

IMPROVING THE OUTCOME OF PATIENTS WITH
PREMALIGNANT AND MALIGNANT DISORDERS
OF THE VULVA

by

JASON KER WEI YAP

A thesis submitted to the University of Birmingham for the degree of

DOCTOR OF PHILOSOPHY



Institute of Cancer and Genomic Sciences

College of Medical and Dental Sciences

University of Birmingham

November 2015

**UNIVERSITY OF
BIRMINGHAM**

University of Birmingham Research Archive

e-theses repository

This unpublished thesis/dissertation is copyright of the author and/or third parties. The intellectual property rights of the author or third parties in respect of this work are as defined by The Copyright Designs and Patents Act 1988 or as modified by any successor legislation.

Any use made of information contained in this thesis/dissertation must be in accordance with that legislation and must be properly acknowledged. Further distribution or reproduction in any format is prohibited without the permission of the copyright holder.

ABSTRACT

Research carried out in this thesis was driven by the need to identify risk factors that predict local recurrence in patients with vulval cancer (VSCC), and the need for more effective treatments for women with usual type vulvar intraepithelial neoplasia (uVIN). To identify the risk factors that predispose women to local recurrences, a multivariate analysis was performed on a well-characterized cohort of women treated for primary VSCC. This analysis revealed that the only independent predictor of local recurrence was the presence of Lichen Sclerosis (LS); here, cancers arising on a background of LS were almost five times more likely to recur compared to those without LS. uVIN is a recognised putative precursor lesion of HPV-positive VSCC. Topical application of Epigallocatechin-3-gallate (EGCG), a green tea polyphenol, has been shown to be an effective treatment for genital warts; a condition caused by low-risk HPV strains. To date, the mechanism(s) by which EGCG exerts its effects on HPV-associated proliferative disorders are unknown. Using HPV18-immortalised keratinocytes as a model, I have shown that EGCG inhibits cell proliferation and promotes apoptosis, an effect that was accompanied by down-regulation of the E6 and E7 proteins and the induction of p53, p21 and pRb. These results were recapitulated in a newly isolated HPV18-positive uVIN keratinocyte clone: VIN clone 11. Biochemical analysis revealed that EGCG did not stimulate E6 degradation by enhancing poly-ubiquitination and proteasome-mediated degradation, suggesting that EGCG-mediated E6 proteolysis occurred through other mechanisms. However, EGCG was found to stimulate mono-ubiquitination of E6, although the relevance of this modification is unknown.

DEDICATION

This thesis is dedicated to the memory of Professor Ciaran Woodman, my supervisor.



ACKNOWLEDGEMENT

First and foremost, I would like to thank my late supervisor, Professor Ciaran Woodman, for his supervision of this thesis, his constructive suggestions in my clinical and laboratory projects, and his constant encouragement throughout the best part of my PhD study. I have been privilege enough to be supervised by Ciaran who has been a “father figure” to me throughout my PhD study, and he will always be an inspiration to me in my academic career.

Next, I would like to express my gratitude to Dr Christopher Dawson who took over as my main supervisor after Ciaran’s passing. I would like to thank him for his guidance, constant support and encouragement, without which I would not have been able to complete my thesis.

I would also like to specially thank Professor David Luesley, my clinical and education supervisor, for his guidance and continue support in my academic career ever since I was a junior doctor. Above all, however, I would like to thank him for the knowledge and skills he has taught me in academia, clinic and operating theatre over the last 8 years.

I would also like to extend my gratitude to:

Cancer Research UK (CRUK) for funding my research.

Mr Richard Fox, for his help in analysing data from the VSCC cohort.

Dr Sally Roberts, Dr Joanna Parish and their group members, for providing technical support and their generosity in providing me with reagents and cell lines for my experiments.

Miss Naheema Gordon, Dr Jennifer Anderton, Dr Sarah Leonard, Dr Roger Grand, and Miss Sara Preigo Moreno for their help in the laboratory, and for their technical advice and assistance.

Professor Sean Kehoe for his mentorship, support and constant encouragement to get me to complete my thesis.

My wife, Yen Lin, and daughter, Chloe, for their understanding, love and support.

And last but not least, my mum, Ah Looi Chon, and dad, Teik Aik Yap, for their love and support.

TABLE OF CONTENTS

ABSTRACT	I
DEDICATION	II
ACKNOWLEDGEMENT.....	III
TABLE OF CONTENTS.....	IV
LIST OF FIGURES	XIII
LIST OF TABLES	XIX
ABREVIATIONS	XXII

Chapter 1: Introduction	1
1.1 Vulval Squamous Cell Carcinoma (VSCC)	2
1.1.1 Epidemiology	2
1.1.2 Aetiology	3
1.1.3 Clinical Symptoms.....	5
1.1.4 Staging.....	5
1.1.5 Management of VSCC.....	7
1.1.6 Prognosis.....	10
1.2 Vulvar Intraepithelial Neoplasia (VIN)	12
1.3 Lichen Sclerosus.....	14
1.4 High-Risk Human Papillomavirus (HR-HPV).....	17
1.5 HPV and Ubiquitination	27
1.5.1 The HPVE6 proteins	29
1.5.2 The HPVE7 Proteins	30
1.6 Stratified Squamous epithelium.....	31
1.6.1 Signals that regulate keratinocyte growth and differentiation	34
1.7 Epigallocatechin-3-gallate (EGCG)	36
1.8 Objectives.....	40

Chapter 2: Materials and Methods	43	
2.1	Part 1: Data collection and analysis of retrospective cohort study	44
2.1.1	Study population	44
2.1.1.1	Identification of study population.....	44
2.1.2	Baseline clinicopathological variables	44
2.1.2.1	Definition of baseline clinic-pathological variables	44
2.1.3	Treatment variables	46
2.1.3.1	Surgery	46
2.1.3.2	Chemo-radiotherapy	47
2.1.4	Outcome variables	47
2.1.4.1	Time to local recurrence.....	48
2.1.4.2	Time to nodal recurrence.....	48
2.1.4.3	Survival	48
2.1.4.4	Anniversary date.....	49
2.1.5	Statistical analysis of the cohort.....	49
2.2	Part 2: Laboratory Techniques.....	50
2.2.1	Tissue culture	50
2.2.1.1	Cell lines and reagents	50
2.2.1.2	3T3 J2 cells.....	51
2.2.1.3	Keratinocyte culture	51
2.2.1.4	Cryopreservation of cell lines.....	51
2.2.1.5	Retrieval of frozen cells.....	52
2.2.2	Drug treatment of cells in monolayer cultures	55
2.2.3	Harvesting of keratinocytes.....	55
2.2.4	Cell proliferation, viability and apoptosis.....	56
2.2.4.1	Cell proliferation and viability assay	56
2.2.4.2	Detection of apoptosis (TUNEL assay)	57
2.2.5	Soft agarose growth assays.....	57
2.2.6	Immunohistochemistry (IHC).....	58
2.2.7	Karyotyping.....	59

2.2.8	Molecular Biology techniques:.....	59
2.2.8.1	Quantitative mRNA analysis of E6/E7 transcript using real-time PCR	59
2.2.8.2	Western blotting analysis.....	60
2.2.9	Cell cycle analysis	63
2.2.10	Immunoprecipitation of HPV18 E6 proteins	64
2.2.10.1	Introduction.....	64
2.2.10.2	Bacterial transformation.....	64
2.2.10.3	Production of plasmid DNA	64
2.2.10.4	Transfection of HEK293 cells.....	65
2.2.10.5	Treatment of transfected cells with drugs.....	66
2.2.10.6	Preparation of cell lysates	66
2.2.10.7	Immunoprecipitation of FLAG-tagged HPV18 E6 protein.....	66
2.2.10.8	Affinity purification of His-tagged ubiquitin protein	67
2.2.11	Endogenous and exogenous proteasome assay	70
2.2.12	Measuring the level of reactive oxidative species (ROS).....	71
2.2.13	Establishment of usual type vulvar intraepithelial neoplasia (uVIN) primary culture	71
2.2.13.1	Establish of primary uVIN keratinocyte cultures	71
2.2.13.2	Single cell cloning	72
2.2.14	HPV genotyping	73
2.2.14.1	HPV 16 and 18 genotyping.....	73
2.2.14.2	HPV genotyping with Luminex PCR.....	73
2.2.14.3	Assessment of HPV E2 integrity	73
2.2.14.4	Determining the changes in relative viral copy number.....	76
2.2.15	Organotypic raft cultures.....	78

Chapter 3: Predicting The Outcome of Women with VSCC.....	81	
3.1	Introduction	82
3.2	Study population	83
3.3	Distribution of explanatory variables.....	83
3.3.1	Demography, behavioural and clinic-pathological variables.....	83

3.3.1.1	Triennia	83
3.3.1.2	Age at diagnosis	83
3.3.1.3	Smoking behaviour.....	84
3.3.1.4	Disease stage.....	84
3.3.1.5	Tumour size	84
3.3.1.6	Multifocal disease	85
3.3.1.7	Histological grade.....	85
3.3.1.8	Lymphovascular space involvement	85
3.3.1.9	Groin node status.....	85
3.3.1.10	Characterisation of epithelium adjacent to invasive component.....	85
3.3.2	Treatment variables (Table 3.2).....	88
3.3.2.1	Type of surgery performed for VSCC.....	88
3.3.2.2	Excision margin status (Table 3.1)	88
3.3.2.3	Type of groin surgery performed	88
3.3.2.4	Radiotherapy and chemotherapy	88
3.3.3	HPV testing.....	91
3.4	Assessment of the correlations between baselines variables ..	91
3.4.1	Overview.....	91
3.4.2	Available information	92
3.4.2.1	Age at diagnosis did not vary over study period	92
3.4.2.2	Smokers/ex-smokers with VSCC are younger than never smokers	92
3.4.2.3	Prevalence of multifocal disease does not vary over time or with age at diagnosis or smoking history	94
3.4.2.4	Women with VSCC associated usual type vulval intraepithelial neoplasia (uVIN) are younger than those with VSCC associated Lichen Sclerosus (LS).....	95
3.4.2.5	Lymphovascular space involvement (LVSI) is more common in never smokers.....	97
3.4.2.6	Tumour size did not vary over time, with age at diagnosis, multifocal disease, smoking status or the presence of LS or VIN	99
3.4.2.7	Grade of tumour differentiation varies over time and with tumour size	102

3.4.2.8	Stage of disease varies over time, with age, grade of tumour differentiation and the presence of uVIN and LS	104
3.4.2.9	Groin node involvement is associated with older age at diagnosis, larger poorly differentiated tumours and associated LS)	106
3.4.2.10	Women with sub-optimally or incompletely excised disease were older with late stage disease and had larger poorly differentiated tumours while those who had LWSI but not GNVI were less likely to have complete excision	109
3.4.2.11	Summary of the relationship of baseline clinic-pathological variables	112
3.4.3	Correlations of HPV positive and negative tumours with baseline variables	112
3.4.4	Missing information	116
3.4.4.1	Smoking history not recorded.....	119
3.4.4.2	Tumour size not recorded	119
3.4.4.3	Tumour differentiation not recorded.....	120
3.4.4.4	Lymphovascular space involvement (LWSI) not recorded	120
3.4.4.5	LS or VIN not recorded.....	121
3.4.4.6	Excision status not determined.....	122
3.4.4.7	Summary	122
3.5	Analysis of local disease recurrence (Time to local recurrence)	122
3.5.1	Overview.....	122
3.5.2	Univariate analysis	127
3.5.2.1	Univariate analysis of local recurrence (local relapse and/or second field tumour).....	127
3.5.2.2	Univariate analysis of local relapse.....	130
3.5.2.3	Univariate analysis of second field tumour	132
3.5.3	Multivariate analysis	134
3.5.3.1	Multivariate analysis of local recurrence (local relapse and/or second field tumour).....	134
3.5.3.2	Multivariate analysis of local relapse.....	135
3.5.3.4	Multivariate analysis of second field tumour	136
3.6	Analysis of groin node recurrence.....	137

3.6.1	Overview, univariate and multivariate analysis	137
3.7	Analysis of disease-specific survival	139
3.7.1	Overview.....	139
3.7.2	Univariate analysis of disease specific survival	140
3.7.3	Multivariate analysis of disease specific survival	143
3.8	Discussion	144
3.9	Overall Summary	154

Chapter 4: The Effect of EGCG on HPV18 Keratinocytes	156	
4.1	Introduction	157
4.2	HFK-HPV18 – the cell model of choice	158
4.3	The effect of EGCG treatment on the proliferation of HFK-HPV18.....	159
4.3.1	EGCG inhibits the proliferation of HFK-HPV18	159
4.3.2	EGCG alters the morphology of HFK-HPV18 keratinocytes.....	161
4.3.3	EGCG treatment does not impose a specific cell-cycle checkpoint blockade in HFK-HPV18 but does increase the proportion of cells in the sub-G1 peak.....	163
4.3.4	EGCG induces apoptosis in HFK-HPV18	165
4.4	The effect of EGCG on episome replication in HFK-HPV18 keratinocytes	168
4.5	The effect of EGCG on expression of the HPV18 E6 and E7 oncogenes	170
4.5.1	EGCG down-regulates expression of the E6 and E7 proteins	170
4.5.2	EGCG does not influence the expression of E6 and E7 mRNA.....	175
4.5.3	E6 and E7 down regulation are accompanied by a decrease in MCM7 and p16 ^{INK4a}	177
4.5.4	E6 and E7 down-regulation are accompanied by an up-regulation in p53 and p21 ^{WAF1}	179
4.5.5	EGCG reverses the effects of HR-HPV on expression of DNA methyltransferases and Polycomb-group proteins.....	182

4.6	The effects of EGCG on the growth and differentiation of HFK-HPV18 keratinocytes in organotypic raft culture	184
4.6.1	EGCG inhibits the proliferation of HFK-HPV18 organotypic raft culture.....	185
4.6.2	EGCG treatment inhibits the incorporation of BrdU label and reduces the expression of the proliferation marker, Ki67, in HFK-HPV18 rafts	188
4.6.3	EGCG treatment of HFK-HPV18 in organotypic raft cultures does not affect the expression of MCM7 or p16 ^{INK4a} , two established targets of the HR-HPVs	191
4.6.4	EGCG treatment increases the expression of tumour suppressor genes (TSGs) p53, p21 ^{WAF1} and pRb in HFK-HPV18 raft cultures.....	193
4.6.5	EGCG treatment does not affect expression of keratinocyte differentiation markers in HFK-HPV18 raft cultures	196
4.6.6	EGCG treatment does not influence expression of the late protein, E4, in HFK-HPV18 raft cultures	199
4.7	EGCG modulates the ubiquitin-proteasome system	201
4.7.1	The proteasome inhibitor MG132 attenuates EGCG-mediated down regulation of E6 and E7 in HFK-HPV18	201
4.7.2	EGCG reduces the half-life of the HPV18 E6 protein	203
4.7.3	EGCG treatment does not increase the pool of poly-ubiquitinated E6 and E6-associated proteins	205
4.7.4	EGCG increases the pool of mono-ubiquitinated E6 protein	218
4.7.5	EGCG selectively inhibit the Chymotrypsin-like activity of the proteasome.....	222
4.8	A role for reactive oxygen species (ROS) in EGCG-mediated degradation of HPV18 E6	227
4.9	Discussion	232

Chapter 5: Establishment of Primary uVIN Clones	249	
5.1	Introduction	250
5.2	Clinicopathological characteristic of the donor	251
5.2.1	Clinical history of donor	251

5.2.2	Pathological description of the surgical specimen	251
5.2.3	HPV status of donor tissue	254
5.3	The establishment of primary keratinocytes from explanted uVIN biopsies.....	255
5.3.1	The morphology of primary keratinocyte outgrowths from explanted VIN biopsies	256
5.3.2	HPV analysis on primary VIN keratinocyte cultures	258
5.4	The establishment of single cell clones from the primary VIN keratinocyte cultures	260
5.4.1	Characterisation of single cell clones isolated from primary keratinocyte outgrowths of the VIN biopsies	260
5.4.2	Characterization of HPV status of VIN cell lines using Luminex PCR	261
5.5	Characterization of VIN cl. 11	263
5.5.1	Karyotypic characterisation of VIN cl.11.....	263
5.5.2	The morphology of VIN cl.11 in monolayer culture.....	267
5.5.3	The morphology of VIN cl.11 in organotypic raft culture	269
5.5.4	The physical status of the HPV18 genome in VIN Clone 11.....	272
5.5.5	Expression of the HPV18 encoded viral oncogenes, E6 and E7, in VIN cl. 11	275
5.6	The effects of EGCG treatment on VIN cl.11 in monolayer culture.....	277
5.6.1	EGCG inhibits the proliferation of VIN cl.11 in monolayer culture ...	277
5.6.2	EGCG treatment changes the morphology of VIN cl.11	279
5.6.3	EGCG treatment does not influence a specific cell-cycle checkpoint, but does increase the proportion of cells undergoing apoptosis	281
5.6.4	EGCG treatment induces apoptosis in VIN cl.11	283
5.7	The effect of EGCG treatment in VIN cl.11 in organotypic raft cultures.....	285
5.7.1	EGCG reduces the proliferation of VIN cl.11 in organotypic raft culture	285
5.7.2	EGCG has little effect, on expression of p16 ^{INK4A} and MCM7 in VIN cl.11 raft cultures	288

5.7.3	EGCG does not influence expression of keratinocyte differentiation markers.....	292
5.7.4	EGCG inhibits the expression of E4 in VIN cl.11 raft cultures	294
5.8	The effect of EGCG treatment on HPV18 E6/E7 oncoprotein and tumour suppressor gene (TSG) expression in VIN cl.11.	296
5.8.1	EGCG treatment down regulates expression of the HPV18 E6 protein in VIN cl.11	297
5.8.2	EGCG up regulates expression of p53 but not p21 ^{WAF1} in VIN cl.11...299	
5.8.3	EGCG treatment stimulates expression of p53, p21 ^{WAF1} and pRb in VIN cl.11 raft cultures	302
5.8.4	EGCG treatment alters the distribution of ΔNp63 in VIN cl.11 raft cultures	306
5.9	Discussion	309
Chapter 6: General Discussion and Future Work		322
Chapter 7: Supplementary Figures.....		330
Chapter 8: References.....		337

LIST OF FIGURES

Figure 1.1: VSCC can be derived from the HPV-dependent and –independent routes.....	4
Figure 1.2: The potential sites in which VSCC can recur locally in the vulva following excision of primary tumour	12
Figure 1.3: The life cycle of human papillomavirus. HPVs (red hexagon) gained access to the basal keratinocytes through a microwound	19
Figure 1.4: The arrangement of the spliced donor (left) and acceptor (right) sites within the E6 open reading frames (ORFs) of the high-risk alpha group of HPVs.....	21
Figure 1.5: The high-risk human papillomavirus E7 oncoprotein modulates its host cellular process by interacting with multiple host cell proteins	23
Figure 1.6: The high-risk human papillomavirus E6 oncoprotein modulates its host cellular process by disrupting cellular signalling pathways.....	24
Figure 1.7: The stepwise progression of cervical neoplasia following persistent HPV infection with high-risk human papillomavirus (HR-HPV)	26
Figure 1.8: Key steps in the ubiquitination pathway	28
Figure 1.9: Organization of the epidermis	33
Figure 1.10: Cross-talk between Notch and ΔNp63 in the Stratified squamous epithelium.....	35
Figure 1.11: Among the catechins, EGCG is the most abundant and biologically active	37
Figure 1.12: Potential molecular targets of EGCG for cancer prevention and treatment	38
Figure 2.1: Flow chart depicting the steps involved in pulling down HPV18 E6 proteins	68
Figure 2.2: pCA.18E6. Based on pcDNA3, the pCA.18E6 plasmid contains a FLAG and double (2x) HA epitope sequence upstream of the HPV18 E6 coding region	69
Figure 2.3: Location of primers used to amplify overlapping regions of the HPV18 E2 gene.....	74

Figure 2.4: qPCR thermal profile for amplifying HPV18 episomes and human TLR primers	77
Figure 2.5: Schematic representation of the steps involved in establishing collagen raft cultures.....	79
Figure 2.6: Typical appearance of a collagen raft culture.....	80
Figure 3.1: The distribution of LS and VIN adjacent to the invasive tumour.....	86
Figure 3.2: The frequency with which tumour size, grade of differentiation and LVI were not recorded in the same surgical sample	121
Figure 3.3: KM-plot for time to local relapse (LR) or 2 nd field tumour (SFT), time to LR and time to SFT	125
Figure 3.4: Plot of baseline hazard ration to time of surgery for local recurrence, LR and SFT	126
Figure 3.5: Kaplan-Meier (KM) plot for disease (VSCC) specific mortality.....	140
Figure 3.6: Kaplan-Meier (KM) plot showing the likelihood patients with local VSCC recurrence (either local relapse, second field tumour or both) went on to develop further episodes of local VSCC recurrence.....	148
Figure 3.7: The relationship between field cancerisation and types of local recurrence is shown.	150
Figure 4.1: EGCG inhibits the proliferation of HFK-HPV18 keratinocytes and the VSCC-derived A431 cell line.....	160
Figure 4.2: Changes in the morphology of HFK-HPV18 following three days treatment with 25μM, 50μM and 100μM	162
Figure 4.3: Representative cell cycle analyses of HFK-HPV18 cells cultured in the presence or absence of EGCG	164
Figure 4.4: TUNEL assay showing EGCG treatment induces apoptosis in HFK-HPV18	167
Figure 4.5: HPV 18 viral copy number increases with EGCG treatment after 48 and 72hrs	169
Figure 4.6: EGCG treatment downregulates expression of the E6 and E7 proteins in HFK-HPV18 and upregulates the expression of p53 and its downstream target gene p21 ^{WAF1}	172

Figure 4.7: EGCG downregulates expression of the HPV18 E6 protein.....	173
Figure 4.8: EGCG downregulates expression of the HPV18 E7 protein.....	174
Figure 4.9: EGCG treatment leads to a slight increase or no change in expression of the HPV18 E6/E7 transcripts.....	176
Figure 4.10: EGCG downregulates expression of MCM7 and p16 ^{INK4a}	178
Figure 4.11: Expression of the p53 protein is upregulated following EGCG treatment	180
Figure 4.12: Expression of the p21 ^{WAF1} protein is not markedly affected by EGCG treatment.....	181
Figure 4.13: EGCG reverses the changes in expression of the DNA methyltransferases and polycomb proteins associated with HR-HPV infection.....	183
Figure 4.14 Organotypic raft culture of HFK-HPV18 showing the overall morphology of the stratified epithelium.....	185
Figure 4.15: EGCG inhibits the proliferation of HFK-HPV18 in organotypic raft culture	187
Figure 4.16 BrdU incorporation and expression of the proliferation marker Ki67 are reduced, while MCM7 remains unchanged, in organotypic raft cultures of HFK-HPV18 treated with EGCG.....	190
Figure 4.17: Expression of p16 ^{INK4a} and MCM7 are not affected by EGCG treatment in organotypic raft cultures of HFK-HPV18.....	192
Figure 4.18: Expression of tumour suppressor genes (TSGs), p53, p21 ^{WAF1} , pRb, and the Polycomb group protein BMI1 are increased in response to EGCG treatment. (A)	195
Figure 4.19: Expression of the keratinocyte differentiation markers: involucrin, Keratin 1/10, β -catenin and Δ Np63 are not affected by EGCG treatment in organotypic raft cultures of HFK-HPV18.....	198
Figure 4.20: Lack of detectable E4 protein expression in control and EGCG-treated HFK-HPV18 raft cultures	200
Figure 4.21: MG132 reverses EGCG-mediated down-regulation of the E6 and E7 proteins in HFK-HPV18.....	202
Figure 4.22: EGCG promotes degradation of the HPV18 E6 protein.....	204

Figure 4.23: Validation of the pCA.18E6 plasmid	207
Figure 4.24: Mono- and poly-ubiquitinated proteins are only detected in HPV18 E6 immunoprecipitates from MG132-treated cells.....	209
Figure 4.25: Input lysates for FLAG immunoprecipitation	210
Figure 4.26: MG132 treatment results in the appearance of ubiquitinated proteins migrating at ~250kDa in HPV18E6 immunoprecipitates	212
Figure 4.27: Validation of the input lysates for the anti-FLAG immunoprecipitation.	214
Figure 4.28: High molecular weight species of ubiquitinated proteins are found in HPV18 E6 immunoprecipitates in cells treated with MG132 or both MG132 & EGCG.....	215
Figure 4.29: Validation of the input lysates for the anti-FLAG protein immunoprecipitation experiment	217
Figure 4.30: EGCG promotes mono-ubiquitination of the HPV18 E6 protein	220
Figure 4.31: Validation of the input lysates for the His-tagged Ub immunoprecipitation experiment	221
Figure 4.32: EGCG and MG132 do not alter the Trypsin-like activity of endogenous and purified 20S proteasomes.....	224
Figure 4.33: EGCG and MG132 do not alter the Caspase-like activity of endogenous or purified 20S proteasomes	225
Figure 4.34: EGCG and MG132 inhibit the Chymotrypsin-like activity of endogenous and purified 20S proteasomes.....	226
Figure 4.35: EGCG treatment reduces the level of reactive oxygen species (ROS) in HFK-HPV18 keratinocytes	229
Figure 4.36: Expression of the HPV18 E6 protein is only marginally affected by ROS	231
Figure 5.1: Representative sections of vulval squamous epithelium within the uVIN biopsies taken from patient Ms S.M.....	253
Figure 5.2: Sections of vulval squamous epithelium from biopsies taken from patient Ms S.M display evidence of HR-HPV infection	254
Figure 5.3: Primary keratinocyte outgrowths and early passage cultures from vulval tissue biopsies obtained from patient Ms S.M.....	257

Figure 5.4: HPV genotyping of primary and subcultured keratinocytes obtained from explanted uVIN biopsies	259
Figure 5.5: Results of the HPV typing analysis performed on uVIN-derived clones using the Luminex multiplex PCR platform.....	262
Figure 5.6: Representative karyotypes from three major clones identified in cultured VIN cl.11 cells.....	266
Figure 5.7: The morphology of VIN cl.11 in monolayer culture.....	268
Figure 5.8: Western blotting analysis confirming the expression of keratinocyte-specific markers in HFK-HPV18 and VIN Cl.11	269
Figure 5.9: Typical morphology of VIN cl. 11 and HFK-HPV18 organotypic raft cultures. H&E stained sections from organotypic raft cultures grown at the air-liquid interface for 14 days.....	271
Figure 5.10: Representative immunostaining for p16 ^{INK4a} in organotypic raft cultures generated from VIN cl.11	273
Figure 5.11: PCR-based HPV18 E2 disruption assay performed to detect the presence of integrated HPV18 genomes.....	274
Figure 5.12: Western blot confirming the expression of HPV18 E6 and E7 in VIN cl.11	276
Figure 5.13: EGCG inhibits the proliferation of VIN cl.11 and HFK-HPV18 keratinocytes.....	278
Figure 5.14: Changes in the morphology of VIN Cl.11 following three days of treatment with 25µM, 50µM and 100µM EGCG.....	280
Figure 5.15: Cell cycle analysis of VIN Cl.11 in the presence or absence of EGCG treatment.....	282
Figure 5.16: TUNEL assay demonstrating that EGCG treatment induces apoptosis in VIN cl.11.....	284
Figure 5.17: H&E staining showing the overall morphology of control and EGCG-treated VIN cl.11 keratinocytes grown in organotypic raft culture.....	286
Figure 5.18: The incorporation of BrdU label and expression of the cell proliferation marker, Ki67, are reduced in VIN cl.11 raft cultures treated with EGCG...	287

Figure 5.19: The expression and distribution of p16 ^{INK4a} and MCM7 are not affected by EGCG treatment in raft cultures of VIN cl11	290
Figure 5.20: EGCG treatment inhibits the proliferation of VIN cl11 cells in organotypic raft culture	291
Figure 5.21: Expression of the differentiation markers, involucrin and Keratin 1/10 are not altered in VIN cl. 11 raft cultures treated with EGCG	293
Figure 5.22: The HPV18 E4 protein is not expressed in VIN.cl11 raft cultures treated with EGCG	295
Figure 5.23: Western blot showing down-regulation of the HPV18 E6 oncoprotein in VIN cl. 11 following EGCG treatment.....	298
Figure 5.24: Western blot showing up-regulation of p53 expression in VIN cl. 11 following EGCG treatment.....	300
Figure 5.25: Western blot showing up-regulation of p21 ^{WAF1} expression in VIN cl. 11 following EGCG treatment.....	301
Figure 5.26: Expression of the p53, p21 ^{WAF1} and pRb are altered in response to EGCG treatment of VIN cl. 11 raft cultures	304
Figure 5.27: EGCG treatment upregulates expression of the key tumour suppressor genes, p53, p21 ^{WAF1} and pRb, targeted by the HPV oncoproteins, E6 and E7, indicating the functions of these TSGs were restored in VIN cl.11 ...	305
Figure 5.28: Unlike β-catenin, expression of the basal cell marker, ΔNp63, is altered in response to EGCG treatment in VIN cl. 11 raft cultures.....	308
Supplementary Figure 1: Expanded image of Western blots taken from Figure 4.6 & 4.13	332
Supplementary Figure 2: Expanded image of Western blots taken from Figure 4.13..	334
Supplementary Figure 3: Immunofluorescence and immunohistochemical staining for p16INK4a on organotypic raft cultures generated from untreated and EGCG-treated HFK-HPV18 keratinocytes	335
Supplementary Figure 4: VIN cl. 11 fails to form colonies in soft-agarose colony formation assays.....	336

LIST OF TABLES

Table 1.1: FIGO staging for vulval cancer (2009)	6
Table 2.1: Information on the cell lines and their respective culture media used for experiments in my thesis	52
Table 2.2: Information on the list of antibodies and their dilutions used for experiments in this thesis	62
Table 2.3: Primer sequences used in PCR assay to detect HPV16 and HPV18 genomes and examine the integrity of E2 genes.....	75
Table 2.4: Primers used to determine episomal copy number changes in HPV18 pre- and post-EGCG treatment.....	77
Table 3.1: Distribution of clinico-pathological variables in Birmingham VSCC cohort.	86
Table 3.2: Distribution of treatment variable in Birmingham VSCC cohort.....	90
Table 3.3: Table showing the relationship between median age and year of diagnosis in 3 triennia.	92
Table 3.4: Table showing the relationship between smoking status and age or year of diagnosis in 3 triennia.	93
Table 3.5: Table showing the relationship between multifocal disease and age, year of diagnosis in 3 triennia or smoking status.....	94
Table 3.6: Table showing types of epithelial abnormalities, either uVIN alone, dVIN alone, Lichen Sclerosus alone or in combination, found adjacent to the primary VSCC.....	96
Table 3.7: Table showing the relationship between lymphovascular space involvement and age, year of diagnosis in 3 triennia, smoking status, disease focality or adjacent epithelial abnormalities.....	98
Table 3.8: Table showing the relationship between tumour size and age, year of diagnosis in 3 triennia, smoking status, disease focality, adjacent epithelial abnormalities or LVSI	100
Table 3.9: Table showing the relationship between grade of tumour differentiation and age, year of diagnosis in 3 triennia, smoking status, tumour size, disease focality, adjacent epithelial abnormalities or LVSI...	103

Table 3.10: Table showing the relationship between disease stage and age, year of diagnosis in 3 triennia, smoking status, tumour differentiation, disease focality, adjacent epithelial abnormalities or LVSI	105
Table 3.11: Table showing the relationship between groin node metastasis (GNVI) and age, year of diagnosis in 3 triennia, smoking status, tumour size, tumour differentiation, disease focality, adjacent epithelial abnormalities or LVSI	108
Table 3.12: Table showing the relationship between adequacy of tumour excision margins and age, year of diagnosis in 3 triennia, smoking status, tumour size, disease stage, tumour differentiation, disease focality, adjacent epithelial abnormalities, LVSI and GNVI.	111
Table 3.13: Table showing the relationship between HPV positive/negative tumour and age, year of diagnosis in 3 triennia, smoking status, tumour size, disease stage, tumour differentiation, disease focality, adjacent epithelial abnormalities, LVSI and GNVI.....	114
Table 3.14: Table showing the associations and determinants of missing information.	117
Table 3.15: Distribution of treatment outcomes in women diagnosed with primary VSCC in Birmingham between 2000 to 2008.	124
Table 3.16: Summary of univariable HR for potential predictors of time to local relapse or second field tumour.....	129
Table 3.17: Summary of univariable HR for potential predictors of time to local relapse	131
Table 3.18: Summary of univariable HR for potential predictors of time to second field tumour.....	133
Table 3.19: Summary of multivariable HR for potential predictors of time to local recurrence	134
Table 3.20: Summary of multivariable HR for potential predictors of time to local relapse	135
Table 3.21: Summary of multivariable HR for potential predictors of time to second field tumour.....	136

Table 3.22: A summary of the univariate analysis for potential predictors of time to nodal recurrence	138
Table 3.23: A summary of the univariate analysis for potential predictors of VSCC specific mortality	142
Table 3.24: Summary of multivariable HR for potential predictors of time to disease specific mortality	143

ABREVIATIONS

BAK:	BCL-2 antagonist/killer protein
BCL-2:	B cell lymphoma 2
BrdU	BromodeoxyUridine
cDNA:	Complementary DNA
Co-IP:	Co-immunoprecipitation
CMV:	Cytomegalovirus
DNA:	Deoxyribonucleic acid
EGCG:	Epigallocatechin-3-gallate
FACS:	Fluorescence-activated cell sorting
FCS:	Foetal calf serum
GAPDH:	Glyceraldehyde-3-phosphate dehydrogenase
HA:	Haemagglutinin
HIS-Ub:	Histidine-tagged Ubiquitin
HR-HPV:	High-Risk Human Papillomavirus
LR-HPV:	Low-Risk Human Papillomavirus
IFN:	Interferon
IHC:	Immunohistochemistry
IL:	Interleukin
IP:	Immunoprecipitation
Kbp:	Kilobase pair
LS:	Lichen Sclerosus
LVSI:	Lymphovascular space invasion
mAb:	Monoclonal antibody
MHC:	Major histocompatibility complex
mRNA:	Messenger RNA
MCM:	Mini chromosome maintenance

ORF:	Open reading frame
P16 ^{INK4a} :	Cyclin-dependent kinase inhibitor 2A
P21 ^{WAF1} :	Cyclin-dependent kinase inhibitor 1/ CDK-interacting protein 1
PBS:	Phosphate buffer saline
PCR:	Polymerase chain reaction
PI:	Propidium iodide
QPCR:	Quantitative polymerase chain reaction
RNA:	Ribonucleic acid
RPM:	Revolutions per minute
RT:	Reverse transcription
SDS:	Sodium dodecyl sulphate
Ub:	Ubiquitin
UTR:	Untranslated region
dVIN:	Differentiated Vulval Intraepithelial Neoplasia
uVIN:	Undifferentiated Vulval Intraepithelial Neoplasia
VSCC:	Vulval Squamous Cell Carcinoma

Chapter 1:

Introduction

1.1 Vulval Squamous Cell Carcinoma (VSCC)

1.1.1 Epidemiology

Vulval cancer is uncommon, comprising only 6% of all gynaecological malignancies reported in the UK. It is predominantly a disease of the elderly with three-quarters of cases affecting those aged over 60 years [1]. The age-standardised incidence of squamous cell carcinoma of the vulva (VSCC) is 2.5 per 100,000 women per year in England and 2.4 per 100,000 in the United States (US) [1, 2]. In England, 966 women were first diagnosed with VSCC in 2011, and there were 364 deaths from the disease in that year. Cancer surveillance systems in England, Denmark and the US point to a significant increase in the incidence of VSCC in women under the age of 65 [1-3]. Consistent with these trends, the Thames Cancer Registry UK has reported an increase in the incidence of vulvar cancer in cohorts born after 1940 [4]. The West Midlands Cancer Registry UK which covers a population of 5.6 million has a reported rate for cases registered between 2001 and 2005, a 5 year relative survival of 80.5% in women < 65 at diagnosis and a rate of 61.6% in older women; the corresponding figures from the SEER programme for cases diagnosed in the US in 2004 were 81.6% and 70.6% [2]. In neither dataset is there evidence of an increase in relative survival over time in these age-groups.

Squamous cell carcinoma (VSCC) make up 90% of all cases of vulval cancers, with the remaining 10% comprised of basal cell carcinoma, adenocarcinoma, malignant melanoma, Paget's disease of the vulva and Bartholin's gland tumours [1]. The scope of this thesis focuses primarily on reducing the risk of local recurrence in those women with VSCC and its precursor lesions.

1.1.2 Aetiology

VSCC is believed to arise through HPV-dependent and independent routes (see Figure 1.1). The current disease paradigm holds that following persistent high-risk HPV infection women develop usual or classical type vulvar intraepithelial neoplasia (uVIN), which subsequently progress into basaloid or warty type squamous cell carcinoma (SCC) [5, 6]. It is estimated that 40% of all VSCC cases arise through the viral-dependent route and, interestingly, the prevalence of HR-HPV positive tumour is 20% higher in the US [7-12]. Most cases of the tumour tested positive for HPV16 and, to a lesser extent, HPV 18 and HPV 33 [13]. HPV-associated tumours typically affect younger women, aged <65 years, and the incidence in this age group is found to be increasing in the UK and elsewhere [1]. This increase is a reflection of the rising incidence of its precursor lesion, uVIN, in young women, which in turn is due to the rise in the prevalence of HR-HPV infection [13].

The virus independent route is associated with the development of keratinising tumours in a background of differentiated intraepithelial neoplasia (dVIN) or Lichen Sclerosus (LS) [5, 6]. It is thought that the main trigger of carcinogenesis in this instance is chronic inflammation, which results in repeated injuries and scarring to the epithelium. The attempt of the epithelium to renew and repair itself continuously predisposes it to DNA damage and mutation, which eventually leads to oncogenic transformation [14]. Nevertheless, it remains unclear if LS gives rise to dVIN as there is no real connection between the two conditions. Women within this age group are usually older (> 65 years) and critically they are also more likely to have other medical comorbidities, which may pose certain challenges in managing their cancer.

Natural history of VSCC

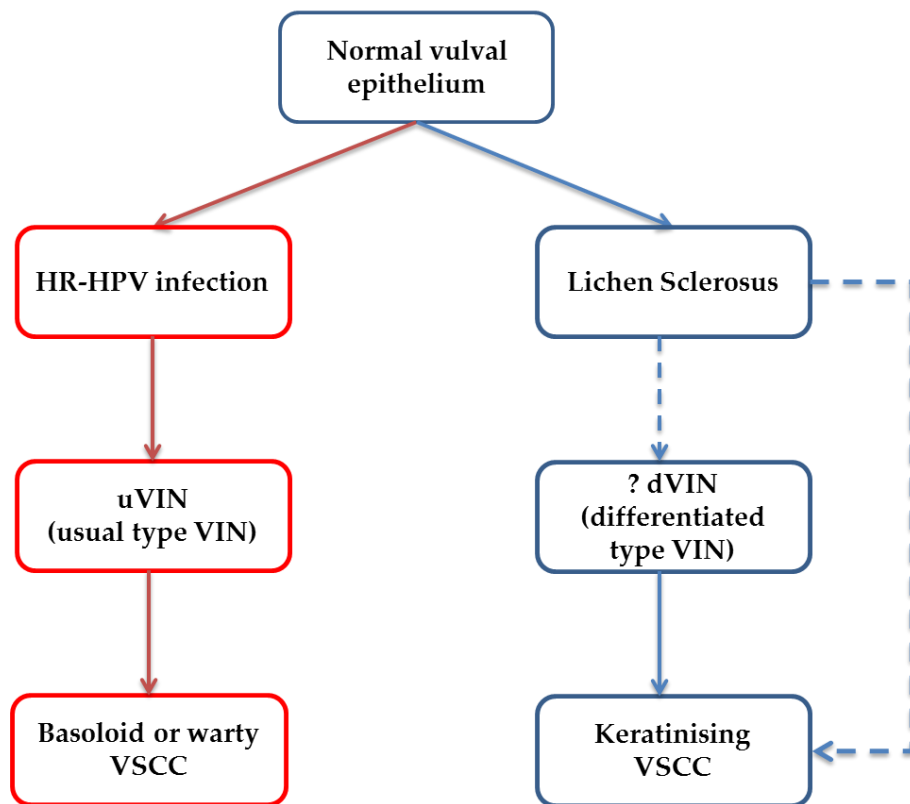


Figure 1.1: VSCC can be derived from the HPV-dependent (red) and –independent (blue) routes. Persistent HR-HPV infection gives rise to uVIN which subsequently developed into basoloid or warty VSCC, if left untreated. Keratinising VSCC is usually found arising in the background of LS and dVIN. It remains unclear if dVIN is a precursor lesion for LS and if LS can give rise directly to VSCC as there is no stepwise histological model of carcinogenesis in the setting of chronic LS (blue dotted lines).

1.1.3 Clinical Symptoms

Women with VSCC usually present with pain, irritation, pruritus, bleeding, a lump, ulcer or discharge. It is well recognised that most women delay in presenting themselves to their medical practitioner, especially the elderly cohort because of embarrassment [15, 16]. However, it is unclear if this affects their treatment outcome, as most VSCC are slow growing.

1.1.4 Staging

Vulval cancer is staged surgicopathologically according to the International Federation of Gynaecology and Obstetrics (FIGO) staging system since 1994. The FIGO staging has been revised and updated over the years according to treatment outcome, and it was last revised in 2009 [17]. The current FIGO staging is presented in Table 1.1.

Table 1.1: FIGO staging for vulval cancer (2009)

FIGO staging for vulval cancer (2009)	
Stage I	Tumour confined to the vulva
<i>Stage Ia</i>	<i>Lesions ≤ 2 cm in size, confined to the vulva or perineum and with stromal invasion ≤ 1mm. No nodal metastasis</i>
<i>Stage Ib</i>	<i>Lesions > 2 cm in size or with stromal invasion > 1 mm confined to the vulva or perineum. No nodal metastasis</i>
Stage II	Tumour of any size with extension to adjacent perineal structures (lower 1/3 urethra; lower 1/3 vagina; anus) with negative nodes
Stage III	Tumour of any size with or without extension to adjacent perineal structures (lower 1/3 urethra; lower 1/3 vagina; anus) with positive inguinofemoral nodes
<i>Stage IIIa</i>	<ul style="list-style-type: none"> i. With 1 lymph node metastasis (≥ 5 mm), or ii. 1–2 lymph node metastasis(es) (< 5 mm)
<i>Stage IIIb</i>	<ul style="list-style-type: none"> i. With 2 or more lymph node metastases (≥ 5 mm), or ii. 3 or more lymph node metastases (< 5 mm)
<i>Stage IIIc</i>	<i>With positive nodes with extracapsular spread</i>
Stage IV	Tumour invades other regional (upper 2/3 urethra; 2/3 vagina) or distant structures
<i>Stage IVa</i>	<i>Tumour invades any of the following</i> <ul style="list-style-type: none"> i. Upper urethral and/or vaginal mucosa; bladder mucosa; rectal mucosa or fixed to pelvic bone, or ii. Fixed or ulcerated inguinofemoral lymph nodes.
<i>Stage IVb</i>	<i>Any distant metastasis including pelvic lymph nodes</i>

1.1.5 Management of VSCC

The Royal College of Obstetricians & Gynaecologists and the British Gynaecological Cancer Society jointly published a guideline detailing the diagnosis and management of vulval cancer [18]. Owing to the rarity of the disease, it is recommended that women with VSCC be referred to and managed in local gynaecological cancer centres to improve treatment outcomes. Surgical excision (radical vulvectomy) is the mainstay of treatment for VSCC and the extent of surgery depends on a number of factors that include: the size of the tumour; its location and proximity to vital organs; fitness to tolerate major surgery; FIGO stage; and wishes of the patient. Over the years, surgical management has become more conservative so as to preserve sexual function and body image [19]; this is particularly important as the incidence of the disease is increasing in younger patients. The main aim of surgery is to achieve adequate surgical resection and to preserve the function of vital organs such as the bowel and genitourinary tract unless these organs are also affected by cancer, in which case they are removed. The current guideline recommends that fresh surgical specimens should consist of at least 15mm of disease-free tissue, lateral and deep margins, so that after fixation a $\geq 8\text{mm}$ histological cancer-free margins can be achieved to avoid local recurrence [18]. This practice is based on a retrospective study that showed that women with histological margins of $<8\text{mm}$ were at significantly increased risks of developing local recurrence when compared to those with histological margin of $\geq 8\text{mm}$ [20]. However, it remains unclear if inadequate surgical excision is the main driver for local recurrence as recent evidence showed that other factors also play an important role in determining the timing and pattern of local recurrence (see Chapter 1 discussion).

More than two-thirds of VSCC arise on a background of atypical skin in the form of VIN, LS or both [21]. While VIN is a putative precursor lesion for VSCC, it is still debatable whether LS is also a pre-malignant lesion. In women, LS is often widespread and affects both the vulva and anal skin in a figure of eight pattern. While there is some evidence to suggest that residual LS left behind after excision of the primary tumour may increase the risk of local recurrence [22, 23], it is unnecessary to remove all the affected skin so as to compromise the function of the vital organs as the absolute risk of recurrence in these women is not well defined. As for VIN, the current guideline recommends that the lesion should be destroyed with diathermy or excised, but not to the extent of a radical vulvectomy because the absolute risk of local recurrence are again not well defined, and VIN often recurs in 1 in 3 women within 3 years of surgical excision [24, 25].

The first point of distant metastasis for vulval cancer is always the lymphatic chain within the groin before it spreads to the pelvis and other parts of the body. Tumours measuring less than 2cm in diameter and confined to the vulva, with stroma invasion of $\leq 1.0\text{mm}$ (FIGO stage Ia) have a negligible risk of spreading to the groin nodes [26]. This group of patients do not normally require further intervention to their groin once their primary tumour is successfully excised. For those with tumours either larger than 2cm, stromal invasion of $>1.0\text{mm}$ or both, require radical treatment to their groin to exclude or remove metastatic disease because undetected groin node disease or nodal recurrence have poor survival outcome [18, 19] Traditionally, lymphadenectomy is the default surgery for managing nodal disease where all lymph nodes in the groin are removed. This can be achieved en bloc or through a separate incision to the primary

tumour (triple incision). Groin lymphadenectomy carries significant long-term morbidity as women often end up with severe lymphedema that often compromise their mobility. The introduction of groin sentinel lymph node biopsy (SLNB), which utilises the combination of radioactive lymphoscintigraphy and methylene blue dye studies to detect the sentinel node, has recently revolutionised the treatment of groin node disease. Instead of performing a complete lymphadenectomy, women with tumour ≤4cm undergo SLNB to remove a small group of lymph nodes (sentinel node) in the groin(s) for histological diagnosis. If the sentinel node(s) is free of disease, then no further treatment is required. Otherwise, the patient will have a full lymphadenectomy if metastasis is detected in the sentinel node. Published data from a multicentre trial practicing SNLB showed that the technique has a great sensitivity and specificity in diagnosing groin node metastasis, and long-term morbidity associated with the procedure is significantly lower than that of a complete lymphadenectomy [27, 28]. The rate of groin node recurrence was also found to be less or comparable to that of a full lymphadenectomy.

The use of radiotherapy is limited to neo-adjuvant or adjuvant setting, to shrink the size of the primary tumour before surgery or to treat potential residual disease locally and in the groin, respectively. Primary radiotherapy, with or without chemotherapy, is increasingly used for those with advanced disease (FIGO stage III and IV) who are not fit enough for surgery; for advanced recurrent disease (distance or local); or for palliation. The benefit of chemotherapy is still under evaluation, and it is used, either alone or in combination with radiotherapy, in neo-adjuvant or adjuvant setting to

complement surgery; in those patients who are not fit enough to tolerate surgery; for palliation; or for advanced recurrence disease [18].

1.1.6 Prognosis

Approximately one-third of women with VSCC exhibit local recurrences [18]. A number of retrospective cohort studies have identified potential risk factors that predispose women to local recurrence. These include: inadequate excision margins; groin node involvement; the presence of LS and VIN (usual and differentiated type) adjacent to the primary tumour; older age group; tumour size; tumour multifocality; histology grade; lymphovascular invasion (LVI); and type of surgery performed [15, 20, 22, 23, 29-36]. However, it remains unclear which of the risk factors best predict local recurrence, as each study identified different predictors, and none were in agreement with each other. This is a reflection of different methods used by each study to collect and analyse its results. Increasingly, two different patterns of local recurrence have been recognised in VSCC. Tumours that arise on a site previously occupied by the primary tumour are usually termed a local relapse (LR), and are thought to be a true local recurrence that usually recurs within 3 years after local excision. Tumours that occur at least 2cm or more away from the primary tumour have been termed second field tumours (SFT) or second primary tumour (SPT) [22, 30, 31, 36, 37], and these are thought to be new tumours that could be genetically related (SFT) or unrelated (SPT) to the primary tumour (see Figure 1.2). Although incompletely resolved, it is thought that both SFT and SPT are likely to arise in a histological normal but molecularly altered epithelium, termed a “field of cancerization” [38]. The theory of field cancerization was first proposed by Slaughter et al. in 1953 who studied the

histology of dysplastic epithelial tissue adjacent to the primary tumour in an attempt to explain the reason for the development of multiple primary tumours and tumour recurrence in the oral cavity and upper respiratory tract [39]. Since the development of molecular biology, the concept of field cancerization has now been redefined in molecular terms. Molecular alterations, such as genetic mutation or epigenetic modulation of genes, predispose an epithelium to undergo oncogenic transformation - this epithelium may even appear macroscopically normal. The accumulation of genetic alterations over a protracted period of time eventually leads to cancer development. In the context of VSCC, one study, which used the pattern of X chromosome inactivation as a marker of clonality, revealed that high-grade uVIN lesions contiguous with VSCC were of the same clonal origin, raising the possibility that these VSCCs were derived from molecularly altered clones within the VIN lesions [40].

The 5-year survival of women without lymph node metastasis was found to be in excess of 80%, but it falls to well below 50% if inguinal nodes are involved. The prognosis of those with iliac or pelvic node involvement is extremely poor with less than 15% surviving in 5 years [18]. Old age, advanced stage disease and groin involvement were repeatedly found to be independent predictors for poor survival. While local recurrence does not normally influence survival, relapse in the groin or pelvic node is almost always fatal as nodal relapse is often refractory to treatment [41].

Site of local recurrences

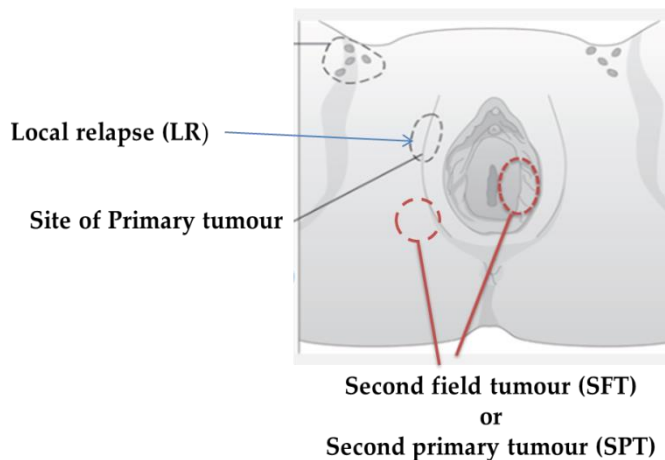


Figure 1.2: The potential sites in which VSCC can recur locally in the vulva following excision of primary tumour.

1.2 Vulvar Intraepithelial Neoplasia (VIN)

According to the International Society for the Study of Vulvovaginal Disease (ISSVD), high-grade vulval intraepithelial neoplasia (VIN), the putative precursor lesion of VSCC, can be divided into usual and differential types, uVIN and dVIN, respectively. While the former is associated with persistent high-risk HPV infection, the aetiology for the latter is less well defined, but it is often found on a background of persistent LS.

Differentiated vulvar intraepithelial neoplasia (dVIN) is believed to be a direct precursor of VSCC and ~80% is found adjacent to VSCC. Studies have shown that when VSCC is found in association with differentiated VIN, it is more likely to recur and to have a shorter disease-specific survival [21, 42]. Most dVIN are associated with TP53 mutations or deletions, and the detection of common mutations in dVIN and its adjacent VSCC points to a genetic relationship between these two entities [43].

However, dVIN is rarely diagnosed in the absence of VSCC. As to why this should be the case is not clear. One possibility is that dVIN progresses rapidly to an invasive disease after a very short pre-invasive phase. However, two groups have recently suggested that dVIN is often under-diagnosed [42, 44]. Both studies found on histological review a failure to recognise dVIN in a substantial proportion of women who were subsequently found to have VSCC; these cases had been originally classified as LS or as “benign changes”. If solitary dVIN is diagnosed, then the preferred choice of treatment is either surgical excision or diathermy destruction of the lesion.

Usual type vulvar intraepithelial neoplasia (uVIN) is associated with persistent infection with high-risk HPV subtypes; predominantly, HPV16 [13]. In most cases, the virus is maintained in episomal form [45]. uVIN primarily affects young women, with a peak age incidence of 30-49 years, and the incidence has increased by more than 3-fold in recent years [46, 47]. Although the malignant potential of uVIN is significantly lower than that of cervical intraepithelial neoplasia (CIN) [24], it often causes debilitating symptoms such as pruritus, pain and sexual dysfunction. Moreover, at least 50% of women were found to have multiple uVIN lesions (multifocal disease); 1 in 3 women were also found to have synchronous or asynchronous multicentric intraepithelial neoplasia of the cervix, vagina and anus [48].

Currently, surgical excision remains the mainstay of treatment for women with uVIN, but it does not offer a cure. More than a third of these women will have recurrences, and surgery may itself result in additional physical and psychosexual problems [25]. Although the risk of malignant transformation in these women is small, clinicians cannot predict those likely to progress and, therefore, place all on extended

surveillance. These arrangements do little to allay patient anxiety while placing an ever increasing burden on NHS resources. Novel alternatives to surgery have been investigated, for example, photodynamic therapy and laser ablation, but both have yielded variable results. Topical treatment with Imiquimod, an immune modulator has been shown to be effective in the management of uVIN but is associated with substantial side effects that frequently result in its premature discontinuation [49, 50]. The results of a recently published Phase II clinical trial (RT3VIN) comparing Imiquimod and Topical Cidofovir (an anti-viral drug) revealed that just under half of women with uVIN from each treatment arm responded to either treatment [51]. Both drugs showed similar side effect profiles and neither treatment was superior over the other. Towards this end, we have started a Phase II randomised control trial (EPIVIN) evaluating the use of a novel topical therapeutic agent, Veregen[®], in the treatment of women with uVIN. Veregen[®] ointment contains Epigallocatechin-3-gallate (EGCG), a major bioactive polyphenol of green tea which has been shown to possess multiple anti-carcinogenic effects in cell culture and animal models of cancer and, more importantly, shown to be safe and effective in treating HPV-associated proliferative disorders [52]. The potential biological activities of EGCG on HPV will be discussed in section 1.5.

1.3 Lichen Sclerosus

Lichen Sclerosus (LS) is a chronic, inflammatory skin condition that affects the genital area and around the anus, where it causes persistent itching and soreness. Scarring after inflammation may lead to severe damage to the genitalia, such as fusion of the

labia, narrowing of the vaginal opening and burying of the clitoris if treatments are not started early. LS affect both men and women, but the disease has a predilection for post-menopausal women. The true incidence and prevalence of the disease remains largely unknown because many patients do not present themselves to the hospital. A long-term follow-up MRC contraceptive study involving 17,000 women found that the risk of developing LS increases with age and the incidence of those aged 50-59 was 14 per 100,000 (95% CI 4-32) [53]. The mean age of onset of the disease in women has been reported to be between the fifth and sixth decade.

There is no single causal factor that attributes to the onset of LS despite numerous studies being conducted to identify the aetiology of the disease [53]. Women who present with LS often have associated autoimmune diseases such as thyroid disease, diabetes mellitus, pernicious anemia, vitiligo and cicatricial pemphigoid [53-56]. The presence of autoantibodies in the serum coupled with histological findings of chronic inflammatory changes point towards an autoimmune aetiology [53]. Genetic factors relate to the human leukocyte antigen (HLA) complex, and traumas that result in a Koebner phenomenon have all been implicated in the development of LS [53, 57, 58]. Unfortunately, there is no curative treatment for women with LS. The treatment regimen involves the use of long-term potent steroids (clobetasol propionate 0.05% and mometasone furoate 0.05%) and emollients aiming to achieve symptomatic control and prevent further anatomical distortion of the genitalia [59]. Surgery has no role in managing a patient with LS except for restoring anatomical function.

The lifetime risk of developing vulval squamous cell carcinoma (SCC) in women with LS has been reported to be 4% to 5% [53, 57, 60]. Clinically, we lack an understanding

of how to separate indolent LS cases from those in danger of progressing to squamous cell carcinoma. Although differentiated vulvar intraepithelial neoplasia (dVIN) is often found in women with LS and VSCC, it remains unclear whether dVIN is the putative precursor lesion linking LS to VSCC because there is no stepwise histological model of carcinogenesis in the setting of chronic LS. It is thought that LS gives rise to the HPV-independent keratinizing SCC where the cohort of patients is often older [61], as opposed to HR-HPV-dependent VSCC which are derived from uVIN in younger patients. Recently, several studies have identified LS as an independent risk factor for developing local VSCC recurrence despite complete removal of the primary tumour [22, 23]. Those tumours that recur on a background of LS were more likely to develop after a long latency period, and to occur at a site distant to the primary tumour; a pattern of recurrence similar to that observed in HPV-negative head and neck SCC [62]. The implications of these findings are that the cancer is more likely to constitute a new primary or second field tumour that arises in a "field of cancerization". Currently there is neither a robust screening method to detect early recurrence nor chemopreventative treatment to prevent recurrence in these patients; consequently, all patients are followed-up for an extended period and many end up having multiple biopsies taken over time. Thus, there is a need to look for better management strategies for those patients with LS and, more importantly, those at risk of developing VSCC, so that they can be identified early and offered chemopreventative therapies. Future research on LS should aim at identifying molecular signatures that separate those with indolent LS from high-risk LS, and developing chemopreventative therapies to prevent the high-risk cohort from progressing to VSCC.

1.4 High-Risk Human Papillomavirus (HR-HPV)

Human papillomaviruses (HPVs) are small DNA viruses (~8kb in size) that are epitheliotropic in nature, displaying a tropism for squamous epithelium. More than 120 subtypes have been described, of which a third have been found to infect the genital mucosa [63]. Of these genital HPVs, 15 subtypes are associated with cervical cancer and, as such, have been classified as high-risk HPVs (HR-HPV). The remaining low-risk subtypes (LR-HPV) cause benign papillomatous lesions [64]. As discussed previously, HR-HPV DNA has been found in approximately 40% of VSCC cases, and in over 90% of uVIN cases, indicating that these viruses are also a causative agent for vulval neoplasia. A multi-national collaborative HPV genotyping study on 2000 cases of pre-invasive and invasive vulval disease found that, like cervical neoplasia, HPV 16 was the commonest type (72.5%) in vulval neoplasia followed by HPV 33 (6.5%) and HPV 18 (4.6%) [65].

The unique and unusual life cycle of HPV explains their propensity to induce malignant transformation of squamous epithelial cells. Unlike most viruses, which produce progeny virus from the same infected cell, lytic replication of HPVs only occurs after infected basal keratinocytes have undergone mitosis and their daughter progeny have committed to the terminal differentiation program [66]. The life cycle of HPV is intimately linked to the differentiation of squamous epithelium (Figure 1.3). The virus gains access to basal keratinocytes through micro-abrasions in the epithelium. Following infection, HPV genomes are established as extrachromosomal elements, termed episomes, which are maintained in basal cells using the host cell's DNA replication machinery. As HPVs do not encode their own DNA polymerases or

other enzymes required for viral replication, they are totally reliant on the host cell for DNA replication. As the infected daughter keratinocytes migrate upwards and begin the terminal differentiation process, the remaining infected keratinocytes are retained within the basal layer as slow-cycling and self-renewing cells to maintain a reservoir of latently infected cells [67]. The early viral genes (E1, E2, E4, E5, E6, E7) are expressed in basal cells, where they function to maintain episomal replication. Low numbers of viral episomes, about 200 copies per cell, are maintained in infected stem/progenitor cell populations, a process termed latent infection. The early genes are also responsible for the initiation of lytic viral replication when the infected daughter cells undergo terminal differentiation. Under normal circumstances, keratinocytes that have migrated into the suprabasal layers can no longer undergo mitosis as they have exited the cell cycle and committed to undergo terminal differentiation. In order to initiate viral genome replication, the E5, E6 and E7 proteins “hijack” the cell cycle machinery to promote host cell DNA replication, which is maintained after keratinocytes exit the basal layer, this also allows the viral genomes to replicate and amplify to high copy numbers. These rapidly dividing suprabasal keratinocytes, also known as koilocytes, display distinctive histological features of an enlarged, irregular and dense nucleus and a perinuclear halo. In the upper layer of the epithelium, E4, L1 and L2 genes are expressed to package the viral DNA into capsids and progeny virions ready to be released and re-initiate infection.

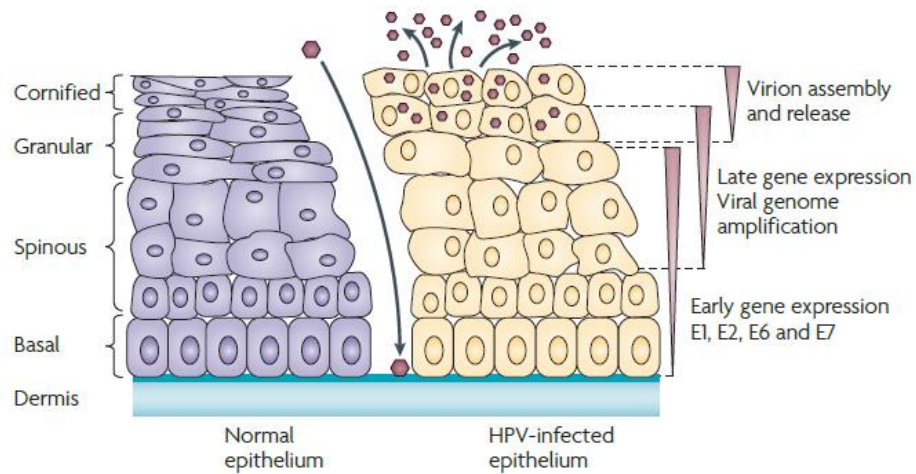


Figure 1.3: The life cycle of human papillomavirus. HPVs (red hexagon) gained access to the basal keratinocytes through a microwound. The uninfected epithelium is shown on left and infected epithelium on the right. On infection, the viral genomes are established in the nucleus of the keratinocytes in low-copy number, typically 200 copies per cell. The virus utilises the host DNA replication machinery to replicate and divide in synchrony with host DNA replication. After cellular division, the infected daughter cell migrates into the suprabasal layer and undergoes terminal differentiation that triggers the vegetative phase of the HPV life cycle. The expression of the oncoproteins E6/E7 deregulates cell cycle control and forces the differentiating keratinocytes to return to S phase so that viral genome amplification can take place. The expression of the late, L1 and L2, and with E4 genes allows the newly synthesised viral genomes to be encapsidated before the virions are released in the upper most layer of the epithelium.

Figure adapted from Moody & Laimins, 2010

The E6 and E7 proteins function as viral oncogenes. Both are essential for initiating and maintaining cellular transformation by modulating cell cycle checkpoint control and preventing apoptosis. E6 and E7 work synergistically to modulate the activity of various cell cycle regulators. This creates an environment conducive to HPV genome replication. However, in doing so, E6 and E7 also deregulate normal cellular gene control, which, over time, leads to genomic instability and carcinogenesis. The E6 and

E7 proteins encoded by high-risk (HR), but not the low-risk (LR), HPVs, are transcribed from a linear bicistronic or spliced polycistronic E6/E7 transcript [68]. The E6 open reading frame (ORF) is usually spliced out at a highly conserved spiced donor site, then spliced back in at E6 ORF splice acceptor site that lies upstream of the E7 promoter, to produce E6* as illustrated in Figure 1.4 [69]. While certain HR-HPV subtypes, such as HPV16, have splicing patterns that allow the expression of up to 4 species of E6*, others such as HPV18 only produce one transcript capable of expressing E6*. The E7 proteins can be translated from either unspliced or spliced variants of the E6/E7 mRNAs and recent evidence suggests that, at least in HPV16 and 18, while unspliced mRNA encode mostly full-length E6, spliced mRNA encodes both E6* and E7 proteins [70]. The E6* proteins have been found to antagonise the functions of full-length E6 protein and probably play an important role in inhibiting keratinocytes proliferation when sufficient viral genomes are amplified so that keratinocytes differentiation can continue to facilitate the release of progeny virions [68].

Like most cellular proteins, E6 and E7 proteins are degraded and recycled through the human ubiquitin-proteasome pathways [71]. However, evidence showing that these viral oncoproteins are poly-ubiquitinated, a prerequisite for proteasome-mediated degradation, is still lacking. For ubiquitination to proceed, at least 4 ubiquitin molecules have to become covalently attached to a protein before they are recognised by the 26S proteasome and targeted for degradation.

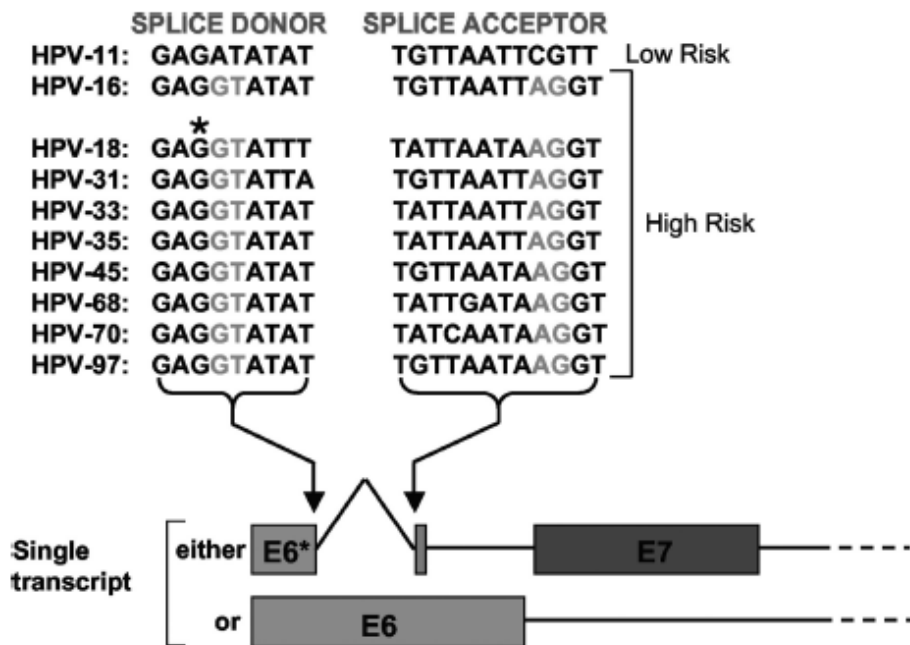


Figure 1.4: The arrangement of the spliced donor (left) and acceptor (right) sites within the E6 open reading frames (ORFs) of the high-risk alpha group of HPVs. Note that splicing is unique to HR-HPV E6. Asterisk denotes that a G is mutated to A to abolish splicing, in which case full-length E6 is produced instead.

Figure adapted from Pim *et al.*, 2009

The transforming functions of E6 and E7 are linked to their ability to target a myriad of cell signalling pathways [66]. The primary target for E7 is the retinoblastoma (Rb) family of proteins, p105 (Rb), p107 and p130. In their hypo-phosphorylated state, the pRb family proteins bind to the E2F transcription factors and repress the expression of S phase genes, which drive DNA replication and cell cycle progression. Phosphorylation of Rb by G1 cyclin-dependent kinases (CDK2, 4) liberates E2F leading to cell cycle progression in S-phase. The E7 protein targets the Rb-E2F pathways in a

number of different ways; it can directly bind to the hypophosphorylated Rb through interaction with the LXCXE motif within its amino-terminus and disrupt the pRb-E2F complexes [72]; it has also been found to promote the degradation of the Rb through the ubiquitin-proteasome system, thus reducing the overall level of Rb protein. In response to Rb inactivation, keratinocytes attempt to counter the effect of E7 by increasing expression of the cyclin-dependent kinase inhibitor, p16^{INK4a}, which prevents the over phosphorylation of Rb [73]. As E2F activation is not due to hyperphosphorylation of Rb, but rather, caused by binding of E7 to Rb, the resultant over-expression of p16^{INK4a} has little, if any effect on E2F activity. Thus, overexpression of p16^{INK4a} has been implicated as a useful surrogate marker for HR-HPV E7 activities [66, 74].

Uncoupling of the G1-S cell-cycle checkpoint induces the expression of p53, a tumor suppressor gene (TSG) that functions to inhibit cell proliferation and induce apoptosis. To counteract the effect of E7 on p53 activation, the HR-HPV E6 proteins have evolved to target p53 proteins for degradation, thus preventing cell growth inhibition. E6 binds to an E3 ubiquitin ligase called E6-associated protein (E6AP), which binds p53 and targets it for ubiquitin-proteasome-mediated degradation [66, 73, 74]. The E6 protein can also interfere directly with other pro-apoptotic proteins such as BAK, FADD and pro-caspase 8 to further inhibit apoptosis [75, 76]. E6 alone appears to play a key role in sustaining continuous cell proliferation, as studies have shown that expression of E6, in the absence of E7, is sufficient to achieve immortalization of a number of normal human keratinocytes [74]. Other molecular targets reported to be modulated by E7 and E6 are illustrated in Figures 1.5 and 1.6.

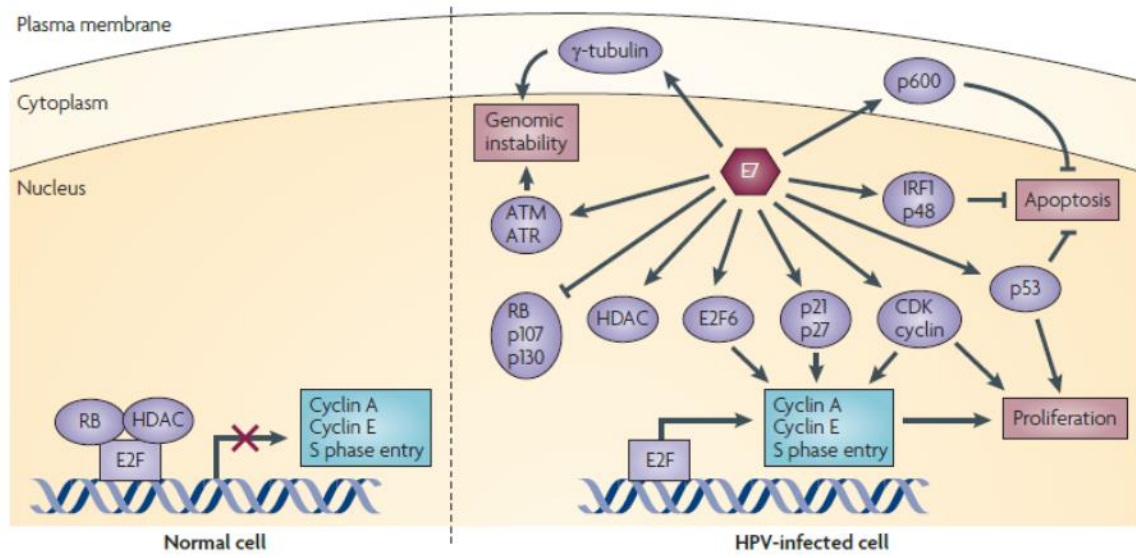


Figure 1.5: The high-risk human papillomavirus E7 oncoprotein modulates its host cellular process by interacting with multiple host cell proteins. E7 oncoprotein disrupts normal cell cycle control by inhibiting the retinoblastoma (Rb) protein family that results in aberrant activation of the E2F transcription factors and drives the cells into S phase. E7 can also deregulate cell cycle control by directly interacting with other cell cycle proteins, for instance it inhibits the cyclin-dependent kinase inhibitors ($p21^{WAF1}$ and $p27$), stimulates the cyclins, and activate the cyclin-dependant kinase 2 (CDK2). Through interaction with histones deacetylases (HDACs) and E2F6, E7 is also able to modulate gene expression. The interactions of E7 with a number of other cellular proteins lead to malignant transformation of the cell, for instance the increase in activity of CDK2 and interaction with γ -tubulin lead to aberrant centrosome synthesis and increases genomic instability; interactions with ATM-ATR (ataxia telangiectasia-mutated-ATM and RAD3-related DNA damage response) causes DNA damage and increases chromosomal instability; and the interactions with p600 prevents anoikis and permits anchorage-dependent growth. E7 also allows the infected cells to escape from host immune surveillance through interactions with the interferon (IFN) signalling proteins.

Figure adapted from Moody and Laimins, 2010

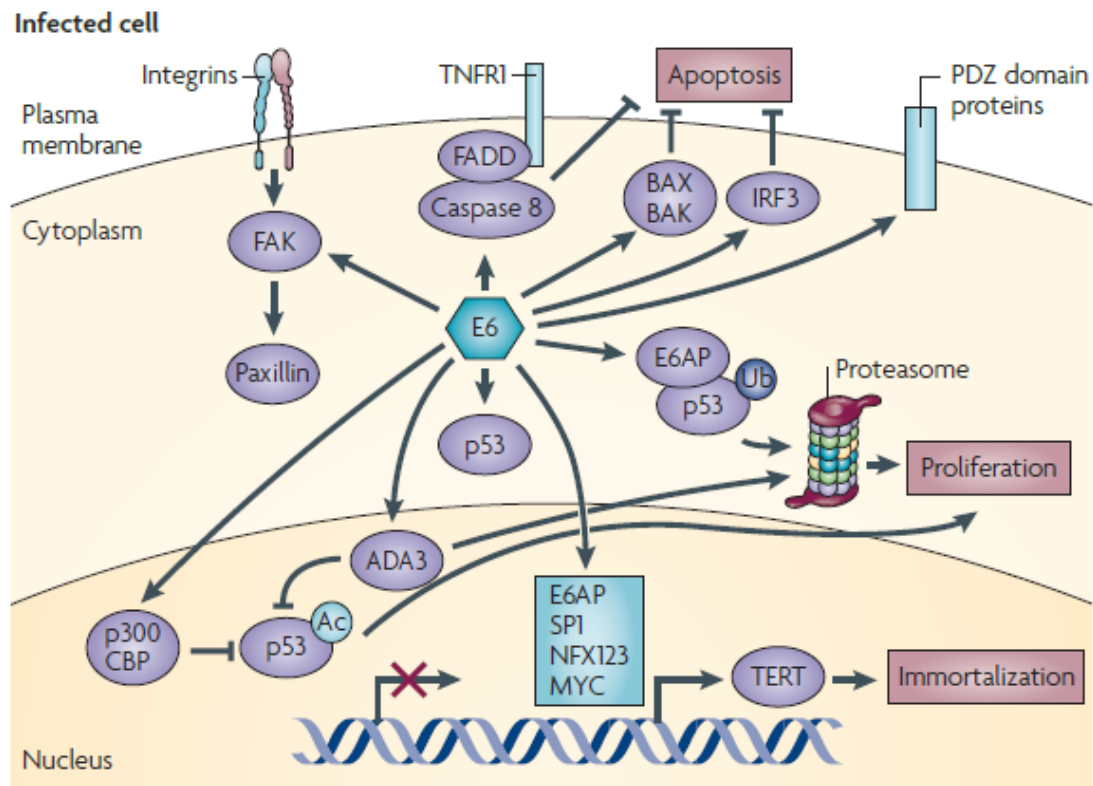


Figure 1.6: The high-risk human papillomavirus E6 oncprotein modulates its host cellular process by disrupting cellular signalling pathways. E6 inhibits p53 mediated growth arrest and apoptosis in a number of ways, it forms a trimeric complex with p53 and E6AP resulting in the degradation of p53 protein through the ubiquitin-proteasome pathways; it also inhibits the transcription of p53-responsive genes by interacting with the histones acetyltransferases p300, CREB binding protein and ADA3 that prevents acetylation of p53. E6 can also induce the degradation of the pro-apoptotic proteins BAX and BAK, and interrupt with the caspase 8, FADD and TNFR1 signalling pathways to inhibit apoptosis. E6 interactions with E6AP, SPI, NFX12 and MYC nuclear transcription factors prevent telomerase shortening and promote cell immortalisation. It promotes anchorage-dependent cell growth by interacting with the focal adhesion protein paxillin and the extracellular matrix protein fibulin. E6 also binds to and mediate the degradation of the PDZ domain proteins resulting in the loss of cell polarity and malignant transformation.

Figure adapted from Moody and Laimins, 2010

HPV-induced transformation was first described in cervical neoplasia [75]. In the cervix, the squamous columnar junction, a meeting point of the stratified non-keratinizing squamous epithelium from the ectocervix and the columnar epithelium from the endocervix, is susceptible to HPV infection and a site where more than 90% of cervical neoplasia arises. Persistent HR-HPV infection is a prerequisite for the initiation of dysplastic changes in the cervical epithelium. The progression from infected lesion to invasive disease is associated with the integration of the HPV genome into the host DNA. Loss or disruption of the E2 gene is accompanied by increased expression of the E6 and E7 oncogenes (see Figure 1.7) [77]. In early pre-invasive cervical dysplasia, cervical intraepithelial neoplasia (CIN) I and II, a relatively low level of E6 and E7 expression is detected when the virus is maintained in episomal form, but overexpression of these oncoproteins is often found in CIN III (high grade) and invasive disease [76]. Unlike cervical neoplasia, the underlying mechanism(s) of how HR-HPVs transform vulval squamous epithelium is less clear, as the vulva lacks a squamo-columnar junction. Moreover, the risk of malignant transformation of uVIN, the putative precursor lesion of viral induced VSCC, is significantly lower when compared to CIN. However, viral genome integration into host chromosomes has been documented in almost all cases of HPV-induced VSCC, indicating that the underlying mechanism of malignant transformation in VSCC, at least that of HPV-induced, is likely to be similar to that of cervical cancer [78]. Therefore, it is likely that the incidence of HPV-related VSCC in future will fall with the introduction of HPV vaccination programme.

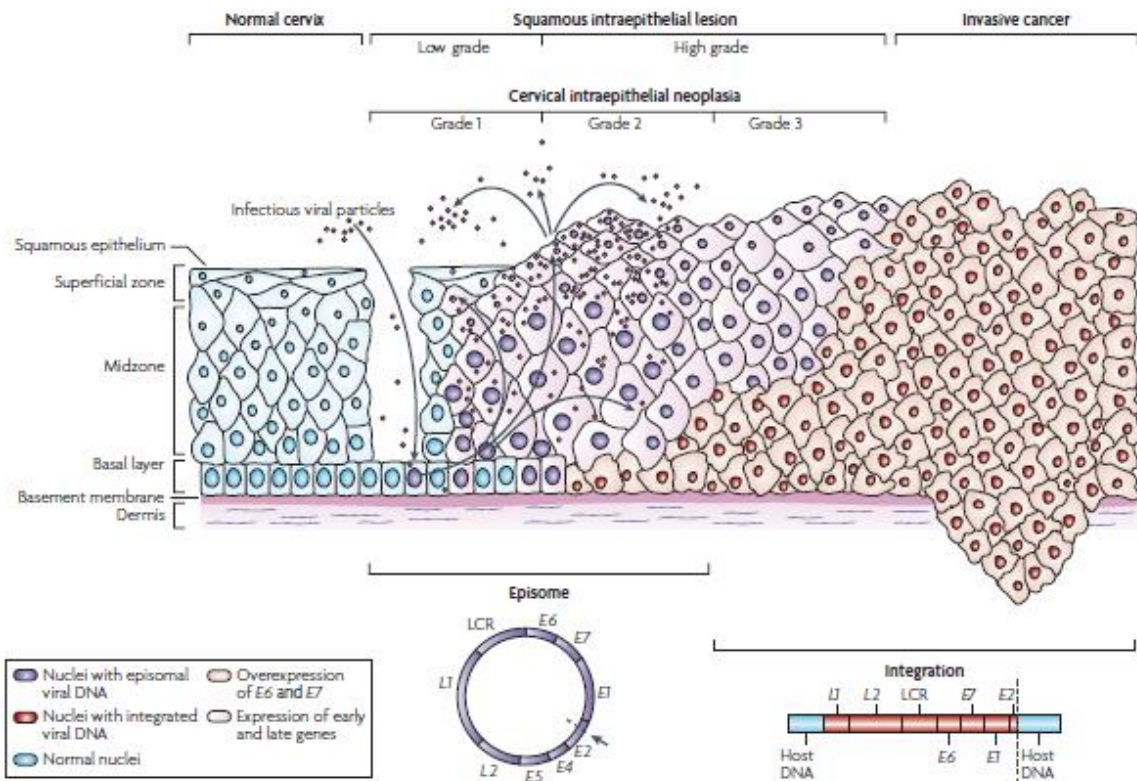


Figure 1.7: The stepwise progression of cervical neoplasia following persistent HPV infection with high-risk human papillomavirus (HR-HPV). HR-HPV is thought to gain access to the basal keratinocytes through micro wound(s) in the cervical epithelium. Following infection, the basal keratinocytes undergo mitosis to produce infected daughter cells (purple nuclei) and one of which will migrate to the suprabasal epithelium to undergo terminal differentiation. The early HPV genes E1, E2, E4, E5, E6 and E7, are responsible for episomal maintenance in the basal cell, and trigger vegetative reproduction when the keratinocytes enter the suprabasal layer. Together, E6 and E7 force the non-replicating suprabasal cell back into S phase which allow HPV genomes amplification as the cells continue to replicate. Expression of the late genes, L1 and L2, and E4 encapsidate the viral genomes to form virions ready for release in the upper epithelium. Low grade intraepithelial neoplasia (CIN I & II) support productive viral replication but not the high grade lesion or invasive disease as the virus is no longer able to replicate when its genomes are integrated into the host chromosomes (red nuclei). The process of integration often leads to the truncation of E2 gene, a negative regulator for E6/E7, and allows the overexpression of E6/E7, which drives mutagenesis and oncogenesis.

Figure adapted from Woodman *et al.*, 2007

1.5 HPV and Ubiquitination

As a small virus, HPV encodes a number of early proteins that have evolved to target or co-opt cellular proteins that function to modulate key cellular processes. As the HPV-encoded early proteins lack intrinsic enzymatic activity, modulation of cell pathways is achieved primarily through protein-protein interactions. In this regard, the ubiquitin system constitutes an attractive target for a number of viruses, given that post-translational modification of cellular proteins not only control the levels of their expression, but also their function and subcellular localization. Although HPV-encoded early and late proteins are themselves subject to regulation by the ubiquitin system, the E6 and E7 proteins are known to target key proteins within the ubiquitin system to influence virus survival and reproduction. By targeting cellular pathways with broad regulatory functions such as the ubiquitin pathway, the HPV early proteins can influence a plethora of biological processes that include cell cycle checkpoint control and differentiation.

The ubiquitin superfamily comprises a number of small proteins that are covalently attached to their protein substrates through a series of defined biochemical steps (Figure 1.8) [79]. Members of this family include ubiquitin (Ub) and a number of ubiquitin-like proteins such as SUMOs, ISG15, NEDD8, and FAT10, amongst others. While these covalent modifications can modulate intracellular localization and function (i.e. target specificity), poly-ubiquitination of proteins earmarks them for proteasome-mediated proteolysis.

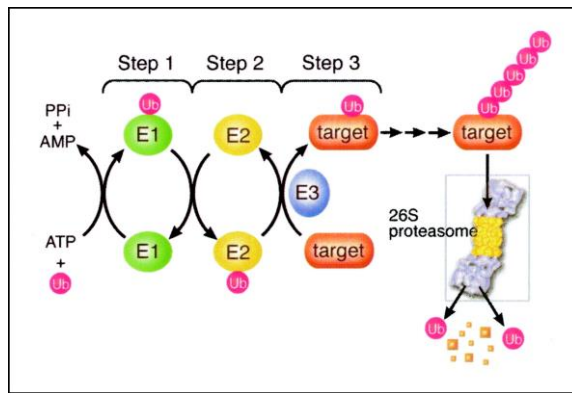


Figure 1.8: Key steps in the ubiquitination pathway.
E1, E2 and E3 are the activating, conjugating and ligase, respectively, that catalyse the transfer of ubiquitin molecules to target proteins.

Figure taken from Wilson, 2014

During the HPV life cycle, the level and temporality of early and late viral protein expression is tightly regulated. While this is achieved primarily at the level of transcription, post-translational modification plays an important role in the stability and half-life of the early proteins. The short half-life of the early proteins (E6 and E7) is due, in part, to post-translational modification. Proteasome inhibitor studies have shown that the E1, E2, E6 & E7 proteins are all subject to ubiquitin-mediated proteasomal degradation. Collectively, these studies show that the ubiquitin system is exploited by HPV to regulate levels of early and late proteins at distinct phases of the virus life cycle. In addition to ubiquitination, a number of viral proteins are subject to Sumoylation, a modification that alters protein function but does not lead to proteolysis. Given that cell regulates distinct aspects of the cell cycle and differentiation utilizes both ubiquitination and Sumoylation, it is not surprising that

HPV utilizes these post-translational modifications to regulate the expression of viral proteins.

1.5.1 The HPVE6 proteins

The HPV-encoded E6 proteins are short-lived proteins that are subject to proteasome-mediated proteolysis [71]. Interestingly, ubiquitination of E6 proteins is E6AP independent, indicating that E6AP is not the E3 ligase responsible for E6 ubiquitination. Although the true E3 ligase(s) for E6 remains unknown, proteomic studies have identified a number of possible candidates. These include HERC2, a putative HECT-domain type E3 ligase, associated with HPV 16E6 [80] and a HECT-domain E3 ligase, called EDD, which binds strongly to HPV 18E6 and weakly to type 16 and 11 E6 proteins [81]. However, their ability to ubiquitinate E6 has not been assayed *in vitro* or *in vivo* and, as such, they may associate with E6 to modify other substrates rather than E6 itself.

The E6 proteins constitute the best-known example of how a virus can modulate host cell gene expression programmes by usurping the ubiquitin-proteasome system. Binding of E6 to E6AP modulates its ligase specificity, allowing E6 to target a number of proteins for proteasome-mediated degradation (Figure 1.6) [66]. The fact that E6AP silencing yields similar effects to the silencing of E6 itself, indicates that the bulk of E6-associated effects on host cell gene expression rely on the activity of E6AP [82]. The ability of the HR-HPV E6 proteins to promote p53 degradation is essential for the transforming activity of these proteins [66, 73, 74]. The HR-HPV E6 proteins also target cellular PDZ proteins, many of which are involved in regulating cell-cell adhesion and

cell polarity [83]. An additional target of E6-E6AP is the pro-apoptotic protein Bak, a protein that is targeted by nearly all tested E6 proteins, Bak [66].

While proteomic approaches have demonstrated associations of various E6 proteins with other E3 ligases, including HERC2, EDD, and the Ccr4-Not complex, the significance of these associations is still unclear. There is also evidence that the E6 proteins can interact directly with various components of the 26S proteasome, with two recent reports describing associations between E6 from HPV16, 11 and 18, binding to the S2, S4, S6a and b, S7, S8, and S10 subunits *in vitro* [84]. The question of how these interactions affect proteasomal function, and/or degradation of E6 targets has not been fully explored, but it suggests that the utilization of the ubiquitin-proteasome system by E6 proteins is multi-faceted and complex.

1.5.2 *The HPVE7 Proteins*

The HR-HPV E7 proteins are incredibly labile, displaying half-lives of the order of 15 minutes. Like E6, proteasome inhibitor studies have revealed that E7 is degraded through the ubiquitin-mediated proteasome-dependent proteolysis. SOCS1, UbcH7 and Cullin 1 and Skp-2 containing E3 ligases have been shown to bind E7 and target it for ubiquitin-mediated degradation. However, the authentic E3 ligase complexes that ubiquitinate E7 still remains uncertain.

The primary target of the HR-HPV E7 proteins is pRb, which is degraded through the ubiquitin-proteasome pathway in an E7-dependent fashion. Interestingly, this activity does not require the authentic E3 ligase for pRB, MDM2 [85]. p130, an additional pRB family member that plays an important role in regulating keratinocyte growth, differentiation and senescence [86], is also degraded through the proteasome in an E7-

dependent fashion by both high and low risk alpha HPVs [87]. Again, the specific E3 ligase components involved are undetermined.

Like the HR-HPV E6 protein, HPV16E7 has been found to associate directly with components of the 26S proteasome, although, unlike E6, E7 has been shown to bind S4 [88]. However, the functional significance of this observation, like the E6- proteasome interactions remain unclear. Nonetheless, this ability to interact with a proteasomal component suggests a complex relationship between E7 and the ubiquitin-proteasome system.

In addition to ubiquitination of cellular targets, the HR-HPV E6 protein has been shown to influence “global” sumoylation, an effect that is likely to impact on keratinocyte differentiation [89, 90]. The E6-E6AP complex has been shown to bind the SUMO conjugating enzyme, Ubc9, and target it for ubiquitin-mediated degradation. This leads to a global change in the cellular sumoylation profile of keratinocytes [90], an effect that might contribute to the aberrant differentiation in the HR-HPV infected epithelium.

1.6 Stratified Squamous epithelium

Both the low and high-risk HPV's target the squamous epithelium, a highly specialised tissue that has evolved to perform an essential barrier function; preventing water loss; resisting mechanical stress; acting as a barrier to pathogens; and orchestrating immune responses. Although keratinocytes constitute the major cell type within the epidermis, dendritic cells, melanocytes and other immune cells are also present. Keratinocytes form an adhesive network of cells organised into multiple cell layers that are highly

polarised. Proliferation is limited to mitotically active cells within the basal layer. These are anchored to the underlying basal lamina, a highly specialised ECM, through hemidesmosomes and integrins, two classes of adhesion receptors that couple to the keratin intermediate filament and actin cytoskeleton, respectively. In response to intrinsic and extrinsic cues, basal keratinocytes down regulate these adhesion receptors and, as a consequence, become less adhesive to the basal lamina. Exit from the basal layer initiates the process of terminal differentiation. This step results in the loss of mitotic activity and profound metabolic and adhesive changes that culminate in the formation of inert cornified squames. Distinct phases of the maturation process have been defined, both morphologically and biochemically (Figure 1.9) [91]. Cells entering the spinous layer increase in size and assemble robust intercellular connections that include tight junctions, desmosomal and cadherin-based junctions whose expression is co-ordinated to create increasingly stronger intercellular contacts. Upon reaching the granular cell layer, cells flatten, assemble a water impermeable cross-linked envelope beneath the plasma membrane, and express numerous keratohyalin granules, which contain histidine and cysteine-rich proteins that induce bundling of the high molecular weight keratins. Finally, upon reaching the cornified layer, cells release lysosomal enzymes to degrade intracellular organelles that culminate in the production of an inert lipid and keratin-rich squame.

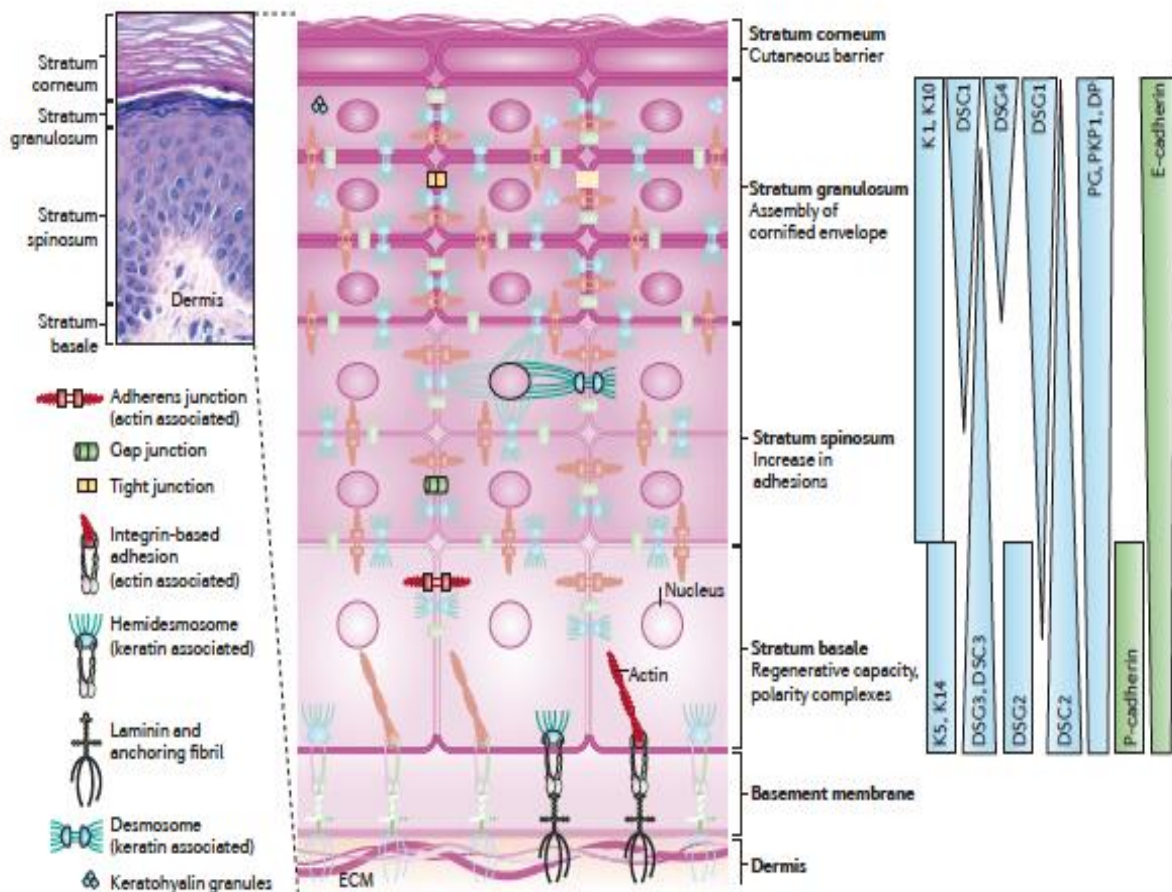


Figure 1.9: Organization of the epidermis. The epidermis is composed of morphologically distinct stratified layers that include: the basal, spinous, granular and cornified cell layers. The basal cell layer contains cells (stem/progenitor and TA-cells), which possess proliferative potential that give rise to differentiated cells. Basal cells are anchored to the basement membrane through hemidesmosomes and integrins. Cells within the spinous cell layer are committed to the differentiation process, and down-regulate integrins and hemidesmosomes but increase their expression of adherens junctions, tight junctions, desmosomes, and gap junctions. They also synthesize the high molecular weight keratins: K1/10. Cells within the granular layer generate a highly cross-linked proteinaceous “envelope” beneath the plasma membrane and produce large numbers of keratohyalin granules that contain proteins that assemble high molecular weight keratin proteins into large insoluble bundles. Cells in the cornified layer are metabolically dead squames that form a protective waterproof barrier.

Figure taken from Simpson *et al.*, 2011

1.6.1 Signals that regulate keratinocyte growth and differentiation

Cells residing within the basal cell layer are heterogenous in their physiology. In addition to stem/progenitor cells, populations of more committed transit-amplifying (TA)-cells exist. This population has a limited proliferative capacity, undergoing several rounds of cell division before commitment to the differentiation process. Many growth factors and soluble morphogens regulate the proliferation of both stem/progenitor and transit-amplifying (TA) populations. These include growth factors and morphogens such as Notch, Hedgehog (HH), Wnt, Epidermal growth factor (EGF), Keratinocyte growth factor (KGF), and transcription factors such as Δ Np63, mitogen-activated protein kinases (MAPKs), nuclear factor kappa-B (NF- κ B), CAAT/enhancer binding protein (C/EBP), Kruppel-like factor 4 (KLF4). In response to intrinsic and extrinsic factors, one of which involves Notch1 activation, TA-cells undergo asynchronous cell division, down-regulate their adhesion receptors and migrate out of the basal cell layer. Notch1-mediated down-regulation of the stem/progenitor cell maintenance protein, Δ Np63, is central to the commitment process, as Δ Np63 directly regulates expression of the integrins (e.g. α 3 β 1) and hemidesmosomal proteins (e.g. α 6 β 4), which are well-known determinants of epithelial integrity and maintain basal cell proliferation (see Figure 1.10) [92, 93].

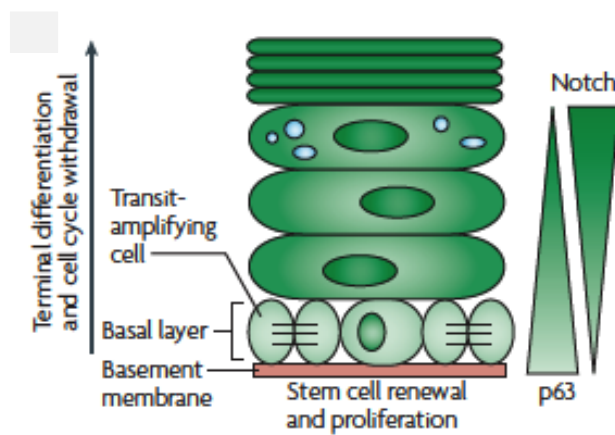


Figure 1.10: Cross-talk between Notch and Δ Np63 in the Stratified squamous epithelium. Reciprocal feedback between Notch and Δ Np63 regulates the balance between self-renewal and terminal differentiation in stem/progenitor and Transit amplifying (TA)-populations. Opposing gradients of Notch and Δ Np63 exist within the proliferative and differentiating cell layers, resulting, in part, through their reciprocal negative regulation. Down regulation of Δ Np63 by Notch plays a key role in the signal for terminal differentiation.

Figure adapted from Dotto *et al.*, 2009

1.7 Epigallocatechin-3-gallate (EGCG)

EGCG is one of the four most abundant bioactive polyphenols found in green tea extracts. The other polyphenols or catechins are Epicatechin, Epigallocatechin and Epicatechin-3-gallate (Figure 1.11). The function and structural differences between the four catechins are attributed to the number of hydroxyl groups present on the B ring and the galloyl moiety [94]. Of all the catechins, EGCG is the most studied flavonoid and its bioactivities have been investigated in a number of human diseases, including cancer. The presence of the galloyl moiety on the B ring of EGCG molecule allows it to interact with both organic and inorganic matter and influences a myriad of biomolecular pathways in the cells (Figure 1.12). Studies have shown that many of the cancer chemopreventative properties of EGCG are mediated through modulation of a number of different molecular pathways particularly those involved in signal transduction. To date, EGCG has been shown to modulate the JAK/STAT, MAPK, PI3K/AKT, Wnt and Notch signalling pathways; to downregulate telomerase expression, and stimulate expression of certain tumour suppressor genes (TSGs) and epigenetic modulators [DNA methyl transferase (DNMT) and Polycomb group of proteins] [95-100]. EGCG can exert its effects at both the transcriptional and translational levels.

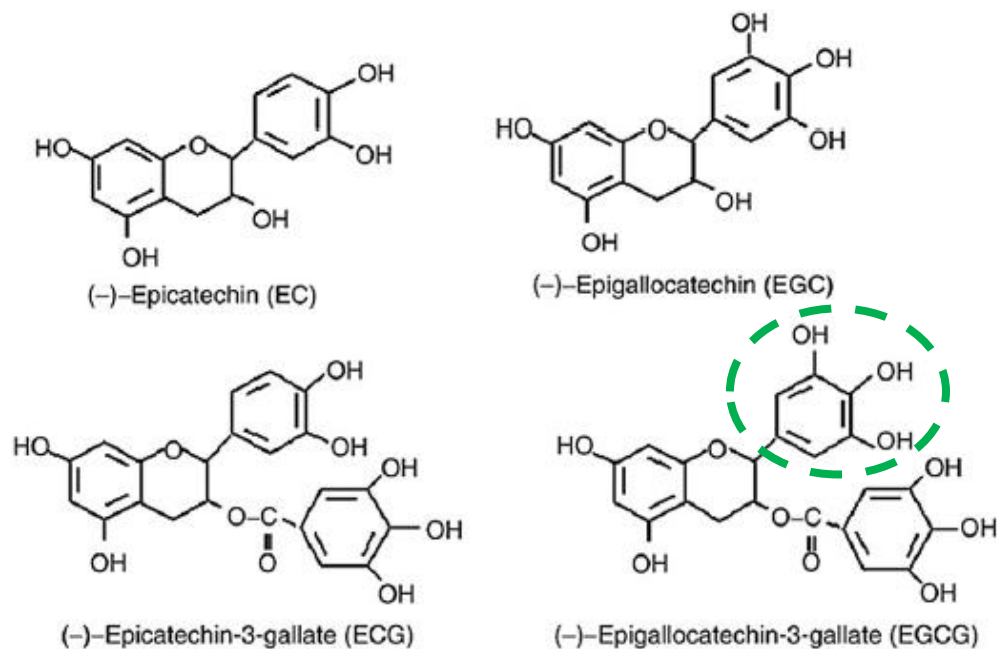


Figure 1.11: Among the catechins, EGCG is the most abundant and biologically active. The biological properties of EGCG are defined by the presence of the galloyl moiety of the B-ring (highlighted green circle), which allows it to form covalent bonds with multiple organic and inorganic molecules.

Figure adapted from Steinmann *et al*, 2013

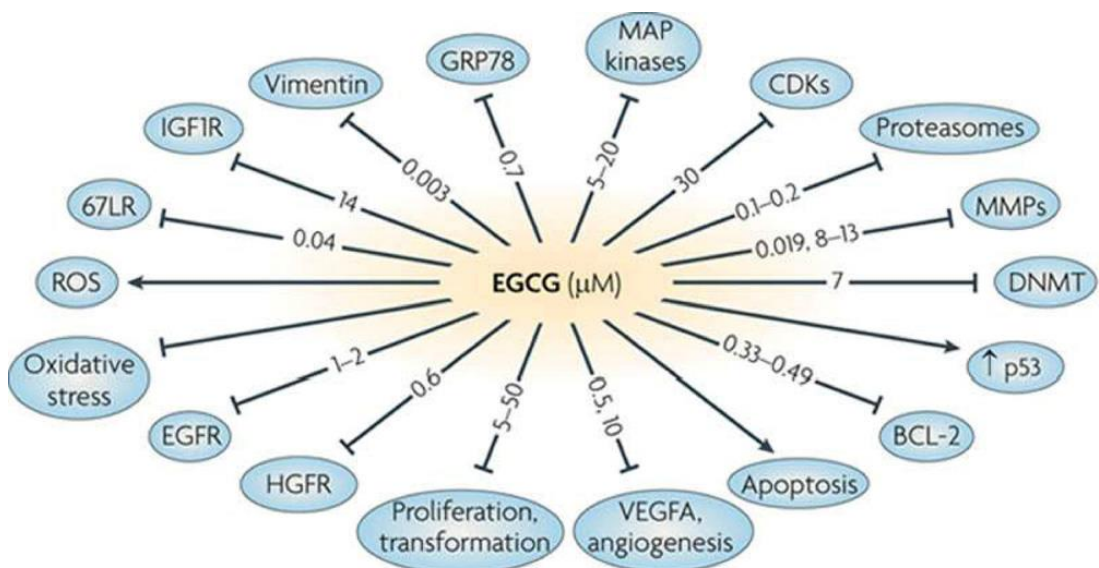


Figure 1.12: Potential molecular targets of EGCG for cancer prevention and treatment. These molecular targets were identified from various *in vitro* studies previously reported. The effective concentrations in IC₅₀, Ki (inhibition constant) or K_d (dissociation constant) are shown in μM ; the first value is derived from cell-free systems and the second is from cell lines experiments.

Figure adapted from Yang *et al.*, 2011

Recently, the NIH database in the US lists 86 clinical trials evaluating the use of EGCG, administered in various routes, for the treatment of a variety of diseases. One-third of these relate to some aspect of the prevention and treatment of pre-neoplastic and invasive diseases. A recent meta-analysis by Tzellos *et al.* has shown that topical application of EGCG to genital warts, a hyperproliferative disorder caused by low risk HPV infection, is effective in eradicating the lesions with a relatively low recurrence rate [52]. Also, the EGCG ointment is well tolerated by most patients, with minimal localised side effects such as skin irritation, which is reversed after treatment cessation.

Although the EGCG ointment has been licensed for the treatment of genital warts in most parts of Europe and US, except the UK, the underlying mechanism of action remains to be elucidated. Furthermore, the notion that EGCG could be used to treat genital warts was not based on experimental evidence, as no laboratory studies had been performed to evaluate if EGCG targets the HPV life cycle. Nevertheless, a range of anti-viral activities has been demonstrated in the laboratory, where EGCG has been shown to affect the growth of a diverse family of viruses such as Retroviridae, Orthomyxoviridae and Flaviviridae. It has also been shown to target a host of potential oncogenic viruses such as EBV, hepatitis B virus (HBV) and HIV by either inhibiting mechanisms of viral replication, gene expression or viral assembly [94]. A number of studies, using transformed cervical cancer cell lines, have shown that EGCG down-regulates transcription of the HPV16 and 18 viral oncogenes through an unknown mechanism [101]. This down-regulation was accompanied by upregulation of the TSGs, p53 and p21^{WAF1}. Whether upregulation of these TSGs is directly stimulated by EGCG or a consequence of E6 and E7 repression remains unclear, as EGCG can also directly stimulate the expression of p53 and p21^{WAF1} by modulating the expression of key epigenetic modulators such as HDAC, DMNTs and the Polycomb group (PcG) of proteins [97-99, 102].

A small number of studies have examined the effects of EGCG on the growth and differentiation of normal epidermal keratinocytes and carcinoma-derived cell lines *in vitro* and *in vivo*. Collectively, these studies show that EGCG promotes differentiation by inducing cell-cycle withdrawal and stimulating the expression of a range of differentiated-associated genes that include involucrin, transglutaminase type I,

keratin 1 (K1), filaggrin, and procaspase 14 [96, 103-105]. Mechanistically, this is achieved through effects on the nPKC, Ras, MEKK1, MEK3, p38δ-ERK1/2 signalling pathways, which modulate the ERK-MAPK and SAP/JNK signalling pathways to modulate expression of the c-Jun and c-Fos transcription factors, components of AP1 [105]. As discussed previously (Section 1.4), the HPV life cycle is intimately linked to keratinocyte differentiation. Thus, disruption of this process is also likely to influence the ability of the virus to undergo lytic replication.

1.8 Objectives

VSCC is a unique cancer as it can arise from HPV-dependent and HPV-independent routes. It is widely recognised that uVIN is a putative precursor lesion of HR-HPV-positive VSCC, and typically affects younger women. The incidence of HR-HPV-positive vulval neoplasia is increasing which is a reflection of the increase in the prevalence of HR-HPV infection. Unlike CIN, uVIN often causes debilitating symptoms and currently available treatments remained unsatisfactory, given that women often suffer from a recurrent disease. It is still unclear how HR-HPV causes VSCC as the progression rate of uVIN to cancer remains comparatively low when compared to CIN.

In the elderly population, VSCC is often found arising in the background of a chronic inflammatory condition, namely Lichen Sclerosus. Again, how LS gives rise to VSCC remained unclear as most women have indolent LS, which never progress to cancer. However, we lack the knowledge of how to separate indolent LS cases from those in danger of progression to VSCC, so most women with LS ended up being followed up

in a hospital for an extended period. Also, it remains unknown whether effective treatments can reduce the risk of development of genital squamous cell carcinoma or genital intraepithelial neoplasia from LS. Although there is a lack of well-defined precursor lesion linking LS to VSCC, dVIN is often widely regarded as the pre-neoplastic lesion for LS.

Topical application of Epigallocatechin-3-gallate (EGCG), a green tea polyphenol, has been shown to be a safe and effective treatment for genital warts. The use of this agent is now being explored in women with uVIN by our group in a phase II randomised control trial (EPIVIN). However, the mechanism of EGCG in the treatment of these associated proliferative disorders has yet to be defined.

Research carried out in this thesis was driven by the need to identify more effective medical treatments for women with uVIN and the need to reduce the risk of recurrent disease in those with VSCC. This need arises because surgical excision that continues to be the treatment most commonly offered to women with VIN does not guarantee a cure; one in three women will require further treatment within three years, and surgery can itself result in additional physical and psychosexual problems. One in four women with an invasive disease who are often elderly and have serious co-morbidity will have a recurrence of their disease within three years of primary surgery. In my thesis I have sought to address the following questions:

1. Using a well-characterized cohort of women with VSCC, identify which iso prognostic groups influence the risk of local recurrence, taking into account those that do not appear to have been considered in detail in earlier analyses of disease-free survival.

2. Using keratinocytes transfected with episomal form of HPV18, explore the biological effects of EGCG on the virus life cycle; their behavior in monolayer and three-dimensional organotypic raft culture; and the underlying mechanisms by which EGCG modulates expression of the E6 and E7 proteins.
3. Establish and characterize HR-HPV positive premalignant keratinocyte clones from authentic uVIN biopsies and evaluate the effects of EGCG on growth, differentiation and apoptosis, as well as the impact on virus behavior.

Chapter 2:

Materials & Methods

2.1 Part 1: Data collection and analysis of retrospective cohort study

2.1.1 Study population

The study population includes 201 women who were first diagnosed with squamous cell carcinoma of the vulva between 2000 and 2008 in the Pan Birmingham Gynaecological Cancer Centre.

2.1.1.1 Identification of study population

The study population was identified from clinical records held on the Pan Birmingham Gynaecological Cancer Centre database.

2.1.2 Baseline clinicopathological variables

Information on the following variables was abstracted: age, smoking behaviour, the presence of unifocal or multifocal disease, tumour differentiation, the involvement of lymphovascular spaces, the presence of perineural invasion, disease stage, groin lymph node status and the presence of concomitant Lichen Sclerosus, usual type VIN or differentiated VIN.

2.1.2.1 Definition of baseline clinic-pathological variables

- i. *Age.* The patients' age was that recorded at the time of surgery.
- ii. *Smoking behaviour.* Smoking history was abstracted from the patients' clinical records. Women were categorized as a smoker if they were still smoking at the time of the referral that led to the diagnosis of VSCC. They were considered to be an ex-smoker if they had stopped smoking prior to

this visit. When the clinical record was silent on smoking behaviour, the patients smoking status was considered to be undetermined.

- iii. *The presence of unifocal or multifocal disease.* The number of disease foci and size of the tumour at the time of primary surgery were abstracted from the operation record; and for those patients who did not have surgery, from the assessment recorded in the out-patient notes.
- iv. *Tumour differentiation.* The degree of tumour differentiation was that recorded in the histopathology report as well, moderate or poor. The degree of tumour differentiation was recorded as undetermined for those women who did not have histological sampling and for those in whom the histopathology report was silent.
- v. *Involvement of lymphovascular space.* The presence or absence of tumour spread to the lymphovascular space was abstracted from the histopathology report. Lymphovascular space involvement was recorded as present or absent when the pathologist had explicitly commented on this feature, and undetermined when the histopathology report was silent.
- vi. *The presence of perineural invasion.* The presence or absence of perineural invasion was abstracted from the histopathology report. Perineural invasion was recorded as present or absent when the pathologist had explicitly commented on this feature, and undetermined when the histopathology report was silent.
- vii. *The presence of concomitant Lichen Sclerosus, usual type VIN or differentiated VIN.* The presence of Lichen Sclerosus (LS), uVIN and dVIN adjacent to the tumour was abstracted from the histopathology report. LS, uVIN and

dVIN was recorded as present when the pathologist had explicitly commented on these features. When the pathologist did not comment on these features, it was assumed that they were not present.

- viii. *Disease stage.* Women were staged according to the FIGO 1995 staging criteria and the operation record. For those women who did not have surgery, their stage was assigned based on the findings at out-patient assessment. When this information was not available, stage of disease was considered to be undetermined.
- ix. *Groin node status.* The presence or absence of tumour in the groin was abstracted from the histopathology report. When no explicit comment was made on groin node status, this variable was considered to be as undetermined. For those patients who did not have groin node surgery, this information was abstracted from the clinical information recorded in the out-patient notes.

2.1.3 Treatment variables

Treatment variables were defined, and information on the variables extracted as follow:

2.1.3.1 Surgery

Details of the surgical procedure were extracted from the operation records. Operations were classified according to the summary provided by the operating surgeon. In every case, the accuracy of the surgical description was verified by a detailed reading of the operation record and by an evaluation of the histology report.

In no case, it was necessary to revise the operation summary provided by the surgeon.

The following procedures were undertaken during the study period:

- i. Simple wide local excision: this refers to the removal of the skin that covers part or all of the vulva.
- ii. Radical WLE or hemi-vulvectomy: this refers to the removal of not just the skin but also the deep tissue from part of or one side of the vulva.
- iii. Total radical vulvectomy: this refers to the removal of the skin and deep tissue of the entire vulva down to the fascia over the bone and muscle.
- iv. Sentinel groin node biopsy referred to the removal of one or a group of groin nodes which the cancer is more likely to spread first.
- v. Groin lymphadenectomy referred to the removal of all the lymphatic in the groin.

2.1.3.2 Chemo-radiotherapy

Women received chemo-radiation in four circumstances:

- i. primary treatment
- ii. neo-adjuvant treatment
- iii. adjuvant treatment
- iv. palliative treatment

2.1.4 Outcome variables

Three outcome variables were measured:

- i. time to local recurrence

ii. time to nodal recurrence

iii. disease-specific survival

2.1.4.1 Time to local recurrence

Information of local recurrence was extracted from clinic records. Time to recurrence was measured from the date of primary treatment to the date of the clinic visit when the diagnosis was made based on either histological confirmation of the presence of invasive disease or recurrence clinically diagnosed or clinically unambiguous evidence of disease progression.

2.1.4.2 Time to nodal recurrence

Information on nodal recurrence was extracted from clinical records. Time to nodal recurrence was measured from the date of the primary treatment to the date of the clinic visit when the diagnosis was made based on either histological/radiological confirmation of the presence of nodal disease or clinically unambiguous evidence of disease progression.

2.1.4.3 Survival

The census date for this study was 31st December 2012. The vital status of all members of the cohort at this time was established in the following ways. If the date of death had not been recorded in the hospital notes or if they had not been seen in the clinic within six months of the census date, the following steps were taken:

- The hospice was contacted when the hospital notes indicated that such a referral had been made.

- Sandwell and City hospital notes/electronic database were interrogated for recent in-patient or out-patient visit to these hospitals for a reason unrelated to vulval neoplasia.
- Patients were contacted by phone.
- The patient's general practitioner was contacted.
- When the patient was transferred to a new general practitioner, the new general practitioner was contacted.
- Records of the remaining patients with uncertain vital status were matched with those held by the West Midlands Cancer Registry. The registry routinely received notification of death occurring in residence of the West Midlands region who have been registered with cancer.

2.1.4.4 Anniversary date

Survival was measured from the date at which primary surgery was performed and in those patients not treated surgically, the date of first histological confirmation of disease. For those patients without histological confirmation of disease the anniversary date was that when the tumour was first clinically diagnosed at the Pan Birmingham Gynaecological Cancer Centre.

2.1.5 Statistical analysis of the cohort

Statistical analysis was performed with the help of Mr Richard Fox, Senior Biostatistician at Institute of Cancer and Genomic Sciences, University of Birmingham. Stata Version 12.1 was used for all analyses. The Chi-square test and Wilcoxon two sample test were used to examine if the categorical and continuous clinico-pathological

variables, respectively, were inter-related to each other. Kaplan-Meier method was used to estimate survival rates across clinico-pathological variables for local recurrence (including local relapse and second field tumour), groin node recurrence, overall survival and disease-specific survival outcome measures.

For each of the time-to-event measures of interest listed above, associations between hazard, or risk of the outcome, and different clinico-pathological variables were assessed using univariate Cox proportional hazard models to estimate hazard ratios with 95% confidence intervals. Then, using a manual forward variable selection method with multivariable Cox models, estimates were adjusted for other significant predictors. The number of predictors entered into the models was limited by the number of events observed, with roughly 4 events required per degree of freedom. All calculated P values were 2-sided and P values less than 0.05 were considered statistically significant.

2.2 Part 2: Laboratory Techniques

2.2.1 *Tissue culture*

2.2.1.1 *Cell lines and reagents*

Information about the cell lines and their culture media are listed in Table 2.1. The cell lines were grown in tissue culture flasks (Corning) or 100mm tissue culture dishes (Falcon) and incubated at 37°C in a humidified atmosphere containing 5% CO₂. Cells were passaged either weekly or biweekly, depending on their growth rate.

2.2.1.2 3T3 J2 cells

3T3 J2 cells were cultivated to provide a supportive feeder layer to HFK-HPV18 and primary keratinocytes. 3T3 J2 cells were routinely maintained in DMEM (Table 2.1) and harvested when the cells were 80% confluent. Cells were then counted and suspended in E-media, and irradiated with 50Gy using a Caesium-¹³⁷ gamma source. Irradiated cells were seeded at a density of 2×10^6 /10cm petri dish, topped up with E-medium and allowed to settle for at least 6 hours or overnight before $1-2 \times 10^5$ keratinocytes were plated. Live 3T3 J2 cells were maintained to no more than 25 passage and unused irradiated cells were kept at 4°C for up to 5 days.

2.2.1.3 Keratinocyte culture

Keratinocytes (HFK-HPV18 and primary uVIN cultures) were seeded at a density of 2×10^5 cells/10cm plate containing 2×10^6 lethally irradiated 3T3 J2 feeder cells. Keratinocytes were cultured in their respective medium, which was refreshed every 2 to 3 days. Keratinocytes were harvested or passaged when cell density reached 80% confluence.

2.2.1.4 Cryopreservation of cell lines

Cell lines or primary keratinocytes marked for long-term storage were preserved in liquid nitrogen or an -80°C freezer. To prepare cells for cryopreservation, cells were harvested at 80% confluence, pelleted and suspended in freezing medium consisting of 50% growth medium, 40% FBS and 10% v/v DMSO (Sigma-Aldrich, UK). Cells were transferred to cryovials, at a density of $1-2 \times 10^6$ cells/ml, and allowed to cool to below -80°C in a Cryo Freezing container (Nalgene®MrFrosty).

2.2.1.5 Retrieval of frozen cells

To retrieve frozen cells, the cryovial was rapidly warmed until completely thawed, and the contents transferred to a sterile 30ml universal tube (Sterilin, UK). Warmed growth medium was added drop-wise, and the cell suspension seeded onto tissue culture dishes or tissue culture flasks at the desired density.

Table 2.1: Information on the cell lines and their respective culture media used for experiments in my thesis

Cell lines	Source	Origin	Tissue culture media and supplements
A431	Gifted by Dr Elena Odintsova from School of Cancer Sciences, University of Birmingham	Derived from vulval epidermal carcinoma of a 85-year old women	Dulbecco's Modified Eagle's Medium (DMEM) (Sigma Aldrich) supplemented with 10% v/v fetal bovine serum (FBS), 100U/ml penicillin, 100mg/l streptomycin and 4mM L-glutamine
HeLa	Gifted by Dr Sally Roberts from School of Cancer Sciences, University of Birmingham	Derived from cervical carcinoma of a 31-year old female; contains integrated form of HPV 18 genomes	DMEM (Sigma Aldrich) supplemented with 10% v/v fetal bovine serum (FBS), 100U/ml penicillin, 100mg/l streptomycin and 4mM L-glutamine
HFK-HPV18		Derived from infant foreskin keratinocytes and transfected with episomal form of HPV 18	E-media: DMEM 60% v/v (Gibco, UK), Ham's F12 32% v/v (Gibco, UK), PenStrep 10,000 U/mL 2% v/v (Gibco, UK), hydrocortisone 0.1% v/v (Sigma), HyClone Defined FBS 10% v/v (Fisher Scientific), mouse epidermal growth factor (EGF) 5ng/ml (BD), L-glutamine 2mM (Gibco, UK), cholera toxin A

			0.1% v/v (Sigma Aldrich), insulin 0.2% v/v (Sigma Aldrich), transferrin 0.2% v/v (Sigma Alrich)), tri-iodo-IL-thyronine T3 4 nM (Sigma Aldrich) and adenine 36 µM (Sigma Aldrich)
3T3-J2		Mouse embryonic fibroblast cell line	DMEM, HEPES modified, (Sigma-Aldrich, UK) supplemented with 10% v/v new born calf serum, 4mM L-glutamine and 100U/ml penicillin and 100mg/l streptomycin
HEK 293	Gifted by Dr E Nagy School of Cancer Sciences, University of Birmingham	Human embryonic kidney cell line	RPMI1640 media (Sigma Aldrich) containing 5% v/v foetal calf serum (FCS), 100U/ml penicillin, 100mg/l streptomycin
VIN cl.11	Generated as part of this study	Primary premalignant keratinocyte clone isolated from a uVIN biopsy	1:1 RPMI 1640 media and Ham's F12 nutrient mixture media containing 5% v/v foetal calf serum (FCS), 0.4µg/ml hydrocortisone, 10ng/ml EGF, 100U/ml penicillin, 100mg/l streptomycin

2.2.2 Drug treatment of cells in monolayer cultures

To treat keratinocytes, cells were first seeded at desire density onto a monolayer of feeder cells and allowed to adhere and form multiple colonies. Feeder cells were selectively removed by using 0.05M EDTA solution (Sigma-Aldrich, UK) and further PBS (phosphate buffer saline) washes. Fresh medium was added before the desired concentration of drug was added to treat keratinocytes for the desired length of time. Drugs used for all the experiments in this thesis were bought and prepared as follow:

- i. EGCG >99% purity was purchased from Tocris, UK Bioscience and was dissolved in sterile distilled water.
- ii. (S) MG-132 was purchased from Cayman Chemical and was dissolved in DMSO (Sigma-Aldrich, UK).
- iii. Cisplatin was purchased from BD Biosciences (UK).

2.2.3 Harvesting of keratinocytes

Keratinocytes cultured in monolayer in petri dishes were harvested by first incubating the cells in trypsin solution (TrypLE Express, Invitrogen, UK) for 10-15mins in humidified incubator. The petri dishes were then gently agitated to detach the keratinocytes, the enzymatic activity of trypsin was neutralised by adding cell culture medium, cells were collected in sterile centrifugation tubes (Corning) and pelleted by centrifugation at 1000rpm for 10mins. Cell pellets were washed with PBS, transferred to 1.5ml Eppendorf tubes and pelleted by centrifugation at 4°C at 1000rpm for 10mins. Supernatant was aspirated off leaving behind the cell pellets which were stored at -80°C. For keratinocytes that were cultured on a monolayer of feeder cells, the feeder

layer was removed by selective washing with a solution of 0.05M EDTA and further PBS washes until all the feeder cells were completely removed.

2.2.4 Cell proliferation, viability and apoptosis

2.2.4.1 Cell proliferation and viability assay

To measure viability and proliferation, 3000 cells/well of HFK-HPV18 or primary keratinocytes were seeded onto a monolayer of lethally irradiated 3T3 J2 feeder cells (1×10^4 cells/well) in a 96-well plate in triplicate. A431 cells were used as a positive control for the assay, and 3000 cells/well were seeded into the same 96-well plate, without any feeder cells, in triplicate. Cells were allowed to establish overnight (A431) or 48 hours (keratinocytes) before treating with EGCG (Tocris, UK) at 0, 20, 40, 60, 80 and 100 μ M for 72 hours. Medium and EGCG were refreshed every 48 hours. Cell proliferation was assessed using 5-bromo-2'-deoxyuridine (BrdU) ELISA assay kit (colorimetric immunoassay, Roche) according to the manufacturer's protocol. In brief, cells were incubated with BrdU for 2 hours so that the synthetic thymidine analogue can be taken-up and incorporated into the DNA of proliferating cells. The incorporated BrdU can then be detected using anti-BrdU antibody and the immune complexes were then detected with the subsequent substrate reaction that gave rise to a colour gradient depending on the number of cells incorporated BrdU. Colorimetric absorbance wavelength was read at 405nm at 0.1s using the Wallac Victor2 plate reader. The reading obtained was compared against control (no treatment) and the results were expressed as a ratio relative to control.

2.2.4.2 Detection of apoptosis (TUNEL assay)

Keratinocytes were seeded at a density of 5×10^4 onto monolayer feeder cells (2.5×10^5) grown on sterile 22x22mm cover slips (Leica Biosystems, UK). Cells were left for 48 hours, and feeder cells were removed by selective washing with a solution of 0.05M EDTA and further PBS washes. Cell medium was refreshed, and cells were treated with either 0, 50 or 100 μM EGCG for 72 hours or 25 μM Cisplatin for 24 hours as a positive control. The presence of DNA fragmentation, a hallmark of apoptosis, was detected using DeadEnd™ Colorimetric TUNEL (Promega) assay according to manufacturer's protocol. Cells were mounted onto a microscope slide with Vectashield containing DAPI (Vector Laboratory) and visualized on a Nikon Eclipse E600 microscope. Images were captured using a Leica DC200 camera and software. The proportion of apoptotic cells (TUNEL positive) was counted against the non-apoptotic cells. The experiment was repeated twice more, and final results were expressed as an average of three experiments. Unpaired Student t-test was used to determine the level of significance for the difference in the proportion of apoptotic cells in drug-treated and untreated cells. The difference was considered significant if $P < 0.005$.

2.2.5 Soft agarose growth assays

Soft agarose colony formation assays were performed as previously described [106]. Briefly, actively growing cells were recovered by trypsinisation, and single cells reconstituted into complete growth medium supplemented with 0.3% low melting point (LMP) agarose (Gibco, UK). This suspension was overlaid onto a pre-set 0.6% LMP agarose base, at a density of 5×10^3 cells per well in 6-well plates. Colony

formation was determined after three weeks and photographs taken on an inverted Nikon microscope at x20 magnification.

2.2.6 *Immunohistochemistry (IHC)*

An Immunohistochemical heat-induced epitope retrieval (HIER) technique was used to stain Formalin-fixed, paraffin-embedded (FFPE) samples. 5 μ m raft sections were incubated for 5 minutes in Histo-ClearTM (National Diagnostics, UK), to clear the paraffin. Following dehydration for 15 minutes in 100% ethanol (IMS), slides were then rinsed three times in water, incubated for 10 minutes in 0.3% (v/v) hydrogen peroxide, and washed three times in water again. The sections were immersed overnight in EDTA buffer (1 mM EDTA-NaOH pH 8, 0.1% v/v Tween) heated to 65°C and continually agitated with a stirrer.

Retrieved raft sections were blocked in 20% v/v heat-inactivated goat serum (HINGS) in PBS, for one hr at room temperature. All incubations took place in a humidified chamber, to prevent evaporation. Primary antibodies were diluted in blocking buffer, applied to raft sections and incubated overnight at 4°C. Excess antibody was removed by washing slides in agitated PBS for 10 min, three times. The appropriate secondary fluorophore-conjugated antibody (Molecular probes®, Life Technologies), made up in the same blocking buffer, was applied to each slide, incubated for an hour at 37°C and washed in agitated PBS as before. Finally, sections were incubated in wash buffer containing 1 μ l of 4',6-diamidino-2-phenylindole (DAPI, Sigma-Aldrich, UK) to stain cell nuclei. Slides were mounted onto coverslips in 80% (v/v) glycerol in PBS containing 2% 4-Diazabicyclo-2,2,2-octane (DABCO, Sigma-Aldrich, UK) and

visualized on a Nikon Eclipse E600 microscope (Nikon, USA). Images were captured using a Leica DC200 camera and software. Slides were stored at -20°C.

2.2.7 Karyotyping

Chromosome analysis was performed on an early passage culture of VIN cl.11 at the West Midlands Regional Genetics Laboratory, Birmingham Women's NHS Trust. Ten metaphase spreads from actively growing cell cultures were examined by G-band chromosome analysis. A detailed examination of the karyotypes was performed by Dr Sally Jeffries (Principal Clinical Scientist at the West Midlands Regional Genetics Laboratory).

2.2.8 Molecular Biology techniques:

2.2.8.1 Quantitative mRNA analysis of E6/E7 transcript using real-time PCR

HFK-HPV18 keratinocytes were seeded onto monolayer feeder cells (2×10^6) at a density of 2×10^5 in 10cm petri dishes. Keratinocytes were left to adhere, form colonies and grow to 60% confluent before feeder cells were removed by selective washing with a solution of 0.05M EDTA and PBS. Keratinocytes were then treated with 0, 50 and 100 μ M EGCG for 3 or 6 days, and cells were then harvested with trypsin solution (TrypLE Express, Invitrogen, UK) and pelleted. Total RNA was extracted from cells using the RNeasy mini kit (Qiagen) and complementary DNA (cDNA) was synthesized through reverse transcription using QuantiTect reverse transcription kit (Qiagen), both according to manufacturer's protocols. Relative quantification of HPV 18 E6/E7 was obtained using FastStart PCR Master master mix (Roche Diagnostics, UK) and primers: forward primer (5'-AGAGGCCAGTGCCATTCGT-3'), reverse primer (5'-

GTTTCTCTGCGTCGTTGGAGT-3'); and probe (5'-TCCTGTCGCTGGTTGCAGC-3'), purchased from Eurofins MWG operon and designed by Lindh et al 2007 [107]. HPV 18 E6/E7 transcript was amplified by real-time PCR with ABI 7700 Sequence Detection System (Applied Biosystems). PCR conditions were: initial enzyme activation step (50°C/2 min), denaturation step at (95°C/10 min), followed by 40 cycles of denaturation (95°C/15 sec) and annealing/extension step (60°C/1 min). Expression levels were normalised to levels of endogenous beta-2 microglobulin gene in samples (Applied Biosystems). Data was analysed using the relative $2\Delta\Delta CT$ method using 7500 SDS software (Applied Biosystems). All experiments were repeated twice more.

2.2.8.2 Western blotting analysis

Analysis of protein expression was performed using Western blot. Cell pellets were lysed in RIPA buffer supplemented with sodium vanadate and 25x complete protease inhibitor (Roche), sonicated at 40Hz for 10s with a microson ultrasonic cell disrupter (Misonix). The protein lysates were then centrifuged at 13,000rpm for 15minutes in 4°C, and the precipitates were removed and proteins (supernatant) were quantified with Bradford assay (Bio-rad). 30 μ g of protein and protein ladder (PageRuler Plus Prestained protein ladder, Thermo scientific) were electrophoresed onto 8-12% Tris-glycine gels and transferred onto Hydronbond nitrocellulose membranes (VWR). Membranes were blocked in TBS-T containing either 5% non-fat dry milk or 5% BSA (Sigma-Aldrich, UK) for 1 hour at room temperature. Membranes were then incubated with antibodies (see Table 2.2) at 4°C overnight followed by secondary anti-mouse or anti-rabbit antibodies. Protein bands were visualized with Fusion FX System (Vilber Lourmat) using SuperSignal West Dura Chemiluminescent Substrate (Thermo

Scientific). Equal protein loading was verified using anti- β -actin antibody. The density of individual protein bands on the nitrocellulose membranes were quantified using the ImageJ 1.48v software; the value of each target protein was normalised to the respective density of the “housekeeping” protein (β -actin or GAPDH).

Table 2.2: Information on the list of antibodies and their dilutions used for experiments in this thesis.

Antibody	1° or 2°	Manufacturer	Catalogue code	Species	Dilutions
Anti-HA	1°	Abcam	Ab9110	Rabbit	WB 1:2000
Anti-His	1°	Milipore	05-531	Mouse	WB 1:1000
β-actin	1°	Sigma-Aldrich, UK	A5316	Mouse	WB 1:1000
BMI-1	1°	Santa-Cruz	SC-10745	Rabbit	WB 1:1000
					IHC 1:100
DNMT1	1°	Abcam	Ab16632	Rabbit	WB 1:1000
DNMT3B	1°	Active Motive	39207	Mouse	WB 1:1000
ΔNp63	1°	Santa-Cruz	SC-8431	Mouse	IHC 1:200
HΠξ18 E4	1°	Gift from Dr Sally Roberts	n/a	Mouse	IHC 1:5
E6	1°	Santa-Cruz	SC-365089	Mouse	WB 1:100
E7	1°	Abcam	Ab100953	Mouse	WB 1:1000
EZH2	1°	Cell Signalling	3147	Mouse	WB 1:1000
FLAG M2	1°	Sigma-Aldrich, UK	F3165	Mouse	WB 1:500
GAPDH	1°	Santa-Cruz	SC-32233	Mouse	WB 1:1000
Involucrin	1°	Sigma	SY5	Mouse	WB 1:200 IHC 1:100
K1/K10	1°	Sigma-Aldrich, UK	8.60	Mouse	IHC 1:100
Ki67	1°	Dako	MIB-1	Mouse	IHC 1:100
MCM7	1°	Sigma-Aldrich, UK	17931	Mouse	WB 1:2000 IHC 1:200
Mono- and polyubiquitinated (HRP conjugate)	1°	Enzo	BML-PW0150-0025	Mouse	WB 1:1000

p16INK4a	1°	Abcam	Ab7962	Mouse	WB 1:200 IHC 1:50
p21WAF1	1°	Santa-Cruz	SC-397	Rabbit	WB 1:100 IHC 1:100
p53	1°	Hybridoma gifted by Dr Roger Grand	n/a	Mouse	WB 1:100 IHC 1:100
pRb	1°	Cell Signalling	9309S	Mouse	WB 1:1000 IHC 1:100
Anti-mouse	2°	Dako	P0447	Goat	WB 1:1000
Anti-rabbit	2°	Dako	P0448	Goat	WB 1:1000

2.2.9 Cell cycle analysis

To perform cell cycle analysis, cells were first harvested and pelleted according to section 2.2.3 (harvesting of cell section) with the exception that the centrifugation speed was reduced to 1000rpm. Iced cold 70% ethanol was then added drop-wise into cell pellet with a continuous vortex to prevent them from clumping together. Cells were then left to fix in ethanol for at least 6 hours at 4°C and then pelleted by centrifugation at 1000rpm for 10mins and then washed twice with PBS. After the second wash, the cell pellet was suspended in 500µl of PBS, 5µl of 10µM proteinase K (Sigma-Aldrich, UK) and 25µl/ml Propidium Iodide (PI) (Sigma-Aldrich, UK) for at least 6 hours at 4°C. Cells were then subjected to flow cytometric analysis using Cyans ADP analyser with 488nm laser (Beckman Coulter) and the data collected were analysed with FlowJo v.10 software to build cell-cycle profiles.

2.2.10 Immunoprecipitation of HPV18 E6 proteins

2.2.10.1 Introduction

Figure 2.1 shows a summary of the steps involved in performing the HPV18 E6 immunoprecipitation or “pull down”. The pCA.18E6 plasmid, containing an amino-terminal FLAG and tandem (2x) HA epitope tagged version of HPV18 E6 (see Figure 2.2) was used in the ubiquitination experiments [69]. This plasmid was a gift from Professor Lawrence Banks (International Centre for Genetic Engineering and Biotechnology, Trieste, Italy).

2.2.10.2 Bacterial transformation

An aliquot (10 μ l) of competent *E. coli* (DH5 α) (New England Biolabs) was mixed with 2 μ l of ice-cold ligation product and, after a quick vortex, incubated for 30 minutes on ice. To facilitate DNA uptake, bacterial cells were incubated at 42°C for 30 seconds in a waterbath and chilled immediately for 2 minutes on ice. The bacterial cells were rescued with 200 μ l LB medium and shaken in an incubator set at 37°C for 30 min at 120rpm. Transformed cells were selected on LB agarose plates containing 100 μ g/ml ampicillin.

2.2.10.3 Production of plasmid DNA

Individual clones were taken from the petridish and transferred to a 1.5ml Eppendorf tube containing 1ml of LB medium and 100 μ g/ml ampicillin. The culture was incubated in a shaking incubator (approximately 120rpm) for 18-24 hours at 37°C. The bacteria were pelleted by centrifugation at 13,000 rpm for 10 seconds, and the

supernatant discarded. Plasmid purification was performed with the Qiagen Plasmid Miniprep Kit® according to the manufacturer's instructions. Bacterial clones containing the desired plasmid constructs (verified by gel electrophoresis and sequencing) were grown in 250ml LB broth containing ampicillin and plasmid purification was performed with Qiagen Plasmid Maxiprep Kit® according to manufacturer's protocol. Final DNA concentration was measured with NanodropTM Spectrophotometer.

2.2.10.4 Transfection of HEK293 cells

HEK293 cells were transfected using Lipofectamine® 2000 (Invitrogen, UK). The transfection mix was prepared as follows. For each well of a 6 well plate, 10µl of Lipofectamine 2000 was added to 150µl of serum- and antibiotic-free OPTIMEM® medium (Invitrogen, UK) in a 5ml bijoux, mixed and incubated for 20 minutes at room temperature. 1-2µg DNA of plasmid (pCDNA3 or pCA.18E6) was then added to 150µl of OPTIMEM® medium in a separate 5ml bijoux, and mixed thoroughly. The DNA was added dropwise to the diluted Lipofectamine, and incubated at RT for a further 30 minutes. After two washes in PBS, 700µl of OPTIMEM® was added to each well. The transfection mix (300µl) was added dropwise onto the adherent cells, swirled gently to mix and incubated overnight. The following day, the transfection medium was replaced with complete growth medium and cells allowed to grow for 24 hours.

2.2.10.5 Treatment of transfected cells with drugs

Transfected HEK293 cells were left in culture medium overnight prior to treatment with either EGCG or MG132 alone, or a combination of the two drugs. An equal volume of water was added to control (no drug treatment).

2.2.10.6 Preparation of cell lysates

Following drug treatment, HEK293 cells were washed with PBS three times and lysed in situ with cold NP40-based lysis buffer (25 mM Tris-HCl pH 7.4, 150 mM NaCl, 1% Nonidet P-40, and 5mM EDTA) containing 20mM Iodacetamide on ice for 30 minutes. Cells were then scraped off with a cell scraper and transferred to 1.5ml Eppendorf tube and sonicated at 40Hz for 10s with a microson ultrasonic cell disrupter (Misonix). The protein lysates were then centrifuged at 13,000rpm for 15 minutes at 4°C to pellet insoluble material, and the supernatant transferred to a new pre-chilled Eppendorf tube. The protein concentration was determined by Bradford assay. Immunoprecipitation or pull-down was performed immediately after the protein determination; unused protein lysates were stored at -80°C.

2.2.10.7 Immunoprecipitation of FLAG-tagged HPV18 E6 protein

For immunoprecipitation of FLAG-tagged HPV18 E6 proteins, first, the agarose beads conjugated to mouse anti-FLAG M2 antibody (Sigma-Aldrich, UK) were washed three times with ice cold lysis buffer. 500µg of protein lysate was then added to 20µl of the pre-washed agarose beads, and the tubes rotated at 4°C for 4 hours. The beads were then washed three times with ice cold lysis buffer and bound proteins eluted off the beads by boiling at 90°C in 20µl of 2x concentrated Laemmli sample buffer (BioRad)

for 5 minutes. All the proteins were then resolved by 12% SDS-PAGE prior to Western blotting.

2.2.10.8 Affinity purification of His-tagged ubiquitin protein

Dynabeads® His-Tag Isolation and Pulldown (Life Technologies) were used to pull down His-tagged ubiquitinated proteins. The magnetic beads were pre-washed with lysis buffer three times. 500µg of protein lysate was denatured in 0.9 times v/v of urea lysis buffer (8M urea, 100mM potassium phosphate, 10mM Tris HCL, 10mM 2-mercaptoethanol, pH 8.0) and left on a rotary wheel at 4°C for 1hour. 20µl of pre-washed magnetic beads were then added into the urea-protein lysate mixtures and left on a rotary wheel at 4°C for 1 hour. Then, the beads were washed for 5 minutes with 1ml urea buffer and 20mM Imidazole; 5 minutes with 1ml urea buffer, 20mM Imidazole and 0.2% Triton; 5 minutes with 1ml urea buffer and 20mM Imidazole; 5 minutes with 1ml urea buffer, 20mM Imidazole and 0.1% Triton; 5 minutes with 1ml urea buffer and 20mM Imidazole. The beads were eluted by boiling in 2x concentrated Laemelli sample buffer at 90°C in 20µl for 5 minutes. All the proteins were then resolved by 12% SDS-PAGE prior to Western blotting.

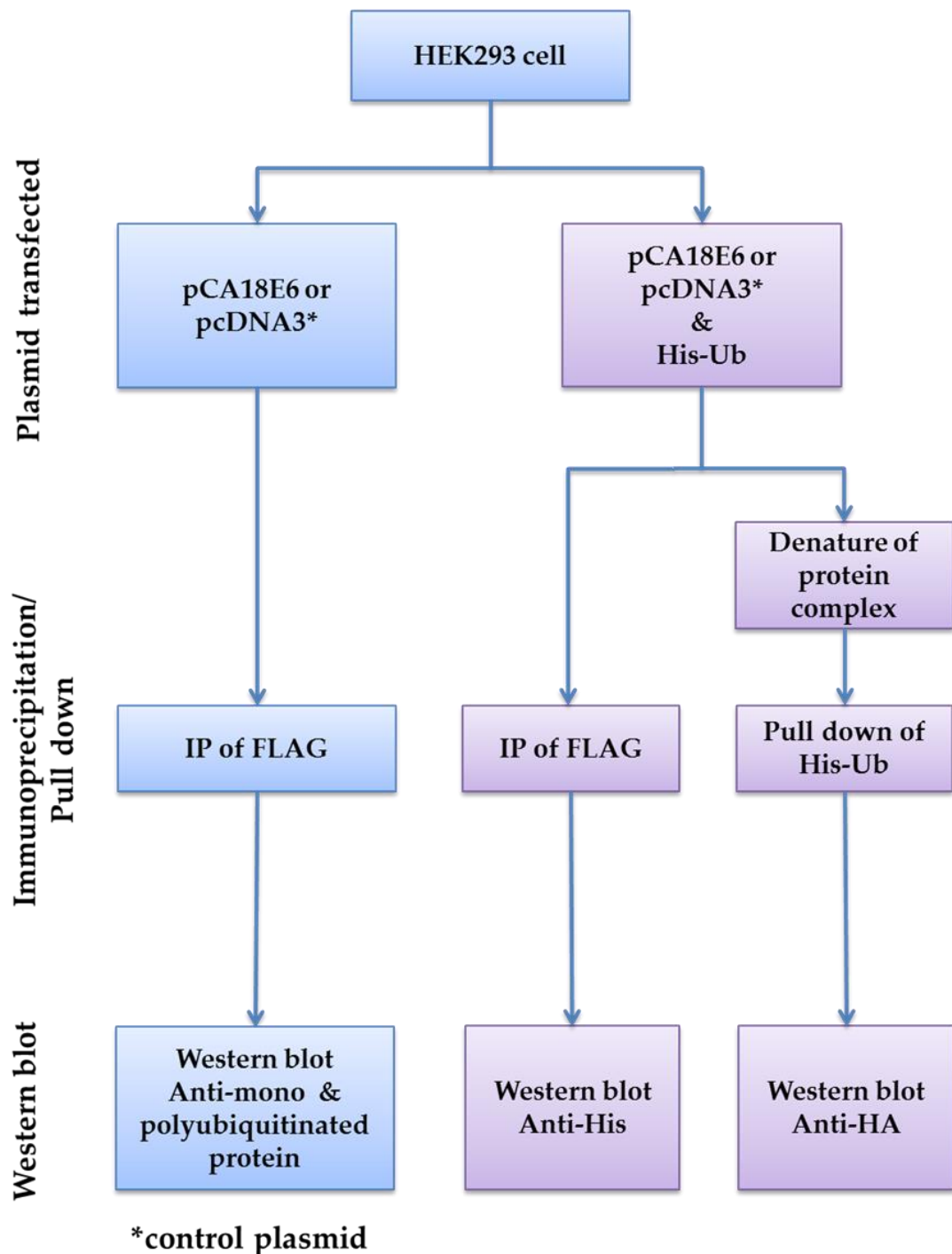


Figure 2.1: Flow chart depicting the steps involved in pulling down HPV18 E6 proteins.

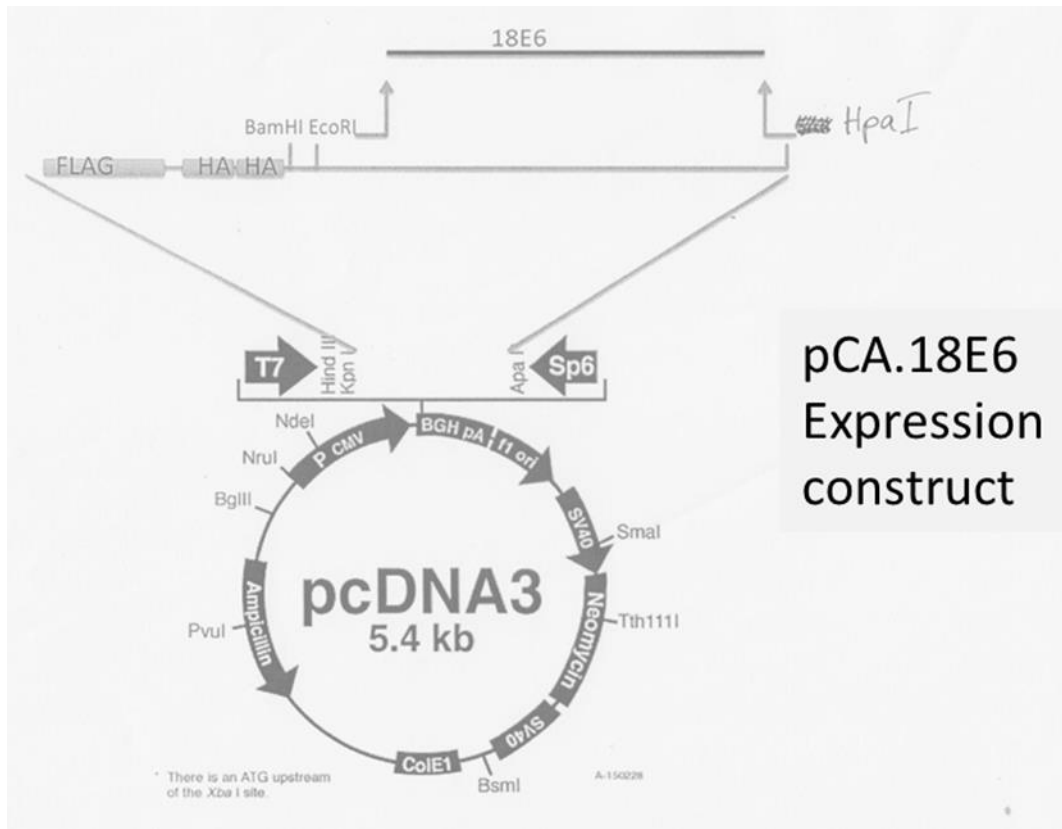


Figure 2.2: pCA.18E6. Based on pcDNA3, the pCA.18E6 plasmid contains a FLAG and double (2x) HA epitope sequence upstream of the HPV18 E6 coding region.

2.2.11 Endogenous and exogenous proteasome assay

The caspase-like, chymotrypsin-like and trypsin-like activities of the endo- and exogenous proteasome were examined in the presence or absence of EGCG using the fluorogenic substrates (Biomol) Z-LLE-AMC, Suc-LLVY-AMC and Bz-VGR-AMC. The substrates were dissolved in DMSO to give a stock concentration of 10mM. To prepare endogenous cellular proteasome, keratinocytes treated with and without 100 μ M EGCG for 72 hours or 10 μ M MG132 for 6 hours were lysed in RIPA buffer and the protein concentration determined by Bradford assay. Purified exogenous 20S human proteasome was purchased from Biomol and was diluted to a working solution of 6.25 μ g/ml.

To measure the endogenous proteasome activities, fluorogenic substrates were first diluted to 200 μ M in assay buffer (50mM Tris pH7.5, 25mM KCL, 10mM NaCl, 1mM MGCl2). Then, 10 μ g of protein lysates were added to 50 μ l of the appropriate substrates in a microfuge tube and incubated at 37°C for 30 minutes. To measure exogenous proteasome activity, 50 μ l of purified 20S proteasome were first primed with 100 μ M EGCG or 150 μ M MG132 for 30 minutes at 37°C before mixing with 50 μ l of appropriate substrates and incubate for a further 30 minutes at 37°C. For a negative control, 50 μ l of substrate solution was added to 50 μ l of assay buffer and incubated at 37°C for 30 minutes. 40 μ l duplicates of each reaction were then transferred to individual 96-well fluorescence plate on ice and the reaction was terminated by adding 200 μ l per well of stop buffer (100mM sodium chloroacetate in 30mM sodium acetate, 70mM acetic acid, pH 4.3). The fluorescence emitted was quantified using the Wallac Victor2 plate reader on “umbelliferone 360nm/460nm”.

2.2.12 Measuring the level of reactive oxidative species (ROS)

To determine the level of ROS in cells treated with EGCG, cells were seeded at a density of 5000 cells/well in triplicates in 96-well plate pre-coated with 10 μ g/ml collagen. The cells were washed with PBS x3 when they were 70% confluent and incubated with 5 μ M cm-H2DCFDA (Life Technologies) for 30 minutes according to manufacturer protocol; excess cm-H2DCFDA was washed off with PBS and replaced with phenol free serum-free keratinocyte media. Baseline ROS activities was measured as fluorescence emitted by breaking down cm-H2DCFDA using the Wallac Victor2 plate reader on 485/535nm; then, variable concentrations of EGCG or 500 μ M hydrogen peroxide (positive control) was added to the cells, and serial fluorescence readings were taken at 5, 15, 30, 60, 90, 180, 360 minutes.

2.2.13 Establishment of usual type vulvar intraepithelial neoplasia (uVIN) primary culture

2.2.13.1 Establish of primary uVIN keratinocyte cultures

Multiple tissue biopsies were taken from a patient with histological proven uVIN and transported to the laboratory in complete growth medium on ice. The tissue biopsies were then rinsed ten times with PBS containing 100U/ml penicillin, 100mg/l streptomycin and Fungizone (2.50 μ g/mL), and minced into 3-5mm cubes. About 10 small cubes were placed 1-2cm apart from each other onto a 9cm petri dish and enough growth medium added just to submerge the tissue cubes (approximately 2-3 mls). The tissue cubes were then left in humidified tissue culture incubator until keratinocytes emerged from the biopsies (7-14 days). Fresh medium was added

intermittently to prevent the tissue from drying out. Fibroblasts were selectively removed at regular intervals by washing with PBS containing 0.02% EDTA. Keratinocytes that grew out from the explants were trypsinized, and $1-2 \times 10^5$ cells seeded onto 9cm petri dishes containing 2×10^6 lethally irradiated 3T3-J2 feeder cells. Cells were maintained by weekly or biweekly passaging onto freshly irradiated 3T3-J2 feeder cells. At every passage, keratinocytes were cryopreserved and stored in liquid nitrogen according to section 2.2.1.4.

2.2.13.2 Single cell cloning

To undertake single cell cloning, primary keratinocytes were seeded at clonal density ($1-2 \times 10^4$ cells/9cm dish) onto a monolayer of irradiated 3T3-J2 feeder cells. Feeder cells were selectively removed with 0.02% EDTA solution and several PBS washes. Keratinocytes were inspected under phase microscopy, and sterile metal ring cylinders were strategically placed over the primary keratinocyte colonies. 50-100 μ l of trypsin (TrypLE Express, Invitrogen, UK) was added into the cylinder to detach the keratinocytes. These were transferred to 6-well plates containing a monolayer of lethally irradiated 3T3-J2 feeder cells (2×10^5 /well). The keratinocytes were then further cultured on 9cm petri dishes by plating onto a monolayer of lethally irradiated 3T3-J2 feeder cells and maintained by weekly or biweekly passages. Cells were cryopreserved at every passage.

2.2.14 HPV genotyping

2.2.14.1 HPV 16 and 18 genotyping

HPV 16 and 18 statuses were determined using multiplex real-time PCR assay. Sequence-specific primers and Fluorescein-labelled probes designed for GAPDH, HPV16 E6 and HPV18 E7 were shown in Table 2.3. Total DNA was extracted from cells using DNeasy kit (Qiagen) according to manufacturer's protocol, and 200ng genomic DNA was amplified using FastStart PCR Master master mix, HPV16 and 18 primers (see Table 2.3) with ABI 7700 Sequence Detection System. PCR conditions were: initial enzyme activation step (50°C/2 min), a denaturation step at (95°C/10 min), followed by 50 cycles of denaturation (95°C/15 sec) and annealing/extension step (55°C/1 min). SiHa and HeLa DNAs were used as positive control for HPV16 and HPV18, respectively.

2.2.14.2 HPV genotyping with Luminex PCR

DNA was extracted from formalin fixed paraffin embedded tissue of uVIN with DNeasy kit according to manufacturer's protocol, and the concentration was measured with Nanodrop™ Spectrophotometer. The DNA was then sent to the Scottish HPV Reference laboratory for HPV genotyping.

2.2.14.3 Assessment of HPV E2 integrity

The integrity of HPV 16/18 E2 genes were assess using sets of sequence-specific primers designed overlapping fragments that spanned the full-length E2 genes (see Figure 2.3). This technique was previously published by our group [108]. 100ng

genomic DNA was amplified using FastStart PCR Master Mastermix and HPV16 and 18 E2 primer sets (see Table 2.3). Cycling conditions for the PCR reactions were as follows: 95°C for 5 min followed by 60 cycles at 95°C for 20s, melting temperatures for 1 min and 72°C for 2 min, then a final extension of 72°C for 10 min. PCR products were analysed with electrophoresis on a 2% agarose gel.

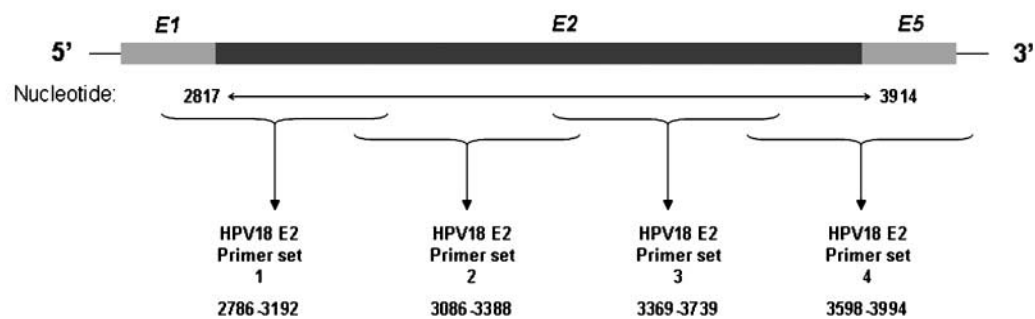


Figure 2.3: Location of primers used to amplify overlapping regions of the HPV18 E2 gene. Nucleotides are numbered according to the HPV18 whole genome sequence.

Table 2.3: Primer sequences used in PCR assay to detect HPV16 and HPV18 genomes and examine the integrity of E2 genes

Target	Accession number	Nucleotide sequence location	Sequence 5' to 3'	Fragment length (bp)	Melting temperature (Tm)
GAPDH	AY340484	3701 3858 3783	5'-GCTCAAGGGAGATAAAATTC-3' 5'-CGACCAAATCTAAGAGACAA-3' FAM-5'-CCT AGG GCT GCT CAC ATA TT-3'-TAMRA	158	55°C
HPV16 E6	NC_001526	368 528 418	5'-GAACAGCAATACAACAAACC -3' 5'-GATCTGCAACAAGACATACA -3' FAM-5'- CTGTCAAAAGCCACTGTGTC-3'-TAMRA	161	55°C
HPV18 E7	NC_001357	76 226 97	5'-GTTGACCTCTATGTCACGA -3' 5'-CAATTCTGGCTTCACACTTA -3' FAM-5'- CAATTAAGCGACTCAGAGGAA-3' TAMRA	151	55°C
HPV18 E2 Primer set 1	NC_001357	2786 3192	5'-TCCAGATTAGATTGCACGA -3' 5'-CAATTGTCTTGTTGCCATC -3'	407	54°C
HPV18 E2 Primer set 2	NC_001357	3086 3388	5'-ATACAAAACCGAGGATTGGA -3' 5'-ACTTCCCACGTACCTGTGTT -3'	303	54°C
HPV18 E2 Primer set 3	NC_001357	3369 3739	5'-AACACAGGTACGTGGGAAGT -3' 5'-TTTCGCAATCTGTACCGTAA -3'	371	54°C
HPV18 E2 Primer set 4	NC_001357	3598 3994	5'-GACCTGTCAACCCACTTCT -3' 5'-ACATGGCAGCACACATACAT -3'	397	54°C

2.2.14.4 Determining the changes in relative viral copy number

Changes in the levels of HPV18 episomes before and after EGCG treatment were measured by qPCR. DNA extracted from HFK-HPV18 keratinocytes were amplified with HPV18 and human TLR primers (see Table 2.4) and SensiMix SYBR master mix (Bioline) with Stratagene MX3000P. The thermo-cycle profiles were shown in Figure 2.4. Serial dilution was performed on DNA of untreated keratinocytes (control) by a factor of 10 up to 1:10 000, and the diluted DNA was amplified, together with the main samples, for human TLR and HPV18 to produce a standard curve for each primer in which a common threshold for both pairs of primers can then be used to calculate changes in viral copy number. The changes in the relative viral copy number in control and EGCG treated keratinocytes were determined from the Ct value using the following formulae [109]:

Step 1: Normalisation of control and EGCG treated sample. The difference in the episomal Ct value and host allele Ct value was calculated as follow:

$$\Delta Ct_{(control)} = Ct_{(\text{episomes of control})} - Ct_{(\text{host gene of control})}$$

$$\Delta Ct_{(EGCG)} = Ct_{(\text{episomes of EGCG})} - Ct_{(\text{host gene of EGCG})}$$

Step 2: The ΔCt value of the EGCG treated sample was normalised against ΔCt of control.

$$\Delta\Delta Ct = \Delta Ct_{(EGCG)} - \Delta Ct_{(control)}$$

Step 3: determining the ratio of EGCG treated episomes per host allele relative to control episomes per host allele; Ratio = $2^{\Delta\Delta Ct}$

Table 2.4: Primers used determine episomal copy number changes in HPV18 pre-and post-EGCG treatment.

Target	Accession number	Nucleotide sequence location	Sequence 5' to 3'	Fragment length (bp)	Melting temperature (Tm)
HPV18 episome FW	AY262282.1	2167-2251	TTATAGGCGAGCCCCAAAAA C	85	59.2°C
HPV18 episome RV	AY262282.1	2167-2251	CCAATCTCCCCCTTCATCTA T	85	59.3°C
Human TLR2 FW	Locus	1893-1957	GCCAGCAAATTACCTGTGT GA	65	61.08°C
Human TLR2 RV	Locus	1893-1957	GGCGGACATCCTGAACCT	65	61.05°C

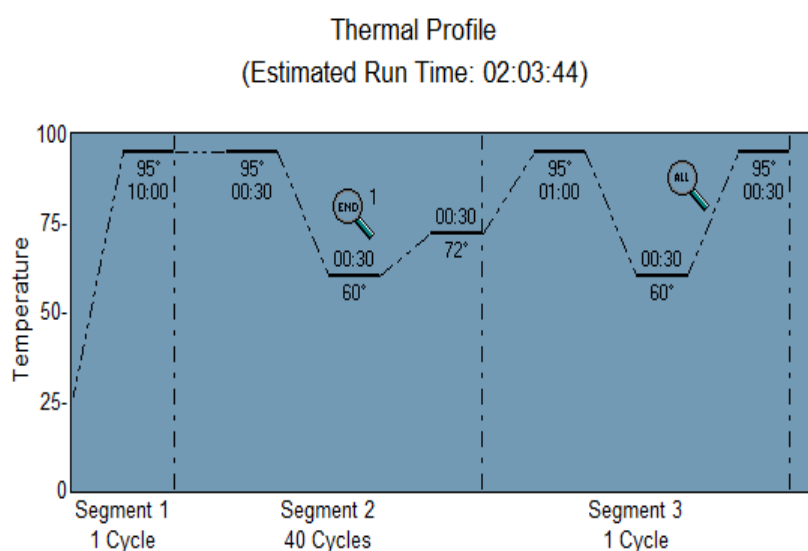


Figure 2.4: qPCR thermal profile for amplifying HPV18 episomes and human TLR primers.

2.2.15 Organotypic raft cultures

Organotypic raft cultures were prepared according to the protocol described in Dawson and Young, 2001 (see Figure 2.5) [110]. Briefly, 2.5-5 x10⁵ keratinocytes (HFK-HPV18 or VIN cl.11) were seeded onto a collagen lattice (Becton Dickinson, UK) containing 3T3-J2 fibroblast feeder cells (10⁵/cells/ml) and grown until confluent. Thereafter, the lattice was carefully transferred to a stainless steel grid, and the epithelial culture was exposed at the air/liquid interface for an additional two to three weeks (see Figure 2.6). Under such conditions, keratinocytes stratify and terminally differentiate. For rafts that were treated with EGCG, the appropriate concentration of EGCG was added into the medium, and equal volume of water was added to the control, EGCG was refreshed every two days along with medium. 5-bromo-2'-deoxyuridine (BrdU) was added into the medium for 12 hours before the raft was fixed with 4% paraformaldehyde in DMEM. The rafts were then sent to Propath Ltd for processing, and 4micron thick sections produced for H&E or immunohistochemical staining.

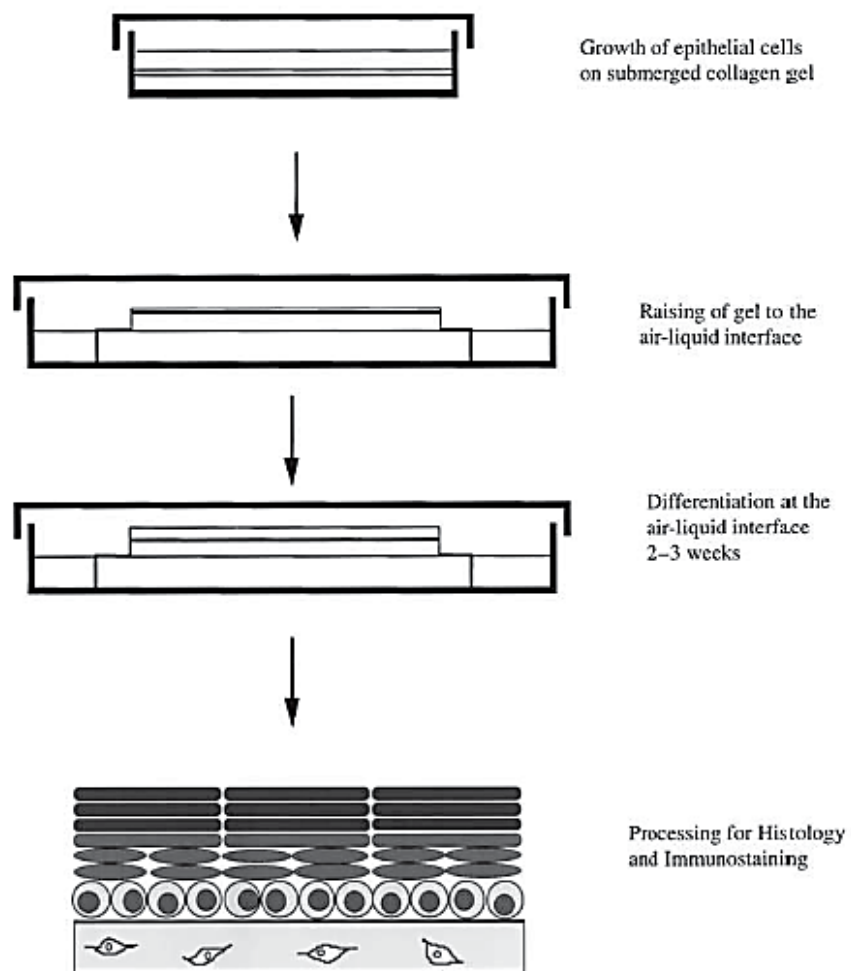


Figure 2.5: Schematic representation of the steps involved in establishing collagen raft cultures.

Adapted from Dawson and Young, 2001

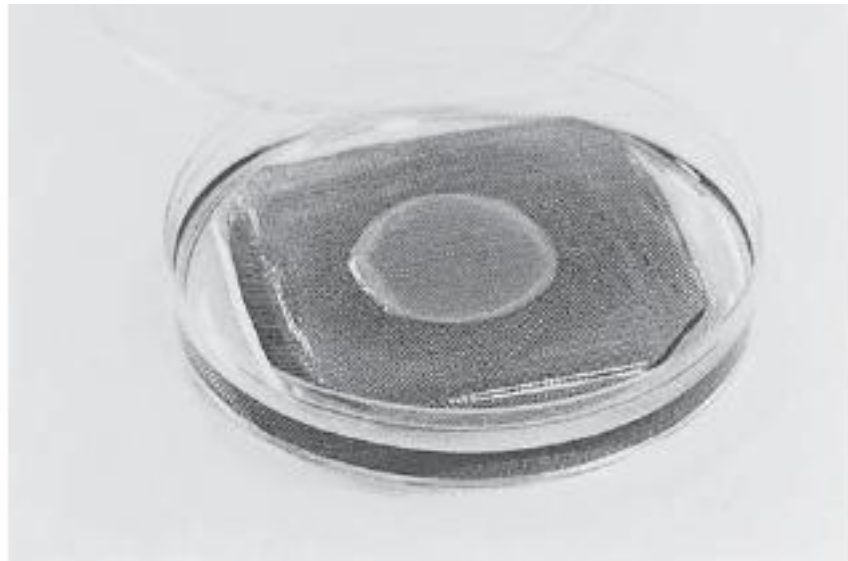


Figure 2.6: Typical appearance of a collagen raft culture.

Adapted from Dawson and Young, 2001

Chapter 3:

Predicting the outcome of women with VSCC:

analysis of the Birmingham VSCC cohort

(2000-2008)

3.1 Introduction

It has been known for some time that the outcome for women with squamous cell cancer of the vulva (VSCC) is influenced by the type of epithelial alteration found adjacent to their tumour. For example, whereas the finding in the resected specimen of usual-type VIN (u-VIN), the putative precursor of HPV-positive VSCC, predicts a prolonged disease-free survival, the detection of Lichen Sclerosus (LS) or differentiated VIN (d-VIN), the putative precursors of virus negative tumours, increases the risk of recurrent disease. Notwithstanding the consistency of these associations, there is as yet no compelling evidence to suggest that the detection of high-risk HPV types in the invasive component of these tumours is an independent predictor of disease-free survival. This is all the more surprising because at other sites of cancer arising through HPV dependent and independent routes (anus, oropharynx, penis and vagina) virus positive tumours have repeatedly been shown to have a longer disease-free survival than virus negative tumours. There are some possible reasons as to why evidence for a similar association in women with VSCC has proven so elusive. For example, u-VIN may co-exist alongside LS or d-VIN in the epithelium adjacent to both HPV positive and negative tumours. Just as it would be unwise to infer the HPV status of a tumour from the nature of its adjacent epithelial abnormality, the HPV status of the invasive component of the tumour may be an imperfect predictor of the epithelial alterations present in the surrounding field. Given that vulvar neoplasia arises in a field of cancerization, revealing a relationship between HPV status and disease free survival may be dependent on those recurrences arising from residual disease left behind at the time of surgery and second field tumours. With a view to gaining a better

understanding of the pathogenesis of recurrent disease at this site and identifying more certain iso prognostic groups, we explore these issues - which do not appear to have been considered in detail in earlier analyses of disease-free survival - using a well characterised cohort of women with VSCC with known HPV status.

3.2 Study population

The study population included 201 consecutive women first diagnosed with squamous cell carcinoma of the vulva (VSCC) between 2000 and 2008 and managed in the Pan Birmingham Gynaecological Cancer Centre.

3.3 Distribution of explanatory variables

3.3.1 Demography, behavioural and clinic-pathological variables (Table 3.1)

3.3.1.1 Triennia

The cohort was divided into three triennia (first: 2000-2, second: 2003-5, third: 2006-8) to reflect on the re-organisation of the gynaecological cancer service within the West Midlands during which this study was undertaken. 53 women were diagnosed in the first triennium (2000-2), with primary VSCC, 50 in the second (2003-5) and 98 in the third (2006-8).

3.3.1.2 Age at diagnosis

The mean and median age at diagnosis of women in this cohort was 68 and 72 years respectively (range 30-95). 67 (33.3%) patients were below the age of 65 years and 134 (66.7%) were ≥65 years.

3.3.1.3 Smoking behaviour

Smoking behaviour was recorded in 164 (82%) of the cohort. Of these, 51 (31.1%) were current smokers, 13 (7.9%) were ex-smokers, and 100 (61%) had never smoked.

3.3.1.4 Disease stage

The disease was staged according to the 1998 FIGO staging system for vulval neoplasia. 198 (98.5%) patients had surgico-pathological staging; 2 were clinically staged, and one patient was unstaged. Of the 198 patients who were surgically staged, 60 (30%) had stage I disease, 74 (37%) had stage II disease, 45 (23%) had stage III disease and 19 (10%) had stage IV disease. Of 60 with stage I disease 29 had stage Ia and 31 had stage Ib disease. Of 19 patients who had stage IV disease 14 had stage Iva and 5 had stage IVb disease. Of the two patients who were clinically staged, one had stage III, and the other had stage IVa disease. Staging information was incomplete in one patient who had synchronous advanced cervical cancer.

3.3.1.5 Tumour size

Tumour size was recorded for 151 (75.1%) patients in this cohort and unrecorded in 50 (24.9%). The median size of tumours was 3cms (range 0-20); 27 (17.9%) were less than 2cms in size, 61 (40.4%) between 2 and 3.9cms, 38 (25.2%) between 4 and 5.9cms and 25 (16.6%) greater than 6cms.

3.3.1.6 Multifocal disease

The site of disease was recorded in the clinical record in 197 (98%) of women in this cohort. Of these, 167 (84.8%) had a unifocal disease and 30 (15.2%) had a multifocal disease.

3.3.1.7 Histological grade

A grade of histological abnormality for the tumour was available for 172 (86%) patients. Of these tumours, 46 (26.7%) were well differentiated, 69 (51.7%) were moderately differentiated, and 57 (33.1%) were poorly differentiated.

3.3.1.8 Lymphovascular space involvement

The presence or absence of LVSI was explicitly recorded in the histopathology record in 173 (86%) of patients. Tumour was reported to have spread to the lymphovascular space in 57 (28%) of these patients.

3.3.1.9 Groin node status

Groin nodes were reported to be positive in 46 patients (22.9%), negative in 150 (74.6%) with disease status undefined in the remaining 5 (2.5%) women.

3.3.1.10 Characterisation of epithelium adjacent to invasive component

Of the 199 patients for whom the histopathology report was available 171 (85.9%) were reported to have LS or intraepithelial neoplasia (uVIN or dVIN) or more than one of these in the surgical specimen. Of these, 75 (43.9%) were reported to have uVIN alone, 8 (4.8%) had dVIN alone and 26 (15.2%) LS alone, 5 (3%) women had both uVIN and

dVIN, 4 (2%) had uVIN, dVIN and LS, 19 (10%) had uVIN and LS, 25 (13%) women had dVIN and LS (Figure 3.1).

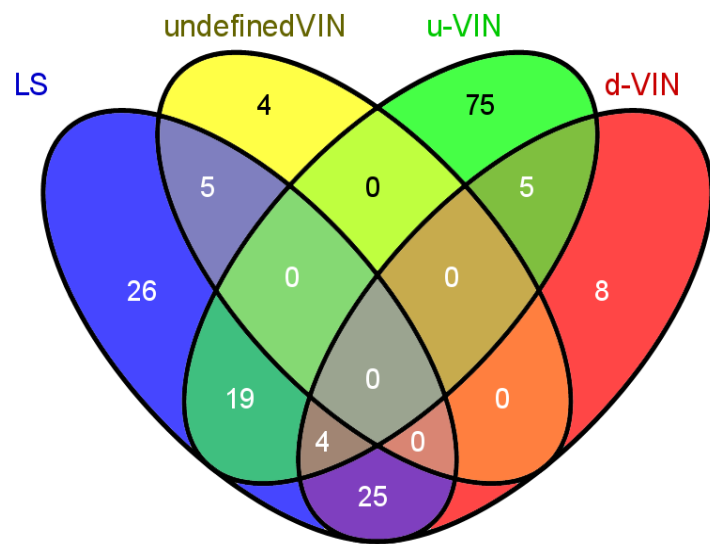


Figure 3.1: The distribution of LS and VIN adjacent to the invasive tumour.

Table 3.1: Distribution of clinico-pathological variable in Birmingham VSCC cohort

Variable		Number of cases	%
Triennium of diagnosis	2000-2	53	26.4%
	2002-5	50	24.9%
	2006-8	98	48.8%
Age	median	72yrs	
	range	30-95yrs	
	<65	67	33.3%
	≥65	134	66.7%
Smoking status	never smoker	100	31.8%
	smoker/ex-smoker	64	49.8%
	missing	37	18.4%
Tumour size	median	3cms	
	range	0-20cms	
	<2cm	27	17.9%
	2-4cm	61	40.4%
	4-6cm	38	25.2%
	≥6cm	25	16.6%
Stage of disease	missing	50	24.9%
	1a	29	14.4%
	1b	31	15.4%
	2	74	36.8%
	3	46	22.9%
	4	20	10.0%
Grade of differentiation	missing	1	0.5%
	well	46	22.9%
	moderate	69	34.3%
	poor	57	28.4%
Focality	missing	29	14.4%
	unifocal	167	83.1%
	multifocal	30	14.9%
Groin node involvement	missing	4	2.0%
	negative	150	74.6%
	positive	46	22.9%
Lymphovascular space involvement	missing	5	2.5%
	negative	116	57.7%
	positive	57	28.4%
LS/VIN	missing	28	13.9%
	No LS/VIN	30	14.9%
	LS alone	26	12.9%
	LS/u-VIN	19	9.5%
	LS/d-VIN	25	12.4%
	LS.u-VIN/d-VIN	4	2.0%
	LS/undefined VIN	5	2.5%
	u-VIN alone	75	37.3%
	d-VIN alone	8	4.0%
Excision status	u-VIN/d-VIN	5	2.5%
	undefined VIN	4	2.0%
	sub-optimal/incomplete	65	32.3%
Excision status	optimal	117	58.2%
	missing	19	9.5%

3.3.2 Treatment variables (Table 3.2)

3.3.2.1 Type of surgery performed for VSCC

183 (91%) patients had surgery to excise their primary tumour. Of these, 4 (2.0%) had simple wide local excision (WLE), 105 (52.2%) had radical WLE or hemi-vulvectomy and 74 (36.8%) had total radical vulvectomy. 16 (8%) patients had a diagnostic biopsy and 2 (1%) did not have any form of surgical procedure.

3.3.2.2 Excision margin status (Table 3.1)

Of the 183 patients having surgery, information for excision margins was available for 182 (99%) of the patients. In 117 (58%) patients the excision margins were considered to be optimum, 56 (30%) were considered to be sub-optimal and 9 (5%) were considered to be incomplete.

3.3.2.3 Type of groin surgery performed

Of the 183 patients who had surgery to excise their VSCC, 138 (75.4%) also had surgery to their groin(s) to diagnose or treat nodal metastatic disease. Of these, 29 (21%) had sentinel groin node biopsy, and 107 (77.5%) had groin node lymphadenectomy. Groin node biopsy was performed on 2 (1.5%) patients.

3.3.2.4 Radiotherapy and chemotherapy

46 (21.9%) patients had radiotherapy or chemotherapy, or both; 35 (76.1%) were given radiotherapy alone, 1 (2.2%) was given chemotherapy alone and 10 (21.7%) were given concurrent radiotherapy and chemotherapy. Of these 46 patients, 3 (6.5%) received concurrent radiotherapy and chemotherapy as primary treatment for their tumour, 3

(6.5%) received treatment as an adjunct before surgery (neo-adjuvant therapy), 35 (76.1%) received treatment as an adjunct after surgery (adjuvant therapy) and 3 received treatment to palliate their disease. Information on one patient who was referred for adjuvant treatment was unavailable, and one patient declined adjuvant radiotherapy. Of those patients who received radiotherapy, 11 (5.5%) had radiotherapy to their vulva (local) only; 7 (3.5%) to their groins only; 5 (2.5%) to their pelvis only; 13 (6.5%) to their vulva and groins; 3 (1.5%) to their vulva, groins and pelvis; 4 (2%) to their groins and pelvis. In 3 patients, the site that radiotherapy was administered was not available. In those patients whose excision margins were recorded as sub-optimal, 21 (37.5%) patients had adjuvant radiotherapy to their vulva.

Table 3.2: Distribution of treatment variable in Birmingham VS&CC cohort

Variable	Number of cases	%
Type of surgery	Biopsy or no surgery	18 9
	Simple WLE	4 2
	Radical WLE/hemi-vulvectomy	105 52.2
	Total radical vulvectomy	74 36.8
Groin node surgery	Sentinel node biopsy	29 21
	Groin node lymphadenectomy	107 77.5
	Others	2 1.5
None surgical interventions	Radiotherapy	35 76.1
	Chemotherapy	1 2.2
	Radio- & chemotherapy	10 21.7
Type of non-surgical interventions	Primary	3 6.5
	Neo-adjuvant	3 6.5
	Adjuvant	35 76.1
	Palliative	3 6.5
	Refused/unknown	2 4.3
Site of radiotherapy	Local	11 5.5
	Groins	7 3.5
	Pelvis	5 2.5
	Local & Groins	13 6.5
	Local, groins & pelvis	3 1.5
	Groins & pelvis	4 2
	Not determined	3 1.5

3.3.3 *HPV testing*

HR-HPV testing was performed on 143 (71.1%) patients in this cohort by Miss Harriet Protheroe (a UoB Medical student) and Dr Sarah Leonard. DNA was extracted from FFPE tissue blocks containing the diagnostic specimen and the presence or absence of HPV16 or HPV18 determined using established PCR protocols previously published (Colin et al.). Of the 143 cases, 78 (54.5%) women were tested positive for HPV16 or HPV18, or both; 72 tested positive for HPV16 alone, 1 for HPV18 alone and 5 for both HPV16 and HPV18. 5 cases were not tested for HPV 18 because of an insufficient amount of DNA. The physical status of the virus is currently being investigated by other members of the group. In the remaining 58 cases, the reasons for not testing for HPV were formalin fixed paraffin embedded (FFPE) histology blocks were unavailable (n=28); insufficient FFPE material available for DNA extraction (n=5); and FFPE blocks were available but not cut (n=25).

3.4 Assessment of the correlations between baselines variables

3.4.1 *Overview*

The aim of this exercise is to examine the relationship between each of the above variables and then determine which of these variables, either alone or in combination, are likely to explain the findings of subsequent analysis on treatment outcomes. The relationship between each pair of potentially explanatory variables is first explored, following which the distribution of missing variables, their associations and possible determinants are described.

3.4.2 Available information

3.4.2.1 Age at diagnosis did not vary over study period (Table 3.3)

The median age of women in this cohort was 72 years (range 30-95). In the first triennium (2000-2), 55 women were diagnosed with VSCC, 52 in the second (2003-5) and 94 in the third (2006-8). Age at diagnosis did not vary significantly across the triennia.

Table 3.3: Table showing the relationship between median age and year of diagnosis in 3 triennia.

Age at diagnosis did not vary over study period					
Variable		Number of cases	median	range	
Year of diagnosis	2000-2	55	69	30-92	Wilcoxon two sample test: p <= 0.5941 (2000-2) vs (2003-5); p<=0.1626 (2000-2 vs 2006-8)
	2003-5	52	72	41-94	
	2006-8	94	74	33-95	

3.4.2.2 Smokers/ex-smokers with VSCC are younger than never smokers (Table 3. 4)

In this cohort, 64 (31.8%) women were either current smokers or ex-smokers, 100 (49.8%) had never smoked, and smoking status was unrecorded in the remaining 37 (18.4%). Among women for whom a smoking history was available, the prevalence of smokers/ex-smokers did not vary over time but did vary with age. The median age of smokers/ex-smokers was 56 (30-85) and never smokers 74.5 (38-92) (Wilcoxon two-sample test, $p <0.001$). Women who were over 80 at diagnosis were less likely to be smokers or ex-smokers than those under 60 (19.4% vs. 70.8%, RR = 0.27 95% CI = 0.1-0.5).

Table 3.4: Table showing the relationship between smoking status and age (in 4 age groups) or year of diagnosis in 3 triennia.

Smokers/ex-smokers were younger than never smokers					
		Number of cases n = 164	smoker/ex-smoker n = 64	never smokers n = 100	% smoker/ex-smoker
Year of diagnosis	2000-2	51	17	34	33.3%
	2003-5	46	17	29	37.0%
	2006-8	67	30	37	44.8%
Age	<60	48	34	14	70.8%
	60-69	33	10	23	30.3%
	70-79	47	13	34	27.7%
	>80	36	7	29	19.4%
	median age		56	74.5	Wilcoxon two sample test: $p \leq 3.964e-05$
	range		30-85	38-92	

Excludes 37 cases with missing smoking status

3.4.2.3 Prevalence of multifocal disease does not vary over time or with age at diagnosis or smoking history (Table 3.5)

In this cohort, 167 (83.1%) women had a unifocal disease, 30 (14.9%) had multifocal disease and this information was unrecorded in the remaining 4 (2%) patients. The prevalence of multifocal disease did not vary significantly over time or with age at diagnosis or smoking history.

Table 3.5: Table showing the relationship between multifocal disease and age (in 4 age groups), year of diagnosis in 3 triennia or smoking status.

Prevalence of multifocal diseases did not vary with year of diagnosis, age or smoking history						
Variable		Number of cases n = 196	Multifocal n = 30	Unifocal n = 167	%multifocal	
Year of diagnosis	2000-2	54	10	44	18.5%	Chi-square = 3.88; 2df; p = 0.144
	2003-5	52	11	41	21.2%	
	2006-8	91	9	82	9.9%	
Age	<60	53	13	40	24.5%	Chi-square = 7.42; 3df: p = 0.0.0598
	60-69	34	2	32	5.9%	
	70-79	60	6	54	10.0%	
	>80	50	9	41	18.0%	
	median age		66.5	73		Wilcoxon two sample test; p <= 0.1761
	range		32-94	30-95		
Smoking status	never smoker	96	14	82	14.6%	Chi-square = 0.03; 1df; p = 0.8559
	smoker/ex-smoker	64	10	54	15.6%	
	recorded	160	24	136	15.0%	Chi-square = 0.03; 1df; p = 0.8537
	missing	37	6	31	16.2%	
excludes 4 patients in whom focality is unknown						

3.4.2.4 Women with VSCC associated usual type vulval intraepithelial neoplasia (uVIN) are younger than those with VSCC associated Lichen Sclerosus (LS) (Table 3.6)

The pathology report described the presence of LS or VIN or both in 171 (85.1%) women in this cohort. In brief, 75 women had usual type VIN (uVIN) alone, 26 had LS alone, 8 had differentiated VIN (dVIN) and 4 had VIN that was not further defined; two or more of these elements were present in the remaining 58 tumours.

The prevalence of uVIN alone was higher in women diagnosed in the last triennium than in the first (46.8% vs. 29.1%, RR = 1.52 95% CI 1.0-2.4) although this association was of borderline significance. Women with uVIN alone were younger than those with LS alone (median 66 years vs. 74.5 years, Wilcoxon two-sample test, p = 0.0242) and younger than those with both LS and dVIN (median 67 years vs. 82 years, Wilcoxon two-sample test, p = 0.0010). Women with LS and uVIN were also younger than those with LS and dVIN (median 67 years vs. 82 years, Wilcoxon two-sample test, p = 0.0010). Women with uVIN alone were not only more likely to be smokers or ex-smokers than those with LS alone (51.6% vs. 7.8%, RR = 2.38 95% CI 1.1-5.3) but also those with both LS and uVIN (51.6% vs. 4.7%, RR = 3.1 95% CI 1.1-8.8). These associations are likely to be confounded by the association between smokers/ex-smokers and young age. The prevalence of LS and VIN did not vary significantly with that of multifocal disease.

Table 3.6: Table showing types of epithelial abnormalities, either uVIN alone, dVIN alone, *Lichen Sclerosus (LS) alone or in combination, found adjacent to the primary VSCC.

Variable	No. of cases	No. *LS/VIN	%	*LS alone	%	*LS/uVIN	%	*LS/dVIN	%	*LS/uVIN/dVIN	%	*LS/undefined VIN	%	uVIN alone	%	uVIN/dVIN	%	dVIN alone	%	undefined VIN	%
	n=30			n=26		n=19		n=25		n=4		n=5		n=75		n=5		n=8		n=4	
Year of diagnosis																					
2000-2	55	9	16.4%	10	18.2%	7	12.7%	4	7.3%	1	1.8%	2	3.6%	16	29.1%	2	3.6%	2	3.6%	2	3.6%
2003-5	52	6	11.5%	5	11.5%	8	15.4%	8	15.4%	2	3.8%	2	3.8%	15	11.5%	1	1.9%	4	7.7%	1	1.9%
2006-8	94	15	16.0%	11	11.7%	4	4.3%	13	13.8%	1	1.1%	1	1.1%	44	46.8%	2	2.1%	2	2.1%	1	1.1%
median range	72	74.5		67		82		80.5		77		66		77		76		73.5		48-78	
Age																					
<60	54	8	14.8%	5	9.3%	4	7.4%	1	1.9%	0	0.0%	0	0.0%	31	57.4%	2	3.7%	2	3.7%	1	1.9%
60-69	35	7	20.0%	4	11.4%	7	20.0%	3	8.6%	1	2.9%	1	2.9%	12	34.3%	0	0.0%	0	0.0%	0	0.0%
70-79	59	7	11.9%	10	16.9%	6	10.2%	7	11.9%	1	1.7%	1	1.7%	20	51.3%	1	1.7%	3	5.1%	3	5.1%
>80	53	8	15.1%	7	13.2%	2	3.8%	14	26.4%	2	3.8%	3	5.7%	12	22.6%	2	3.8%	3	5.7%	0	0.0%
Smoking status																					
missing	37	6	16.2%	4	10.8%	2	5.4%	8	21.6%	1	2.7%	1	2.7%	14	37.8%	0	0.0%	1	2.7%	0	0.0%
recorded	164	24	14.6%	22	13.4%	17	10.4%	17	10.4%	3	1.8%	4	2.4%	61	37.2%	5	3.0%	7	4.3%	4	2.4%
never	100	17	17.0%	17	17.0%	14	14.0%	10	10.0%	2	2.0%	3	3.0%	28	28.0%	3	3.0%	4	4.0%	2	2.0%
smoker/ex-smoker																					
recorded	64	7	10.9%	5	7.8%	3	4.7%	7	10.9%	1	1.6%	1	1.6%	33	51.6%	2	3.1%	3	4.7%	2	3.1%
missing	197	28	14.2%	26	13.2%	19	9.6%	25	12.7%	4	2.0%	5	2.5%	73	37.1%	5	2.5%	8	4.1%	4	2.0%
Focality																					
multifocal	30	4	13.3%	4	13.3%	4	13.3%	3	10.0%	1	3.3%	0	0.0%	9	30.0%	2	6.7%	3	10.0%	0	0.0%
unifocal	167	24	14.4%	22	13.2%	15	9.0%	22	13.2%	3	1.8%	5	3.0%	64	38.3%	3	1.8%	5	3.0%	4	2.4%

**3.2.4.5 Lymphovascular space involvement (LVI) is more common in never smokers
(Table 3.7)**

LVI was present in 57 (28.4%) tumours, absent in 116 (57.8%) and unrecorded in 28 (13.9%). The prevalence of LVI did not vary over time, with age at diagnosis, multifocal disease or the presence of LS or VIN. Compared with never smokers, smokers and ex-smokers were less likely to have tumours with LVI (20.5% vs. 46.0%, RR = 0.45 95% CI 0.3-0.7). As yet, there is no compelling reason to believe that this association is confounded by age.

Table 3.7: Table showing the relationship between lymphovascular space involvement (LWSI) and age (in 4 age groups), year of diagnosis in 3 triennia, smoking status, disease focality or adjacent epithelial abnormalities.

LWSI more common in never smokers						
Variable		Number of cases n = 173	LWSI			
			Yes n = 57	No n = 116	%LWSI	
Year of diagnosis	2000-2	43	13	30	30.2%	Chi-square = 0.22; 2df: p = 0.8962
	2003-5	46	16	30	34.8%	
	2006-8	84	28	56	29.8%	
Age of diagnosis	<60	43	14	29	32.6%	Chi-square = 1.26; 3df: p = 0.7387
	60-69	32	10	22	31.3%	
	70-79	55	16	39	29.1%	
	>80	43	17	26	39.5%	
	median age	74	72			Wilcoxon two sample test: p <= 0.5152
	range	33-95	33-94			
Smoking status	never smoker	63	29	34	46.0%	Chi-square = 10.45; 1df: p = 0.0012
	smoker/ex-smoker	78	16	62	20.5%	
	missing	32	12	20	37.5%	Chi-square = 0.37; 1df: p = 0.5441
	recorded	141	45	96	31.9%	
Focality	missing	4	2	2	50.0%	At least 20% of expected frequencies are less than 5
	recorded	169	55	114	32.5%	
	multifocal	27	11	16	40.7%	Chi-square = 0.98; 1df: p = 0.3215
	unifocal	142	44	98	31.0%	
Adjacent epithelial abnormalities	No LS/VIN	24	8	16	33.3%	At least 20% of expected frequencies are less than 5
	LS alone	21	6	15	28.6%	
	LS/u-VIN	18	6	12	33.3%	
	LS/d-VIN	23	4	19	17.4%	
	LS/u-VIN/d-VIN	3	0	3	0.0%	
	LS/undefined VIN	4	0	4	0.0%	
	u-VIN alone	63	26	37	41.3%	
	d-VIN alone	8	3	5	37.5%	
	u-VIN/d-VIN	5	2	3	40.0%	
	undefined VIN	4	2	2	50.0%	

3.4.2.6 Tumour size did not vary over time, with age at diagnosis, multifocal disease, smoking status or the presence of LS or VIN (Table 3.8)

Tumour size did not vary over time, with age at diagnosis, multifocal disease, smoking status or the presence of LS or VIN.

Table 3.8: Table showing the relationship between tumour size and age (in 4 age groups), year of diagnosis in 3 triennia, smoking status, disease focality, adjacent epithelial abnormalities or LVSI.

Tumour size does not vary with year of diagnosis, age, smoking status, multifocal disease or lymphovascular space involvement											
Variable	Number of cases n = 151*	median size (cms)	range	<2 cms n = 27	2-4 cms n = 61	4-6 cms n = 38	>6 cms n = 25				
Year of diagnosis	2000-2	32	2.5	1-10	7	21.9%	13	40.6%	4	12.5%	
	2003-5	44	3	0.5-7	7	15.9%	19	43.2%	5	11.4%	
	2006-8	75	3	0.5-20	13	17.3%	29	38.7%	17	22.7%	
				Wilcoxon two sample test: p <= 0.3712 (2000-2 vs 2003-5); p <= 0.2391 (2000-2 vs 2006-8)							
Age	<60	29	3	0.5-10	7	24.1%	12	41.4%	5	17.2%	
	60-69	25	3	1-20	5	20.0%	8	32.0%	9	36.0%	
	70-79	55	3	0.5-9	10	18.2%	23	41.8%	15	27.3%	
	>80	52	3	0.9-10	5	9.6%	18	34.6%	9	17.3%	
				Wilcoxon two sample test: p <= 0.4505 (<60 vs 60-69); p <= 0.9625 (<60 vs 70-79); p <= 0.2614 (<60 vs >80)							
Smoking status	missing	30	3.8	0.5-10	4	13.3%	11	36.7%	6	20.0%	
	recorded	121	3	0.5-20	23	2.5%	50	41.3%	32	26.4%	
	never smoker	78	3	0.5-9	16	3.8%	33	42.3%	20	25.6%	
	smoker/ex-smoker	43	3	0.5-20	7	16.3%	17	39.5%	12	27.9%	
				Wilcoxon two sample test: p = 0.0042 (missing vs. recorded); p <= 0.0977 (never vs ex-smoker)							
Focality	missing	4	NA	NA	NA	NA	NA	NA	NA	NA	
	recorded	151	3	0.5-20.0	27	17.9%	61	40.4%	38	25.2%	
	multifocal	19	3	1.0-8.0	3	15.8%	9	47.4%	4	21.1%	
	unifocal	132	3	0.5-20.0	24	18.2%	52	39.4%	34	25.8%	
				Wilcoxon two sample test: p <= 0.7705 (unifocal vs multifocal)							
Adjacent abnormal epithelia	No LS/VIN	23	5	2-20	0	0.0%	8	34.8%	7	30.4%	
	LS alone	22	2	0.5-10	5	22.7%	10	45.5%	5	22.7%	
	LS/u-VIN	15	3	1.0-7	2	13.3%	7	46.7%	3	20.0%	
	LS/d-VIN	22	2.5	0-5	6	27.3%	9	40.9%	7	31.8%	
				Wilcoxon two sample test: p <= 0.2489 (u-VIN alone vs. LS alone);							
Ls/u-VIN/d-VIN	LS,u-VIN/d-VIN	3	3	2.5-3	0	0.0%	3	100.0%	0	0.0%	
	LS/undefined VIN	4	1.3	1-2	3	75.0%	1	25.0%	0	0.0%	
	u-VIN alone	49	3	0.5-9	9	18.4%	18	36.7%	13	26.5%	
	d-VIN alone	3	3	1-4	1	33.3%	1	33.3%	0	0.0%	
				At least 20% of expected frequencies are less than 5							
lymphovascular space involvement**	u-VIN/d-VIN	7	3	1-10	1	14.3%	3	42.9%	1	14.3%	
	undefined VIN	3	5	2-7	0	0.0%	1	33.3%	1	33.3%	
	missing	14	3.5	1-7	3	21.4%	4	28.6%	3	21.4%	
	recorded	131	3	0.5-20	24	18.3%	57	43.5%	34	26.0%	
				Wilcoxon two sample test: p <= 0.0637 (negative vs positive)							
lymphovascular space involvement**	negative	88	3	0.5-20	17	19.3%	41	46.6%	20	22.7%	
	positive	49	4	0.9-10	7	14.3%	16	32.7%	14	28.6%	
				Wilcoxon two sample test: p <= 0.1252							
				At least 20% of expected frequencies are less than 5							

**50 cases with missing tumour size were excluded

3.4.2.7 Grade of tumour differentiation varies over time and with tumour size

(Table 3.9)

Women diagnosed in the last triennium were less likely to have well-differentiated tumours than those diagnosed in the first (16.5% vs. 34.8%, RR = 0.47 95% CI 0.3-0.9). Poorly differentiated tumours were larger (median 4cms) than those which were moderately (median 3cms) and well (median 2.5cms) differentiated (Wilcoxon two-sample test, p = 0.0027 and p<=0.0045, respectively). Tumours larger than 6cms were more than twice as likely to be poorly differentiated as those smaller than 2cms (54.2% vs. 24.0%, RR = 2.26 95% CI 1.0-5.0), although this association was of borderline significance. Tumours with LVI were more likely to be poorly differentiated than those without (42.9% vs. 29.0%, RR = 1.48 95% CI 1.0-2.3), although this association was again of borderline significance. Grade of tumour differentiation did not vary with age at diagnosis, multifocal disease, smoking status or the presence of LS or VIN.

Table 3.9: Table showing the relationship between grade of tumour differentiation and age (in 4 age groups), year of diagnosis in 3 triennia, smoking status, tumour size, disease focality, adjacent epithelial abnormalities or LVSI.

		Grade of tumour differentiation varies with tumour size						
Variable		Number of cases n = 172	Grade of tumour differentiation					
			well n = 46	moderate n = 69	poor n = 57			
Year of diagnosis	2000-2	46	16	34.8%	16	34.8%	14	30.4%
	2003-5	47	17	36.2%	16	34.0%	14	29.8%
	2006-8	79	13	16.5%	37	46.8%	29	36.7%
Age	<60	40	13	32.5%	18	45.0%	9	22.5%
	60-69	30	4	13.3%	13	43.3%	13	43.3%
	70-79	54	12	22.2%	22	40.7%	20	37.0%
	>80	48	17	35.4%	16	33.3%	15	31.3%
	median age	172	75		73		73	
	range		33-92		39-94		35-95	
Smoking status	missing	33	6	18.2%	13	39.4%	14	42.4%
	recorded	139	40	28.8%	56	40.3%	43	30.9%
	never smoker	87	25	28.7%	32	36.8%	30	34.5%
	smoker/ex-smoker	52	15	28.8%	24	46.2%	13	25.0%
Size of tumour	missing	32	14	43.8%	10	31.3%	8	25.0%
	recorded	140	32	22.9%	59	42.1%	49	35.0%
	<2	25	10	40.0%	9	36.0%	6	24.0%
	2-4	56	12	21.4%	31	55.4%	13	23.2%
	4-6	35	6	17.1%	12	34.3%	17	48.6%
	>6	24	4	16.7%	7	29.2%	13	54.2%
	median size		2.5		3		4	
Focality	range		0.5-10		0.5-9		0.9-20	
	missing	3	1	33.3%	2	66.6%	0	0.0%
	recorded	169	45	26.6%	67	39.6%	57	33.7%
	multifocal	25	8	32.0%	10	40.0%	7	28.0%
	unifocal	144	37	25.7%	57	39.6%	50	34.7%
Adjacent abnormal epithelia	No LS/VIN	26	9	34.6%	8	30.8%	9	34.6%
	LS alone	23	4	17.4%	9	39.1%	10	43.5%
	LS/u-VIN	18	6	33.3%	6	33.3%	6	33.3%
	LS/d-VIN	24	7	29.2%	11	45.8%	6	25.0%
	LS/u-VIN/d-VIN	4	1	25.0%	2	50.0%	1	25.0%
	LS/undefined VIN	4	2	50.0%	2	50.0%	0	0.0%
	u-VIN alone	56	9	16.1%	26	46.4%	21	37.5%
	d-VIN alone	5	1	20.0%	3	60.0%	1	20.0%
	u-VIN/d-VIN	8	6	75.0%	2	25.0%	0	0.0%
	undefined VIN	4	1	25.0%	0	0.0%	3	75.0%
LVSI	missing	16	9	56.3%	3	18.8%	4	25.0%
	recorded	156	37	23.7%	66	42.3%	53	34.0%
	negative	100	27	27.0%	44	44.0%	29	29.0%
	positive	56	10	17.9%	22	39.3%	24	42.9%

*29 cases with missing grade of differentiation were excluded;

3.4.2.8 Stage of disease varies over time, with age, grade of tumour differentiation and the presence of uVIN and LS (Table 3. 10)

60 (29.9%) women had stage 1 disease, 74 (36.8%) stage 2 disease, 46 (22.9%) stage 3 disease, 20 (10%) stage 4 disease and 1 patient was unstaged. Variation in stage distribution across the study period was in large part explained by changes in the prevalence of stage 1 and 2 disease. For example, the prevalence of stage 2 disease increased from the first to the second triennium (25.9% vs. 61.5%, RR = 2.37 95% CI = 1.4-3.9), but fell again from the second to third triennium (61.5% vs. 29%, RR = 0.48 95% CI = 0.3-0.7); this shift was mirrored by changes in the prevalence of stage 1 disease. The median age of women with stage 1 to 4 disease was 61.5, 75, 77.5 and 75 respectively. Compared to women with stage 1 disease, those with more advanced disease were older (Wilcoxon two sample test: p <= 0.01, stage 1 vs. 2; p <= 2.588e-05, stage1 vs. 3; p <= 0.0010, stage 1 vs. 4). Women over 80 were less likely to have stage 1 disease than those under 60 (7.7% vs. 53.7%, RR = 0.12 95% CI = 0-3.0).

Smokers/ex-smokers were more likely to have stage 1 disease (43.8% vs. 27.3%, RR = 0.12 95% CI = 0-0.3) than never smokers. However, this association is likely to be confounded by the younger age of smokers and ex-smokers. Compared to women with well-differentiated tumours, those with poorly differentiated tumours were less likely to have stage 1 disease (12.5% vs. 32.6%, RR = 0.38 95% CI = 0.2-0.9).

Compared to women who had uVIN alone with their primary tumour, those with associated LS alone were less likely to have stage 1 disease (19.2% vs. 42.7%, RR = 0.45 95% CI = 0.2-1.0) although this association was of only borderline significance. Neither multifocal disease (Chi-square = 2.06; 3df: p < 0.56) nor LVI (Chi-square = 4.73; 3df: p < 0.1928) were associated with disease stage.

Table 3.10: Table showing the relationship between disease stage and age (in 4 age groups), year of diagnosis in 3 triennia, smoking status, tumour differentiation, disease focality, adjacent epithelial abnormalities or LVSI.

Stage of disease varies with year of diagnosis, age, smoking status and tumour differentiation						
Variable		Number of cases n = 200*	Stage 1 n = 60 (%)	Stage 2 n = 74 (%)	Stage 3 n = 46 (%)	Stage 4 n = 20 (%)
Year of diagnosis	2000-2	54	23 (42.6%)	14 (25.9%)	13 (24.1%)	4 (7.4%)
	2003-5	52	7 (13.5%)	32 (61.5%)	10 (19.2%)	3 (5.8%)
	2006-8	94	30 (31.9%)	28 (29.8%)	23 (24.5%)	13 (13.8%)
Age	<60	54	29 (53.7%)	15 (27.8%)	7 (13.0%)	3 (5.6%)
	60-69	35	9 (25.7%)	13 (37.1%)	10 (28.6%)	3 (8.6%)
	70-79	59	18 (30.5%)	21 (35.6%)	13 (22.0%)	7 (11.9%)
	>80	52	4 (7.7%)	25 (48.1%)	16 (30.8%)	7 (13.5%)
	median age		61.5	75	77.5	75
	range		30-95	33-94	35-95	46-90
Smoking status	never smoker	99	24 (27.3%)	42 (42.4%)	25 (25.3%)	8 (8.1%)
	smoker/ex-smoker	64	28 (43.8%)	21 (32.8%)	9 (14.1%)	6 (9.4%)
	recorded	163	52 (31.9%)	63 (38.7%)	34 (20.9%)	14 (8.6%)
	missing	37	8 (21.6%)	11 (29.7%)	12 (32.4%)	6 (16.2%)
Tumour differentiation	well	46	15 (32.6%)	22 (47.8%)	5 (10.9%)	4 (8.7%)
	moderate	69	14 (20.3%)	33 (47.8%)	16 (23.2%)	6 (8.7%)
	poor	56	7 (12.5%)	16 (28.6%)	24 (42.9%)	9 (16.1%)
	recorded	171	36 (21.1%)	71 (41.5%)	45 (26.3%)	19 (11.1%)
	missing	29	24 (82.8%)	3 (10.3%)	1 (3.4%)	1 (3.4%)

Table continue below

Variable		Number of cases n = 200*	Stage 1 n = 60 (%)	Stage 2 n = 74 (%)	Stage 3 n = 46 (%)	Stage 4 n = 20 (%)	
Adjacent epithelial abnormalities	No LS/VIN	30	4 13.3%	11 36.7%	4 13.3%	11 36.7%	At least 20% of expected frequencies are less than 5
	LS alone	26	5 19.2%	10 38.5%	9 34.6%	2 7.7%	
	LS/u-VIN	19	5 26.3%	8 42.1%	5 26.3%	1 5.3%	
	LS/d-VIN	25	5 20.0%	14 56.0%	5 20.0%	1 4.0%	
	LS.u-VIN/d-VIN	4	1 25.0%	2 50.0%	1 25.0%	0 0.0%	
	LS/undefined VIN	5	3 60.0%	2 40.0%	0 0.0%	0 0.0%	
	u-VIN alone	75	32 42.7%	20 26.7%	20 26.7%	3 4.0%	
	d-VIN alone	5	2 40.0%	3 60.0%	0 0.0%	0 0.0%	
	u-VIN/d-VIN	8	2 25.0%	4 50.0%	1 12.5%	1 12.5%	
	undefined VIN	3	1 33.3%	0 0.0%	1 33.3%	1 33.3%	
Focality	missing	4	1 25.0%	0 0.0%	2 50.0%	1 25.0%	At least one expected frequency is less than 1 Chi-square = 2.06; 3df: p < 0.5600
	recorded	196	59 30.1%	74 37.8%	44 22.4%	19 9.7%	
	multifocal	30	9 30.0%	14 46.7%	4 13.3%	3 10.0%	
	unifocal	166	50 30.1%	60 36.1%	40 24.1%	16 9.6%	
LVSI	missing	28	14 50.0%	8 28.6%	6 21.4%	0 0.0%	Chi-square = 8.26; 3df: p < 0.041 Chi-square = 4.73; 3df: p < 0.1928
	recorded	172	46 26.7%	66 38.4%	40 23.3%	20 11.6%	
	negative	115	35 30.4%	45 39.1%	25 21.7%	10 8.7%	
	positive	57	11 19.3%	21 36.8%	15 26.3%	10 17.5%	

*Excluded 1 unstaged case

3.4.2.9 Groin node involvement is associated with older age at diagnosis, larger poorly differentiated tumours and associated LS (Table 3.11)

Groin nodes were reported to be positive in 46 patients (22.9%), negative in 150 (74.6%) with disease status undefined in the remaining 5 (2.5%) women. The prevalence of groin node disease did not vary over the study period (Chi-square = 2.33; 2df; p = 0.3121).

Women with positive groin nodes were older (median age 77 vs. 69.5, Wilcoxon two sample test: $p \leq 0.0012$) and those over 80 had a more than nine-fold greater risk of groin node involvement (GNVI) than those under 60 (36.0% vs. 3.8%, RR = 9.36 95% CI = 2.3-38.3). Smokers/ex-smokers were less likely to have groin node disease than never smokers (14.1% vs. 27.3%, RR = 0.52 95% CI = 0.3-1.0) but this association is of borderline significance and is likely to be confounded by the younger age of smokers/ex-smokers.

Women with positive groin nodes had larger tumours (median size 3.5 vs. 3cms, Wilcoxon two-sample test: $p \leq 0.0219$) and those with tumours >6cms were more likely to have GNVI than those with tumours <2cms in size (41.7% vs. 14.8%, RR = 2.81 95% CI = 1.0-7.8) although this association was of only borderline significance. Women with poorly differentiated tumours were more likely to have GNVI (41.8% vs. 15.6%, RR = 2.69 95% CI = 1.3-5.7).

Compared to women who had uVIN alone in their primary tumour, those with associated LS alone had an increased risk of GNVI (38.5% vs. 16.4%, RR = 2.34 95% CI = 1.2-4.8). Not surprisingly, women with LVS1 were more likely to have GNVI (40.0% vs. 18.6%, RR = 2.15 95% CI = 1.3-3.6). Groin node involvement was not associated with multifocal disease (Chi-square = 0.67; 1df; $p = 0.4127$).

Table 3.11: Table showing the relationship between groin node metastasis (GNVI) and age (in 4 age groups), year of diagnosis in 3 triennia, smoking status, tumour size, tumour differentiation, disease focality, adjacent epithelial abnormalities or LVSI.

Groin node involvement (GNVI) varies with age, tumour size and grade of differentiation					
Variable	Number of cases n = 196	Groin node involvement			
		Yes n = 46	No n = 150	%GNVI	
Year of diagnosis	2000-2	54	40	25.9%	Chi-square = 2.33; 2df; p = 0.3121
	2003-5	51	43	15.1%	
	2006-8	91	67	26.4%	
Age	<60	52	50	3.8%	Chi-square = 16.88; 3df; p = 0.00007
	60-69	35	24	31.4%	
	70-79	59	44	25.4%	
	>80	50	32	36.0%	Wilcoxon two sample test; p <= 0.001195
	median age	77	69.5		
	range	41-90	30-95		
Smoking status	never smoker	99	72	27.3%	Chi-square = 3.76; 1df; p = 0.0526
	smoker/ex-smoker	63	54	14.1%	
	recorded	172	126	20.9%	Chi-square = 0.81; 1df; p = 0.3684
	missing	34	24	29.4%	
Size of tumour	median size	3.5	3		Wilcoxon two sample test; p <= 0.0219
	range	1.0-20	0.5-10		
	<2	27	23	14.8%	
	2-4	61	45	26.2%	Chi-square = 4.68; 3df; p = 0.1968
	4-6	36	26	27.8%	
	>6	24	14	41.7%	
	present	148	108	27.0%	Chi-square = 4.26; 1df; p = 0.0390
Grade of differentiation	missing	48	42	12.5%	
	well	45	38	15.6%	Chi-square = 9.9; 2df; p = 0.0073
	moderate	67	52	22.4%	
	poor	55	32	41.8%	
	present	167	122	26.9%	Chi-square = 7.6; 1df; p = 0.0058
Focality	missing	29	28	3.4%	
	unifocal	162	124	23.5%	Chi-square = 0.67; 1df; p = 0.4127
	multifocal	30	25	16.7%	
	present	192	149	22.4%	
	missing	4	1	25.0%	At least one expected frequency is less than 1
Adjacent epithelial abnormalities	No LS/VIN	29	19	34.5%	At least one expected frequency is less than 1
	LS alone	26	16	38.5%	
	LS/u-VIN	19	13	31.6%	
	LS/d-VIN	24	20	16.7%	
	LS,u-VIN/d-VIN	4	3	25.0%	
	LS/undefined VIN	5	5	0.0%	
	u-VIN alone	73	61	16.4%	
	d-VIN alone	5	5	0.0%	
	u-VIN/d-VIN	8	6	25.0%	
	undefined VIN	3	2	33.3%	
LVSI	missing	28	25	10.7%	Chi-square = 2.96; 1df; p = 0.0854
	recorded	168	125	25.6%	
	negative	113	92	18.6%	Chi-square = 8.91; 1df; p = 0.0028
	positive	55	33	40.0%	

*5 cases with missing information on GNVI were excluded;

3.4.2.10 Women with sub-optimally or incompletely excised disease were older with late stage disease and had larger poorly differentiated tumours while those who had LSVI but not GNVI were less likely to have complete excision (Table 3.12)

In this cohort, 117 (58.2%) tumours were optimally excised and 65 (32.4%) sub-optimally or incompletely excised. No information on excision status was available for 19 (9.5%) women of whom two did not have surgery and 16 had only a biopsy.

Compared to women presenting in the first triennium, those presenting in the last were more likely to have incompletely or sub-optimally excised tumours although this association was of only borderline significance (43.2% vs. 25.5%, RR = 1.7 95% CI = 1.2-1.7). Women with sub-optimally or incompletely excised tumours were older (median age 77 vs. 70, Wilcoxon two-sample test: $p \leq 0.0061$), and those over 80 more than twice as likely to have inadequate excised tumours as those under 60 (54.3% vs. 25.5%, RR = 2.12 95% CI = 1.2-3.7).

Smokers and ex-smokers were no more likely to have sub-optimally or incompletely excised tumours than never smokers (Chi-square = 0.0; 1df; $p = 0.9496$). Sub-optimally or incompletely excised tumours were larger (median size 4 vs. 2.3cms, Wilcoxon two-sample test: $p < 0.0001$), and the risk of inadequate excision increased with increasing tumour size being more than four times greater for tumours larger than 6cms compared with those smaller than 2cms (78.9% vs. 18.5%, RR = 4.26 95% CI = 1.9-9.7).

Not surprisingly, the risk of a sub-optimally or incompletely excised tumour also increased progressively with stage of disease and was more than five times higher in those with stage 4 compared to those with stage 1 disease (66.7% vs. 12.7%, RR = 5.23 95% CI = 2.4-11.7). Poorly differentiated tumours were more than twice as likely to be

inadequately excised as well differentiated tumours (60% vs. 23.3%, RR = 2.58 95% CI = 1.4-4.6).

Women with tumours reported to have LS alone were more likely to have inadequately excised tumours than those with uVIN alone (50.0% vs. 27.9 %, RR = 1.79 95% CI = 1.0-3.1) although this association was of borderline significance. Although the risk of inadequate excision increased in tumours with groin node involvement (59.0% vs. 28.3%, RR = 2.1 95%CI = 1.4-3.0), it was not significantly increased in the presence of LVSI (44.2% vs. 35.6%, RR = 1.24 95%CI = 0.8-1.9).

However, when this analysis was repeated but this time removing those cases with GNVI, LVSI in the absence of groin disease was associated with an increased risk of inadequate excision (51.5% vs. 22.7%, RR = 2.34 95%CI = 1.4-3.9).

Table 3.12: Table showing the relationship between adequacy of tumour excision margins (complete margins vs. sub-optimal or incomplete excision margins) and age (in 4 age groups), year of diagnosis in 3 triennia, smoking status, tumour size, disease stage, tumour differentiation, disease focality, adjacent epithelial abnormalities, LVS and GNVI.

Sub-optimal or incomplete excision of primary VSCC associated with year of diagnosis, age, tumour size, stage of disease, groin node involvement and lymphovascular space involvement in the absence of groin node disease					
Variable	Incompletely or sub-optimally excised*				
	Yes	No	Odds ratio	95%CI	
Year of surgery	2000-2	13	38	1 (ref)	Chi-square = 4.37; 1df: p = 0.1126
	2002-5	17	33	1.33	
	2006-8	35	46	1.70	
Age	<60	12	35	1 (ref)	Chi-square = 9.86; 3df: p = 0.0198
	60-69	11	22	1.31	
	70-79	17	39	1.19	
	>80	25	21	2.12	
	median age	77	70		
	range	30-91	33-95		
Smoking status	never smoker	31	65	1 (ref)	Wilcoxon two sample test: p <= 0.0061
	smoker/ex-smoker	19	39	1.01	
	recorded	50	104	1 (ref)	
	missing	15	13	1.65	
Size of tumour	median size	4	2.3		Wilcoxon two sample test: p <= 5.446e-06
	range	0.5-7	0.9-10		
	recorded	60	82	1 (ref)	
	missing	5	35	0.30	
	<2	5	22	1 (ref)	
	2-4	21	39	1.89	
	4-6	19	17	2.85	
	>6	15	4	4.26	
Stage of disease	1	7	48	1 (ref)	Chi-square = 28.01; 3df; p = 0.0000
	2	25	48	2.69	
	3	25	17	4.68	
	4	8	4	5.23	
grade of differentiation	well	10	33	1 (ref)	Chi-square = 13.69; 2df; p = 0.0011
	moderate	24	42	1.56	
	poor	30	20	2.58	
	recorded	64	95	1 (ref)	
focality	missing	1	22	0.11	Chi-square = 9.77; 1df: p = 0.0018
	unifocal	56	85	1 (ref)	
	multifocal	8	21	0.69	
	recorded	64	106	1 (ref)	
groin node involvement	missing	1	1	1.33	Chi-square = 1.51; 1df; p = 0.2194
	negative	40	101	1 (ref)	
	positive	23	16	2.10	
	recorded	63	117	1 (ref)	
LVSI	missing	2	0	Infinity	Chi-square = 11.28; 1df; p = 0.0008
	negative	37	67	1 (ref)	
	positive	23	29	1.24	
	recorded	60	96	1 (ref)	
LVSI**	missing	5	21	0.5	Chi-square = 12.58; 1df; p = 0.0004
	negative	20	68	1 (ref)	
	positive	17	15	2.34	
	recorded	37	83	1 (ref)	
No LS/VIN	missing	3	18	0.46	At least one expected frequency is less than 1
	negative	19	9	10	
	LS alone	26	13	13	
	LS/u-VIN	19	7	12	
	LS/d-VIN	25	8	17	
	LS,u-VIN/d-VIN	4	2	2	
	LS/undefined VIN	5	0	5	
	u-VIN alone	68	19	49	
	d-VIN alone	8	4	4	
	u-VIN/d-VIN	5	1	4	
undefined VIN	undefined VIN	3	2	1	Chi-square = 10.19; 1df: p = 0.0014
				65	
*19 cases with missing excision status were excluded; restricted to cases without GNVI					

3.4.2.11 Summary of the relationship of baseline clinic-pathological variables

Women with sub-optimally or incompletely excised disease were older and more likely to have late stage disease and larger, poorly differentiated tumours. Those who have GNVI were more likely to have LVSI. Age at diagnosis was not associated in this cohort with tumour size, grade of differentiation or LVSI. However, increasing tumour size was associated with worsening tumour differentiation that in turn was associated with late stage disease and GNVI. Although women with VSCLC associated LS were older than those with VSCLC associated uVIN and more likely to have GNVI, their modest excess risk of sub-optimal or incomplete excision was of borderline significance.

3.4.3 Correlations of HPV positive and negative tumours with baseline variables

(Table 3.13)

This was determined for 143 (71.1%) women with 78 (54.6%) cases tested positive for HPV 16 or HPV 18, or both. Compared to never smokers and ex-smokers, current smokers were more likely to test positive for HPV16 or HPV18, or both (79.4% vs. 44.0%, RR = 1.8, 95% CI = 1.3 – 2.5). Stage 1 tumours were more likely to test positive for HPV16 or HPV18 (72.4% vs. 27.6%, RR = 2.22, 95% CI = 1.05 – 4.67) than those staged 2 or more. LVSI was more likely to be found in HPV-positive than in HPV-negative tumours (66.0% vs. 34.0%, RR = 1.52, 95% CI = 1.1 – 2.1). Compared to women in whom LS alone was detected when VSCLC was diagnosed, those with u-VIN alone were more likely to test positive for high-risk HPV types (70.8% vs. 17.6%, RR = 4.01, 95% CI = 1.4 – 11.4). Those with VIN or no LS were more likely to test positive for HPV types when compared to LS with or without VIN (69.4% vs. 37.3%, RR = 1.86, CI = 1.3 –

2.7). Excision margins were more likely to be reported as incomplete in those who tested positive for HPV types when compared to those who had complete excision (77.8% vs. 50%, RR = 1.55, CI = 1.0-1.25) although this last observation was of only borderline significance.

Triennium of diagnosis, age at diagnosis, the size of the tumour, groin node involvement, tumour differentiation or multifocal disease did not vary significantly with HPV status of the tumour.

Table 3.13: Table showing the relationship between HPV positive/negative tumour and age (in 4 age groups), year of diagnosis in 3 triennia, smoking status, tumour size, disease stage, tumour differentiation, disease focality, adjacent epithelial abnormalities, LVI and GNVI.

Clinicopathological associations of VSCC which test positive for HPV16 and HPV18					
Clinicopathological feature	HPV-ve VSCC	HPV+ve VSCC	Significance testing		
	n = 65 (%)	n = 78 (%)			
Age	median	75	70	Wilcoxon two sample test; p <= 0.0813	
	range	41-92	30-95		
Triennium of diagnosis	first	12 37.5%	20 62.5%	1 (ref)	Chi-square = 1.94;2df: p = 0.3787
	second	20 54.1%	17 45.9%	RR = 0.74, 95%CI 0.5-1.1	
	third	33 44.6%	41 55.4%	RR = 0.89, 95%CI 0.6-1.2	
Smoking status	never smoker	42 56.0%	33 44.0%	1 (ref)	Chi-square = 11.86;1df: p = 0.0006 (current smokers vs never smokers)
	ex-smoker	4 44.4%	5 55.6%	RR = 1.26, 95%CI 0.7-2.4	
	current smoker	7 20.6%	27 79.4%	RR = 1.8, 95%CI 1.3-2.5	
	not known	12 48.0%	13 52.0%	RR = 1.2, 95%CI 0.7-1.9	
Tumour size	median	3	4	Wilcoxon two sample test; p <= 0.1174	
	range	0.5-10	0.9-10		
Focality	unifocal	52 44.8%	64 55.2%	1 (ref)	Chi-square = 0.21;1df: p = 0.6437
	multifocal	12 50.0%	12 50.0%	RR = 0.91, 95%CI 0.6-1.4	
	not known	1 33.30%	2 66.60%	RR = 1.21, 95%CI 0.5-2.7	
Stage of disease	1	8 27.6%	21 72.4%	1 (ref)	Chi-square = 7.6;3df: p = 0.055
	2	34 53.1%	30 46.9%	RR = 0.65, 95%CI 0.5-0.9	
	3	13 39.4%	20 60.6%	RR = 0.84, 95%CI 0.6-1.2	
	4	10 62.5%	6 37.5%	RR = 0.52, 95%CI 0.3-1.0	
	unstaged	0	1		
GNVI	negative	43 41.7%	60 58.3%	1 (ref)	Chi-square = 2.95;1df: p = 0.0857
	positive	21 58.3%	15 41.7%	RR = 0.72, 95%CI 0.5-1.1	
	not known	1	3		
Tumour differentiation	well	14 43.8%	18 56.3%	1 (ref)	Chi-square = 2.12;3df: p = 0.5483
	moderate	27 51.9%	25 48.1%	RR = 0.85, 95%CI 0.6-1.3	
	poor	20 43.5%	26 56.5%	RR = 1.0, 95%CI 0.7-1.5	
	not known	4 30.8%	9 69.2%	RR = 1.23, 95%CI 0.8-2.0	

Continue below

Clinicopathological feature		HPV-ve VSCC	HPV+ve VSCC	Significance testing	
		n = 65 (%)	n = 78 (%)		
LVSI	negative	46 56.8%	35 43.2%	1 (ref)	Chi-square = 10.86;2df: p = 0.0044
	positive	17 34.0%	33 66.0%	RR = 1.52, 95%CI 1.1-2.1	
	not known	2 16.7%	10 62.5%	RR = 1.93, 95%CI 1.4-2.8	
LS or VIN or both	LS-alone	14 82.4%	3 17.6%	1 (ref)	Chi-square = 12.50;1df: p = 0.0004
	no LS/VIN	9 40.9%	13 59.1%	RR = 3.35, 95%CI 1.1-9.9	
	u-VIN alone	14 29.2%	34 70.8%	RR = 4.01, 95%CI 1.4-11.4	
	u-VIN/d-VIN	1 33.3%	3 75.0%	RR = 4.25, 95%CI 1.3-13.7	
	undefined VIN	0 0.0%	3 100.0%	Infinity	
	d-VIN	4 57.1%	3 42.9%	RR = 2.43, 95%CI 0.6-9.2	
	LS/ungraded VIN	1 33.3%	2 66.7%	RR = 3.78, 95%CI 1.0-13.9	
	LS/u-VIN/d-VIN	2 66.7%	1 33.3%	RR = 1.89, 95%CI 0.3-12.6	
	LS-d-VIN	10 47.6%	11 52.4%	RR = 2.97, 95%CI 1.0-9.0	
	LS-u-VIN	10 66.7%	5 33.3%	RR = 1.89, 95%CI 0.5-6.5	
LS+/-VIN vs. any VIN	LS+/-VIN	37 62.7%	22 37.3%	1 (ref)	Chi-square = 12.50;1df: p = 0.0004
	VIN/no LS	19 30.6%	43 69.4%	RR = 1.86, 95%CI 1.3-2.7	
Excision margins	complete	39 50.0%	39 50.0%	1 (ref)	Chi-square = 1.51;1df: p = 0.2193 (complete excision vs incomplete and sub-optimal excision)
	suboptimal	20 42.6%	27 57.4%	RR = 1.15, 95%CI 0.8-1.6	
	incomplete	2 22.2%	7 77.8%	RR = 1.55, 95%CI 1.0-2.4	
	not known	4 44.4%	5 55.6%	RR = 1.11, 95%CI 0.6-2.1	

3.4.4 Missing information (Table 3.14)

Before performing a multivariate analysis, those variables for which information is missing in ~10% of cases are considered in more detail. This analysis focuses on how missing information varies over time and with age at diagnosis, stage of disease and the sample provided for histological examination.

Table 3.14: Table showing the associations and determinants of missing information.

		Associations and determinants of missing information							
Variable	No. of cases	Smoking status n %	Grade of differentiation n %	Tumour size n %	Excision margins n %	No VIN/LS recorded n %	LVSI n %		
Year of surgery	2000-2	55	4 7.3%	9 16.4%	23 41.8%	4 7.3%	9 16.4%	12 21.8%	
	2002-5	52	6 11.5%	5 11.5%	Chi-square = 1.32; 2df: $p = 0.5166$	2 4.32%; 2df: $p = 0.0024$	Chi-square = 4.32; 2df: $p = 0.1154$	6 11.5%	Chi-square = 0.64; 2df: $p = 0.7269$
	2006-8	94	27 28.7%	15 16.0%	19 20.2%	13 13.8%	15 16.0%	10 10.6%	= 3.95; 2df: $p = 0.1386$
Age	<60	54	6 11.1%	14 25.9%	25 46.3%	7 11.7%	8 14.8%	11 20.0%	
	60-69	35	3 8.6%	5 8.6%	10 28.6%	2 5.7%	7 20.0%	3 8.6%	Chi-square = 1.22; 3df: $p = 0.7480$
	70-79	60	12 20.0%	6 10.0%	Chi-square = 8.65; 3df: $p = 0.0344$	5 8.3%	4 6.7%	7 11.7%	= 4.77; 3df: $p = 0.1895$
	>80	52	16 30.8%	4 7.7%	10 23.8%	6 11.5%	8 15.4%	9 17.3%	
					median (status unknown) = 57 (30-92), median (status known) = 75 (33-95);Wilcoxon two sample test, $p \leq 0.0009$	median (status unknown) = 75 (39-90), median (status known) = 75 (33-95);Wilcoxon two sample test, $p \leq 0.909$	median (status unknown) = 72 (42-90), median (status known) = 72 (33-95);Wilcoxon two sample test, $p \leq 0.9742$	median (status unknown) = 70.5 (30-88), median (status known) = 72 (33-95);Wilcoxon two sample test, $p \leq 0.6514$	
					median (status unknown) = 63 (30-87), median (status known) = 74 (33-95);Wilcoxon two sample test, $p \leq 0.0039$	median (status unknown) = 72 (30-95);Wilcoxon two sample test, $p \leq 0.9636$	median (status unknown) = 72 (30-95);Wilcoxon two sample test, $p \leq 0.9742$	median (status unknown) = 70.5 (30-88), median (status known) = 72 (33-95);Wilcoxon two sample test, $p \leq 0.6514$	
Stage	1a	29	3 10.3%	18 62.1%	19 65.5%	3 10.3%	1 3.4%	8 27.6%	
	1b	31	5 16.1%	6 19.4%	11 35.5%	2 6.5%	3 9.7%	8 25.8%	
	2	74	11 14.9%	Chi-square = 67.17; 4df: $p = 0$, but >20% of expected frequencies are < 5	10 13.5%	1 1.4%	11 20% of expected frequencies are less than 5	6 At least 20% of expected frequencies are less than 5	At least 20% of expected frequencies are less than 5
	3	46	12 26.1%	1 2.2%	5 10.9%	4 26.1%	4 8.7%	6 8.1%	
	4	20	6 30.0%	1 5.0%	4 20.0%	8 40.0%	11 55.0%	5 10.9%	
	Unstaged	1	0 0.0%	0 0.0%	0 100.0%	1 0.0%	0 0.0%	0 5.0%	0 0.0%

Continue below

Variable	No. of cases		Smoking status		Grade of differentiation		Tumour size		Excision margins		No VIN/LS recorded		LVSI	
	n	%	n	%	n	%	n	%	n	%	n	%	n	%
Treatment	Radical Vulvectomy	56	14	2	3.6%	5	8.9%	1	1.8%	6	10.7%	3	5.4%	
	En Bloc vulvectomy	12	0	0	0.0%	2	16.7%	0	0.0%	2	16.7%	2	16.7%	
	Biopsy	16	6	4	26.7%	9	56.3%	16	100.0%	9	56.3%	4	25.0%	
	Ano-vulvectomy	6	1	0	0.0%	0	0.0%	0	0.0%	1	16.7%	0	0.0%	
	Lt Hemivulvectomy	2	0	0	0.0%	1	50.0%	0	0.0%	1	50.0%	1	50.0%	
	Rt Hemivulvectomy	12	2	At least 20% of expected frequencies are less than 5	8.3%	0	At least 20% of expected frequencies are less than 5	0	0.0%	0	At least 20% of expected frequencies are less than 5	1	At least 20% of expected frequencies are less than 5	
	Posterior Hemivulvectomy	4	0	0	0.0%	1	25.0%	5	100.0%	0	0.0%	0	0.0%	
	Ant hemivulvectomy	29	0	5	6.9%	6	20.7%	5	100.0%	4	13.8%	5	17.2%	
	Radical WLE	57	12	15	26.3%	21	36.8%	0	0.0%	3	5.3%	8	14.0%	
	Radical WLE of scar	1	0	0	0.0%	1	100.0%	0	0.0%	1	100.0%	0	0.0%	
Surgery	Simple vulvectomy	1	0	0	0.0%	1	100.0%	0	0.0%	0	0.0%	1	100.0%	
	No surgery	2	2	2	100.0%	0	0.0%	2	100.0%	2	100.0%	2	100.0%	
	Simple WLE	3	0	3	100.0%	3	100.0%	0	0.0%	0	0.0%	1	33.3%	

3.4.4.1 Smoking history not recorded

A smoking history was not available for 37 women (18.4%). How often a smoking history went unrecorded varied over time and with age. It was nearly four times more likely to be unrecorded in the last triennium of the study period than in the first (28.7% vs. 7.3%, RR = 3.95 95% CI = 1.5-10.7), and three times more likely to be unrecorded in women over 80 than those under 60 (30.8% vs. 10.0%, RR = 3.1 95% CI = 1.3-7.3). A woman who was over 80 and diagnosed in the last triennium was nine times more likely to have her smoking history unrecorded than a woman under 60 diagnosed in the first triennium, (51.9% vs. 5.6%, RR = 9.3 95% CI = 1.3-64.9).

3.4.4.2 Tumour size not recorded

No tumour size was available for 50 (24.9%) women in this cohort. How often tumour size went unrecorded varied over time, with age and with the stage of the disease. Tumours diagnosed in the second and third triennium were less likely to have tumour size unrecorded than those diagnosed in the first (15.4% vs. 41.8%, RR = 0.37 95% CI = 0.2-0.7; 20.2% vs. 41.8%, RR = 0.48 95% CI = 0.3-0.8). Women with missing information on tumour size were younger (median 57 vs. 75 years, Wilcoxon two sample test: p <= 7.09e-05). Most (n = 30) had stage 1 disease, and those with stage 1a and stage 1b disease were nearly five and three times more likely to have tumour size unrecorded than those with stage 2 disease, (65.5% vs. 13.5%, RR = 4.85 95% CI = 2.6-9.1; 35.5% vs. 13.5%, RR = 2.98 95% CI = 1.4-6.3).

3.4.4.3 Tumour differentiation not recorded

Grade of tumour differentiation was not available for 29 (14.4%) women in this cohort.

How often grade of differentiation went unrecorded varied with age and stage of disease and the sample provided. Women with missing information on grade of differentiation were younger (median 63 vs. 74 years, Wilcoxon two sample test: $p \leq 0.0009$). Most ($n = 24$) had stage 1 disease; those with stage 1a and stage 1b disease were fifteen and four times more likely to have grade of differentiation unrecorded than women with stage 2 disease (62.1% vs. 4.1%, RR = 15.3 95% CI = 4.9-48.1; 19.4% vs. 4.1%, RR = 4.77 95% CI = 1.3-17.9).

In addition to the two women who did not have surgery, 19 of the women with missing information on tumour differentiation had a wide local excision and 4 had a biopsy alone. Compared to women who had a radical vulvectomy, those who had a biopsy or a wide local excision (simple or radical) were seven and eight times more likely to have grade of differentiation unrecorded (26.7% vs. 3.6%, RR = 7.0 95% CI = 1.4-34.8; 30% vs. 3.6%, RR = 8.4 95% CI = 2.0-34.6).

3.4.4.4 Lymphovascular space involvement (LVSI) not recorded

No information on LVSI was available for 28 (13.9%) of women in this cohort. How often LVSI went unrecorded varied significantly with the stage of disease and the surgical sample provided. Most ($n = 16$) of these women had stage 1 disease; those with stage 1a and stage 1b disease were three times more likely to have their grade of differentiation unrecorded than those with stage 2 disease (27.6% vs. 8.1%, RR = 3.4 95% CI = 1.3-9; 25.8% vs. 8.1%, RR = 3.18 95% CI = 1.2-8.4).

Compared to women who had a radical vulvectomy, those who had a biopsy alone were more than four times as likely to have grade of differentiation unrecorded (25.0% vs. 5.4%, RR = 4.67 95% CI = 1.2-18.7). Figure 3.2 shows how often tumour size, grade of differentiation and LVSIs went unrecorded in the same surgical samples.

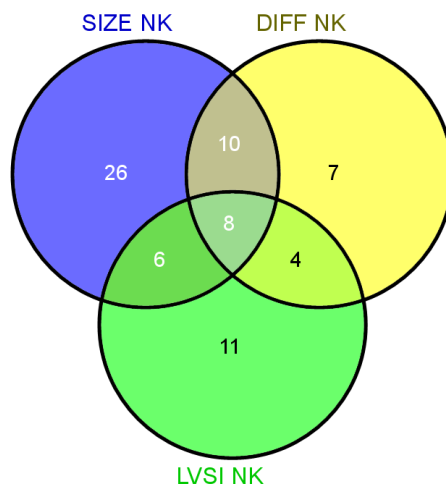


Figure 3.2: The frequency with which tumour size, grade of differentiation and LVSIs were not recorded in the same surgical sample (NK = not known; DIFF = tumour differentiation).

3.4.4.5 LS or VIN not recorded

There was no comment on LS or VIN in the pathology report of 30 (14.9%) women in this cohort. How often LS or VIN went unrecorded varied with the stage of disease and the sample provided.

Half of these women ($n = 15$) had stage 3 or 4 disease; those with stage 4 disease were nearly four times as likely not to have LS or uVIN as women with stage 2 disease (55% vs. 14.9%, RR = 3.7 95% CI = 1.9-7.3). Women who had a biopsy alone were more than

five times as likely not to have a comment on LS or VIN in their pathology report than those who had a radical vulvectomy (56.3% vs. 10.7%, RR = 5.25 95% CI = 2.2-12.5).

3.4.4.6 Excision status not determined

Excision status was unknown for 19 (9.5%) women in this cohort. Women with stage 4 disease were nearly 30 times more likely to have inadequately excised tumours than those with stage 2 disease (40.0% vs. 1.4%, RR = 21.4 95% CI = 2.8-163.7). However, the main determinant of undetermined excision status was the sample provided for histological analysis. Excision status was unknown in all 16 women who had had a biopsy alone, two who had no surgery and one who had a radical vulvectomy.

3.4.4.7 Summary

Enthusiasm for taking a smoking history appears to be less in recent years. Whereas missing information on tumour size, tumour differentiation and LVI is more common in those with early stage disease, no mention of LS or VIN on the pathology and the absence of a comment on excision status is more common in women with late stage disease and in those who provided a biopsy alone for histological examination.

3.5 Analysis of local disease recurrence (Time to local recurrence)

3.5.1 Overview

44 (21.9%) women in this series were found to have local disease recurrence following surgery that was unlikely to be explained by treatment failure. For this analysis, local recurrence was further classified into local relapse and second field tumour (see Figure 1.2 in introduction). Tumour that recurred within 2cm of the primary tumour was

termed local relapse (LR) while those tumour that recurred more than 2cm away from the primary tumour was termed second field tumour (SFT). Of the 44 patients who had local recurrence, 29 had local relapse alone, 26 had second field tumour alone and 11 had both local relapse and second field tumour (Table 3.15). Figure 3.3 shows the Kaplan-Meir (KM) plots of time to local recurrence, time to local relapse and time to second field tumour. The proportion of patients who developed local recurrence, LR and SFT in 5 years were 25.8% (95% CI 19.4-33.9%; 13.4%, 95% CI 8.7-20.5%) and 16.5% (95% CI 11.3-23.8%), respectively. There is no significant difference in the time taken to develop local relapse and second field tumour but patients were at the greatest risks of developing LR and SFT within the first five years after their treatment.

Figures 3.4 represents underlying risk (rate) over time for LR and SFT outcomes for those with women LS associated VSCC which were estimated by survival modelling procedures: patient characteristics, or covariates, in a statistical survival model, modify this hazard proportionally. For example groin node involvement, a known prognostic factor, would proportionally increase the magnitude of this function throughout the time period. Although not formally compared, visual inspection indicates that patients are at an increasing risk of recurrent disease in the years following surgery and that this risk dissipates after 4-5 years, and 2 years for LR and SFT respectively. These observations indicate that SFT are likely to occur earlier than local relapses.

Univariate and multivariate analyses were performed to identify possible prognostic markers that were likely to influence disease recurrence.

Table 3.15: Distribution of treatment outcomes in women diagnosed with primary VSCC in Birmingham between 2000 to 2008.

Distribution of treatment outcomes in Birmingham VSCC cohort			
Outcomes		Number of cases	%
Local recurrence	Yes	44	21.9
	No	157	78.1
Local relapse	Yes	29	14.4
	No	172	85.6
Second field tumour	Yes	26	12.9
	No	175	87.1
Groin node recurrence	Yes	16	8.0
	No	185	92.0
Disease related mortality	Yes	41	20.4
	No	160	79.6

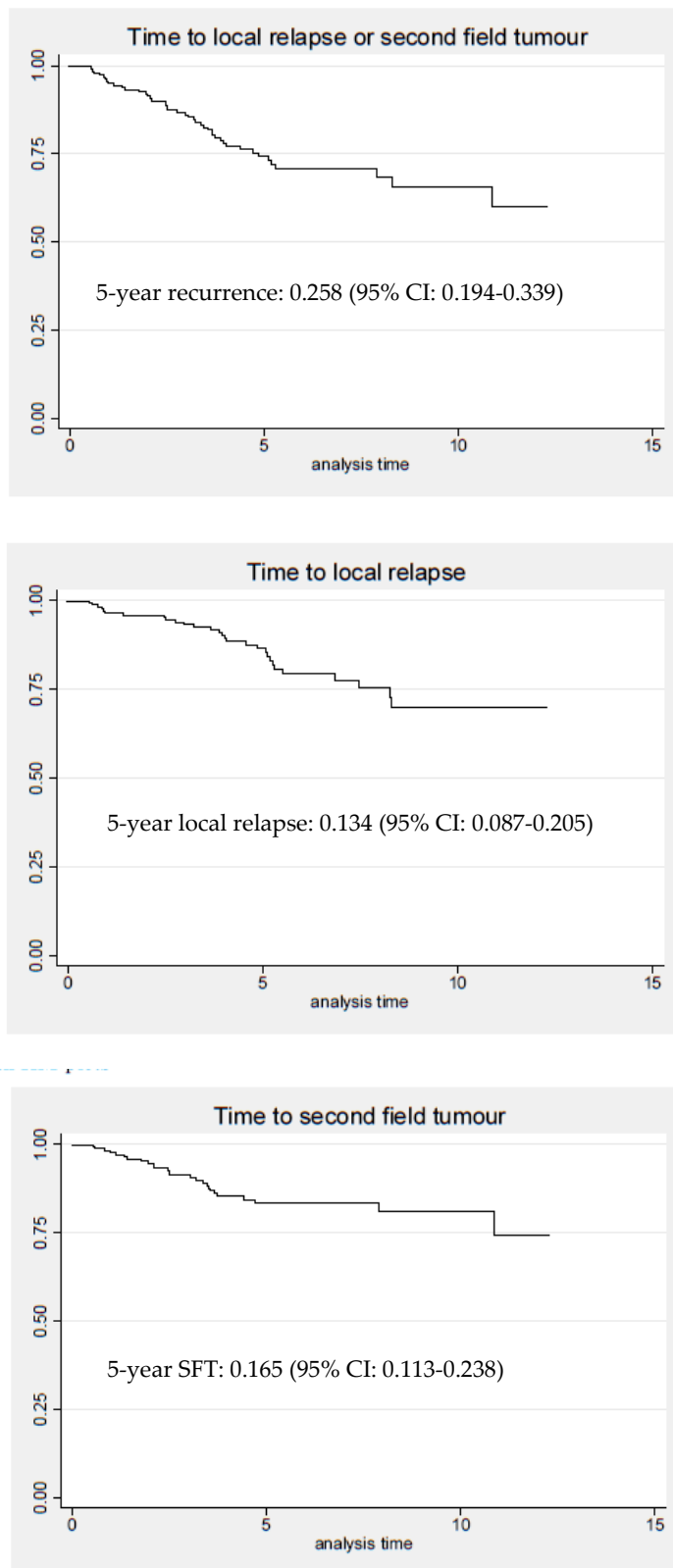


Figure 3.3: KM-plots for time to local relapse (LR) or 2nd field tumour (SFT), time to LR and time to SFT.

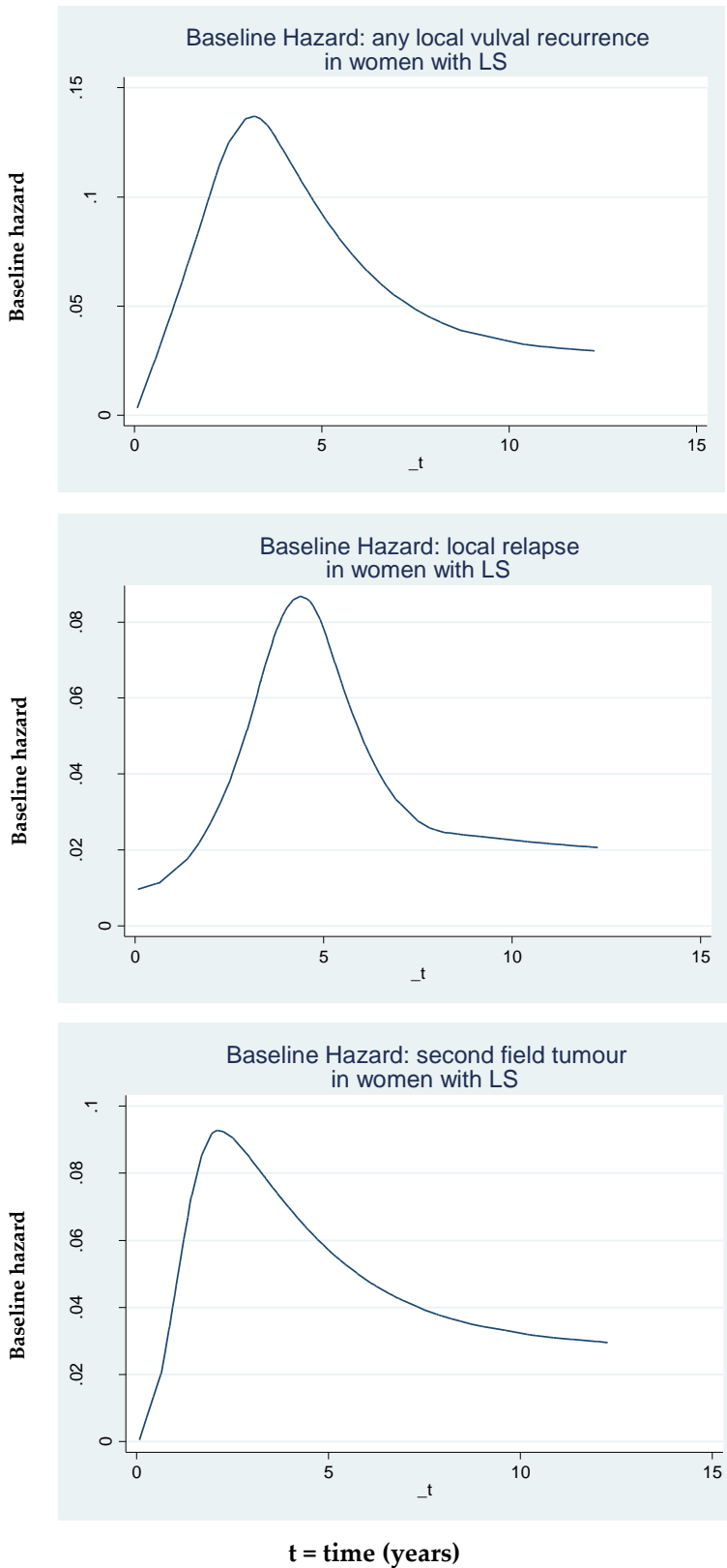


Figure 3.4: Plots of baseline hazard ratio to time of surgery for local recurrence, LR and SFT.

3.5.2 Univariate analysis

3.5.2.1 Univariate analysis of local recurrence (local relapse and/or second field tumour (Table 3.16)

Univariate analyses revealed seven variables which modulated the risk of women with VSCC developing a local recurrence, either a local relapse or a second field tumour or both: the presence of Lichen Sclerosus with or without associated VIN in the pathological specimen; age; smoking status; groin node metastasis; LVSI; advanced disease stage; and HPV test positivity.

Compared to women who were younger than 65 years at diagnosis those who were 65 and older had an increased risk of a local recurrence (HR: 3.13, 95% CI: 1.49-6.55, p= 0.003) as did women found to have LS+/-VIN (HR: 3.61, 95% CI: 1.91-6.82, p<0.001) in the surgical specimen. Compared to never smokers, current smokers had a reduced risk of developing a local recurrence (HR: 0.32, 95% CI: 0.14-0.73, p= 0.007) as did patients with tumours in which lymphovascular spaces (HR: 0.36, 95% CI: 0.14-0.93, p= 0.035) were reported to be involved. Women with advanced stage disease were twice more likely to develop local recurrence when compared to those with early stage disease (HR: 2.76, 95% CI 1.14-4.10, p=0.007). Patients who were tested negative for HR-HPV were more likely to have disease recurrence when compared to those who tested positive (HR: 2.26, 95% CI: 1.07-4.76, p= 0.032). Those with groin node metastasis at baseline were also more likely to develop local recurrence when compared to those without groin node metastasis (HR: 3.39, 95% CI: 1.76-6.53, p<0.001).

As previously shown some of these variables were found to be correlated with each other. For instance, women with LS+/-VIN were older than those without LS+/-VIN

(Wilcoxon two-sample test, $p \leq 0.0014$) as were women with groin node involvement compared to those without (Wilcoxon two-sample test, $p \leq 0.0012$). Current smokers were younger than never smokers (Wilcoxon two-sample test, $p \leq 3.964e-05$). The inverse relationship between smoking and age which is almost certainly a cohort effect could explain in large part why compared to never smokers, current smokers were less likely to have LS+/-VIN (19.6% vs. 46%, RR = 0.43 95% CI = 0.2-0.8) and GNVI (14.1% vs. 27.3%, RR = 0.52 95% CI = 0.3-1.3) although this is borderline significant.

Table 3.16: Summary of univariable HR (95%CI) for potential predictors of time to local relapse or second field tumour.

Covariate (LR p-value)	HR (95% CI)	P-value
Age (years) (p<0.01)		
<65 (Ref. Category)		
≥65	3.13 (1.49, 6.55)	0.003
Smoking status (p<0.01)		
No (Ref. Category)		
Smoker/Ex-Smoker	0.32 (0.14, 0.73)	0.007
Stage (simplified) (p=0.026)		
1/2 (Ref. Category)		
3/4	2.16 (1.13, 4.10)	0.019
Tumour Size (p=0.983)		
< 2cm (Ref. Category)		
2-<4cm	1.00 (0.42, 2.36)	0.999
4-<6cm	0.95 (0.35, 2.55)	0.920
≥ 6cm	0.79 (0.21, 3.00)	0.724
Disease Multifocal (p=0.990)		
No (Ref. Category)		
Yes	0.99 (0.44, 2.23)	0.990
Groin node involvement (p<0.01)		
No (Ref. Category)		
Yes	3.39 (1.76, 6.53)	0.000
Groin Node Surgery (p=0.637)		
No nodal surgery (Ref. Category)		
SNLB/GLND	0.86 (0.45, 1.62)	0.633
LVSI (p=0.045)		
No (Ref. Category)		
Yes	0.36 (0.14, 0.93)	0.035
Unavailable	0.59 (0.25, 1.41)	0.236
Excision Margins (p=0.933)		
Optimum (Ref. Category)		
Sub-optimum	1.09 (0.54, 2.18)	0.817
Incomplete	1.27 (0.30, 5.33)	0.743
Histology grade (p=0.689)		
Well (Ref. Category)		
Moderate	1.03 (0.46, 2.30)	0.942
Poorly	1.39 (0.61, 3.16)	0.435
LS, +/- Vin (p<0.01)		
No LS (Ref. Category)		
LS, +/- Vin	3.61 (1.91, 6.82)	0.000
Type of Surgery (p=0.587)		
Biopsy or No Surgery (Ref. Category)		
Simple wide local excision	1.86 (0.12, 29.80)	0.661
Radical WLE or hemi-vulvectomy	1.77 (0.24, 13.19)	0.576
Total radical vulvectomy	2.55 (0.34, 19.12)	0.363
RT given for sub-optimal surgery (p=0.316)		
No (Ref. Category)		
Yes	1.60 (0.67, 3.79)	0.288
HPV 16/18 E6 (p=0.028)		
X (Ref. Category)		
P	0.44 (0.21, 0.93)	0.032

3.5.2.2 Univariate analysis of local relapse

Univariate analysis revealed 3 variables which modulate the risks of women with VSCC developing a local relapse: the presence of Lichen Sclerosus with or without associated VIN in the pathological specimen; age; and groin node metastasis (Table 3.17).

Women aged 65 years and older were more likely to develop local relapse when compared to those that were younger than 65 (HR: 3.01, 95% CI: 1.22-7.40, p= 0.017) as did women found to have groin node metastasis (HR: 3.55, 95% CI: 1.60-7.87, p=0.002) or those found to have LS+/-VIN in the surgical specimen (HR: 2.85, 95% CI: 1.32-6.13, p=0.007).

Table 3.17: Summary of univariable HR (95%CI) for potential predictors of time to local relapse (LR)

Covariate (LR p-value)	HR (95% CI)	P-value
Age (years) (p<0.01)		
<65 (Ref. Category)		
≥65	3.01 (1.22, 7.40)	0.017
Smoking status (p=0.201)		
No (Ref. Category)		
Smoker/Ex-Smoker	0.56 (0.22, 1.42)	0.220
Stage (simplified) (p=0.078)		
1/2 (Ref. Category)		
3/4	2.13 (0.96, 4.73)	0.063
Tumour Size (p=0.678)		
< 2cm (Ref. Category)		
2-<4cm	1.66 (0.54, 5.10)	0.378
4-<6cm	0.95 (0.24, 3.81)	0.043
≥ 6cm	1.08 (0.20, 5.93)	0.932
Disease Multifocal (p=0.784)		
No (Ref. Category)		
Yes	1.15 (0.44, 3.01)	0.781
Groin node involvement (p<0.01)		
No (Ref. Category)		
Yes	3.55 (1.60, 7.87)	0.002
Groin Node Surgery (p=0.505)		
No nodal surgery (Ref. Category)		
SNLB/GLND	0.77 (0.36, 1.65)	0.498
LVSI (p=0.090)		
No (Ref. Category)		
Yes	0.33 (0.10, 1.09)	0.070
Unavailable	0.56 (0.19, 1.62)	0.282
Excision Margins (p=0.587)		
Optimum (Ref. Category)		
Sub-optimum	1.21 (0.51, 2.91)	0.663
Incomplete	2.26 (0.53, 9.71)	0.274
Histology grade (p=0.665)		
Well (Ref. Category)		
Moderate	0.92 (0.37, 2.33)	0.865
Poorly	0.60 (0.18, 1.96)	0.398
LS, +/- Vin (p<0.01)		
No LS (Ref. Category)		
LS, +/- Vin	2.85 (1.32, 6.13)	0.007
Type of Surgery (p=0.628)		
Biopsy or No Surgery (Ref. Category)		
Simple wide local excision	0.00 (0.00, .)	1.000
Radical WLE or hemi-vulvectomy	0.92 (0.12, 7.05)	0.939
Total radical vulvectomy	1.20 (0.15, 9.36)	0.861
RT given for sub-optimal surgery (p=0.431)		
No (Ref. Category)		
Yes	1.57 (0.54, 4.50)	0.406
HPV 16/18 E6 (p=0.188)		
X (Ref. Category)		
P	0.55 (0.23, 1.35)	0.194

3.5.2.3 Univariate analysis of second field tumour

Univariate analysis revealed 3 variables which modulate the risk of women with VSCC developing a second field tumour: the presence of LS with or without associated VIN in the pathological specimen; age; and smoking status (Table 3.18).

Compared to women who were younger than 65 years at diagnosis those who are 65 and older had an increased risk of developing a second field tumour (HR: 3.32, 95% CI: 1.23-8.92, p= 0.017). Those patients who were found to have LS+/-VIN in the surgical specimen were also more likely to develop a second field tumour (HR: 5.43, 95% CI: 2.18-13.52, p<0.001). Compared to never smokers, current smokers had a reduced risk of developing a second field tumour (HR: 0.18, 95% CI: 0.06-0.62, p= 0.006).

Table 3.18: Summary of univariable HR (95%CI) for potential predictors of time to second field tumour (SFT).

Covariate (LR p-value)	HR (95% CI)	P-value
Age (years) (p<0.01)		
<65 (Ref. Category)		
≥65	3.32 (1.23, 8.92)	0.017
Smoking status (p<0.01)		
No (Ref. Category)		
Smoker/Ex-Smoker	0.18 (0.06, 0.62)	0.006
Stage (simplified) (p=0.320)		
1/2 (Ref. Category)		
3/4	1.58 (0.66, 3.80)	0.302
Tumour Size (p=0.627)		
< 2cm (Ref. Category)		
2-<4cm	0.65 (0.24, 1.77)	0.395
4-<6cm	0.57 (0.17, 1.97)	0.374
≥ 6cm	0.32 (0.04, 2.65)	0.292
Disease Multifocal (p=0.168)		
No (Ref. Category)		
Yes	0.41 (0.10, 1.73)	0.225
Groin node involvement (p=0.139)		
No (Ref. Category)		
Yes	2.10 (0.84, 5.27)	0.113
Groin Node Surgery (p=0.837)		
No nodal surgery (Ref. Category)		
SNLB/GLND	0.92 (0.40, 2.11)	0.836
LVSI (p=0.535)		
No (Ref. Category)		
Yes	0.57 (0.19, 1.68)	0.309
Unavailable	0.75 (0.25, 2.22)	0.603
Excision Margins (p=0.233)		
Optimum (Ref. Category)		
Sub-optimum	0.69 (0.26, 1.83)	0.449
Incomplete	0.00 (0.00, .)	1.000
Histology grade (p=0.629)		
Well (Ref. Category)		
Moderate	1.18 (0.41, 3.40)	0.763
Poorly	1.66 (0.57, 4.81)	0.351
LS, +/- Vin (p<0.01)		
No LS (Ref. Category)		
LS, +/- Vin	5.43 (2.18, 13.52)	0.000
Type of Surgery (p=0.361)		
Biopsy or No Surgery (Ref. Category)		
Simple wide local excision	1.36 (0.17, 10.67)	0.767
Radical WLE or hemi-vulvectomy	0.78 (0.35, 1.78)	0.561
Total radical vulvectomy	1.00 (., .)	.
RT given for sub-optimal surgery (p=0.775)		
No (Ref. Category)		
Yes	1.20 (0.36, 3.99)	0.770
HPV 16/18 E6 (p=0.081)		
X (Ref. Category)		
P	0.42 (0.16, 1.14)	0.089

3.5.3 Multivariate analysis

3.5.3.1 Multivariate analysis of local recurrence (local relapse and/or second field tumour)

Multivariate analyses revealed that the three independent predictors that best describe risk of women with VSCC developing a local recurrence, either a local relapse or a second field tumour or both: age; groin node metastasis; and LS+/-VIN (see Table 3.19). Compared to women who were younger than 65 years at diagnosis those who are 65 and older were twice more likely to develop a local recurrence (HR 2.202, 95% CI: 1.026-4.727, p = 0.043). Patients with groin node metastasis and LS +/- VIN found in the surgical specimen were 2.6 times (HR: 2.568, 95% CI: 1.327-4.967, p= 0.005) and 2.8 times (HR: 2.792, 95% CI: 1.464-5.322, p= 0.002), respectively, were at greater risk of developing a local recurrence. It is noted that when adjusting for other prognostic characteristics the hazard ratio associated with LS+/-VIN is reduced compared to those observed in the univariate analysis, HR: 2.568 vs. 3.61 (see Table 3.16).

Table 3.19: Summary of multivariable HR (95%CI) for potential predictors of time to local recurrence

Variable	Level	HR (95% CI)	P-value
LS, +/- Vin	No LS	1.000 (Ref. Category)	-
	LS, +/- Vin	2.792 (1.464, 5.322)	0.002
Groin node involvement	No	1.000 (Ref. Category)	-
	Yes	2.568 (1.327, 4.967)	0.005
Age (years)	<65	1.000 (Ref. Category)	-
	≥65	2.202 (1.026, 4.727)	0.043

3.5.3.2 Multivariate analysis of local relapse

Multivariate analyses revealed two independent predictors that modulated the risk of women with VSCC developing a local relapse: groin node metastasis and LS+/-VIN (see Table 3.20).

Women with groin node disease were three times more likely to develop a local relapse when compared with those without nodal disease (HR: 2.909, 95% CI: 1.295-6.533, p= 0.010). Patients who were found to have LS +/- VIN in the surgical specimen were twice more likely to develop local relapse when compared to those without LS (HR: 2.380, 95% CI: 1.088-5.204, p= 0.30). It is noted that when adjusting for other prognostic characteristics the hazard ratio associated with LS +/- VIN is reduced compared to those observed in the univariate analysis, HR: 2.38 vs. 2.85 (see Table 3.17).

Table 3.20: Summary of multivariable HR (95%CI) for potential predictors of time to local relapse (LR).

Variable	Level	HR (95% CI)	P-value
LS, +/- Vin	No LS	1.000 (Ref. Category)	.
	LS, +/- Vin	2.380 (1.088, 5.204)	0.030
Groin node involvement	No	1.000 (Ref. Category)	.
	Yes	2.909 (1.295, 6.533)	0.010

3.5.3.4 Multivariate analysis of second field tumour

Multivariate analyses revealed two independent predictors that modulated the risk of women with VSCC developing a second field tumour: LS+/-VIN and smoking status (see Table 3.21).

Women with LS +/- VIN found in the histological specimen were 5 times more likely to develop a second field tumour when compared to those without LS (HR 4.932, 95% CI: 1.957-12.431, p= 0.001). Compared to never smokers, current smokers were four times less likely to develop a second field tumour (HR: 4.178, 95% CI: 1.241-14.074, p= 0.021).

After adjusting for smoking, the risk associated with LS is slightly reduced when compared to the results of the univariate analysis, HR: 4.932 vs. 5.43 (see Table 3.18).

Table 3.21: Summary of multivariable HR (95%CI) for potential predictors of time to second field tumour (SFT)

Variable	Level	HR (95% CI)	P-value
LS, +/- Vin	No LS	1.000 (Ref. Category)	.
	LS, +/- Vin	4.932 (1.957, 12.431)	0.001
Smoking status	Smoker/Ex-Smoker	1.000 (Ref. Category)	.
	No	4.178 (1.241, 14.074)	0.021

3.6 Analysis of groin node recurrence

3.6.1 Overview, univariate and multivariate analysis

Groin node recurrence was found in 16 (8%) patients in this series and half of them previously had treatment for groin metastasis along with their primary tumour (Table 3.15). Univariate analysis (see Table 3.22) revealed four prognostic factors that modulate the risk of groin node recurrence: those women older than 65 years (HR: 4.96, 95% CI 1.04-23.70, p=0.044); poorly differentiated histology grade (HR: 5.73, 95% CI: 1.24-26.53, p= 0.026); advance disease stage (HR: 4.89, 95% CI 1.72-13.98, p=0.003); and previous groin node metastasis (HR: 5.83, 95% CI: 2.10-16.26, p<0.001). However, multivariate analysis revealed that only those women with previous groin node disease were at risk of developing groin node recurrence (HR: 5.849, 95% CI: 2.104-16.259, p= 0.001).

Table 3.22: A summary of the univariate analysis for potential predictors of time to nodal recurrence.

Covariate (LR p-value)	HR (95% CI)	P-value
Age (years) (p=0.018)		
<65 (Ref. Category)		
≥65	4.96 (1.04, 23.70)	0.044
Smoking status (p=0.121)		
No (Ref. Category)		
Smoker/Ex-Smoker	0.33 (0.07, 1.55)	0.161
Stage (simplified) (p<0.01)		
1/2 (Ref. Category)		
3/4	4.89 (1.72, 13.94)	0.003
Tumour Size (p=0.276)		
< 2cm (Ref. Category)		
2-<4cm	0.63 (0.11, 3.79)	0.617
4-<6cm	2.35 (0.47, 11.65)	0.296
≥ 6cm	1.49 (0.21, 10.61)	0.690
Disease Multifocal (p=0.021)		
No (Ref. Category)		
Yes	0.00 (0.00, .)	1.000
Groin node involvement (p<0.01)		
No (Ref. Category)		
Yes	5.85 (2.10, 16.26)	0.001
Groin Node Surgery (p=0.363)		
No nodal surgery (Ref. Category)		
SNLB/GLND	1.75 (0.49, 6.21)	0.387
LVSI (p=0.497)		
No (Ref. Category)		
Yes	0.92 (0.29, 2.94)	0.890
Unavailable	0.34 (0.04, 2.69)	0.308
Excision Margins (p=0.470)		
Optimum (Ref. Category)		
Sub-optimum	1.91 (0.65, 5.58)	0.237
Incomplete	1.95 (0.24, 15.75)	0.529
Histology grade (p=0.010)		
Well (Ref. Category)		
Moderate	1.28 (0.21, 7.71)	0.785
Poorly	5.73 (1.24, 26.53)	0.026
LS, +/- Vin (p=0.290)		
No LS (Ref. Category)		
LS, +/- Vin	1.73 (0.63, 4.77)	0.290
Type of Surgery (p=0.245)		
Total radical vulvectomy (Ref. Category)		
Biopsy or No Surgery	0.00 (0.00, .)	1.000
Simple wide local excision	0.00 (0.00, .)	1.000
Radical WLE or hemi-vulvectomy	0.49 (0.17, 1.41)	0.185
RT given for sub-optimal surgery (p=0.266)		
No (Ref. Category)		
Yes	2.18 (0.61, 7.75)	0.228
HPV 16/18 E6 (p=0.400)		
X (Ref. Category)		
P	0.61 (0.19, 1.93)	0.404

3.7 Analysis of disease-specific survival

3.7.1 Overview

All the patients who were still alive in this series were being followed up for at least five years and the median follow-up duration for the cohort was 4.6 years (IQR: 1.8-7.1 years). 110 (54.7%) patients within this cohort were still alive when the information on follow-up was last updated on 31st December 2012. There were 91 (45.3%) deaths and 41 (45.1%) of those were attributed to VSCC. The remaining 50 (54.9%) patients died of causes other than VSCC related. Figure 3.5 shows the Kaplan-Meier (KM) plot for VSCC specific mortality where 10% of death from VSCC occurs within the first year after treatment. The proportion of patients who were still alive in 5 years was 81.4%, 95% CI: 74.8-86.3%. A univariate and multivariate analysis were constructed to identify possible prognostic markers that influence VSCC specific mortality.

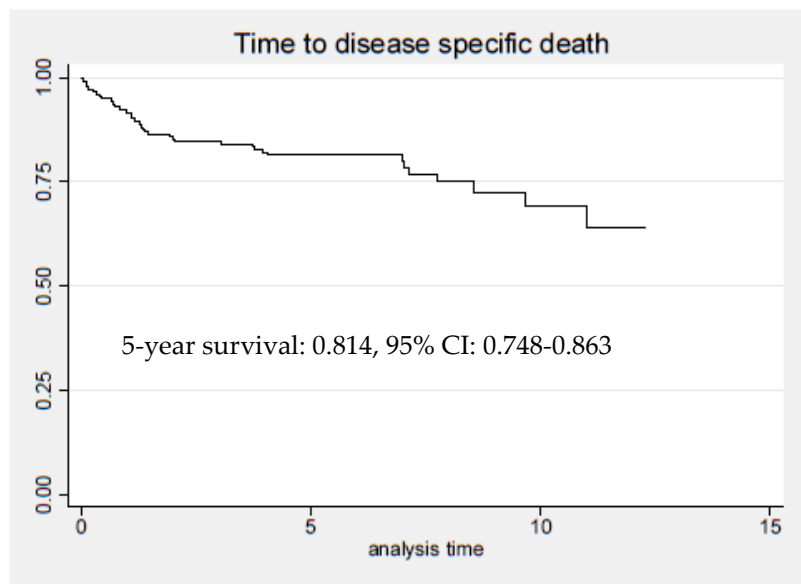


Figure 3.5: Kaplan-Meier (KM) plot for disease (VSCC) specific mortality.

3.7.2 *Univariate analysis of disease specific survival*

Univariate analysis revealed 8 prognostic factors which modulate the risk of women dying from VSCC: age; type of non-surgical interventions; disease stage; tumour size; groin node metastasis; surgical excision margins; histology grade; and type of surgery performed (Table 3.23).

Compared to women who were younger than 65 years at diagnosis those who are 65 and older were at greater risk of dying from VSCC (HR: 5.26, 95% CI: 2.03-13.63, p=0.01). Women with tumour size 4cm or greater (HR: 3.21, 95% CI: 1.04-9.89, p= 0.043), advanced staged disease (HR: 8.45, 95% CI: 4.23-16.87, p<0.001), poorly differentiated histology grade or groin node metastasis (HR: 8.54, 95% CI: 4.41-16.52, p<0.001) were also at higher risks of dying from VSCC. Compared to patients who underwent

simple wide local excision, those who did not have surgery (HR: 7.07, 95% CI: 2.88-17.34, p<0.001) or had total radical vulvectomy (HR: 2.52, 95% CI: 1.23-5.15, p= 0.012) were also at greater risks of dying from VSCC as did women found to have sub-optimally (HR: 2.41, 95% CI: 1.15-5.07, p= 0.020) or incompletely excised surgical specimen (HR: 3.92, 95% CI: 1.31-11.75, p= 0.015). Patients who received palliative radiotherapy and/or chemotherapy were also at risks of dying from VSCC. (HR: 6.84, 95% CI: 1.80-26.07, p= 0.005).

Table 3.23: A summary of the univariate analysis for potential predictors of VSCC specific mortality

Covariate (LR p-value)	HR (95% CI)	P-value
Age (years) (p<0.01)		
<65 (Ref. Category)		
≥65	5.26 (2.03, 13.63)	0.001
Smoking status (p=0.216)		
No (Ref. Category)		
Smoker/Ex-Smoker	0.61 (0.27, 1.37)	0.231
Stage (simplified) (p<0.01)		
1/2 (Ref. Category)		
3/4	8.45 (4.23, 16.87)	0.000
Tumour Size (p<0.01)		
< 2cm (Ref. Category)		
2-<4cm	1.33 (0.42, 4.29)	0.628
4-<6cm	3.21 (1.04, 9.89)	0.043
≥ 6cm	4.84 (1.46, 16.08)	0.010
Disease Multifocal (p=0.105)		
No (Ref. Category)		
Yes	0.42 (0.13, 1.37)	0.152
Groin node involvement (p<0.01)		
No (Ref. Category)		
Yes	8.54 (4.41, 16.52)	0.000
Groin Node Surgery (p=0.267)		
No nodal surgery (Ref. Category)		
SNLB/GLND	0.70 (0.37, 1.31)	0.260
LVSI (p=0.586)		
No (Ref. Category)		
Yes	1.21 (0.61, 2.43)	0.585
Unavailable	0.71 (0.27, 1.87)	0.487
Excision Margins (p=0.017)		
Optimum (Ref. Category)		
Sub-optimum	2.41 (1.15, 5.07)	0.020
Incomplete	3.92 (1.31, 11.75)	0.015
Histology grade (p=0.013)		
Well (Ref. Category)		
Moderate	1.46 (0.57, 3.72)	0.426
Poorly	3.22 (1.34, 7.74)	0.009
LS, +/- Vin (p=0.095)		
No LS (Ref. Category)		
LS, +/- Vin	1.69 (0.91, 3.12)	0.095
Type of Surgery (p<0.01)		
Biopsy or No Surgery (Ref. Category)		
Simple wide local excision	0.00 (0.00, .)	1.000
Radical WLE or hemi-vulvectomy	0.14 (0.06, 0.35)	0.000
Total radical vulvectomy	0.36 (0.15, 0.82)	0.015
RT given for sub-optimal surgery (p=0.167)		
No (Ref. Category)		
Yes	1.85 (0.82, 4.18)	0.139
HPV 16/18 E6 (p=0.136)		
X (Ref. Category)		
P	0.59 (0.29, 1.19)	0.140

3.7.3 Multivariate analysis of disease specific survival

Multivariate analyses revealed the three prognostic factors that best describe the risk of women dying from VSCC: age; disease stage; and groin node metastasis (Table 3.24).

Women aged 65 years and older were more likely to die from VSCC compared to those who were younger than 65 (HR: 3.951, 95% CI: 1.313-11.889, p=0.015) as did those with groin node metastasis (HR: 4.791, 95% CI: 2.238-10.256, p<0.001) and advanced staged disease (HR: 2.466, 95% CI: 1.056-5.758, p=0.037).

Table 3.24: Summary of multivariable HR (95%CI) for potential predictors of time to disease specific mortality

Variable	Level	HR (95% CI)	P-value
Groin node involvement	No	1.000 (Ref. Category)	.
	Yes	4.791 (2.238, 10.256)	0.000
Age (years)	<65	1.000 (Ref. Category)	.
	≥65	3.951 (1.313, 11.889)	0.015
Stage (simplified)	1-3	1.000 (Ref. Category)	.
	4	2.466 (1.056, 5.758)	0.037

3.8 Discussion

As the prevailing orthodoxy holds that adverse outcomes following primary surgery for VSCC are more likely when the tumour has been inadequately excised, this belief is increasingly being challenged with new clinical evidence. Tumour free pathological margins of 8mm or more, measured after formalin fixation, is considered to be the gold standard practice to minimise local disease recurrence. This recommendation is based on a study conducted by Heap *et al.* on a small retrospective cohort consisting of 135 patients [20]. The study found that none of the patients with pathological margins of $\geq 8\text{mm}$ had recurrent disease, and local recurrence was only found in those with pathological margins of $<8\text{mm}$. To achieve a tumour free pathological margin of $\geq 8\text{mm}$, a surgical excision margin of at least 2cm around the primary tumour is required to account for 25% shrinkage when the surgical specimen is fixed in formalin [18]. Removing a large section of the normal vulval skin would inadvertently lead to physical and psychosexual comorbidities, especially if the tumour is located near to major functional organs such as the clitoris, urethra and anus.

Despite current surgical practice advocating the removal of at least 1.5cm of normal vulval skin, and most cohort studies showing a relatively high proportion of patients achieving histological margins in excess of $>8\text{mm}$, the 5-year local recurrence rate for VSCC has not improved over the last years and remained steady at around 30% in any given study population [20, 22, 23, 29-37, 111, 112]. Whereas some studies report that surgical excision margins independently predict the risk of local recurrence, others report no difference. Interestingly, other clinicopathological variables, such as groin node metastasis, disease stage, histologic grade, depth of tumour invasion, the

presence of usual type VIN, differentiated VIN or LS adjacent to the primary tumour, tumour size, tumour multifocality and LVI have all been reported to independently predict local recurrence [22, 23, 29-37, 109, 110]. It is worth pointing out that Heap *et al.* drew their inferences solely from p-values, not from a multivariate analysis, and their findings are likely to be confounded by other clinicopathological variables given that most patients with excision margins of <8mm in their cohort had advanced staged disease. When we examined the relationships between each of the clinicopathological variables in our own cohort, we found that women who had sub-optimal excision margins (<8mm) were older and more likely to have late stage disease as well as larger, poorly differentiated tumours. Although somewhat speculative, it is possible that tumour recurrence in these women was more likely to arise from surgical spillage of tumour cells due to the technical difficulty in performing the surgery and not inadequate excision margins. Moreover, it is also possible that the biology and thus, the behaviour, of advanced staged tumours are different from that of early stage disease, and women with the former are at higher risk of local recurrence.

Although a number of more recent studies have used multivariable analysis to identify clinicopathological variables that are most likely to predict local recurrence, none of them came out with a satisfying conclusion as each of these studies found different predictive variables. There are some reasons why these studies failed to find common prognostic factors that accurately predict local disease recurrence. Firstly, the selection of prognostic variables collected from each cohort study were different from each other with many not including associated epithelial disorders found adjacent to the primary tumour, e.g. VIN and LS [20, 29, 31, 37]. In those studies that include associated epithelial disorders, many did not make the distinction between differentiated,

undifferentiated VIN and LS [30, 34, 35, 111]. Secondly, the definition of local recurrence used in each study differs and some are vague, an important consideration when measuring disease recurrence. For instance, some investigators neither distinguish vulval recurrences from more distant disease nor separately identify recurrences and reoccurrences [20, 23, 29, 30, 34, 35]. The term “reoccurrences” is poorly defined and often used inconsistently with one investigator defining it as “the development of VSCC lesions in the vulva or groin lymph nodes after 5 years of follow-up” and another defining it as “vulval tumour occurring at a site remote from the initial primary tumour” [22, 31, 32, 37]. Thirdly, many studies have a relatively short follow-up duration and losses to follow-up are rarely defined. It was found that a second field tumour (tumour that recurs >2cm away from the primary tumour), took longer than 2 years to recur when compared to local relapse (a tumour that recurs within 2cm of the primary tumour [22, 31, 37]. Thus, any studies with a relatively short follow-up period are likely to overlook tumours that recur away from the primary. Lastly, it is often not clear how the multivariate analysis model was built in many studies as certain prognostic variables were deliberately excluded from the analysis [30, 31, 78]. Thus, the lack of standardised definition and methodology used in these cohort studies has failed to identify the common prognostic variable(s) for local recurrence. Although some authors proposed the use of a standardised prospective and multicentre collaborative cohort study to improve the accuracy of the study, this is unlikely to happen for two reasons. Firstly, such a study will not be completed in a reasonable time frame because of the rarity of the disease; secondly, the elderly population which it affects are more likely to die of causes other than vulval cancer, before they develop local recurrence.

To improve on the analysis of previous studies mentioned above, we repeated the retrospective cohort studies on our own cohort of patients who have been extensively followed-up for at least five years. None of these patients were "lost" in follow-up and all clinicopathological variables previously described to modulate the risk of local recurrence, were abstracted from the patients' case notes. Also, we performed HPV testing on 71% of our cohort. The relationships between each of these variables were examined, and a multivariable analysis model was built based on all the variables to identify the prognostic markers for local recurrence, groin node metastasis and disease-specific survival. We also dichotomised local recurrence into local relapse (LR), tumour which recurs within 2cm of the primary tumour, and second field tumour (SFT), tumour which recurs more than 2cm away from the primary tumour. The results of our multivariate analysis showed that age; groin node metastasis and the presence of LS are independent predictors for any local recurrence: LR alone, SFT or both. The independent predictors for LR are groin node metastasis and LS while LS is the only independent predictor for SFT. Women with LS are five times more likely to develop an SFT when compared to those without LS. Women with a local recurrence were also at risk of developing subsequent recurrences, with 50% of those with local recurrences going on to develop further episodes of LR, SFT or both (Figure 3.6).

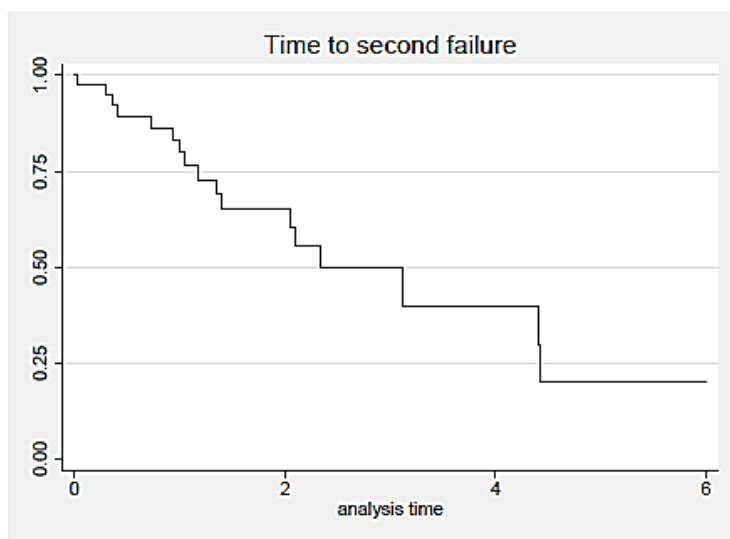


Figure 3.6: Kaplan-Meier (KM) plot showing the likelihood patients with local VSCC recurrence (either local relapse, second field tumour or both) went on to develop further episodes of local VSCC recurrence. Note that 50% of patients with local recurrence went on and had a further recurrence within 2.34 years.

Consistent with a number of previous studies, women with groin node metastasis were at risk of developing LR. This is probably due to the retrograde migration of microscopic tumour emboli in the groin lymphatics to the site of the primary tumour [34]. Although it was not always clear how some studies defined distance to local recurrence, some authors have acknowledged that recurrences that occur more than 2 years after initial treatment were more likely to be away from the primary tumour [31, 37, 111], and arise in vulva with underlying LS [22]. Here, we have used the term distant recurrence as SFT and our analysis have shown that these tumours were more likely to arise in those with underlying LS, but contrary to other studies, we found that

SFT occurs sooner than LR in those with VSCC arising in the background of LS. Currently, we do not yet have an explanation for the discrepancy observed in the timing of LR and SFT occurring between ours and others studies. Interestingly, head and neck squamous carcinoma (HNSCC) also exhibit similar patterns of recurrence, with HPV-negative HNSCC displaying a tendency to recur away from the primary tumour [62]. This has led to the suggestion that those tumours that recur some distance away from the primary tumour are likely to constitute a new primary tumour that arises in a "field of cancerization" [62].

The concept of field cancerization was first proposed by Slaughter *et al.* in 1953 who studied the histology of dysplastic epithelial tissue adjacent to the primary tumour in an attempt to explain the reason for the development of multiple primary tumours and tumour recurrence in the oral cavity and upper respiratory tract [39]. Since the development of molecular biology, the concept of field cancerization has now been redefined in molecular terms. Field cancerization predicts that local recurrences which develop following surgery could arise in one of two ways: either because of a failure to completely excise the tumour at primary surgery or the intra-operative spillage of tumour cells; or secondly, through the development of second field tumours in un-resected epithelium which is already molecularly altered but not yet malignantly transformed - this epithelium may even appear microscopically normal [62] (Figure 3.7).

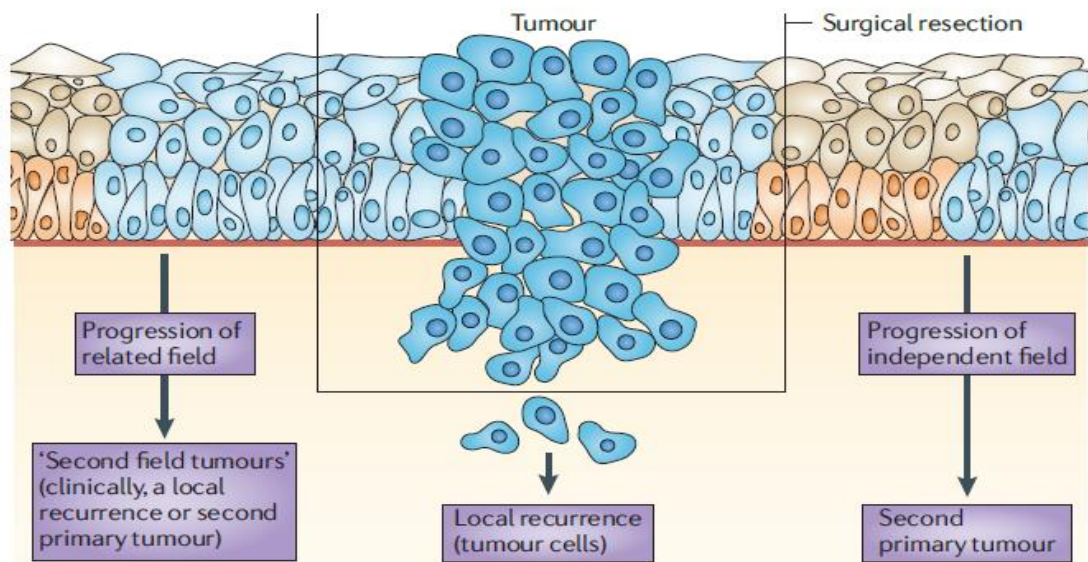


Figure 3.7: The relationship between field cancerisation and types of local recurrence is shown. Field of cancerisation is defined based on recent molecular understanding as the presence of one or more epithelial areas consisting of keratinocytes that have acquired cancer associated genetic or epigenetic alterations. A precursor field (shown here in light blue) is monoclonal in origin and lacks the ability to invade and metastasise. A field is pre-neoplastic in nature and it may have histological features of dysplasia (for instance uVIN and dVIN in the vulva), but not necessarily. We hypothesise that most VSCC probably arise from within this field after complete resection of the initial tumour. Local recurrence is likely to arise from intra-operative spillage of cancer cells or retrograde migration of these cells within the lymphatic; a molecularly altered" field probably results in a "second field tumour" which can occur at a site previously occupied by or distant to the primary tumour. However, additional molecular alterations are required to transform this field into new carcinoma. Based on current evidence, the field and primary tumour share common genetic alterations and are considered to have a common clonal origin. We believe that LS is a precursor lesion of field cancerisation in those women with VSCC and LS found adjacent to their tumour. Additional molecular alterations acquired as a result of chronic inflammation in this already abnormal field (LS) leads to the development of new VSCC (second field tumour). Moreover, it is also possible that new tumour may arise from an independent field and give rise to a second primary tumour, which is genetically distinct from the primary tumour.

Figure taken from Leemans *et al.* 2011

The notion that LS generates a field of cancerization much like that observed in HPV-negative HNSCC is a tenable but as yet unproven concept. However, such an idea is not without foundation. It is now well-established that chronic inflammation, coupled with sustained episodes of wound-healing and epithelial scarring, can predispose epithelial tissues to oncogenic transformation, allowing molecularly altered clones to expand and generate a pre-cancerous “field” [62]. LS is an autoimmune condition with an unknown aetiology. While precancerous fields in oral mucosa are likely generated through the pro-carcinogenic effects of cigarette smoke, alcohol and other ingested compounds (e.g. volatile nitrosamines) [62], the external and intrinsic factors involved in the aetiology of LS are less well defined (of course, this presumes that LS does generate a field). A number of studies have shown that LS lesions overexpress p53 protein and, in a significant proportion of cases, harbour mutated *TP53* genes [14, 113, 114]. The induction of p53 is most likely associated with a DNA damage response, induced through the production of reactive oxygen species (ROS) or by ischaemic stress, both of which are induced during chronic inflammation. Chronic or sustained bouts of inflammation are also associated with abnormal cytokine and growth factor production (e.g. TGF β , IL1 α/β , TGF α) which causes significant alterations to the underlying stroma, leading to tissue scarring and sclerosus; and the latter is a characteristic feature of LS.

In HPV-positive VSCC, the HPV-encoded E6 and E7 oncoproteins, play key roles in early disease pathogenesis, by targeting the key cellular targets p53, and pRb [115]. Subsequent mutation of these HR-HPV-driven clones or, HPV infection of molecularly altered clones, may lead to cellular transformation and the generation of premalignant lesions typified by high grade VIN. However, it is not clear at this stage whether virus

infection *per se* results in the expansion of clones which proliferate to generate a pre-cancerous field. One study, using molecular analyses involving X chromosome inactivation, revealed that high-grade VIN lesions contiguous with VSCC were of clonal origin, raising the possibility that these VSCCs were derived from molecularly altered clones from the VIN lesions [40].

Unlike HPV-positive VSCC, comparatively little is known about the molecular defects and genetic alterations that contribute to the development of HPV-negative VSCC and, just as importantly, the molecular changes that occur in the precursor lesion, dVIN and LS. Although comprehensive molecular profiling has yet to be performed, a number of studies have identified both overexpression of p53 protein and/or mutation of the TP53 gene in a high proportion of HPV-negative VSCC [116, 117]. Given that the same mutations are also frequently found in dVIN precursor lesions, mutant p53 may act as an essential “driver” mutation during the early stages of the disease [118]. Further support for the concept that LS generates a precancerous “field” comes from a recent study by Rolfe et al., who have shown that the p53 mutations identified in LS lesions were found to be identical to those found in the LS-associated VSCC [113]. This finding lends further weight to the concept that LS lesions contain molecularly altered clones that have the potential to undergo malignant transformation. In addition to p53, mutations in *PTEN*, amplification of the *EGFR* and *HER2* genes and epigenetic silencing of *p16^{INK4a}*, *RASSF2A*, *MGMT* and *TSPY* have been documented in a high proportion of HPV-negative LS-associated VSCCs, compared to VSCCs that were not [119-121]. The same study revealed that the extent of promoter methylation increased upon disease progression from LS to and LS-associated with VSCC, suggesting that

epigenetic inactivation of genes is a common event in vulvar SCC and, more importantly, is present in adjacent lesions, implying a possible precursor role for these molecular alterations in LS-associated VSCC [121].

Based on the available data for HNSCC and the current concept of field cancerization, it is possible that LS generates a field of pre-neoplastic basal keratinocytes, as a consequence of mutations in key “driver” genes (e.g. TP53). These mutation(s) confer a growth or survival advantage over neighbouring keratinocytes, allowing them to expand laterally within the basal layer and to displace or replace their neighbouring keratinocytes. Over time, this generates a field of molecularly abnormal epithelium that is susceptible to additional mutation (see Figure 3.7). Further exposure of these abnormal keratinocytes to carcinogens, in this instance, pro-inflammatory cytokines or some as yet unidentified carcinogen, causes more genetic alterations (multistep field cancerization) which eventually give rise to SCC either on the site of previous tumour (LR), site distance to previous tumour (SFT) or both; as observed in our cohort study where women with LS were more likely to have LR, SFT or both.

Our analysis, along with others, have showed that local VSCC recurrence is likely to arise in a field of cancerization, and future work should focus on identifying potential molecular biomarkers that predict the risk of local recurrence. The contiguous nature and ease of accessibility of the vulva made this organ an ideal model to study how the field of cancerization develops. Also, VSCC almost always arises in a field with adjacent abnormal epithelium. By identifying the molecular defect(s), field therapy can then be developed and applied topically onto the potential defective field to treat or prevent the field from expanding.

Although LS is an independent predictor for LR and SFT, it is neither a predictor for groin node recurrence nor disease-specific mortality. Groin node recurrence only occurs in those who were previously diagnosed with groin node metastasis. The main prognostic factors that independently predict mortality are age (older than 65 years), advanced disease stage and groin node metastasis. While there is compelling evidence to suggest that in cancers of the vagina, anus, penis and oropharynx, patients with HPV-positive tumours display better disease-specific survival, the relationship between virus positivity and outcome is less clear in women with VSCC. Whereas some studies report a substantial survival advantage for HPV-positive patients, others report no difference [12, 122-124]. In our own cohort study, we found that HPV positivity did not confer any survival advantage. It is now apparent that testing tumours for oncogenic HR-HPV infection has remained problematic for two main reasons: firstly, the different molecular techniques used have different levels of sensitivity and specificity in detecting HPV DNA; secondly, the small HPV DNA fragments are likely to have been degraded and lost following the process of fixing the tumour in formalin and embedding it in paraffin [125]. These limitations will invariably influence the reliability of the reported prevalence rates and prognostic data.

3.9 Overall Summary

Field cancerization is a well-known and well-documented process of malignant transformation. Numerous studies attest to the importance of this phenomenon in the development of tumours at anatomical sites such as the oral cavity, oesophagus, colon,

stomach and the vulva [38]. The advent of more advanced molecular biology technology such as DNaseq and RNAseq, will aid the identification of genetic markers and cell signalling pathways whose aberrant expression or dysregulation may not only provide useful diagnostic biomarkers but viable targets for therapy. An obvious shortcoming in almost all the studies of field cancerization is the lack of extensive genome-wide scans that will enable early and important genetic changes in tumour evolution to be uncovered. To date, most studies have relied heavily on established “tumour-specific” markers. Whilst useful, these highly selected tumour markers might constitute later acquisitions in the disease process that are not present in preneoplastic or dysplastic epithelium, or whose expression may be key to the very earliest stages of disease. It is clear from this, and other studies, that analyses aimed at identifying relevant genetic changes in histologically normal epithelium adjacent to dysplastic and cancerous lesions is required. The information obtained from such studies will be essential for early detection, risk assessment and development of chemoprevention of VSCC.

Chapter 4:

The effects of EGCG on the growth and
differentiation of HPV18 immortalised
keratinocytes: insights into the mechanism of
action of EGCG

4.1 Introduction

EGCG is currently used as a topical ointment to treat and prevent the recurrence of genital warts [52], a proliferative disorder induced by low-risk HPV subtypes - notably HPV6 and HPV11. Recently, a clinical case study reported that topical EGCG treatment was used successfully to treat an immunodeficient patient suffering from usual-type vulvar intraepithelial neoplasia (uVIN), a pre-neoplastic lesion of the vulval skin induced by high-risk HPV subtypes [126]. While it is encouraging to learn that EGCG could be used to cure uVIN, we are still awaiting the outcome of our Phase II randomised control trial that attempts to evaluate the effectiveness and safety of topical EGCG (EPIVIN) for the treatment of uVIN.

Although the clinical evidence, thus far, suggests that topical EGCG is effective in treating proliferative disorders induced by both low and high risk HPV subtypes, the underlying mechanism of action of EGCG remains to be elucidated. A number of studies have shown that EGCG inhibits the growth and malignant potential of HPV-transformed cervical cancer cell lines through a mechanism involving repression of the HPV-encoded viral oncogenes, E6 and E7, and induction of the tumour suppressor genes, Rb and p53 [101, 127, 128]. However, given that EGCG has been shown to influence a myriad of cell signalling pathways [95], the precise mechanism by which EGCG influences the growth of HPV18-infected keratinocytes and expression of the E6 and E7 proteins remains unclear.

The objective of this chapter was to examine the effects of EGCG treatment on the growth and differentiation of HPV18-immortalised keratinocytes. In addition to this, I set out to establish whether EGCG influenced the HPV life-cycle, and expression of the E6 and E7 proteins. I also considered whether this study could identify potential

biomarkers (i.e. molecular targets of EGCG) that could be used to predict patient response to treatment, and, therefore, stratify patients into responders and non-responders. This could be performed on tissue biopsies collected from patients participating in our EPIVIN trial and our planned Phase III clinical trial.

4.2 HFK-HPV18 – the cell model of choice

The cell model chosen to investigate the mechanism of action of EGCG was HFK-HPV18, an HPV18-immortalised human foreskin keratinocyte line carrying episomal forms of the virus. This cell line was chosen for the following reasons:

1. Firstly, at the time this study was undertaken, uVIN-derived keratinocyte cell lines were not available for study, and, although not proven, it was felt that HFK-HPV18 was more likely to behave like uVIN than the highly transformed HeLa and SiHa cell lines. In common with uVIN lesions, HFK-HPV18 maintains viral genomes in an episomal form and exhibits features of pre-invasive intraepithelial neoplasia such as hyperproliferation and parakeratosis, yet lacks the malignant and invasive potential of the highly transformed HeLa and SiHa cell lines.
2. HFK-HPV18 is ideal for studying the HPV18 life cycle because the majority of cells maintain the virus in an episomal, non-integrated form. In organotypic raft culture, HFK-HPV18 keratinocytes stratify into a full thickness epithelium, where the virus undergoes vegetative replication through a process that is linked to keratinocyte differentiation. This feature allows us to study the effects of EGCG treatment on the viral life cycle in both monolayer and organotypic

raft culture. In this regard, HPV18-HFK has been used successfully to investigate factors that influence the HPV18 life cycle.

3. The E6 and E7 oncogenes are subject to normal transcriptional control in HFK-HPV18 (i.e. their expression is not deregulated through integration), allowing an investigation into whether EGCG influences their transcription in the context of a normal infection programme.
4. HFK-HPV18 expresses functional tumour suppressor genes (TSGs) such as p53, p21^{WAF1} and pRb that are targets for E6 and E7 oncogenes. The effects of EGCG treatment on their expression can be studied following treatment.

4.3 The effect of EGCG treatment on the proliferation of HFK-HPV18

EGCG has previously been shown to inhibit the proliferation of the vulval cancer-derived cell line, A431 [129], and the cervical cancer cell lines, SiHa and HeLa [130], but its effect on HPV-immortalised keratinocytes has not been investigated. To address this question I set out to examine the effect of EGCG on the proliferation of HFK-HPV18 keratinocytes in monolayer culture.

4.3.1 EGCG inhibits the proliferation of HFK-HPV18

To examine the effects of EGCG on the proliferation of HFK-HPV18 keratinocytes, cells were recovered into single cell suspensions and seeded in triplicate into 96-well plates pre-coated with fibronectin. Cells were allowed to attach and grow for 48hours prior to treatment with increasing concentrations of EGCG. 72hours later, control and EGCG-treated cells were pulsed with 10μM BrdU and cell proliferation measured using the

BrdU ELISA kit. A431 cells were included as positive control given their responsiveness to EGCG [131].

As shown in Figure 4.1, cell proliferation was progressively inhibited in both A431 and HFK-HPV18 cells subjected to increasing concentrations of EGCG. The IC₅₀ dose, a concentration of drug at which 50% of cell proliferation is inhibited, was 60μM and 100μM for A431 and HFK-HPV18, respectively. Maximum cell inhibition was achieved at 80μM for A431 and 150μM for HFK-HPV18. These findings show that while the HPV18-immortalised HFK and malignant vulvar cancer-derived cell lines are responsive to EGCG, for some reason, the A431 cell is more sensitive to EGCG than HFK-HPV18.

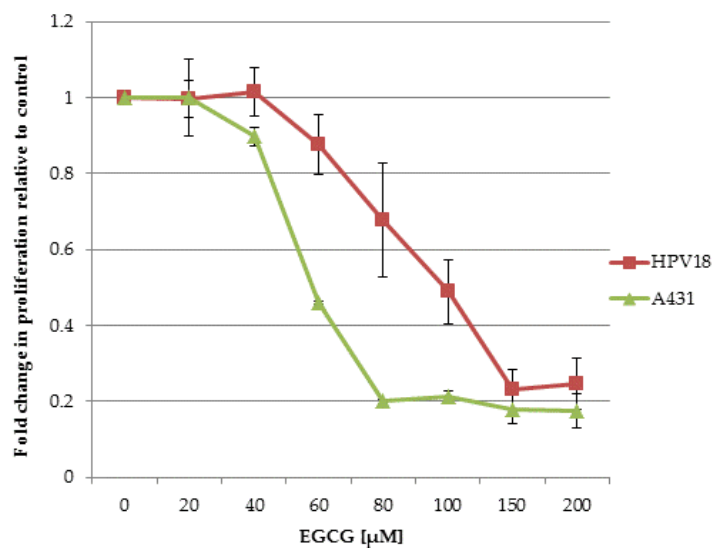


Figure 4.1: EGCG inhibits the proliferation of HFK-HPV18 keratinocytes and the VSCC-derived A431 cell line. Cells were treated with increasing concentrations of EGCG and proliferation was measured 72 hours later using the BrdU ELISA assay kit (Roche). The fold change in proliferation in EGCG treated cells was measured against untreated cells (control). Cell proliferation decreased as the concentration of EGCG increased. The IC₅₀ for HFK-HPV18 and A431 were ~100μM and ~60μM, respectively. Data shown is an average of 3 independent experiments.

4.3.2 EGCG alters the morphology of HFK-HPV18 keratinocytes

Having established that EGCG inhibits the proliferation of HFK-HPV18, I next examined the effects of EGCG treatment on cell morphology. HFK-HPV18 cells were seeded into petri dishes pre-coated with fibronectin and allowed to establish small colonies for at least 48 hours prior to treatment with 50 μ M and 100 μ M EGCG. The morphology of control and EGCG treated cells was then examined 72 hours later by phase contrast microscopy. Representative images, Figure 4.2, show that the colony size of EGCG-treated cells was noticeably smaller than untreated cells, confirming that these doses of EGCG inhibited cell proliferation. Furthermore, EGCG-treated cells developed cytoplasmic vacuoles and assumed a spindle-like appearance. These changes were most apparent at cell treated with 100 μ M EGCG.

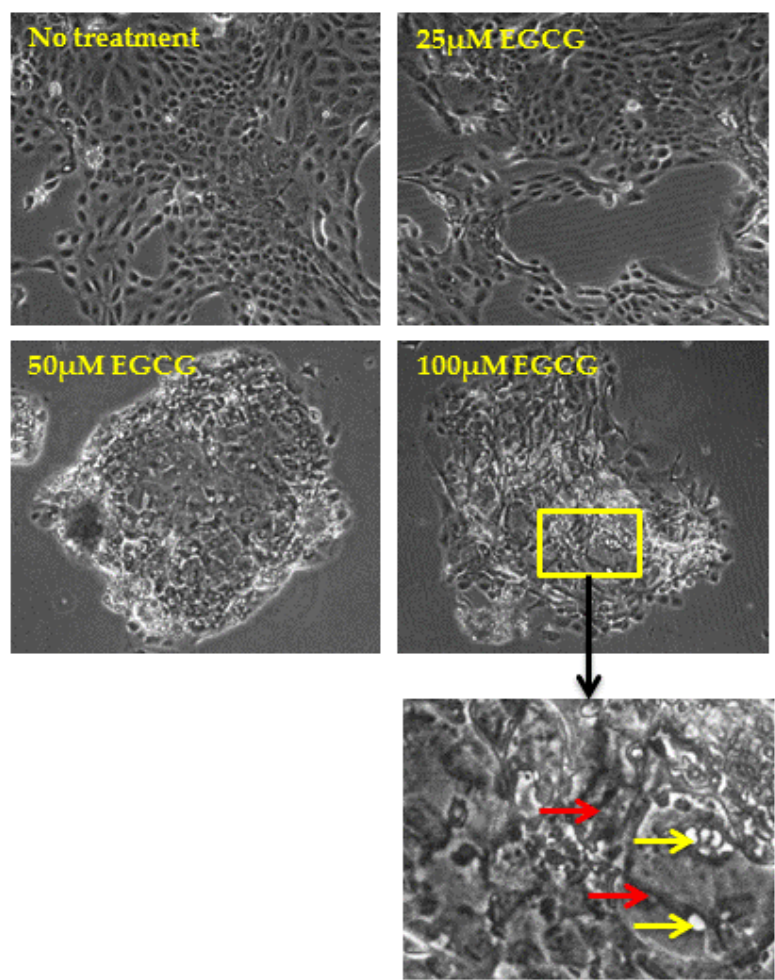


Figure 4.2: Changes in the morphology of HFK-HPV18 following three days treatment with 25 μ M, 50 μ M and 100 μ M. Single cell suspensions of HFK-HPV18 were seeded onto fibronectin-coated petri dishes and allowed to grow for three days before various concentrations of EGCG were added for an additional three days. Changes in cell morphology were evident as the concentration of EGCG was increased. The cells assumed spindle-like appearance (red arrows) with intracellular vacuole (yellow arrows) at 100 μ M. Images were taken using a Nikon Eclipse E600 microscope at x200 magnification.

4.3.3 EGCG treatment does not impose a specific cell-cycle checkpoint blockade in HFK-HPV18 but does increase the proportion of cells in the sub-G1 peak

The possibility that EGCG inhibited cell proliferation by imposing a cell-cycle checkpoint was investigated further using Propidium Iodide (PI) staining coupled with flow cytometry. HFK-HPV18 cells were treated with 100µM EGCG for 24, 48 and 72 hours or 100ng/ml Nocodazole for 12 hours, an agent that results in cell cycle arrest at the G2/M checkpoint. Control and EGCG treated cells were trypsinised into single cell suspensions, permeabilised in 70% ethanol and stained with 25µg/ml PI. Cells were then subjected to flow cytometric analysis, and the data collected analysed with FlowJo v.10 software to build cell-cycle profiles.

Representative cell-cycle profiles are shown in Figure 4.3. Compared to untreated cells, cell-cycle analysis of Nocodazole-treated cells revealed an increase in the number of cells in G2/M and a corresponding decrease in the size of the G1 and S phase populations. Interestingly, however, EGCG treatment did not induce a specific cell-cycle check-point blockade but did result in an accumulation of cells in the sub-G1 population. Cells found in the sub-G1 phase have depleted DNA content as a result of a loss of DNA fragments from permeabilised cells. DNA fragmentation is a characteristic hallmark of apoptosis and the accumulation of HFK-HPV18 in sub-G1 suggested that EGCG-treated cells had undergone apoptosis. The number of cells underwent apoptosis increased progressively when treatment duration was extended to 48 and 72 hours.

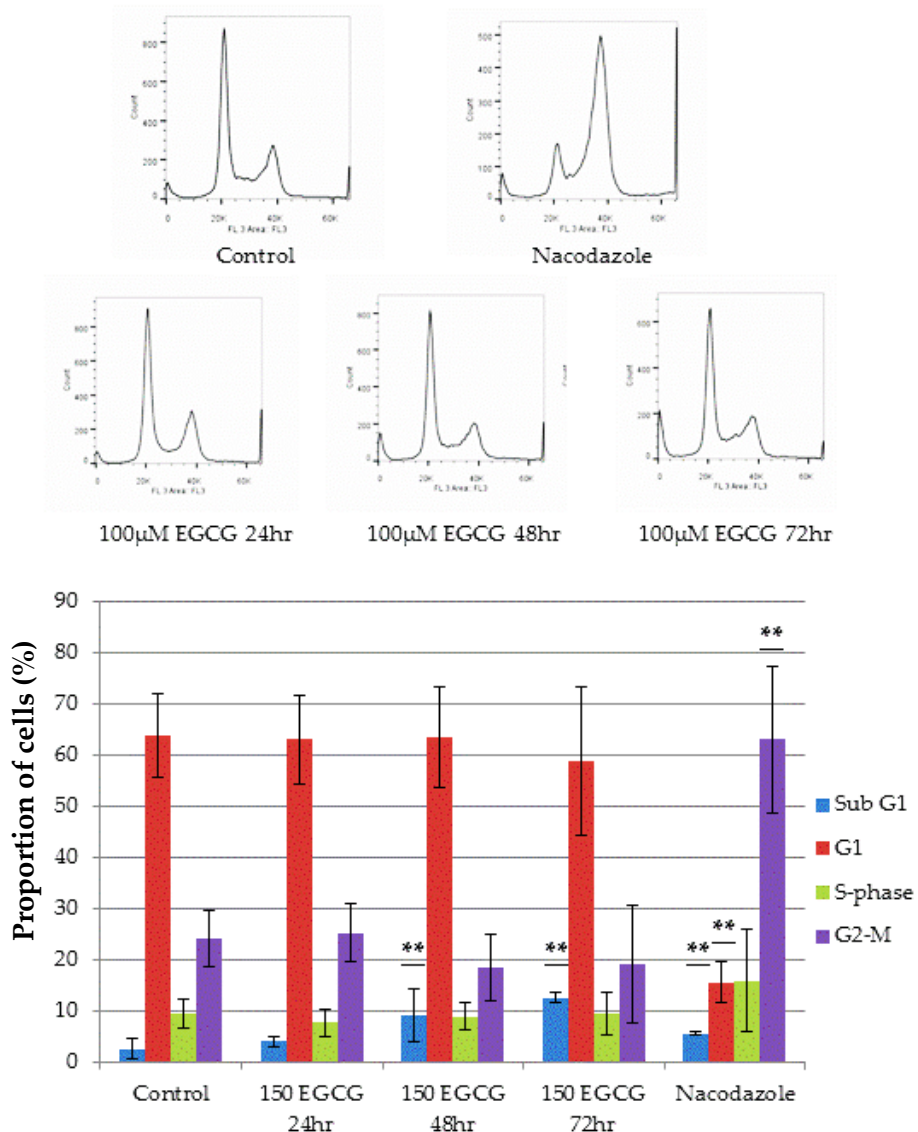


Figure 4.3: Representative cell cycle analyses of HFK-HPV18 cells cultured in the presence or absence of EGCG. Cells were treated with 150μM EGCG for 24, 48 and 72 hrs and, after harvesting, fixed and stained with propidium iodide for flow cytometric analysis. Nocodazole treatment was used as positive control for the assay. Data was analysed with FlowJo v.10. Data shown is an average of 3 independent experiments. **P<0.05, unpaired student t-test indicates that the difference in the proportion of cells is significant when compared to control. The proportion of Sub-G1 cells was significantly increased following treatment with EGCG for 48hrs.

4.3.4 EGCG induces apoptosis in HFK-HPV18

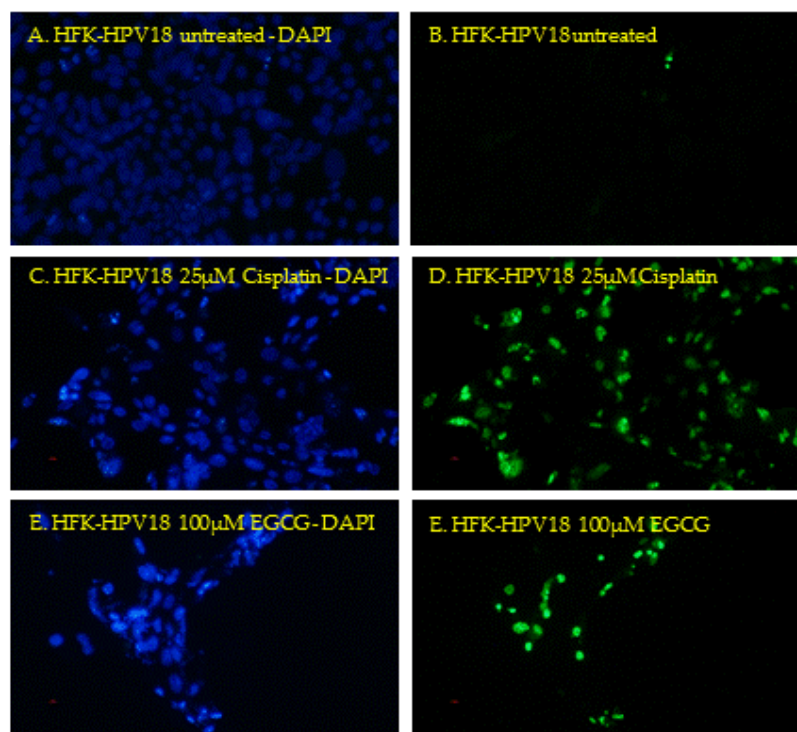
The accumulation of cells in the sub-G1 phase of the cell cycle, coupled with the profound morphological change in response to EGCG treatment, suggested that EGCG treated cells were undergoing apoptosis. To confirm this, a TUNEL assay was performed to detect the presence of DNA fragmentation, a classical feature of apoptotic cells. The TUNEL assay catalytically incorporates fluorescein-12-dUTP at 3'-OH ends of the DNA using the enzyme Terminal Deoxynucleotidyl Transferase (TdT) and forms a polymeric tail. The nucleus of apoptotic cells, which is labelled with fluorescein-12-dUTP, can then be visualised with a fluorescence microscope.

HFK-HPV18 cells were seeded onto sterile cover slips pre-coated with fibronectin and, after 24 hours, treated with 100 μ M EGCG for an additional 72hours. As a positive control, cells were treated for 24 hours with 25 μ M Cisplatin a DNA-damaging agent commonly used to induce apoptosis. Cell nuclei were then fixed and stained with TUNEL according to the manufacturer's instructions. Cell nuclei were identified using the DAPI DNA stain. The number of TUNEL positive nuclei was counted, and results expressed as the number of TUNEL positive nuclei expressed as a percentage of total stained cell nuclei. A Two-tailed unpaired Student t-test was used to determine the level of significance between the proportion of TUNEL positive cell in drug-treated and untreated cells.

Figure 4.4 shows a summary of the results obtained from the TUNEL assays performed on control, Cisplatin or EGCG treated HFK-HPV18 cells. The baseline level of apoptosis in HFK-HPV18 was approximately 1%. 24 hour treatment with Cisplatin increased the number of apoptotic cells to greater than 50%, while treatment with

EGCG for 72 hours led to apoptosis in approximately 40% of cells. In comparison, the DNA-damaging agent cisplatin is a more potent apoptotic inducing agent as lower drug concentrations, and shorter treatment duration are sufficient to induce apoptosis in more than 50% of the cell population.

A.



B.

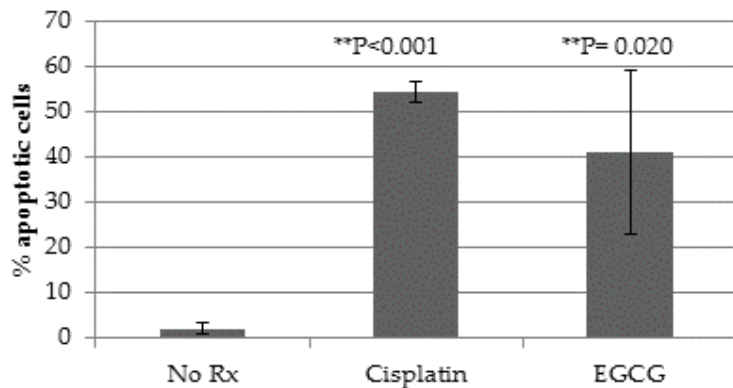


Figure 4.4: TUNEL assay showing EGCG treatment induces apoptosis in HFK-HPV18. (A). HFK-HPV18 cells were cultured in monolayer and treated with 100 μ M EGCG for 72 hours or 25 μ M Cisplatin for 24 hours as a positive control to induce apoptosis. TUNEL assay was used to label apoptotic cell (green) and cell nuclei were counter stained with DAPI (blue). Magnification x200. (B) TUNEL positive cells were expressed as a percentage of total cell nuclei. Unpaired Student t-test was used to determine the level of significance for the difference in the proportion of apoptotic cells in drug-treated and untreated cells. Experiments were repeated three times in triplicate.

4.4 The effect of EGCG on episome replication in HFK-HPV18 keratinocytes

Unlike HPV18 immortalised HFK cell lines, primary HFK cell strains have a limited lifespan *in vitro*, proliferate slowly and undergo differentiation after a number of passages. The introduction of HR-HPV genomes significantly extends the lifespan and proliferative potential of keratinocytes, leading ultimately to cell immortalisation. EGCG treatment inhibits the proliferation of HR-HPV infected keratinocytes, forcing them to undergo apoptosis. One obvious possibility as to how EGCG re-programmes these cells to “commit suicide” is to inhibit replication of the viral genome such that genome loss results in senescence or differentiation. I sought, therefore, to investigate whether EGCG influences HPV replication using an established qPCR-based technique that measures viral load (genome copy number) before and after EGCG treatment.

HFK-HPV18 keratinocytes were cultured in the presence of lethally irradiated 3T3-J2 feeder cells for at 48 hours or until multiple small keratinocyte colonies had formed (48-72 hours). The feeder cells were selectively removed and cells treated with 100 μ M of EGCG for 24, 48 and 72 hours. Cellular DNA was extracted using a commercially available kit from Qiagen. qPCR was performed to determine the relative change in viral load before and after EGCG treatment on triplicate samples using primers that amplify the E2 region of HPV18 genome. The experiments were repeated three times. As shown in Figure 4.5, no significant change in viral copy number was observed between treated and untreated cells 24 hours after EGCG treatment. However, there was 0.2 and 0.5 fold increase in viral copy number relative to untreated cells after 48 and 72 hours of EGCG treatment, respectively. The increase in viral copy number is

statistically significant, a finding which indicates that viral genome replication is slightly increased in HFK-HPV18 following EGCG treatment.

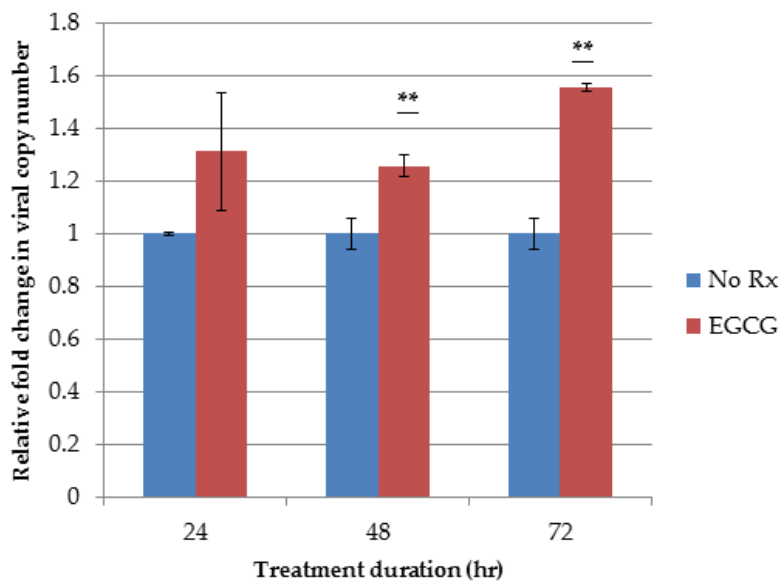


Figure 4.5: HPV 18 viral copy number increases with EGCG treatment after 48 and 72hrs. HFK-HPV18 cells were treated with 100 μ M EGCG for 24, 48 and 72hrs and DNA were harvested. qPCR was performed to quantify the relative fold change in viral copy number. **P<0.05, unpaired student t-test indicates that the difference in the level of viral load is significant when compared to control. Averaged results from three experiments.

4.5 The effect of EGCG on expression of the HPV18 E6 and E7 oncogenes

As EGCG treatment appeared to have only a marginal effect on HPV genome replication in HFK-HPV18, it appeared unlikely that the reduction in cell proliferation occurred as a result of the loss of HPV18 genomes. I next explored the possibility that the effects of EGCG on cell growth were mediated through its effects on the HPV-encoded oncoproteins: E6 and E7. This seemed pertinent given that EGCG has been shown to down-regulate expression of these oncogenes in cervical cancer cell lines.

To investigate the effect of EGCG on the expression of HPV18 E6 and E7 mRNA and protein, HFK-HPV18 cells were cultured with lethally irradiated 3T3 J2 feeder cells until 60-70% confluent. The feeder cells were removed with EDTA washing, and keratinocytes treated with 50 μ M or 100 μ M EGCG for 3 and 6 days. Cells were harvested and divided into two pellets: one for mRNA and the other for protein.

4.5.1 EGCG down-regulates expression of the E6 and E7 proteins

Cells were lysed in RIPA buffer and equal amounts of protein resolved by SDS-PAGE. Western blotting was performed using antisera specific for HPV18 E6 or E7. The membranes were re-probed with an antibody to β -actin to ensure equal protein loading. The density of the bands detected on the Western blots was quantified using the ImageJ software. The density values of the E6 and E7 bands were then normalised to the corresponding β -actin density values. The fold change in protein expression was compared to untreated cells (control). Two-tailed Student unpaired t-test was used to determine the level of significance in the difference in the oncoprotein expression before and after EGCG treatment.

Figure 4.6 shows the dose-dependent reduction in the levels of E6 and E7 protein in HFK-HPV18 72 hours following treatment either 50 μ M and 100 μ M EGCG. An expanded version of the original western blots is shown in Supplemental Figure 1. Having established that E6 and E7 down-regulation was more pronounced at 72 hours post-EGCG treatment, further experiments were performed to examine the treatment time required to observe the down regulation of E6 and E7 expression. As the reduction in levels of E6 and E7 protein was most pronounced using 100 μ M EGCG, further experiments were performed using this concentration. The effect of EGCG on the levels of E6 and E7 proteins was examined at 24, 48 and 72 hours post-EGCG treatment by Western blotting. Figure 4.7 and 4.8 show representative examples of Western blots for the E6 and E7 proteins, respectively. The levels of E6 protein were significantly reduced by more than 50 percent following 24-hour treatment with EGCG, and continued to decrease further at 48 and 72 hours post-treatment. Similarly, E7 protein started to decrease after 24 hours treatment with EGCG and continued to do so at 48 and 72 hours treatment. However, unlike E6, the level of E7 protein was only reduced by half after 48 hours treatment.

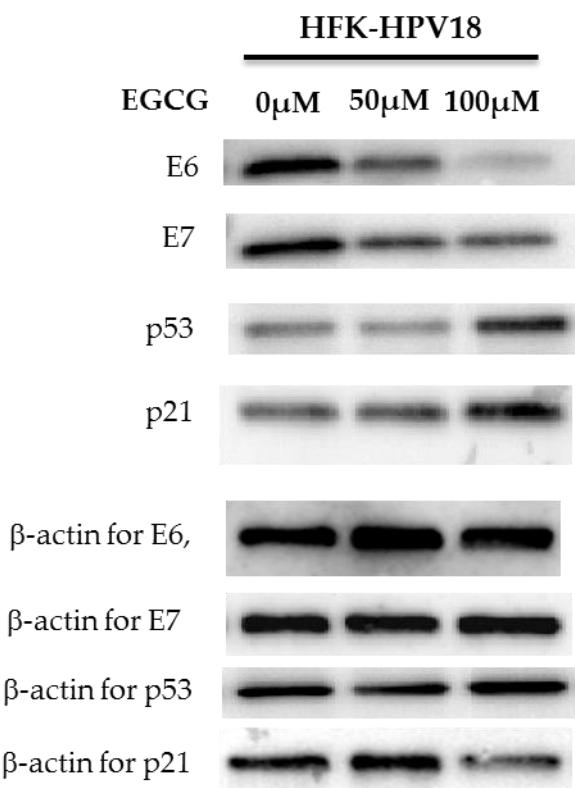
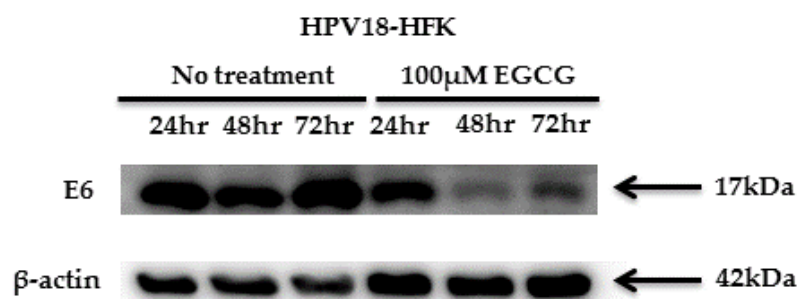


Figure 4.6: EGCG treatment downregulates expression of the E6 and E7 proteins in HFK-HPV18 and upregulates the expression of p53 and its downstream target gene p21^{WAF1}. HFK-HPV18 cells were either left untreated or treated with 50μM or 100μM EGCG for three days. Cell were harvested and lysed in RIPA buffer. 30μg of total protein lysate were resolved by SDS-PAGE and the levels of HPV18 E6, E7, p53, p21^{WAF1} and β-actin determined by Western blotting analysis. Experiments were repeated twice.

A.



B.

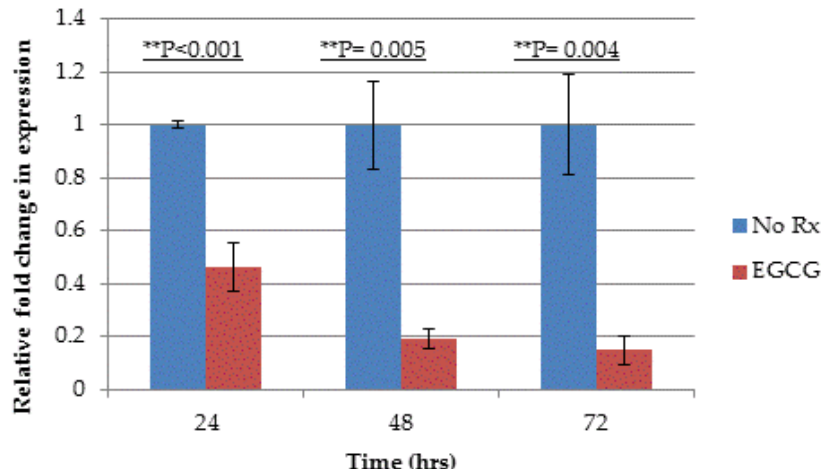


Figure 4.7: EGCG downregulates expression of the HPV18 E6 protein. (A). HFK-HPV18 cells were treated with 100 μ M EGCG for 24, 48 and 72hrs. Cells were lysed with RIPA buffer and 30 μ g of total protein lysate resolved by SDS-PAGE. E6 expression was determined by Western blotting analysis. (B) Densitometry analysis of the Western blots. E6 densitometry value was normalised against β -actin. Fold change in E6 expression was compared against untreated cells (control). **P<0.05, unpaired student t-test indicates that the difference in E6 expression is significant when compared to control. Averaged results from three experiments.

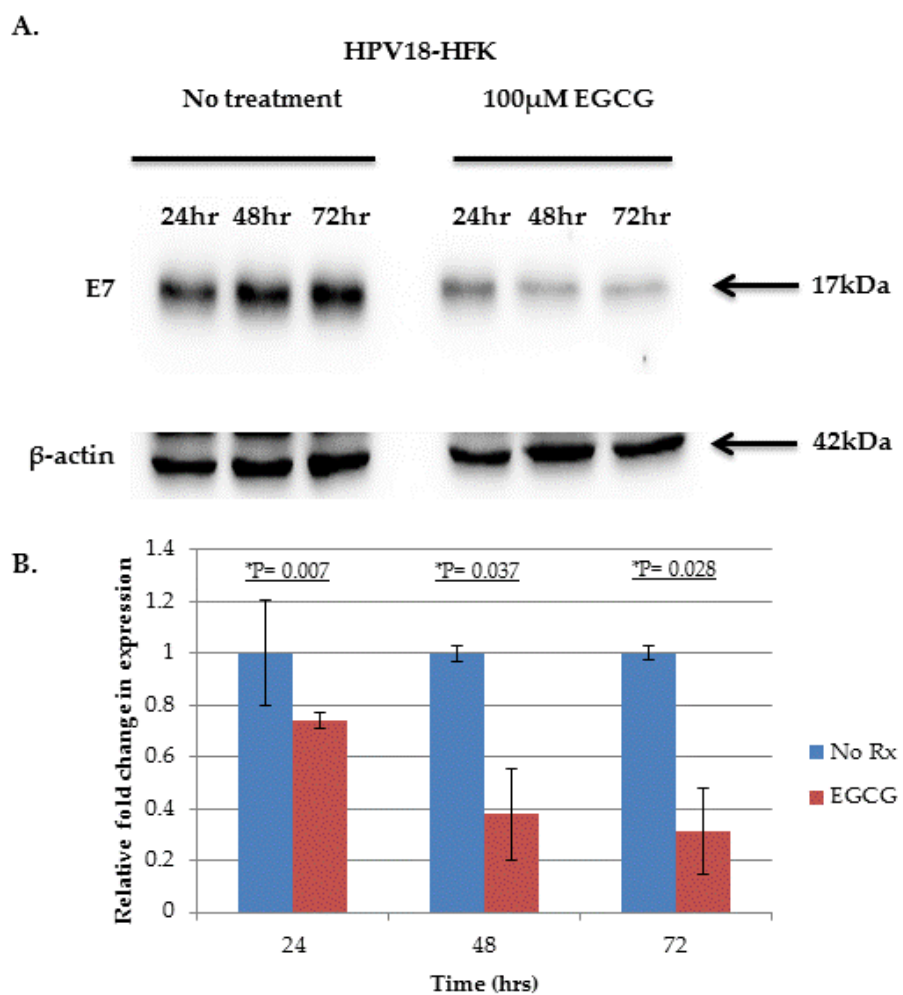


Figure 4.8: EGCG downregulates expression of the HPV18 E7 protein. HFK-HPV18 cells were treated with 100 μ M EGCG for 24, 48 and 72hrs. Cells were lysed in RIPA buffer and 30 μ g of total protein lysate resolved by SDS-PAGE. E7 expression was determined by Western blotting analysis. (A). Western blot showing down-regulation of E7 protein following EGCG treatment. (B) Densitometry analysis of the Western blots. E7 densitometry value was normalised against β -actin. Fold change in E7 expression was compared against untreated cells (control). **P<0.05, Student unpaired t-test indicates that the difference in E7 expression is significant when compared to control. *P = 0.09 indicates borderline not significance. Averaged results from three experiments.

4.5.2 EGCG does not influence the expression of E6 and E7 mRNA

To explore the possibility that the reduction in HPV18 E6 and E7 protein occurred as a result of decreased expression of E6 and E7 mRNA, the levels of E6 and E7 mRNA were quantified by q-PCR. The levels of E6 and E7 mRNA were normalised to the levels of endogenous beta-2 microglobulin gene within the sample. Data was analysed using the relative $2\Delta\Delta CT$ method using 7500 SDS software (Applied Biosystems). All experiments were repeated twice.

qPCR analysis, Figure 4.9, revealed that levels of E6/E7 mRNA transcripts were not reduced following three days of EGCG treatment. In fact, a small increase in E6/E7 mRNA of approximately 0.5 fold was observed in HFK-HPV18 cells treated with 50 μ M EGCG compared to untreated cells. No change was observed in cells treated with 100 μ M EGCG. Furthermore, extending the EGCG treatment for a further three days did not alter the levels of E6/E7 substantially. There was a small but significant rise in the level of E6/E7 transcripts by 0.3 fold at 100 μ M EGCG on day 6. The findings here suggest that the down regulation of E6 and E7 expression following EGCG treatment does not occur through effects on transcription of E6/E7 mRNA.

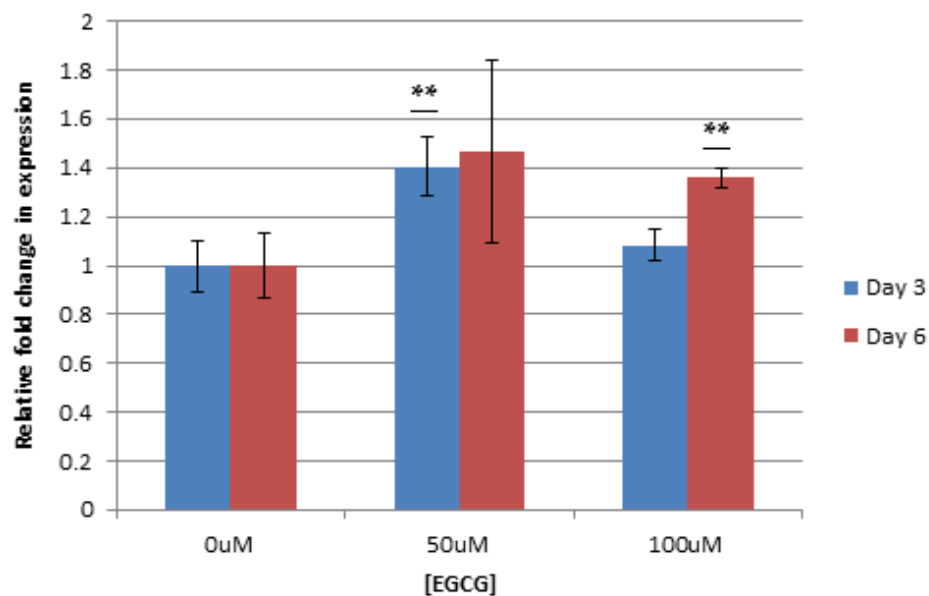
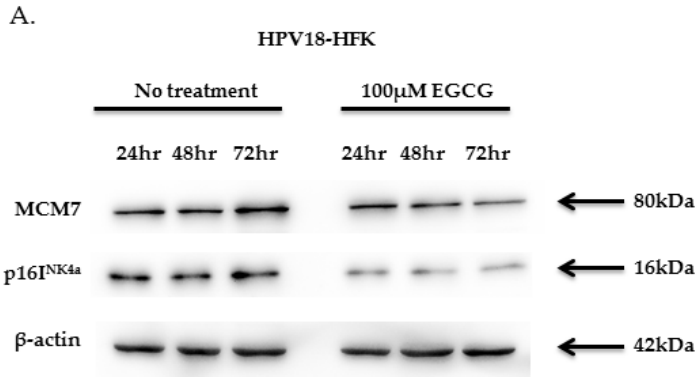


Figure 4.9: EGCG treatment leads to a slight increase or no change in expression of the HPV18 E6/E7 transcripts. HFK-HPV18 cells were treated with 50 μ M or 100 μ M EGCG for 3 and six days and RNA were harvested from which cDNA were synthesized by reverse transcription. qPCR was performed to quantify relative fold change in E6/E7 transcripts level pre- and post-EGCG treatment. Expression levels were normalised to levels of endogenous beta-2 microglobulin gene in samples. Data was analysed using the relative $2\Delta\Delta CT$ method using 7500 SDS software. All experiments were repeated three times. **P<0.05, unpaired student t-test indicates that the difference in the level of mRNA expression is significant when compared to control.

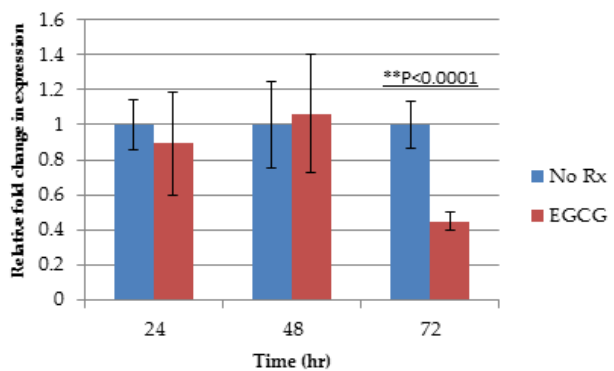
4.5.3 E6 and E7 down regulation are accompanied by a decrease in MCM7 and

p16^{INK4a}

MCM7 and p16^{INK4a} are both used as surrogate markers of transcriptionally active HR-HPV infection as their expression is increased in following HR-HPV infection [115, 132-135]. Having previously established that EGCG down regulates the E6 and E7 proteins in HFK-HPV18 keratinocytes, it seemed pertinent to examine the impact of E6 and E7 loss on expression of these markers. Equal amounts of protein lysate from untreated and EGCG-treated HFK-HPV18 cells were resolved by SDS-PAGE and Western blotting performed using antsera specific for MCM7 and p16^{INK4a}; β-actin was included to ensure equal protein loading. As expected, the down regulation of E6 and E7, which followed EGCG treatment, was accompanied by a reduction in MCM7 and p16^{INK4a} expression (Figure 4.10A-C). Although the expression of p16^{INK4a} was reduced 24 hours after treatment with EGCG (Figure 4.10A,C), the expression of MCM7 was only reduced 72 hours after treatment (Figure 4.10A,B).



B. MCM7



C. p16^{INK4a}

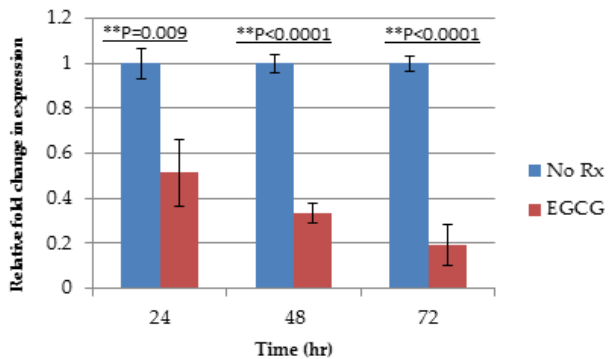


Figure 4.10: EGCG downregulates expression of MCM7 and p16^{INK4a}. (A) HFK-HPV18 cells were treated with $100\mu\text{M}$ EGCG for 24, 48 and 72hrs. Cells were lysed in RIPA buffer and $30\mu\text{g}$ of total protein lysate resolved by SDS-PAGE. Expression of MCM7 and p16^{INK4a} were determined by Western blotting analysis. (B&C). Densitometric analysis of the Western blots. MCM7 and p16^{INK4a} densitometry values were normalised against β -actin. The fold change in expression of MCM7 and p16^{INK4a} in EGCG treated cells were compared against untreated cells (control). Unpaired Student t-test was used to determine the difference in gene expression was significant when compared to control. Averaged results from three experiments.

4.5.4 E6 and E7 down-regulation are accompanied by an up-regulation in p53 and

p21^{WAF1}

Given that E6 and E7 target the tumour suppressor genes, p53 and pRb, I set out to determine whether E6 and E7 down-regulation was associated with their up-regulation in response to EGCG treatment. Protein lysates used in the experiments above were resolved by SDS-PAGE and Western blotting performed using monoclonal antibodies (mAbs) specific for p53, its downstream target, p21^{WAF1}, and pRb. The blots were reprobed with antibodies specific for GAPDH or β-actin to ensure equal protein loading. A preliminary investigation, Figure 4.6, revealed that expression of p53 and p21^{WAF1} were increased 72 hours after EGCG treatment. A more detailed investigation (Figure 4.11) revealed that p53 upregulation was not significant until 48 hours after EGCG treatment but remained elevated at 72 hours. Unlike p53, the expression of p21^{WAF1} was somewhat variable (Figure 4.12). Whilst a modest induction in p21^{WAF1} levels was observed 24 hours after EGCG treatment, they dipped at 48 hours and then increased 72 hours after treatment. Unfortunately, the Western blot for pRb were inconclusive as the antibody used failed to identify differences between the basal phosphorylated and hyperphosphorylated forms of pRb in response to EGCG treatment.

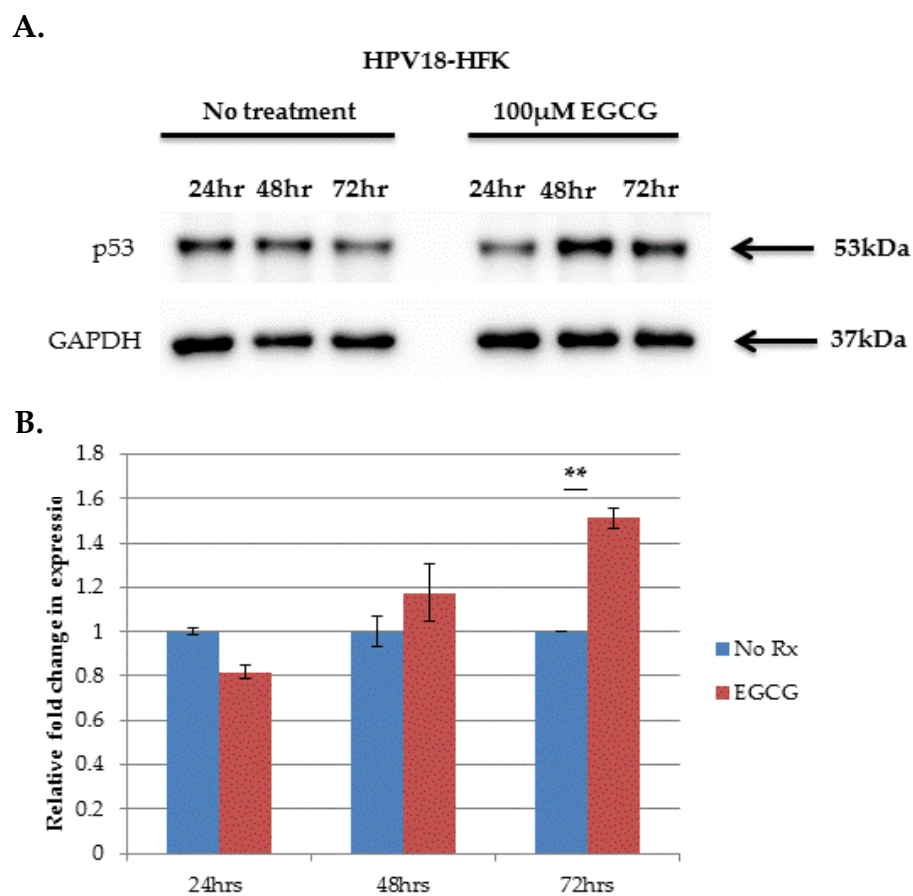
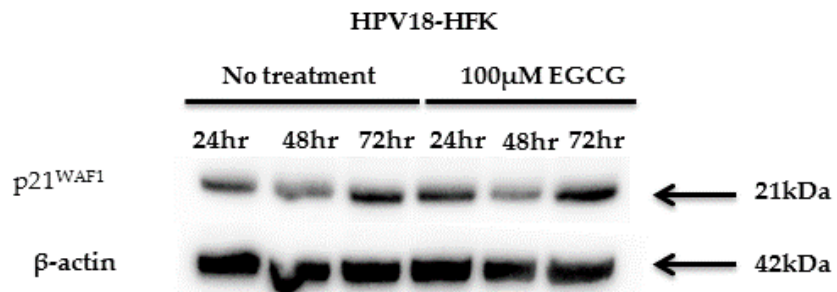


Figure 4.11: Expression of the p53 protein is upregulated following EGCG treatment. (A) HFK-HPV18 cells were treated with 100 μ M EGCG for 24, 48 and 72hrs. Cells were lysed in RIPA buffer and 30 μ g of total protein lysate resolved by SDS-PAGE. The levels of p53 were determined by Western blotting analysis (B) Densitometry analysis of the blots. p53 densitometry values were normalised against GAPDH. The fold change in p53 expression was compared against untreated cells (control). **P<0.05, Student unpaired t-test indicates that the difference in p53 expression is significant when compared to control. Averaged results from three experiments.

A.



B.

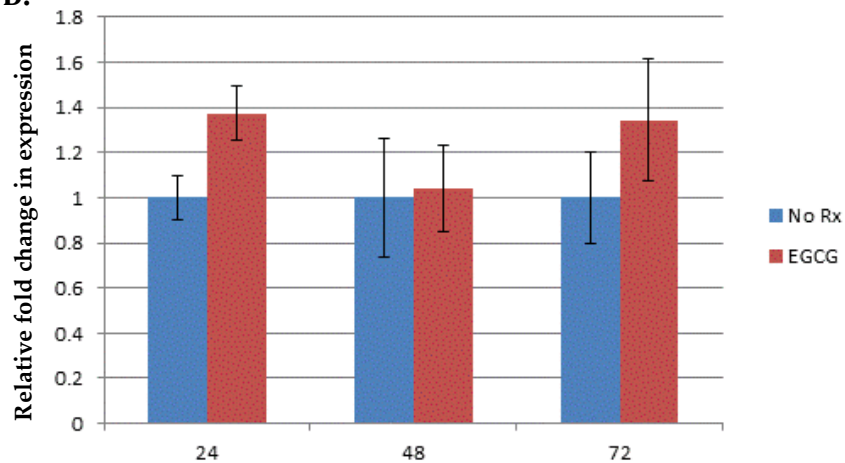


Figure 4.12: Expression of the p21^{WAF1} protein is not markedly affected by EGCG treatment. (A) HFK-HPV18 cells were treated with 100μM EGCG for 24, 48 and 72hrs. Cells were lysed in RIPA buffer and 30μg of total protein lysate resolved by SDS-PAGE. The expression of p21^{WAF1} was determined by Western blotting analysis (B) Densitometry analysis of the blots. p21 densitometry value was normalised against β-actin. The fold change in p21 expression was compared against untreated cells (control). Unpaired Student t-test was used to determine the difference in p21^{WAF1} expression was significant when compared to control. Averaged results from three experiments.

4.5.5 EGCG reverses the effects of HR-HPV on expression of DNA methyltransferases and Polycomb-group proteins

Previous studies have identified alterations in key epigenetic regulators following HR-HPV infection [136]. As E6 and E7 are likely effectors in this response, I set out to investigate whether down regulation of the HPV18 E6 and E7 proteins influenced the expression of DNA methyltransferases and the Polycomb-group proteins in HFK-HPV18 keratinocytes. Previously generated protein lysates were resolved by SDS-PAGE and Western blotting performed using antibodies specific for DNMT1, DNMT2, EZH2 and BMI-1; β -actin was included as a loading control. A representative Western blot, Figure 4.13, shows that compared to untreated cells, the expression of DNMT1, DNMT2 and EZH2 were down regulated, while expression of BMI-1 was up-regulated following 72 hour treatment with EGCG. An expanded version of the original western blots is shown in Supplemental Figure 2. Again, the changes in the level of expression of these epigenetic regulators were most pronounced at 100 μ M concentration of EGCG.

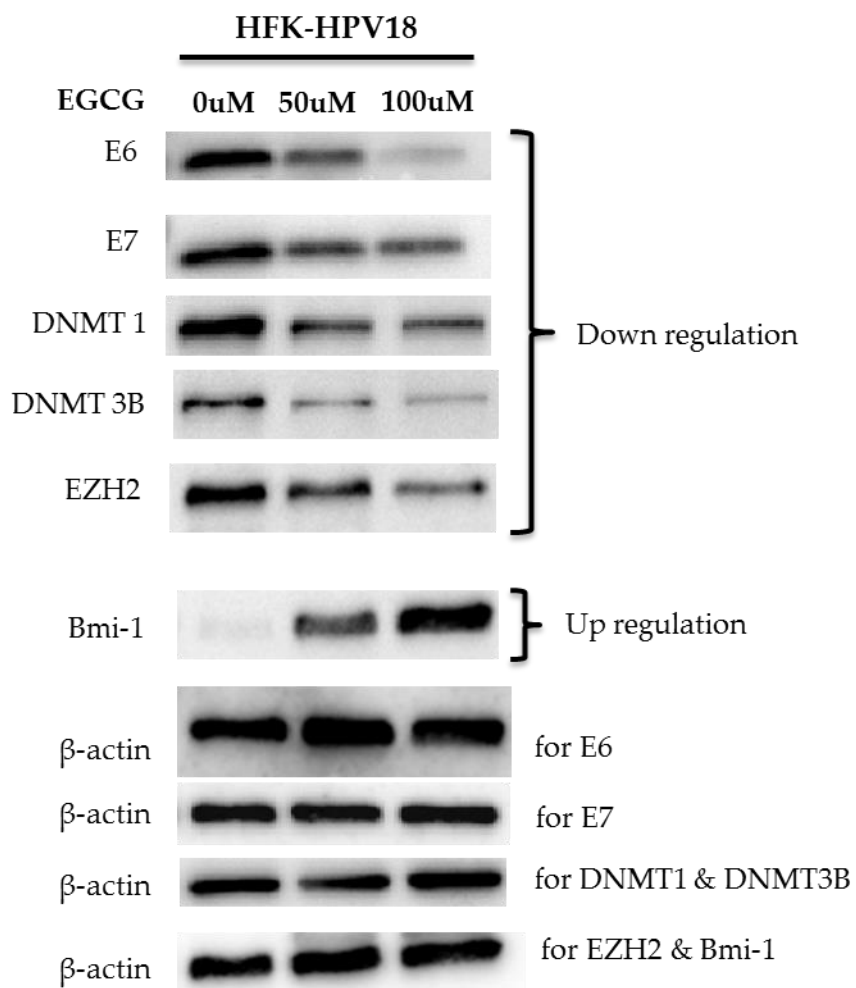


Figure 4.13: EGCG reverses the changes in expression of the DNA methyltransferases and polycomb proteins associated with HR-HPV infection. HFK-HPV18 cells were treated with 50 and 100 μ M EGCG for 72hrs. Cells were lysed with RIPA buffer and 30 μ g of total protein lysate resolved by SDS-PAGE. The expression of HPV18 E6 and E7, DNMT1, DNMT3B, EZH2, BMI-1 and β -actin were determined by Western blotting analysis. Experiments were repeated twice.

4.6 The effects of EGCG on the growth and differentiation of HFK-HPV18 keratinocytes in organotypic raft culture

The growth of keratinocytes in organotypic raft culture induces cells to stratify and differentiate into a fully organised epithelium that resembles histomorphological normal epidermis. This system enables investigators to study the impact of pharmacological drugs on keratinocyte differentiation in the context of a three-dimensional tissue and, in the context of HPV infection, the consequences of drug action on the HPV18 life cycle. To establish organotypic raft cultures, HFK-HPV18 keratinocytes were seeded onto a collagen gel containing 3T3-J2 feeder cells. Once confluent, the gels were raised to the air-liquid interface to allow the keratinocytes to stratify and differentiate. After two weeks, raft cultures were fixed in formal saline and processed for histology. Figure 4.14 shows a haematoxylin and eosin (H&E) stained section of representative HFK-HPV18 raft cultures grown at the air-liquid interface for two weeks. As with normal epidermal keratinocytes, HFK-HPV18 keratinocytes formed a fully differentiated cornified epithelium, with characteristic basal, spinous and granular layers reminiscent of a normal epidermis.

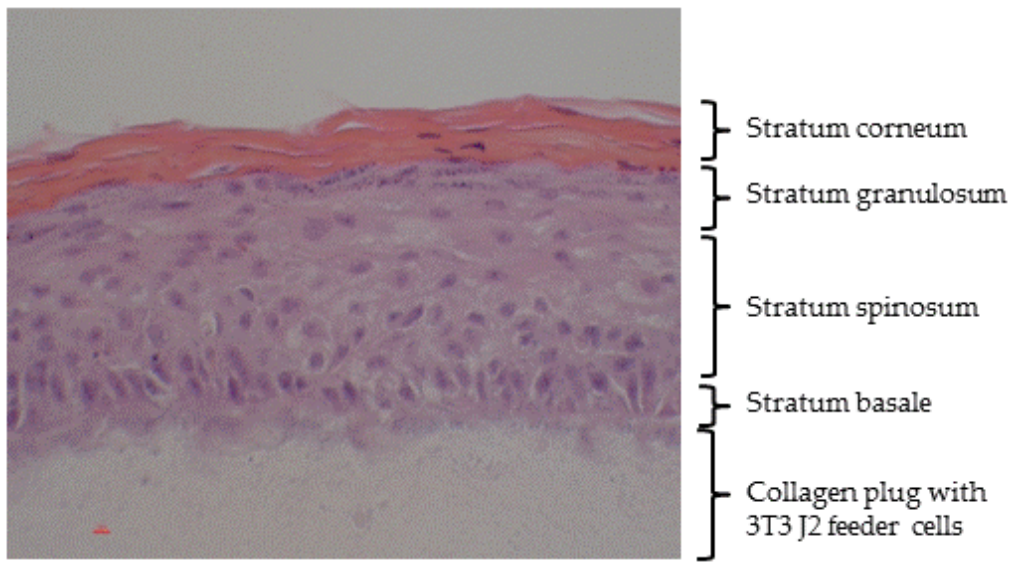


Figure 4.14 Organotypic raft culture of HFK-HPV18 showing the overall morphology of the stratified epithelium. Haematoxylin and Eosin (H&E) stained section showing a typical raft structure formed by HFK-HPV18.

4.6.1 EGCG inhibits the proliferation of HFK-HPV18 organotypic raft culture

As the effects of EGCG on the growth of HPV-infected keratinocytes in organotypic raft culture had not been performed previously, three different experiments were set up to examine the effects of EGCG treatment on the morphology of HFK-HPV18 keratinocytes in raft culture. In the first experiment, 100 μ M EGCG was added to the culture medium as soon as the collagen plug was lifted to the air-liquid interface, and the raft culture refed with EGCG every 2 days for a total of 13 days. In the second and third experiments, the raft cultures were allowed to stratify for 7 and ten days at the air-liquid interface, respectively, before 100 μ M EGCG was added into the culture medium. In experiment 2, raft cultures were treated with EGCG for seven days while those in experiment 3 were treated for ten days. Corresponding control raft cultures

were also set up for all the three experiments where an equal volume of sterile water was added in place of EGCG to the culture medium.

Figure 4.15 shows representative H&E stained sections of raft cultures obtained from the three experiments described above. The duration in which all the three raft cultures were allowed to stratify was 13, 14 and 20 days before they were fixed and processed for histology. Note that the latter raft culture has a thinner epithelium and a thickened cornified layer compared to raft cultures harvested at the 13 and 14-day time points. All three raft cultures treated with 100 μ M EGCG formed significantly thinner epithelia compared to control untreated rafts. However, EGCG did not prevent the rafts from stratifying, as the keratinocytes were still able to differentiate and form stratum corneum albeit a less well-defined stratum spinosum and granulosum.

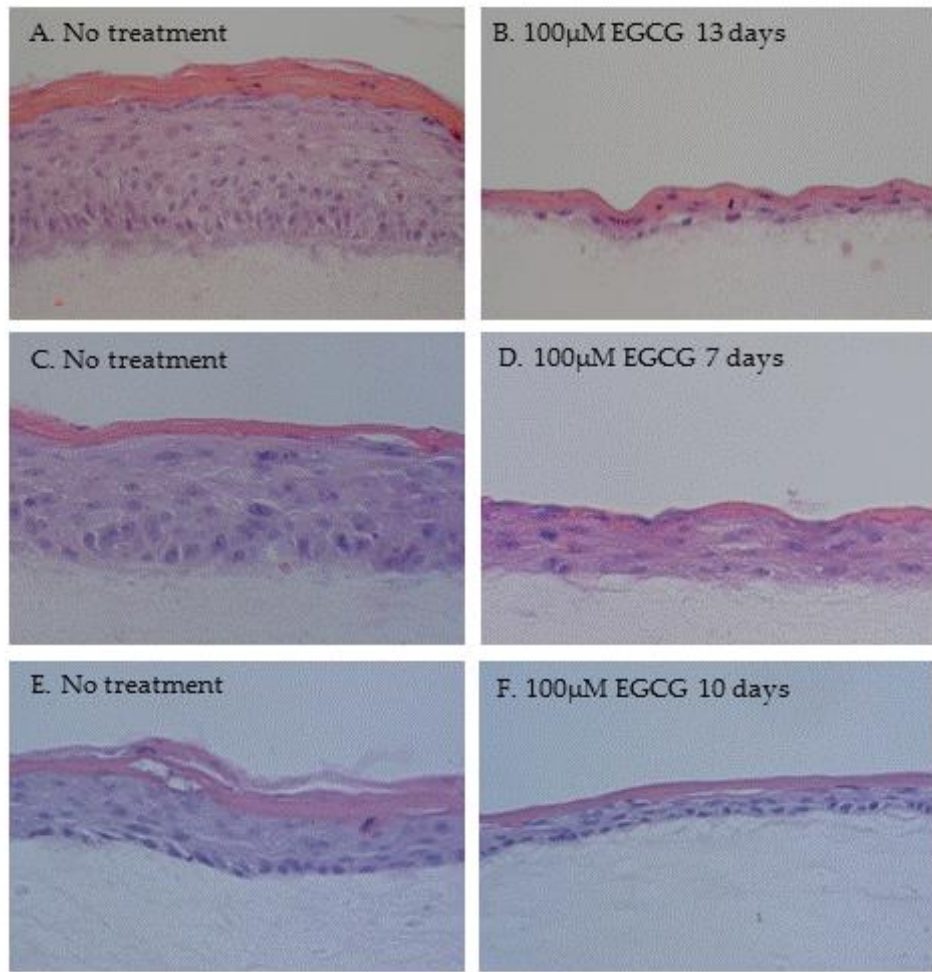


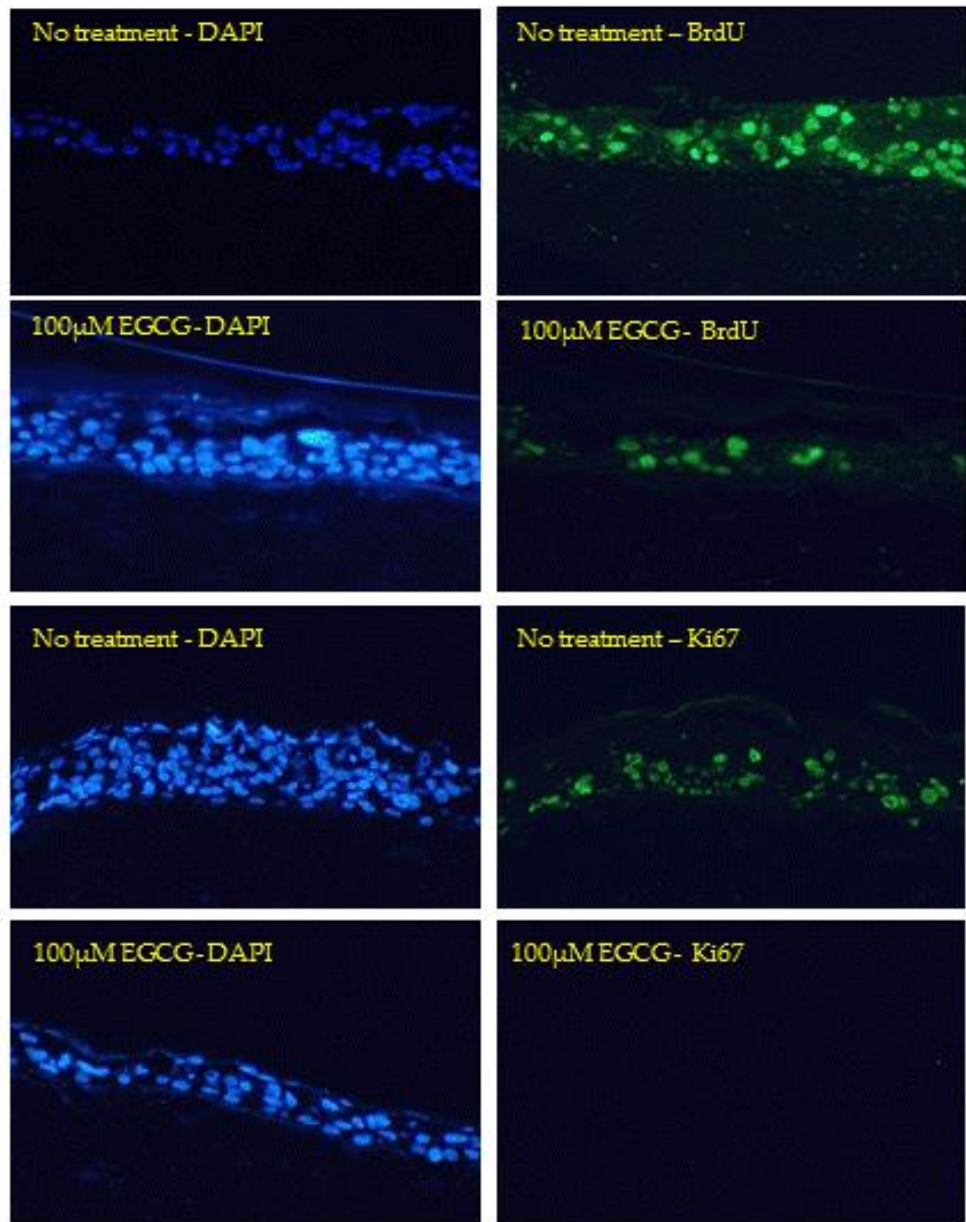
Figure 4.15: EGCG inhibits the proliferation of HFK-HPV18 in organotypic raft culture. Panels A-F show representative haematoxylin and eosin (H&E) stained sections of HFK-HPV18 keratinocytes grown in the absence or presence of 100 μ M EGCG in raft culture. HFK-HPV18 cells were seeded onto collagen plugs impregnated with 3T3 cells and then lifted onto metal grids to stratify at the air-liquid interface. 100 μ M EGCG or an equal volume of water was added into growth media of the raft cultures for the indicated times. In panel B, the raft culture was treated with EGCG for 13 days when the collagen plug was laid onto the metal grid. In panels C & D, rafts were allowed to stratify for 7 days before EGCG was added to the growth media for a further 7 days (panel D). In panels E and F, rafts were allowed to stratify for 10 days before treatment with EGCG for a further 10 days (panel F).

4.6.2 EGCG treatment inhibits the incorporation of BrdU label and reduces the expression of the proliferation marker, Ki67, in HFK-HPV18 rafts

Having observed that EGCG treatment reduces the thickness of the epithelium in raft culture, I set out to determine whether this stemmed from the effects of EGCG on cell proliferation. Prior to fixation and processing, raft cultures were treated with 25 μ g/ml BrdU for 12 hours to label cells replicating their DNA. Immunofluorescence staining was performed with a monoclonal antibody to BrdU and a monoclonal antibody specific for the cell proliferation marker, Ki67; DAPI was used as counter stain cell nuclei. As shown in Figure 4.16A, a significant number of cells were labelled throughout the full thickness of the epithelium in control, untreated raft cultures. In marked contrast, fewer cell nuclei were labelled in raft cultures treated with EGCG. Essentially similar findings were observed when rafts were stained for Ki67, with fewer labelled cells being observed in sections obtained from EGCG treated raft cultures. The number of cell nuclei labelled with BrdU, or expressing Ki67, was counted manually in control and EGCG treated rafts and these expressed as a proportion of the total DAPI stained cell nuclei. Results were presented as the proportion of cells stained positive for targeted proliferative markers. Two-tailed unpaired Student t-test was used to determine the difference in the proliferative marker expression of in EGCG treated rafts is significant when compared to control.

Figure 4.16B shows the results of IF staining for BrdU and Ki67, shown as a percentage of total DAPI stained nuclei. BrdU and Ki67 expression were significantly reduced in response to EGCG treatment compared to control rafts, indicating that DNA replication and cell proliferation were inhibited by EGCG.

A.



B.

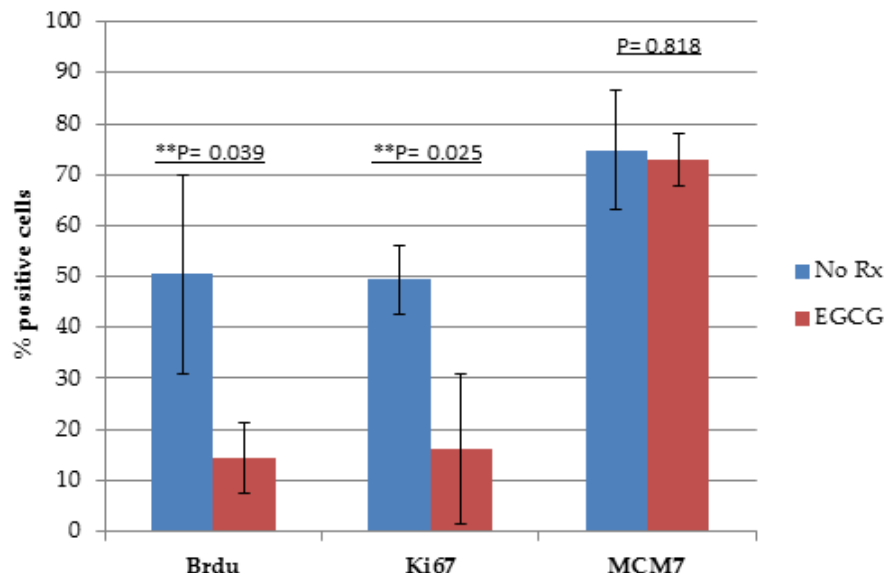


Figure 4.16 BrdU incorporation and expression of the proliferation marker Ki67 are reduced, while MCM7 remains unchanged, in organotypic raft cultures of HFK-HPV18 treated with EGCG. Organotypic raft cultures were allowed to stratify for ten days prior to the addition of 100 μ M EGCG, which was added to the growth media for a further ten days. 25 μ g/ml BrdU was added to growth media for 12 hours prior to processing to label cells replicating DNA. (A) Immunofluorescence (IF) staining of FFPE sections of HFK-HPV18 for anti-BrdU, Ki67 or MCM7 (Green) and counterstained with DAPI (Blue) to detect cell nuclei. Magnification $\times 200$. (B) Summary of the results obtained for cells incorporating BrdU label or staining positive for the proliferation antigens Ki67 and MCM7 in control and EGCG treated organotypic raft cultures. The total number of cell nuclei (DAPI stained) and those nuclei expressing BrdU, Ki67 or MCM7 were counted manually. Results were presented as the proportion of cells stained positive for targeted proliferative markers. **P<0.05, two-tailed Student unpaired t-test indicates that the difference in BrdU or Ki67 expression is significant when compared to control. No Rx = No treatment.

4.6.3 EGCG treatment of HFK-HPV18 in organotypic raft cultures does not affect the expression of MCM7 or p16^{INK4a}, two established targets of the HR-HPVs

As stated in section 4.4.3, infection of epithelial tissues with HR-HPV is accompanied by increased expression of the minichromosome maintenance (MCM) proteins, MCM6/MCM7 and p16^{INK4a}. Indeed, p16^{INK4a}, in conjunction with HPV genotyping, is often used as a surrogate marker of a transcriptionally active HR-HPV infection. The expression of MCM7 and p16^{INK4a} was next examined on control and EGCG-treated raft sections using antibodies specific for MCM7 and p16^{INK4a}; raft sections were counter-stained with DAPI to visualise cell nuclei. Figure 4.17 confirmed high levels of MCM7 and high levels of “block” staining for p16^{INK4a} in untreated raft cultures. Interestingly, very similar levels were observed in EGCG-treated raft sections, indicating that chronic EGCG treatment at this particular dose did not abrogate, completely, the biological actions of the E6 and E7 proteins. Results obtained from the p16^{INK4a} IF staining were consistent with findings from immunohistochemical (IHC) staining performed at the Histopathology Department at City Hospital, Birmingham (Supplementary Figure 1). Thus, both IF and IHC staining showed diffuse cytosolic and nuclear p16^{INK4a} staining in untreated and EGCG-treated raft sections of HFK-HPV18.

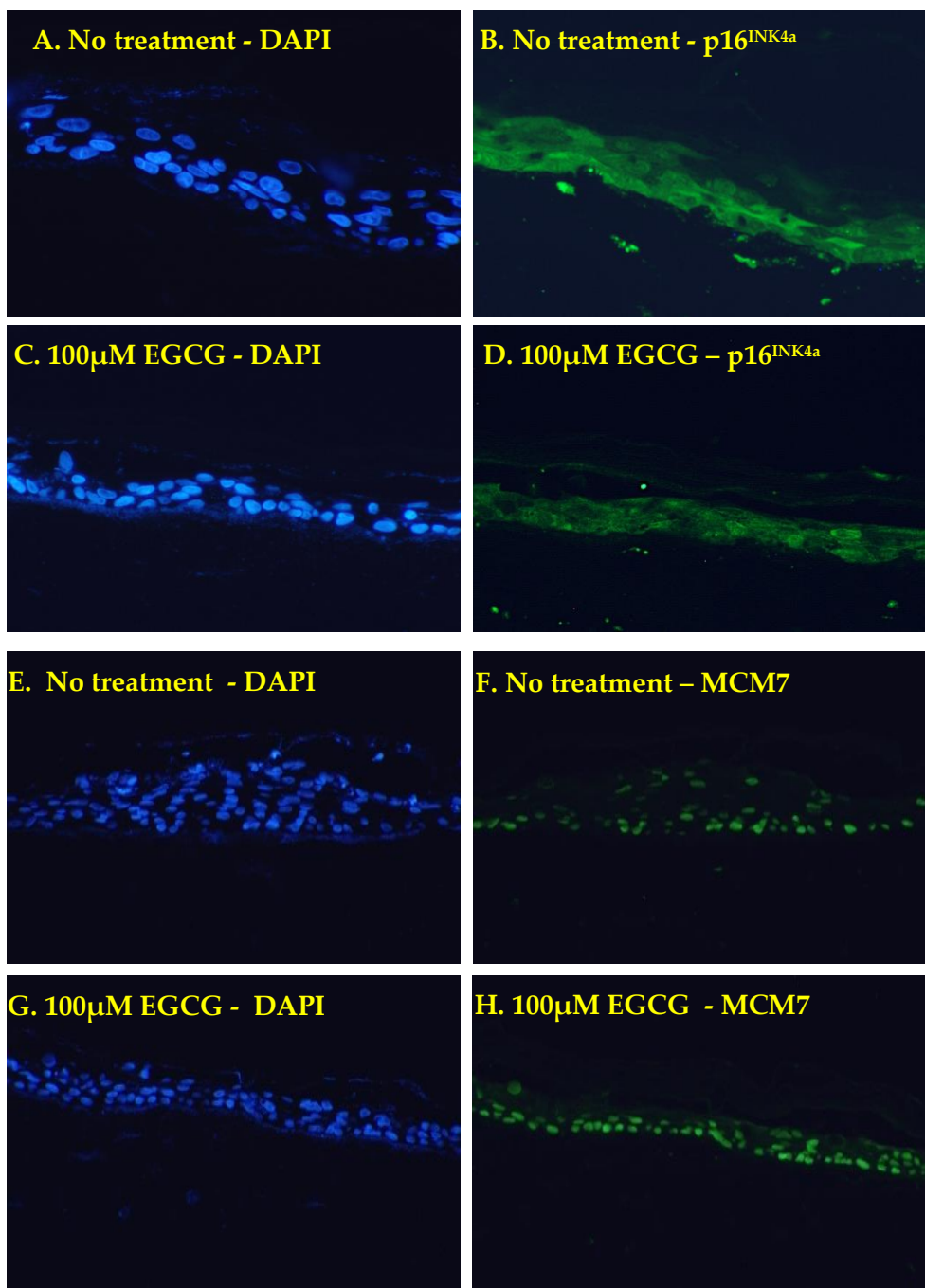


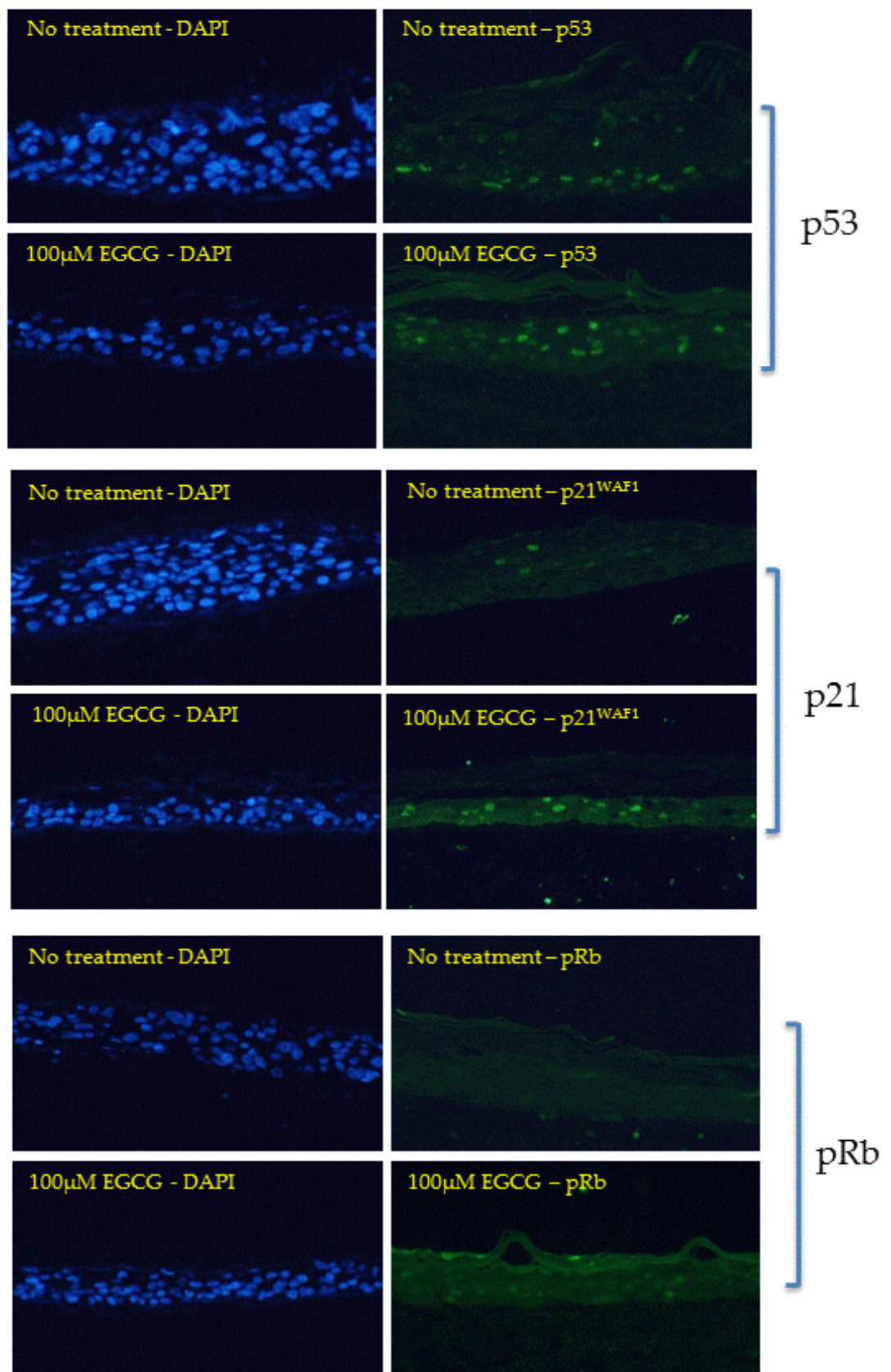
Figure 4.17: Expression of p16^{INK4a} and MCM7 are not affected by EGCG treatment in organotypic raft cultures of HFK-HPV18. FFPE sections of HFK-HPV18 raft cultures were stained for (A-D) p16^{INK4a} or (E-H) MCM7 (Green) and counter stained with DAPI (Blue) to label cell nuclei. Panels A-D show raft sections with diffuse cytosolic and nuclear p16^{INK4a} staining in untreated and EGCG-treated raft cultures. Panels E-H show nuclear staining of MCM7. Magnification x200.

4.6.4 EGCG treatment increases the expression of tumour suppressor genes (TSGs)

p53, p21^{WAF1} and pRb in HFK-HPV18 raft cultures

Given the lack of an effect of EGCG on the expression of p16^{INK4a} and MCM7, I sought to examine raft cultures for expression of p53, p21^{WAF1} and pRb, given that these are established targets of E6 and E7. Raft sections were stained with monoclonal antibodies specific for p53, p21^{WAF1} or pRb (Green) and counter stained with DAPI (Blue) to identify cell nuclei. Compared to untreated raft cultures, EGCG-treated rafts displayed overall increases in the expression of p53, p21^{WAF1} and pRb (Figure 4.18A & B). Quantification of these results revealed that EGCG-treated rafts displayed a 35% increase in p53; a 23% increase in p21^{WAF1}; and a 23% increase in pRb expression (Figure 4.18C). The increase in p53 and p21^{WAF1} expression from baseline following EGCG treatment seen here in the raft cultures are consistent with results obtained by Western blotting analysis in section 2.4.3 also showing an increase in the expression of these TSGs following EGCG treatment of HFK-HPV18 in monolayer culture.

A.



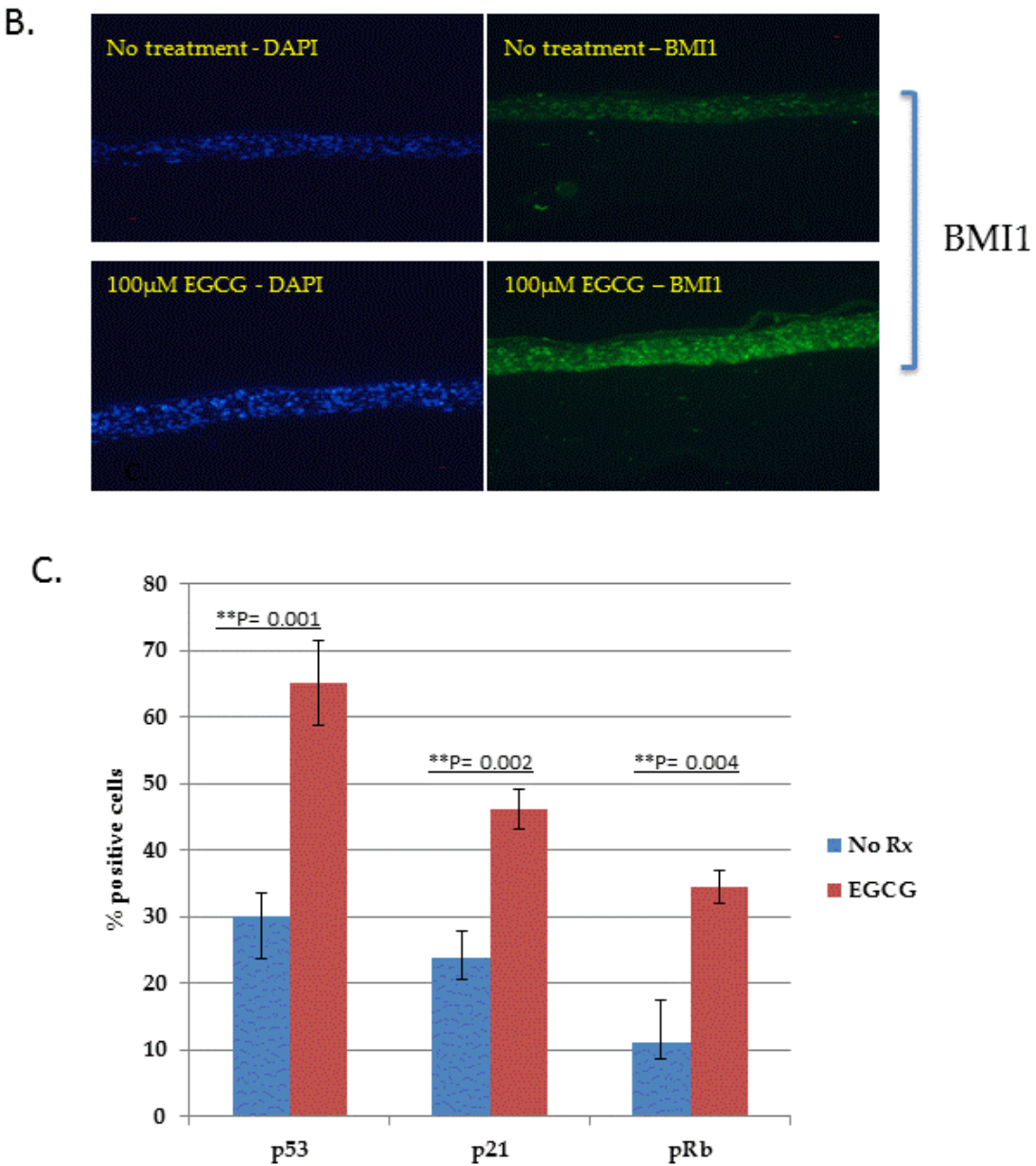


Figure 4.18: Expression of tumour suppressor genes (TSGs), p53, p21^{WAF1}, pRb, and the Polycomb group protein BMI1 are increased in response to EGCG treatment.

(A). Immunofluorescence (IF) staining of FFPE sections of HFK-HPV18 for p53, p21^{WAF1} and pRb (Green) and counterstained with DAPI (Blue) to detect cell nuclei.

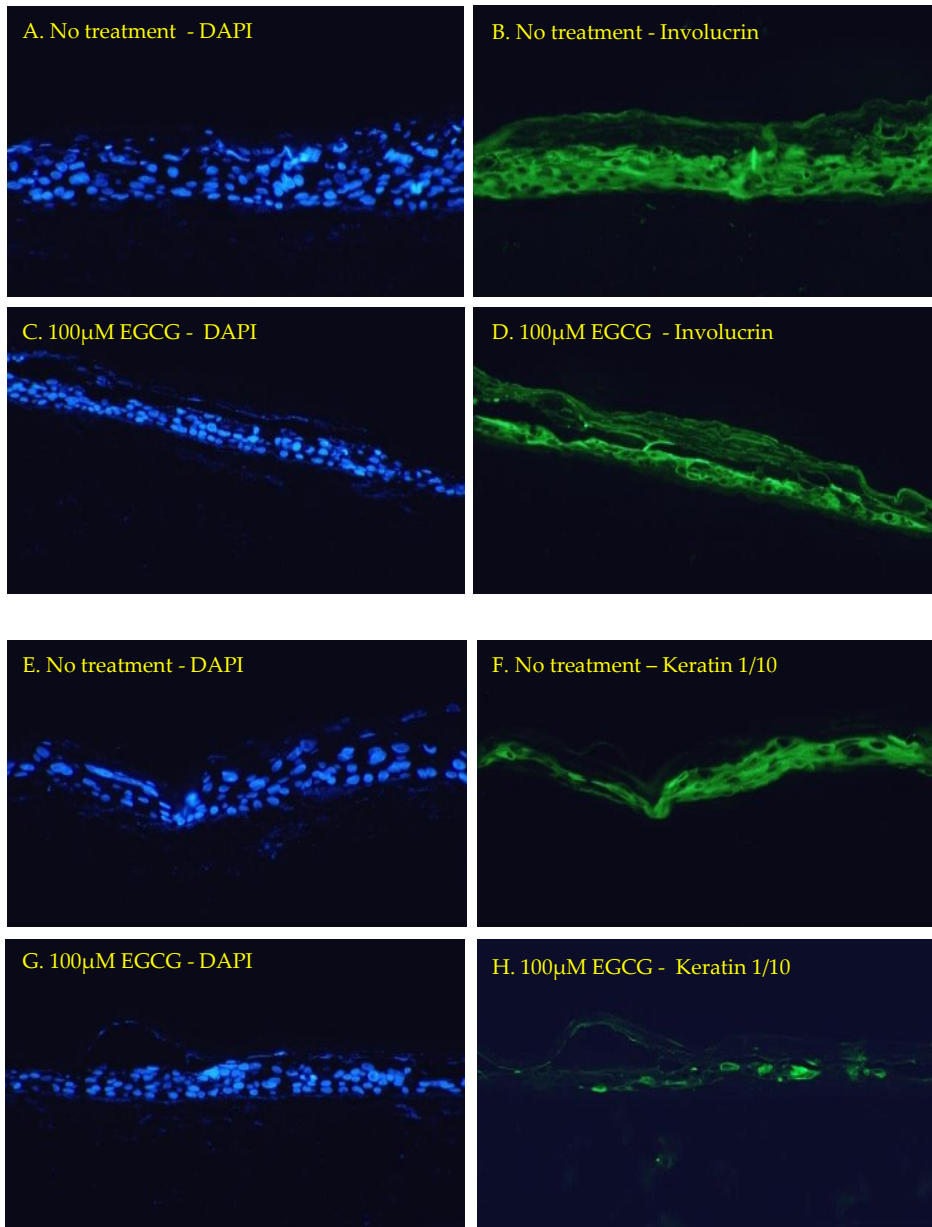
(B). Immunofluorescence (IF) staining of FFPE sections of HFK-HPV18 for BMI1 (Green) and counterstained with DAPI (Blue) to detect cell nuclei. Magnification x200.

(C) Summary of the results obtained for positive nuclear staining of the TSGs in control and EGCG treated raft cultures. Total number of cell nuclei (DAPI stained) and those nuclei expressing p53, p21^{WAF1} and pRb were counted manually. Results were presented as proportion of cells stained positive for targeted proliferative markers. **P<0.05, two-tailed student unpaired t-test indicates that the difference in p53, p21^{WAF1} and pRb expression is significant when compared to control.

4.6.5 EGCG treatment does not affect expression of keratinocyte differentiation markers in HFK-HPV18 raft cultures

Evidence in the literature supports the notion that EGCG promotes the differentiation of normal epidermal keratinocytes [103]. Although EGCG treated HFK-HPV18 rafts were considerably thinner than control rafts, I nonetheless wanted to determine whether EGCG treatment influenced keratinocyte differentiation. Control and EGCG treated raft sections were subjected to staining with mAbs specific for a number of differentiation-associated proteins. These included involucrin and the high molecular-weight keratins, K1/10, whose expression is confined to differentiating keratinocytes, and β -catenin and Δ Np63, whose expression is confined to basal and immediate suprabasal cells, and basal cells, respectively (Green). Rafts were counter stained with DAPI (Blue) to identify cell nuclei. Figure 4.19A revealed that both involucrin and K1/10 were expressed in the suprabasal differentiating layers of HFK-HPV18 rafts, with sparing of the undifferentiated basal cell layers. Expression of β -catenin was localised to cell membranes of basal and suprabasal cell layers, whereas expression of Δ Np63 was restricted to the basal cell layer (4.19B). Objectively there was no change in the expression of these differentiation markers in EGCG treated and untreated rafts indicating that the differentiation of HFK-HPV18 in raft culture was not affected by EGCG treatment.

A.



B.

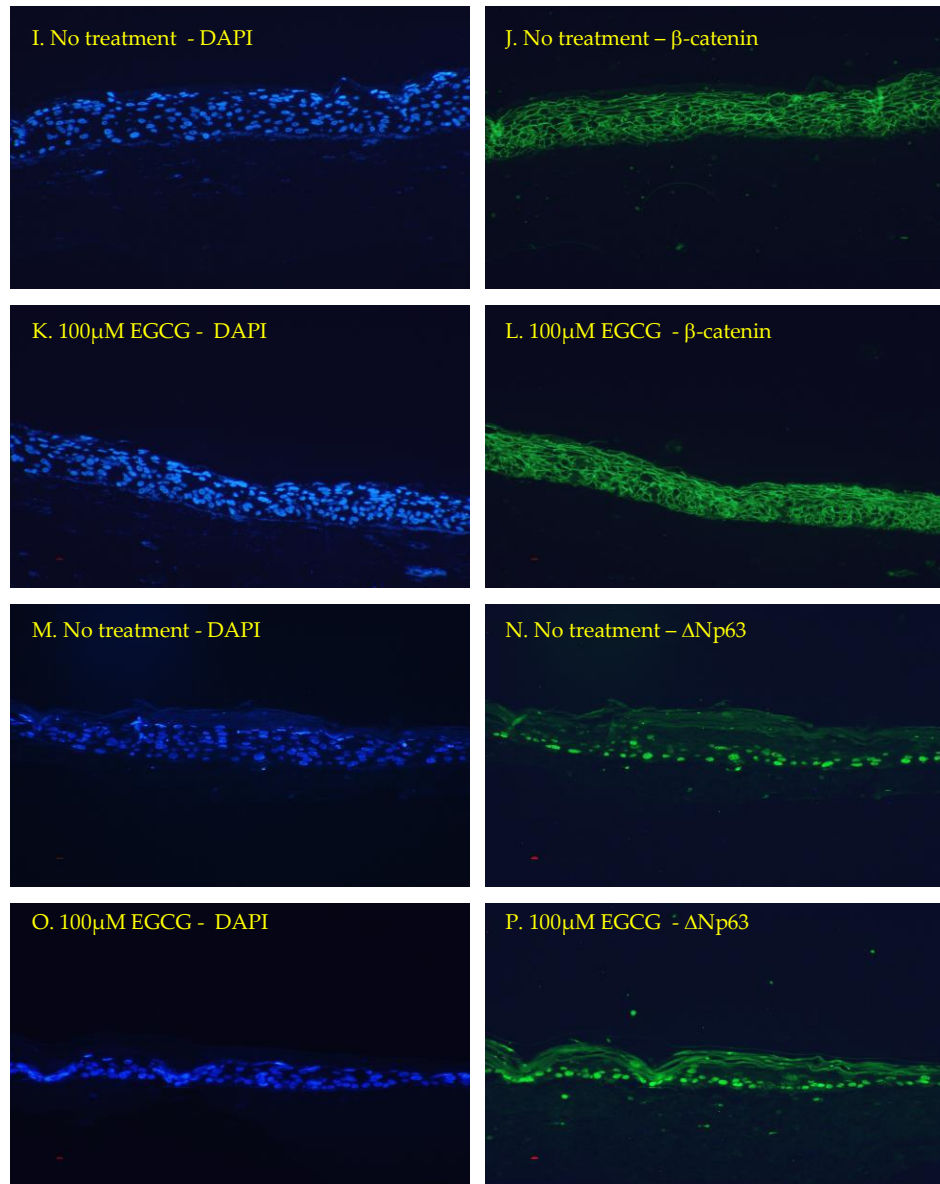


Figure 4.19: Expression of the keratinocyte differentiation markers: involucrin, Keratin 1/10, β -catenin and Δ Np63 are not affected by EGCG treatment in organotypic raft cultures of HFK-HPV18. FFPE sections from control and EGCG treated HFK-HPV18 were stained with mAbs specific for (A-D) involucrin, (E-H) Keratin 1/10, (I-L) β -catenin, or (M-P) Δ Np63 (Green) and counterstained with DAPI (Blue) to label cell nuclei. Magnification x200.

4.6.6 EGCG treatment does not influence expression of the late protein, E4, in HFK-HPV18 raft cultures

One possible mechanism by which EGCG could inhibit the growth of uVIN lesions is to stimulate lytic replication of the virus. To examine the impact of EGCG on lytic replication, immunofluorescence staining was performed for E4, a viral-encoded late protein whose expression is induced during the lytic phase of the virus life cycle. Previous studies have confirmed suprabasal expression of E4 protein in HFK-HPV 18 keratinocytes induced to differentiate in the organotypic raft culture system. Raft sections were stained with an antiserum specific for HPV18 E4 (kindly provided by Dr Sally Roberts) and counter-stained with DAPI to visualise cell nuclei. Despite numerous attempts, Figure 4.20, I was unable to confirm expression of the E4 protein in the suprabasal differentiating cell layers of raft structures generated by HFK-HPV18 keratinocytes. A similar lack of staining was observed in EGCG-treated rafts, precluding an assessment of the effects of EGCG treatment on lytic replication.

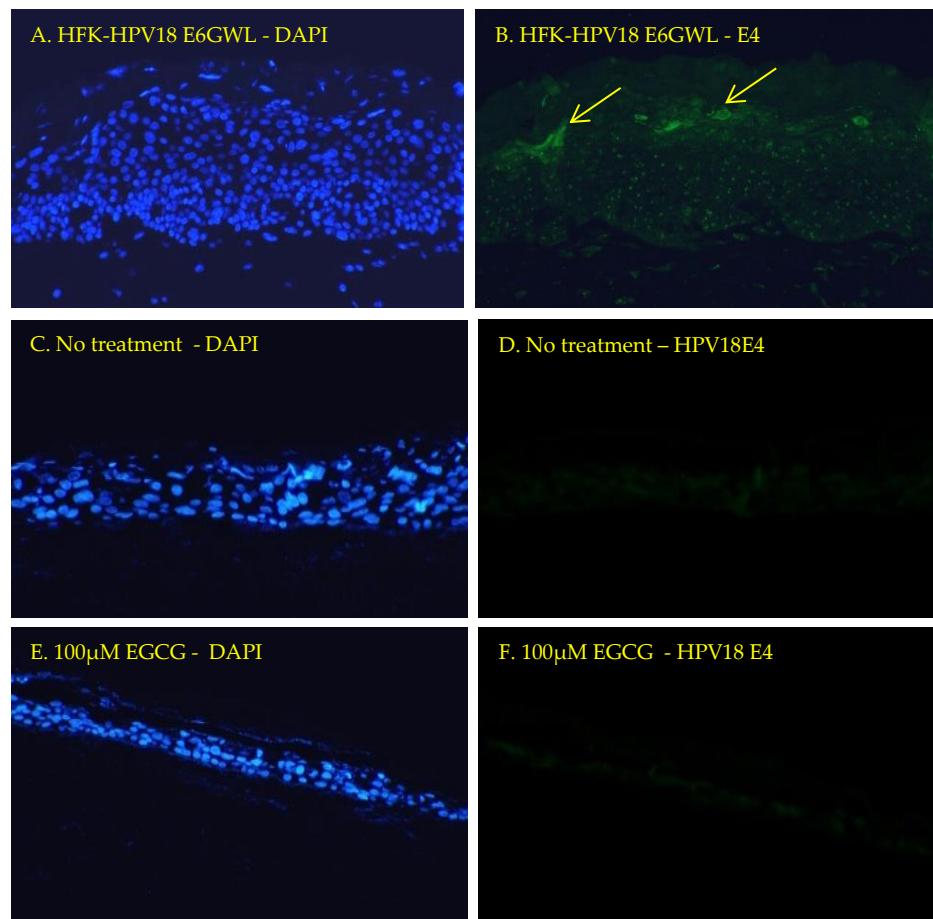


Figure 4.20: Lack of detectable E4 protein expression in control and EGCG-treated HFK-HPV18 raft cultures.

(A-F) FFPE sections were stained with an antiserum specific for HPV18 E4 (Green) and counterstained with DAPI (Blue) to label cell nuclei. (A, B) Positive staining for HPV18 E4 in suprabasal keratinocyte layers of rafts generated from HFK-HPV18 keratinocytes carrying the E6 mutant E6-GWL. (D, E) Lack of staining of HPV18 E4 in suprabasal keratinocyte layers in rafts generated from HFK-HPV18 keratinocytes. Magnification x200.

4.7 EGCG modulates the ubiquitin-proteasome system

Thus far, I have shown that EGCG influences the cellular levels of the HPV18 E6 and E7 proteins through a mechanism that does not appear to involve effects on transcription. These findings suggest that EGCG must influence the stability of E6 and E7 through effects on protein translation or protein turnover (i.e. post-translational events). Previous studies have shown that the E6 and E7 proteins are degraded through the ubiquitin-proteasome system, as MG132, a broad-spectrum proteasome inhibitor, inhibits the turnover of these proteins. Given that EGCG has previously been shown to modulate the turnover of proteins through the ubiquitin-proteasome system, it seemed reasonable to assume that EGCG might also promote the turnover of E6 and E7 proteins by enhancing their ubiquitination or by modulating proteasome activity.

4.7.1 The proteasome inhibitor MG132 attenuates EGCG-mediated down regulation of E6 and E7 in HFK-HPV18

To establish whether EGCG enhances E6 and E7 degradation through the ubiquitin-proteasome pathway, MG132, a commonly used proteasome inhibitor, was used to block proteasome activity in untreated and EGCG treated HFK-HPV18 keratinocytes. Cells were treated with 100 μ M EGCG for 72 hours to induce maximum E6 and E7 down-regulation before the addition of 10 μ M MG132 for the final 6 hours; HFK-HPV18 keratinocytes were also treated with MG132 alone. Cells were lysed in RIPA buffer and equal amounts of protein lysate resolved by SDS-PAGE. Western blotting was then performed using antisera specific for E6 and E7; β -actin was included to ensure equal protein loading.

Figure 4.21 shows that MG132 treatment leads to an accumulation of E6 and E7 protein, indicating that both proteins are degraded through the ubiquitin-proteasome pathway. As expected, the levels of E6 and E7 protein were both down-regulated following 72 hours treatment with of EGCG; however, MG132 treatment led to the accumulation of E6 and E7 protein albeit to lower levels than those observed in untreated cells. This finding suggests that EGCG stimulates E6 and E7 protein turnover through the ubiquitin-proteasome pathway.

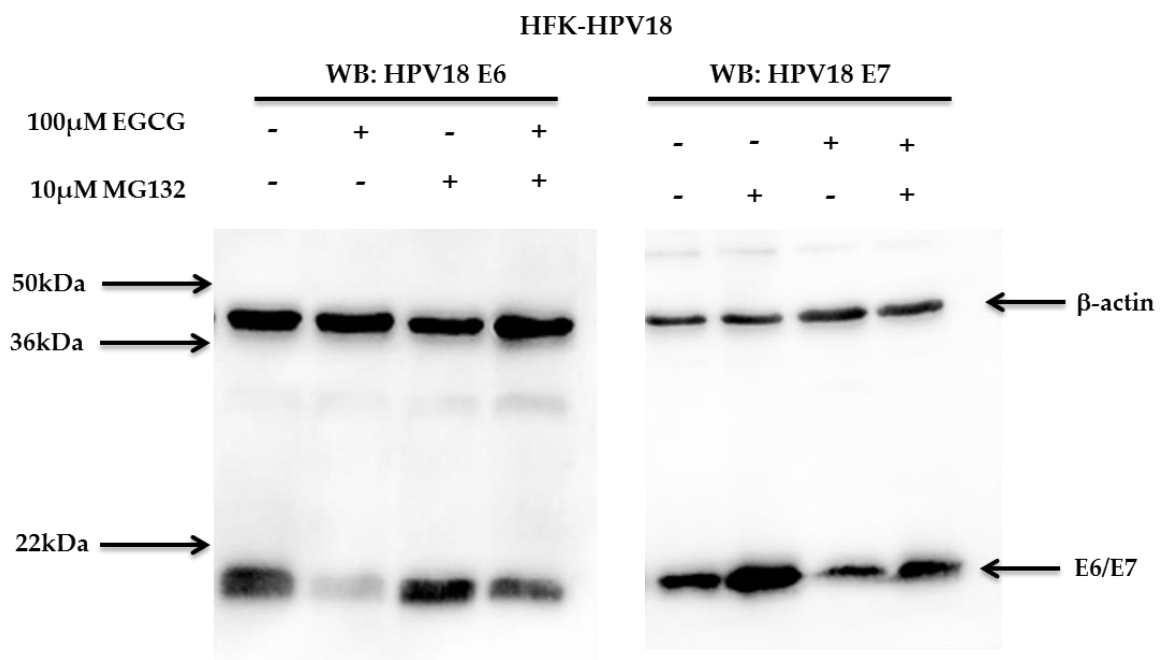


Figure 4.21: MG132 reverses EGCG-mediated down-regulation of the E6 and E7 proteins in HFK-HPV18. HFK-HPV18 cells were treated with either 10μM MG132 for 6hrs, 100μM EGCG for 72hrs or 100μM EGCG for 72hrs followed by 10μM MG132 for 6hrs. Cells were lysed with RIPA buffer and 30μg of total protein lysate resolved by SDS-PAGE. The levels of HPV18 E6, E7 and β-actin, were determined by Western blotting analysis. Experiments were repeated three times.

4.7.2 EGCG reduces the half-life of the HPV18 E6 protein

To further strengthen the hypothesis that EGCG stimulates the turnover and degradation of the E6 and E7 proteins, the half-life of E6 was measured in the absence and presence of EGCG. HFK-HPV18 keratinocytes were cultured in 6cm petri dishes on 3T3-J2 fibroblasts until 70% confluent. The feeder cells were then removed and the remaining HFK-HPV18 keratinocytes treated with 100 μ g/ml cycloheximide (CHX), in the presence or absence of 100 μ M EGCG for 1hr, 2hrs, 4hrs and 6hrs. At the allotted time points, cells were lysed in RIPA buffer and sonicated. Equal amounts of total protein lysate were resolved by SDS-PAGE prior to Western blotting with an antibody to E6; blots were reprobed with an antibody to β -actin to ensure equal protein loading. A representative experiment, Figure 4.22, shows that the rate of E6 degradation was increased significantly within the first hour of EGCG treatment. The half-life of E6 was approximately 3 hours but this was significantly reduced to just under an hour following EGCG treatment. Interestingly, the rate of protein degradation increased only in the first 1.5 hours after EGCG treatment and, thereafter, appeared to stabilise, with the rate of protein degradation similar to that of the control. If HFK-HPV18 cells were pre-treated with 100 μ M EGCG for 2 hours before CHX was added to block protein synthesis, note that although the pool of E6 was significantly lower following EGCG treatment, but the rate of protein degradation was identical to that of control, indicating that EGCG treatment increases the rate of E6 degradation only during the first 1.5 hours of treatment.

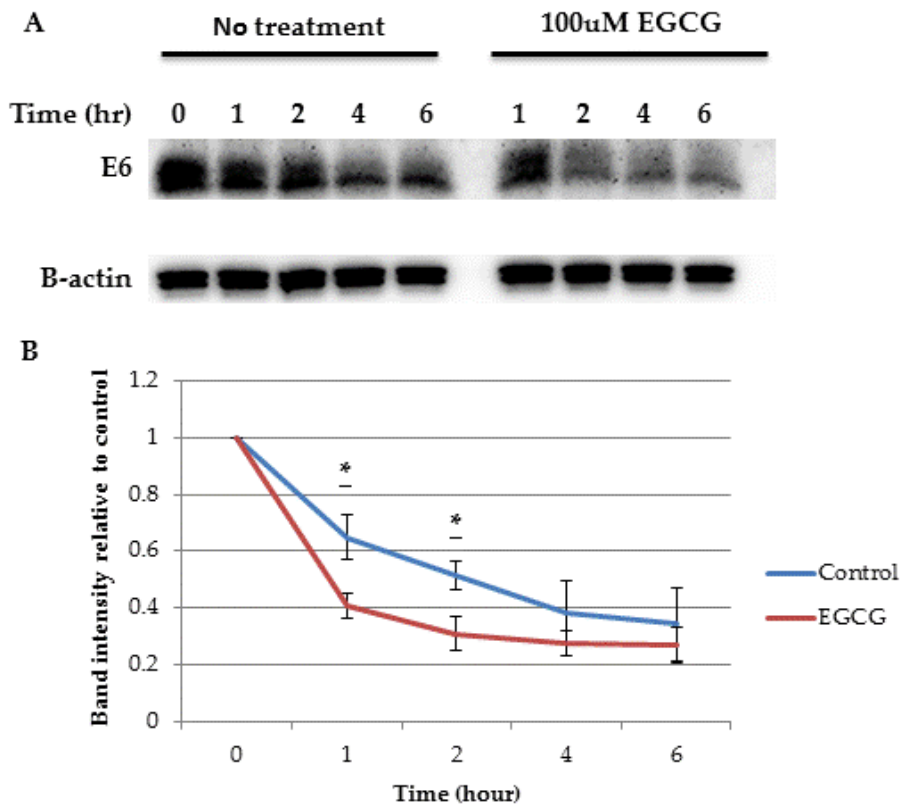


Figure 4.22: EGCG promotes degradation of the HPV18 E6 protein.
HFK-HPV18 cells were treated with and without 100 μ M EGCG in the presence of 100 μ g/ml Cycloheximide (CHX) to inhibit protein synthesis. Cells were harvested at 0, 1, 2, 4 and 6hrs post CHX treatment and lysed in RIPA buffer. 30 μ g of total protein lysate were resolved by SDS-PAGE and the expression of HPV18 E6 and β -actin determined by Western blotting analysis. Experiments were repeated twice. (A) Western blot showing down-regulation of E6 expression following EGCG treatment. (B) Densitometric analysis of the Western blots. E6 densitometry values were normalised against β -actin. The fold change in E6 expression was compared against untreated cells (control). **P<0.05, unpaired student t-test indicates that the difference in band intensity (protein concentration) was significant when compared to control. Averaged results from three experiments.

4.7.3 EGCG treatment does not increase the pool of poly-ubiquitinated E6 and E6-associated proteins

Proteins that are destined for degradation undergo post-translational modification. In most instances, ubiquitination, a process that involves the covalent attachment of ubiquitin molecules to lysine residues on the target protein, is a prerequisite for proteasome targeting and proteolysis. At least four ubiquitin monomers are required before the protein can be recognised by the proteasome [137]. One mechanism by which EGCG may increase the rate of E6 degradation is to enhance its ubiquitination. To investigate this possibility, a transient expression system was employed in which the E6 protein was overexpressed and evidence of E6 ubiquitination examined by immunoprecipitating the HPV18 E6 protein and Western blotting with a monoclonal antibody that recognises both mono and poly-ubiquitin.

Briefly, a plasmid, pCA.18E6, encoding an epitope tagged form of HPV18 E6 [69], was transiently transfected into HEK293 cells. Following EGCG treatment, the epitope-tagged HPV18E6 protein was purified using anti-FLAG conjugated agarose beads. After a series of washes to remove non-specific protein binding, eluted proteins were resolved by SDS-PAGE and subjected to Western blotting with an antibody to HPV18-E6, or a monoclonal antibody that recognises both mono and poly-ubiquitin.

As a starting point, the pCA.18E6 plasmid was transiently transfected into HEK293 cells. 48 hours later, cells were lysed in an NP40-based lysis buffer containing 20mM Iodacetamide, and equal amounts of protein lysate resolved by SDS-PAGE. To confirm that the tagged HPV18 E6 protein was expressed, and that the epitope tags were intact, Western blotting was performed using antibodies specific for HPV18 E6, or to the

FLAG or HA epitopes. Total cell lysates from HEK293 cells transfected with the pcDNA3 plasmid were included as a negative control, while protein lysates from HFK-HPV18 were included as a positive control for HPV18 E6. As shown in Figure 4.23, Western blotting confirmed the expression of the HPV18 E6 protein in HEK293 cells transfected with pCA.18E6, at levels that were higher than those observed in HFK-HPV18 keratinocytes. Importantly, Western blotting with antibodies specific for the HA and FLAG epitopes confirmed the presence of the tagged HPV18 E6 protein, as no signals were observed in HFK-HPV18 cells which carry a non-tagged E6 protein. No signals were detected in HEK293 cells transfected with pcDNA3, confirming the specificity of the antibodies used for detection. Compared to HFK-HPV18, the E6 band detected in HEK293 was at a slightly higher molecular weight, consistent with the fact that the E6 protein derived from the plasmid carries an extra 3kDa in weight from the FLAG (~1kDa) and double HA (2x 1kDa) tagged epitopes.

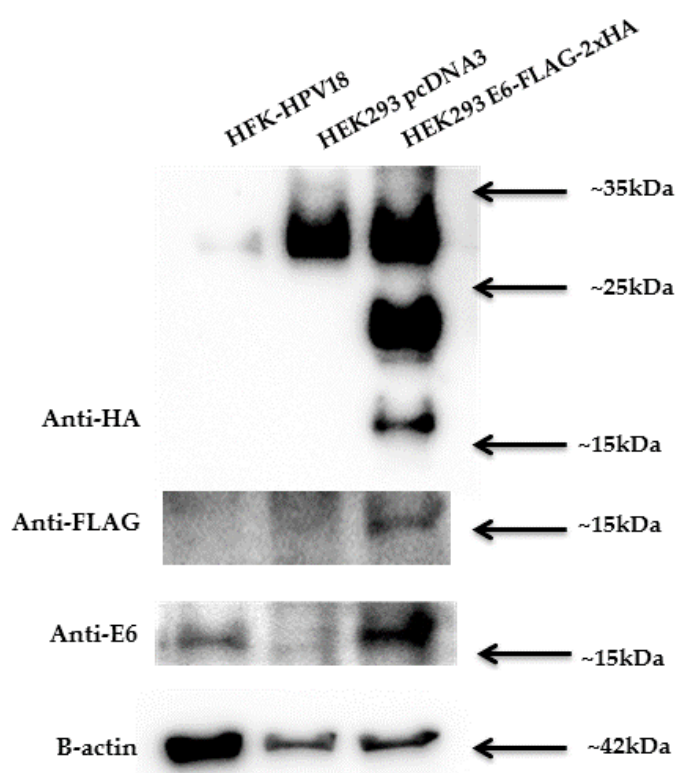


Figure 4.23: Validation of the pCA.18E6 plasmid. HEK293 cells were transfected with either control (pCDNA3) or HPV18 E6 (pCA.18E6) plasmids. 48 hours post-transfection, cells were lysed in an NP40-based lysis buffer containing 20mM Iodoacetamide. 50 μ g of total protein lysates were resolved by SDS-PAGE prior to Western blotting with antibodies specific for the HA or FLAG epitopes, or HPV18 E6, to confirm expression of the protein epitopes and E6 in HEK293 cells following transfection. The HFK-HPV18 cell was used as positive control for HPV18 E6 expression.

Having confirmed that HEK293 cells transfected with pCA.18E6 expressed the tagged E6 protein, HEK293 cells were next transfected with pCA.18E6 or pcDNA3 and, 48 hours later, treated with 40 μ M MG132 or 100 μ M EGCG for 2 hours. Cells were then lysed in an NP40-based lysis buffer containing 20mM Iodoacetamide to inhibit the activity of deubiquitinating enzymes (DUBs). Equal amounts of total cell lysate (500 μ g) were incubated with anti-FLAG agarose beads to immunoprecipitate the tagged HPV18 E6 protein. After 3 washes, proteins retained by the beads were dissolved in Laemmli buffer and resolved by SDS-PAGE. Western blotting was then performed using an HRP-conjugated monoclonal antibody that detects mono and poly-ubiquitinated proteins. The results of a representative immunoprecipitation (IP) experiment (Figure 4.24 - upper panel) revealed a general increase in the pool of mono and poly-ubiquitinated proteins in E6 immunoprecipitates from MG132-treated cells. Interestingly however, no such effects were observed for HPV18 E6 immunoprecipitated from EGCG-treated cells, with essentially similar levels of mono and poly-ubiquitinated proteins being found in HPV18 E6 immunoprecipitates from EGCG-treated and untreated samples. The increased amounts of mono and poly-ubiquitinated proteins found in E6 immunoprecipitates from MG132-treated cells appeared to be of moderate to high molecular weight, and in excess of 55kDa. Although speculative, this finding suggested that the majority of these high molecular weight mono and poly-ubiquitinated proteins were likely to be HPV18 E6-associated proteins, and that the amounts of ubiquitinated HPV18 E6 protein present in the eluted samples were beyond the limit of detection. Reprobing of the blots with a high-affinity monoclonal antibody specific for the HA epitope (Figure 4.24 - bottom panel), confirmed the presence of the epitope-tagged HPV18 E6 protein in the IP eluates from

the three sets of lysates. Moreover, significantly higher amounts of E6 protein were found in the anti-FLAG IP's prepared from MG132-treated cells, further supporting the notion that E6 is degraded through the proteasome. Unlike the situation with MG132, EGCG treatment did not result in an increase in the levels of epitope-tagged HPV18 E6, with broadly similar levels being observed compared to untreated cells.

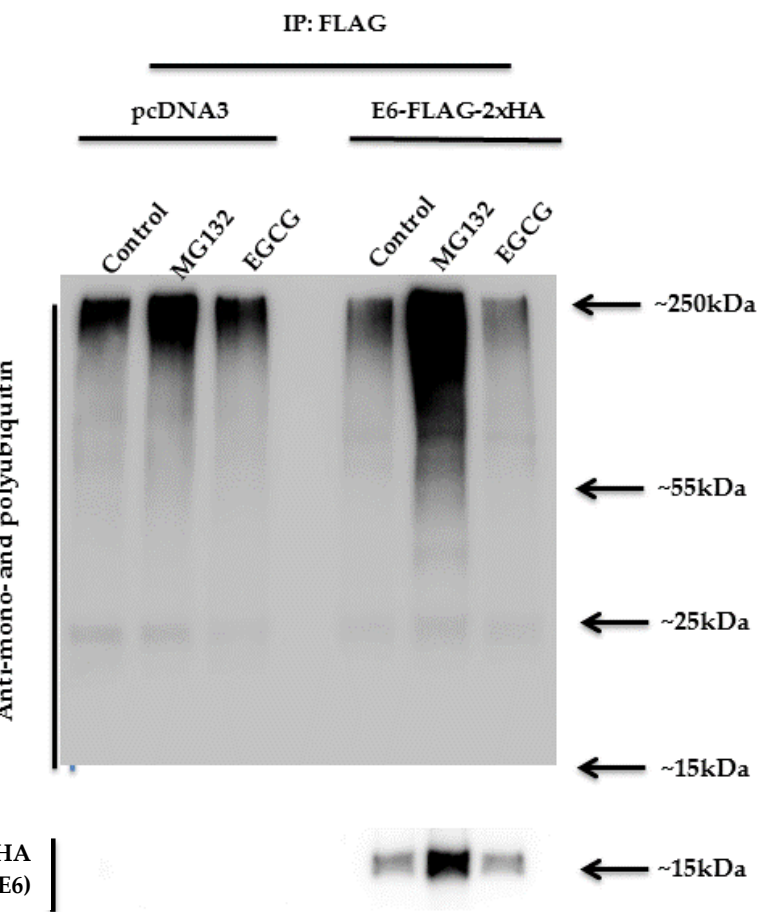


Figure 4.24: Mono- and poly-ubiquitinated proteins are only detected in HPV18 E6 immunoprecipitates from MG132-treated cells. HEK293 cells were transfected with plasmids expressing HPV18 E6 (pCA.18E6) or control plasmid (pCDNA3) and treated with 100 μ M EGCG or 40 μ M MG132 for 2 hours prior to lysis in an NP40-based buffer containing 20mM Iodoacetamide. 500 μ g of protein lysates were incubated with Anti-FLAG®M2 agarose beads. FLAG-tagged proteins were immunoprecipitated and resolved by SDS-PAGE followed by Western blotting with a mAb recognising mono- and poly-ubiquitin or the HA epitope to identify the epitope tagged HPV18 E6 protein. Experiment was repeated twice.

Western blotting of total cell lysates with a monoclonal antibody specific for the HA epitope (Figure 4.25), confirmed expression of epitope-tagged HPV18E6 in lysates generated from pCA.18 E6 transfected cells but not in lysates generated from control, pcDNA3 transfected cells. Again, MG132 treatment led to an accumulation in the total amounts of E6 protein, whereas EGCG had no such effect.

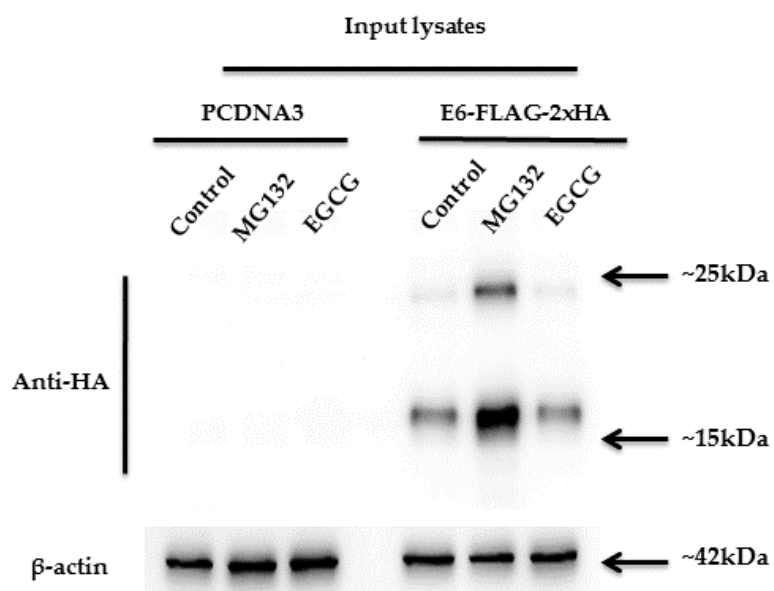


Figure 4.25: Input lysates for FLAG immunoprecipitation.
HEK293 cells were transfected with pCA18E6 or the control plasmid, pCDNA3, and treated with 100 μ M EGCG or 40 μ M MG132 for 2 hours. Transfected HEK293 cells were then lysed in NP40 containing 20mM Iodoacetamide and sonicated. 50 μ g (10% input) of protein lysates were resolved by SDS-PAGE followed by Western blotting for anti-HA and anti- β -actin to confirm successful transfection of E6-FLAG-2xHA plasmid into HEK293 cells.

Thus far, it appeared difficult to confirm the existence of ubiquitinated forms of the HPV18 E6 protein in response to proteasome inhibition or EGCG treatment, even though MG132 treatment increased the total amount of ubiquitinated proteins in HPV18 E6 immunoprecipitates. To further refine these experiments, and in an attempt to improve the sensitivity of detecting ubiquitinated forms of HPV18 E6, the E6 protein was co-expressed with a Histidine-tagged form of ubiquitin (His-Ub). HEK293 cells were co-transfected with a plasmid encoding a Histidine (His)-tagged ubiquitin, pHis-Ub, in conjunction with pCA.18E6 or pcDNA3. The conditions of treatment remained the same as described in the previous section. Protein lysates were incubated with anti-FLAG M2 agarose beads to immunoprecipitate the epitope-tagged HPV18E6 protein and Western blotting performed with a monoclonal antibody specific for the His-tag, to detect the presence of His-tagged ubiquinated proteins in the anti-FLAG immunoprecipitates. The results, Figure 4.26, revealed the presence of high molecular weight His-tagged ubiquitinated proteins only in E6 immunoprecipitates purified from MG132-treated samples. These high molecular weight species were not observed in EGCG or control samples.

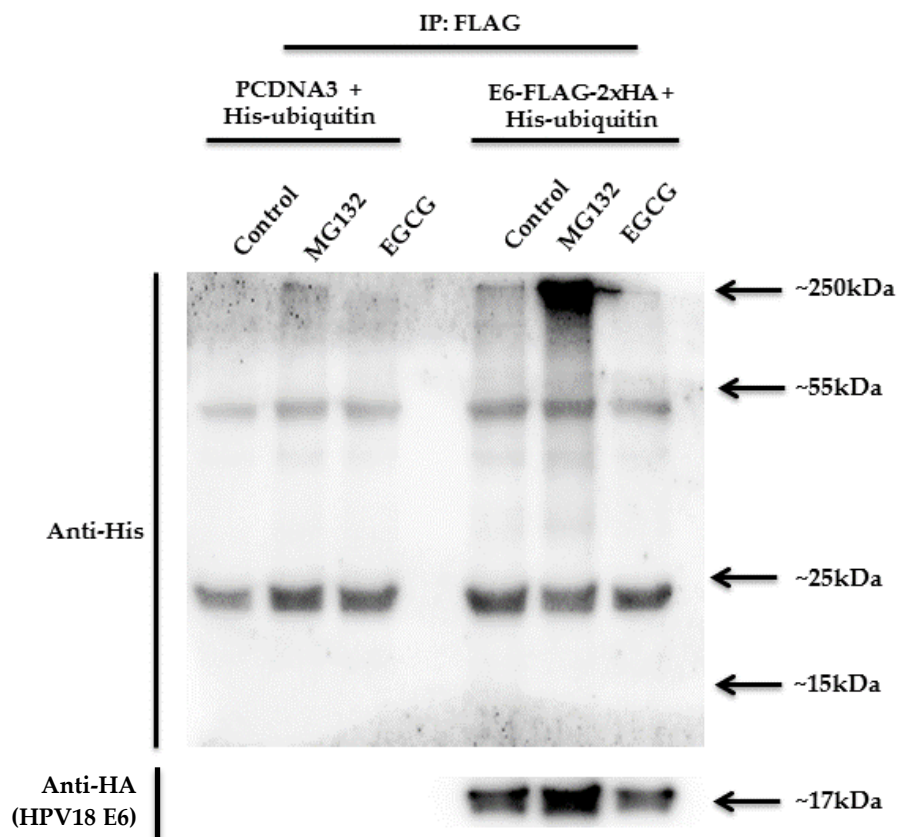


Figure 4.26: MG132 treatment results in the appearance of ubiquitinated proteins migrating at ~250kDa in HPV18E6 immunoprecipitates. HEK293 cells were co-transfected transfected with Histidine-tagged ubiquitin (His-Ub) and E6-FLAG-2xHA or control (pcDNA3) plasmid and treated with 100 μ M EGCG or 40 μ M MG132 for 2hours. Transfected HEK293 cells were lysed in NP40 containing 20mM Iodoacetamide. 500 μ g of protein lysates were incubated with Anti-FLAG®M2 agarose beads. FLAG-tagged proteins were immunoprecipitated and resolved by SDS-PAGE followed by Western blotting for the His and HA epitope tags to identify His-Ub tagged proteins and HPV18 E6, respectively. Experiment was repeated twice.

Again, this analysis failed to identify the presence of ubiquitinated forms of HPV18 E6 migrating at 17kDa, or at higher molecular weights, in either MG132 or EGCG-treated cell lysates (Upper panel), even though Western blotting with a monoclonal antibody to HA confirmed the presence of the epitope-tagged E6 protein in the anti-FLAG immunoprecipitates (Lower panel). Western blotting of protein lysates generated from pCA.18E6 transfected cells confirmed the presence of the HA-tagged E6 protein, and its absence in pcDNA3 transfected cells (Figure 4.27). Again, higher levels of HPV18 E6 protein were observed in cells treated with MG132. Higher molecular weight proteins were also observed migrating at approximately 20kDa that may constitute ubiquitinated forms of HPV18 E6; again this species was increased in MG132 treated cells but not in control or EGCG-treated cells. Thus far, attempts to demonstrate EGCG-mediated ubiquitination of the HPV18 E6 protein had proved problematic. I reasoned that the inability to detect ubiquitinated lower molecular weight forms (<100kDa) of HPV18 E6 might stem from the fact that they are rapidly degraded through the proteasome. To examine this possibility, the same experimental procedure was performed, but this time, MG132 was added to EGCG-treated cells. Given that the most significant drop in E6 expression occurred between 1-2 hours after EGCG treatment (Figure 4.15), transfected cells were treated with either 40µM MG132 2hrs, 100µM EGCG 2hrs or first primed with 40µM MG132 for 2hr then with 100µM EGCG for 2hrs.

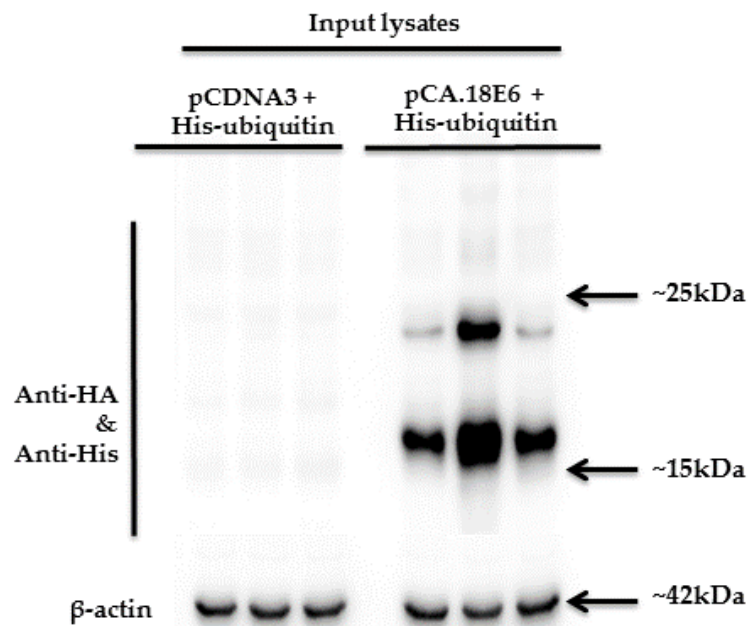


Figure 4.27: Validation of the input lysates for the anti-FLAG immunoprecipitation. HEK293 cells were co-transfected with plasmids encoding His-tagged ubiquitin (His-Ub) and either pCA.18E6 or pcDNA3 and treated with 100 μ M EGCG or 40 μ M MG132 for 2 hours. Transfected HEK293 cells were then lysed in NP40 containing 20 mM Iodoacetamide and sonicated. 50 μ g (10% input) of protein lysates were resolved by SDS-PAGE followed by Western blotting with mAbs to the His or HA epitopes, and anti- β -actin, to confirm successful transfection of pCA.18E6 and His-Ub plasmids into HEK293 cells.

Anti-FLAG immunoprecipitates were subjected to SDS-PAGE and Western blotting performed with an antibody to the His-tag epitope to detect ubiquitinated proteins. This analysis (Figure 4.28) revealed the presence of ubiquitinated high molecular weight proteins (>200kDa) in anti-FLAG-immunoprecipitates from MG132 treated and EGCG and MG132-treated cells, compared to controls, suggesting that E6 and/or E6-associated proteins are highly ubiquitinated. Interestingly, anti-FLAG immunoprecipitates from EGCG and MG132 treated cells did not appear to contain

increased amounts of ubiquitinated high molecular weight proteins, or proteins of lower molecular weights.

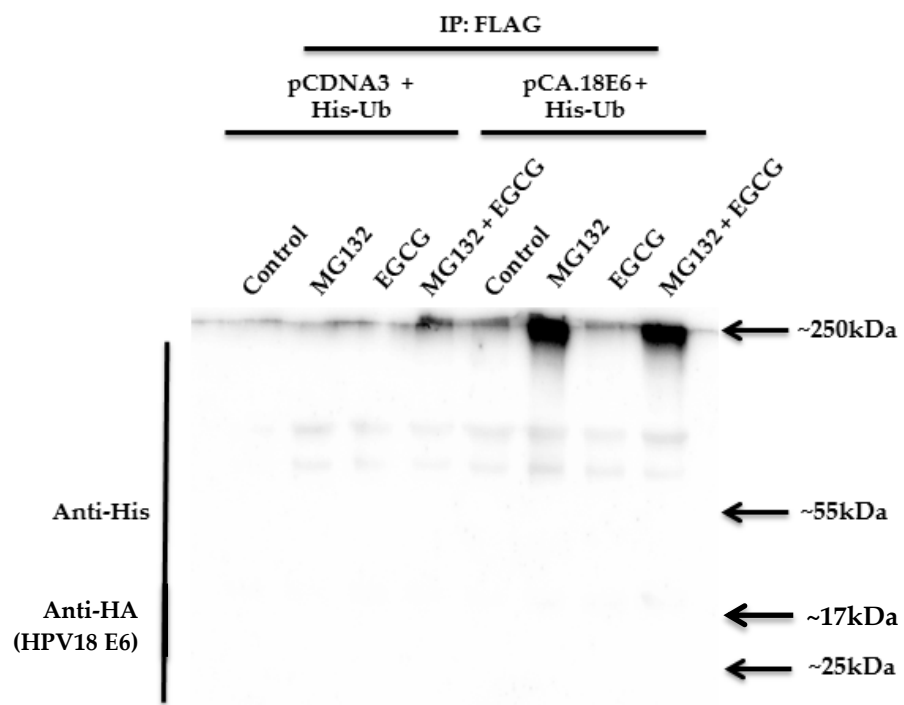


Figure 4.28: High molecular weight species of ubiquitinated proteins are found in HPV18 E6 immunoprecipitates in cells treated with MG132 or both MG132 & EGCG. HEK293 cells were co-transfected with plasmids encoding His-tagged ubiquitin (His-Ub) and either the pCA.18E6 or pcDNA3 plasmids. Transfected cells were treated with either 40 μ M MG132 2hrs, 100 μ M EGCG 2hrs or first primed with 40 μ M MG132 for 2hr then with 100 μ M EGCG for 2hrs. Transfected HEK293 cells were then lysed in NP40 containing 20mM Iodoacetamide. 500 μ g of protein lysates were incubated with Anti-FLAG®M2 agarose beads. FLAG-tagged proteins were immunoprecipitated and resolved by SDS-PAGE followed by Western blotting with mAbs specific for the His-tag epitope (upper panel) or the HA-tag epitope (lower panel). Experiment was repeated twice.

Reprobing of the blot with an antibody specific for the HA-epitope confirmed expression of HPV18 E6 protein in pCA.18E6 transfected cells, with a prominent band migrating at approximately 17kDa-20kDa (Figure 4.28). Again, larger amounts of E6 protein were found in anti-FLAG-immunoprecipitates from MG132 treated cells, whereas lower amounts were found in immunoprecipitates from EGCG-treated cells. While higher molecular weight species migrating at 25kDa, ~40kDa, 55kDa, and above, were observed in MG132-treated cells, EGCG treatment in combination with MG132 did not influence the amounts of His-tagged HPV18 E6 protein or the amount of these higher molecular weight species. Western blotting of cell lysates with an antibody to HA (Figure 4.29) confirmed the presence of HPV18 E6 protein in pCA.18E6 transfected cells, and increased amounts of the E6 protein in MG132-treated cells. Here, E6 proteins migrating at 17kDa and ~ 20kDa, with lower levels migrating between 30kDa and 45kDa were observed in treated cells. Whilst EGCG treatment did not increase the amounts of E6 protein, larger amounts were observed in EGCG and MG132-treated cells. A slight reduction in E6 protein was observed in cells treated with EGCG.

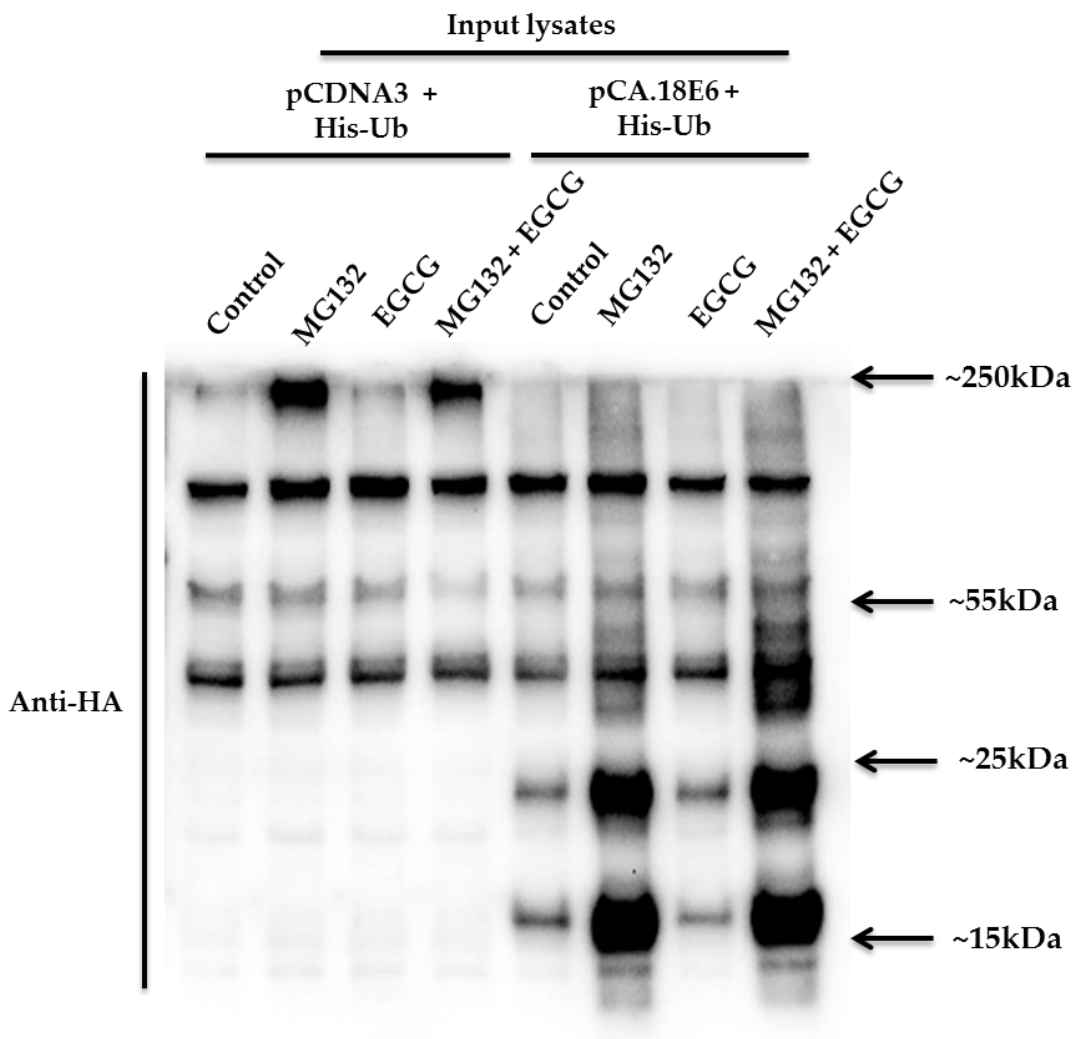


Figure 4.29: Validation of the input lysates for the anti-FLAG protein immunoprecipitation experiment. HEK293 cells were co-transfected with a His-tagged ubiquitin plasmid and either pCA.18E6 or pCDNA3. Transfected cells were treated with either 40 μ M MG132 2hrs, 100 μ M EGCG 2hrs or first primed with 40 μ M MG132 for 2hr then with 100 μ M EGCG for 2hrs. Cells were then lysed in NP40 buffer containing 20mM Iodoacetamide and sonicated. 50 μ g (10% input) of protein lysates were resolved by SDS-PAGE followed by Western blotting with mAbs specific for the His or HA-epitope tags to confirm successful transfection of E6-FLAG-2xHA and His-ubiquitin plasmids into HEK293 cells.

4.7.4 EGCG increases the pool of mono-ubiquitinated E6 protein

Thus far, I have shown that unlike MG132, EGCG failed to increase the pool of ubiquitinated HPV18E6 protein when over-expressed in HEK293 cells. Given that the immunoprecipitation procedure was performed under non-denaturing conditions, it is likely that the purified E6 proteins immunoprecipitated with the anti-FLAG beads contain complexes of E6 and E6-associated proteins (see Introduction Chapter 1). Thus, rather than assuming that the higher molecular weight ubiquitinated proteins are indeed ubiquitinated forms of E6, it is possible that they constitute high molecular weight E6-associated proteins that are themselves mono or poly-ubiquitinated.

To address this question, an additional protocol was employed to examine purified HPV18 E6 for evidence of ubiquitination. Protein lysates from HEK293 cells co-transfected with His-tagged ubiquitin and pCA.18E6 or pcDNA3, and treated with MG132 or EGCG, or both, were incubated with Urea lysis buffer for 1 hour to denature protein complexes (i.e. to break E6 - E6-associated protein interactions). The protein lysates were then incubated with high-affinity nickel beads to “pull-down” His-tagged proteins. After a series of washes to remove non-specific binding, bound proteins were eluted from the Nickel beads and resolved by SDS-PAGE prior to Western blotting with an antibody specific for the HA-epitope to detect HPV18 E6. Figure 4.30 shows the detection of a single species of E6 protein migrating at ~ 25kDa. This mono-ubiquitinated pool of E6 protein was increased following MG132 treatment, to a lesser extent by EGCG treatment, and in response to a combination of EGCG and MG132 treatment, indicating that both treatments resulted in an increase the amounts of mono-ubiquitinated E6 proteins. Western blotting of cell lysates (Figure 4.30)

confirmed the presence of HPV18E6 protein in pCA.18E6 transfected cells, revealed a significant increase in the amounts of HPV18E6 protein in MG132-treated cells, and a slight reduction in E6 protein in cells treated with EGCG.

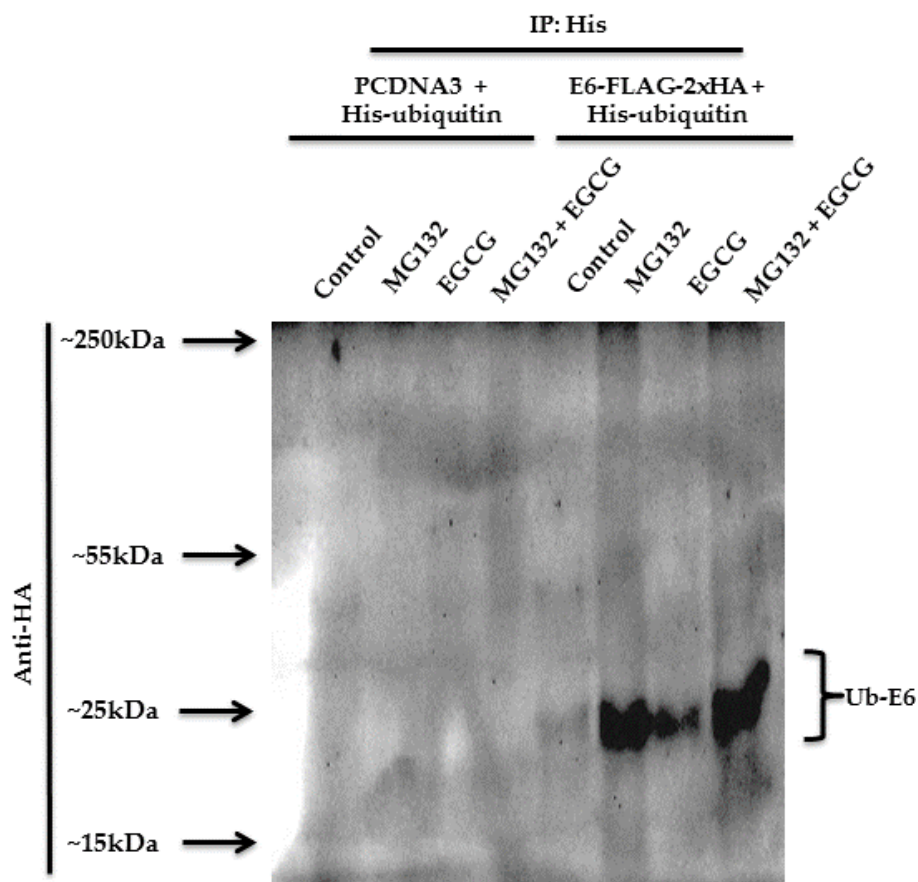


Figure 4.30: EGCG promotes mono-ubiquitination of the HPV18 E6 protein. HEK293 cells were co-transfected with Histidine-tagged ubiquitin (His-Ub) and E6-FLAG-2xHA or control (PCDNA3) plasmid. Transfected cells were treated with either 40 μ M MG132 2hrs, 100 μ M EGCG 2hrs or first primed with 40 μ M MG132 for 2hr then with 100 μ M EGCG for 2hrs. Cells were lysed in NP40 lysis buffer containing 20mM Iodoacetamide and sonicated. 500 μ g protein lysates were denatured with 5M urea lysis buffer. Denatured protein lysates were incubated with His-Select® Nickle Magnetic Agarose beads for 2hrs. Histidine-tagged proteins were immunoprecipitated and resolved by SDS-PAGE followed by Western blotting with an mAb specific for the HA epitope on HPV18E6. Experiment was repeated twice.

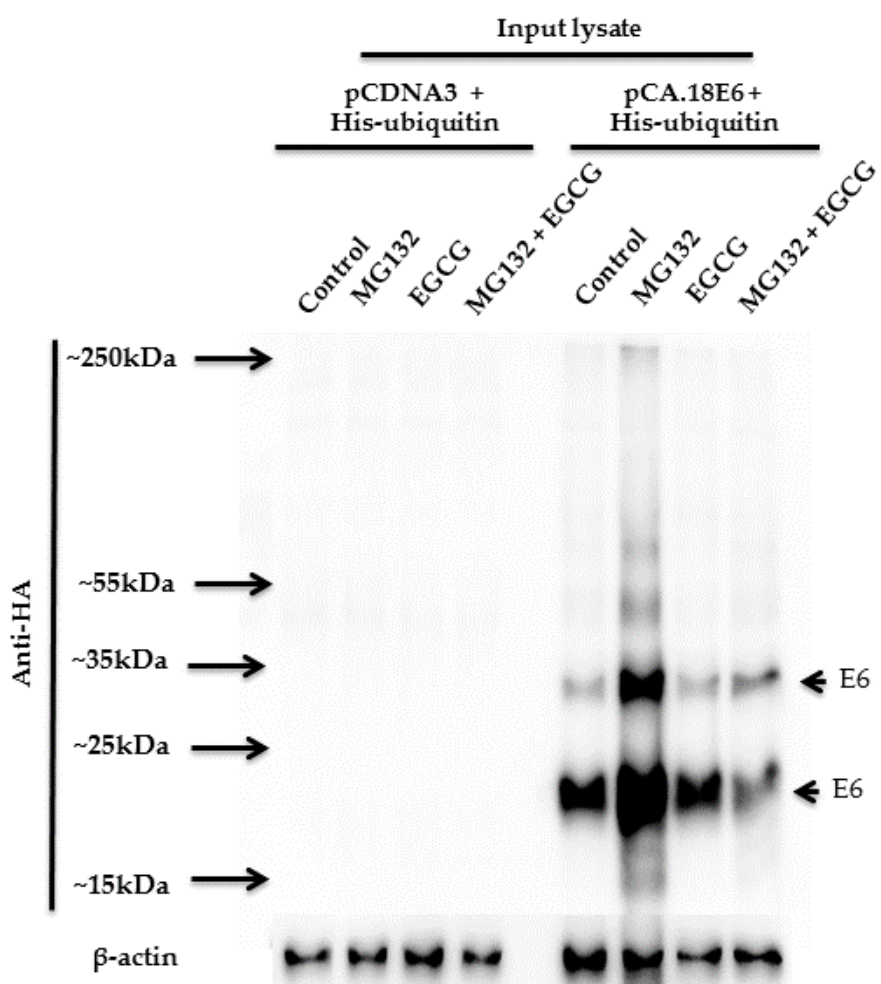


Figure 4.31: Validation of the input lysates for the His-tagged Ub immunoprecipitation experiment. HEK293 cells were co-transfected with plasmids encoding His-tagged ubiquitin (His-Ub) and either pCA.18E6 or pcDNA3. Transfected cells were treated with either 40 μ M MG132 2hrs, 100 μ M EGCG 2hrs or first primed with 40 μ M MG132 for 2hr then with 100 μ M EGCG for 2hrs. Cells were lysed in NP40 lysis buffer containing 20mM Iodoacetamide. 50 μ g (10% input) of protein lysates were resolved by SDS-PAGE followed by Western blotting with mAbs specific for the His and HA epitopes to confirm successful transfection of E6-FLAG-2xHA and His-ubiquitin plasmids into HEK293 cells.

4.7.5 EGCG selectively inhibit the Chymotrypsin-like activity of the proteasome

The inner core of the proteasome contains the main catalytic enzymatic activities, including Trypsin-like (TL), Chymotrypsin-like (ChTL) and caspase-like (CGPH) activity, all of which are involved in protein proteolysis, degrading poly-ubiquitinated proteins into smaller peptides [138]. These enzymatic activities can be selectively inhibited or accelerated by endogenous and exogenous agents. It is possible that EGCG can selectively influence one or more of these three enzymatic activities leading to an increase in the processing of the viral oncoproteins. To investigate whether any of these enzymatic activities was modulated by EGCG, experiments were conducted to measure the rate of degradation of fluorogenic peptide substrates specific for TL, ChTL and CGPH activities in endogenous and exogenous proteasomes. Purified exogenous proteasome (20S proteasome) and selected fluorogenic peptide substrates specific for the TL, ChTL and CGPH activities were purchased from Enzo-Lifesciences. Endogenous proteasomes, in the form of "crude" cytosolic preparations, were generated from HFK-HPV18 cells using an NP40-based lysis buffer. HFK-HPV18 cells were treated with 10 μ M MG132 for 6 hours or 100 μ M EGCG for 72 hours before cell lysis *in situ*. To measure endogenous proteasome activities, the fluorogenic peptide substrates were incubated with 10 μ g of protein lysate for 30 minutes, and the fluorescence emitted when the peptides were cleaved were measured at 450nm on a fluorescence plate reader. The strength of the fluorescence signal emitted corresponds to the amount of the fluorogenic peptide cleaved by the enzymes during the 30-minute incubation. The fluorescence readings of EGCG and MG132 treated lysates were then compared to that of untreated control lysates.

To measure the proteolytic activity of the exogenous proteasome, the 20S proteasome were incubated with 150 μ M MG132 or 100 μ M EGCG for 30 minutes prior to adding the fluorogenic peptide substrates. The fluorescence emitted was measured with a fluorescence plate reader as described above.

Figures 4.32, 4.33 and 4.34 show the three enzymatic activities of the proteasome for Trypsin-like, Caspase-like and Chymotrypsin-like activities, respectively. The activities were expressed as relative fold change in activity relative to control (no drug treatment). When compared to control, little or no change was observed in the Trypsin-like and Caspase-like activities of endogenous and purified 20S proteasomes following EGCG or MG132 treatment. However, Chymotrypsin-like activities of the exogenous and endogenous proteasomes were significantly inhibited following EGCG or MG132 treatment. Collectively, these findings show that EGCG, like MG132, and some other proteasome inhibitors, modulates the Chymotrypsin-like activity of the proteasome [139, 140].

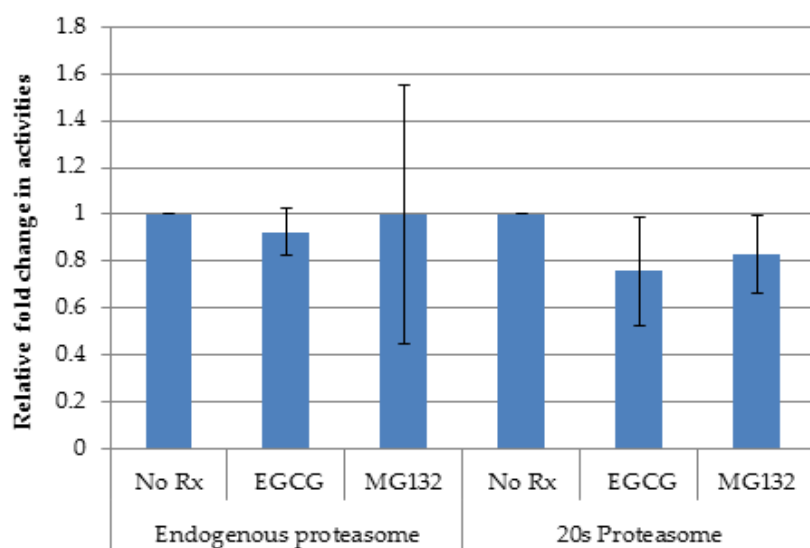


Figure 4.32: EGCG and MG132 do not alter the Trypsin-like activity of endogenous and purified 20S proteasomes. Fluorogenic peptide substrates specific to Trypsin-like enzymatic activities, were incubated with endogenous proteasomes from HFK-HPV18 protein lysate treated with EGCG or MG132, or 20S (exogenous proteasomes) treated with MG132 or EGCG. Fluorescence emitted from peptide cleavage was measured with fluorescence plate reader and the fold change in florescence emission was compared against the control (no drug treatment). **P<0.05, unpaired student t-test indicates that the difference in enzymatic activities was significant when compared to control. Average results from three experiments.

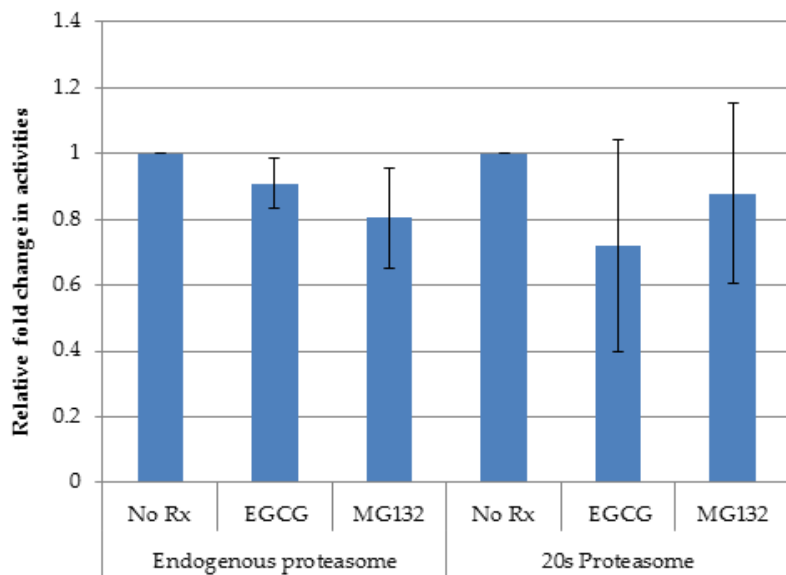


Figure 4.33: EGCG and MG132 do not alter the Caspase-like activity of endogenous or purified 20S proteasomes. Fluorogenic peptide substrates specific to Caspase-like enzymatic activities were incubated with endogenous proteasomes from HFK-HPV18 protein lysate treated with EGCG or MG132, or 20S (exogenous proteasomes) treated with MG132 or EGCG. Fluorescence emitted from peptide cleavage was measured with fluorescence plate reader and the fold change in fluorescence emission compared against a control (no drug treatment). **P<0.05, unpaired student t-test indicates that the difference in enzymatic activities was significant when compared to control Average results from three experiments.

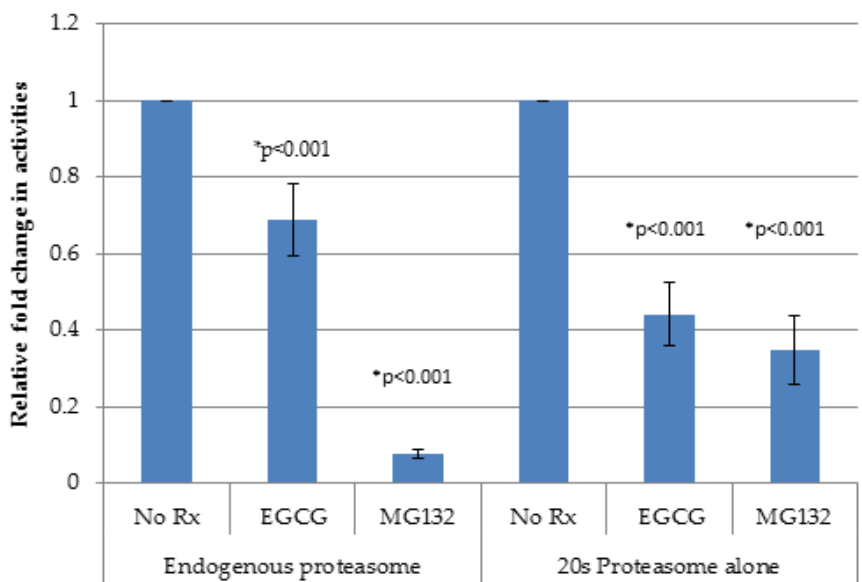


Figure 4.34: EGCG and MG132 inhibit the Chymotrypsin-like activity of endogenous and purified 20S proteasomes. Fluorogenic peptide substrates specific to Caspase-like enzymatic activities were incubated with endogenous proteasomes from HFK-HPV18 protein lysate treated with EGCG or MG132, or 20S (exogenous proteasomes) treated with MG132 or EGCG. Fluorescence emitted from peptide cleavage was measured using a fluorescence plate reader, and the fold change in fluorescence emission compared against a control (no drug treatment). **P<0.05, unpaired student t-test indicates that the difference in enzymatic activities was significant when compared to control. Average results from three experiments.

4.8 A role for reactive oxygen species (ROS) in EGCG-mediated degradation of HPV18 E6

A recent study has shown that Docosahexaenoic acid (DHA), an omega-3 fatty acid, promotes ubiquitin/proteasome-mediated proteolysis of the HPV16 and HPV18 E6 and E7 oncoproteins through a mechanism involving ROS [141]. EGCG has previously been shown to induce ROS overproduction, leading to oxidative stress-induced cell damage and apoptosis [142, 143]. Based on this evidence it is plausible that the down-regulation of the HPV oncoproteins E6 and E7 in response to EGCG is mediated through the overproduction of mitochondrial ROS. I set out to investigate whether EGCG stimulates the production of ROS, and whether this was responsible for E6 proteolysis through the ubiquitin-proteasome pathway.

To detect the levels of intracellular ROS in HFK-HPV18 cells following EGCG treatment, cells were plated in triplicate, into 96-well plates pre-treated with collagen. Cells were allowed to attach and grow for 48 hours prior to treatment. Cells were then incubated with the general oxidative stress Indicator (CM-H2DCFDA) for 1 hour prior to treatment with increasing concentrations of EGCG (0, 25, 50, 100, 150 and 200 μ M EGCG). To induce endogenous ROS, cells were treated with 500 μ M hydrogen peroxide (H_2O_2). The effects of 500 μ M H_2O_2 in combination with 200 μ M EGCG were also examined to look for possible synergistic effects on ROS production. The fluorescence signal emitted from the breakdown of the fluorogenic ROS indicator CM-H2DCFDA was measured on a fluorescence plate reader. Figure 4.35 shows the results of a representative experiment (one of three). As predicted, treatment with H_2O_2 , promoted cleavage of the fluorogenic CM-H2DCFDA substrate, giving rise to a strong

fluorescence signal that increased over time (5 - 360 mins). This confirmed that H₂O₂ treatment stimulated the levels of ROS within these cells. The level of ROS in H₂O₂ treated cells was significantly higher than that of control and continued to rise steadily over the 6 hours period. In contrast, EGCG treated cells had significantly lower levels of ROS compared to control. Furthermore, EGCG suppressed ROS induction in H₂O₂ treated cells to levels that were significant below that of control, indicating that EGCG is an anti-oxidant and not a pro-oxidant in this context.

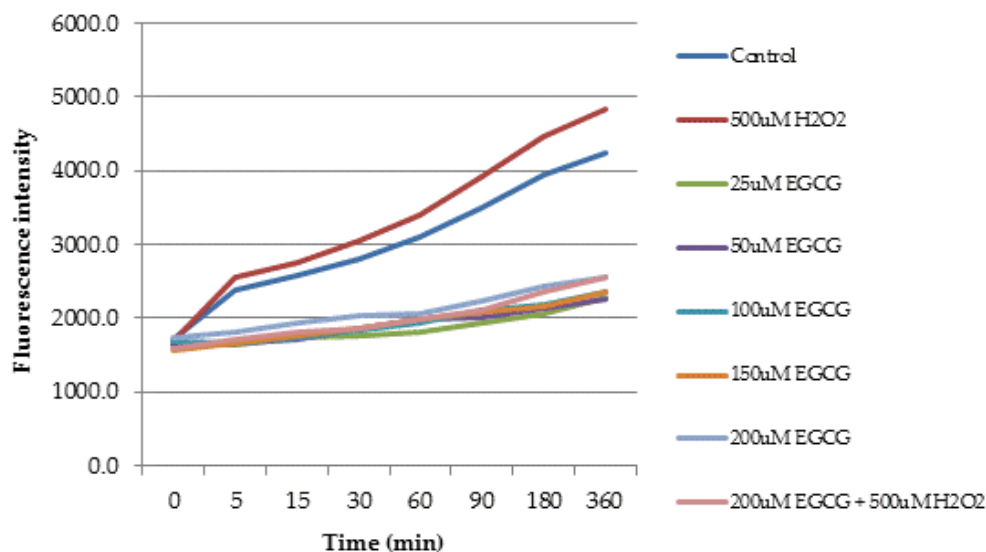


Figure 4.35: EGCG treatment reduces the level of reactive oxygen species (ROS) in HFK-HPV18 keratinocytes. HFK-HPV18 cells were incubated with the General Oxidative Stress Indicator (CM-H2DCFDA) for 1 hour prior to treatment with increasing concentrations of EGCG (0 to 200 μ M), 500 μ M hydrogen peroxide (H₂O₂) and 200 μ M EGCG plus 500 μ M H₂O₂. Fluorescence signals emitted following the cleavage of the fluorogenic CM-H2DCFDA molecule were measured with fluorescence plate readers at increasing time points for up to 360 minutes. The difference in fluorescence signals detected between EGCG treated cells and controls were statistically significant when tested with two-tailed unpaired Student t-test ($P<0.05$). This is a representative result of 3 experiments.

To examine the impact of ROS on the expression of the E6 protein, HFK-HPV18 cells were plated into petri dishes and, when 70-80% confluent, treated with 100 μ M EGCG; 500 μ M hydrogen peroxide (H₂O₂); 5mM N-acetylcysteine (NAC); primed with 5mM NAC for 1hr then 100 μ M EGCG; 5mM NAC then 500 μ M H₂O₂ for 6 hours or 48 hours. NAC is a powerful anti-oxidant that scavenges intra-cellular superoxide and free radicals [144]. Cells were then lysed with RIPA buffer *in situ* and protein lysates were resolved by SDS-PAGE. Western blotting was performed to assess the level of E6

protein expression following EGCG, H₂O₂ and NAC treatment using antisera specific for HPV18 E6; blots were reprobed with an antibody to β-actin to confirm equal protein loading. Figure 4.36 shows that the level of E6 protein expression following treatment with EGCG alone, H₂O₂ alone, NAC alone, EGCG plus NAC and H₂O₂ plus NAC for 6 and 48 hours. At 6 hours, the level of E6 protein was slightly reduced following EGCG treatment but not following H₂O₂ or NAC treatment. It appears that the down regulation of E6 induced by EGCG was reversed by NAC. When treatment duration was extended to 48 hours E6 expression was found to be reduced following EGCG, H₂O₂ and NAC treatment, and NAC did not reverse the down regulation of E6 induced by EGCG as seen following 6 hours treatment.

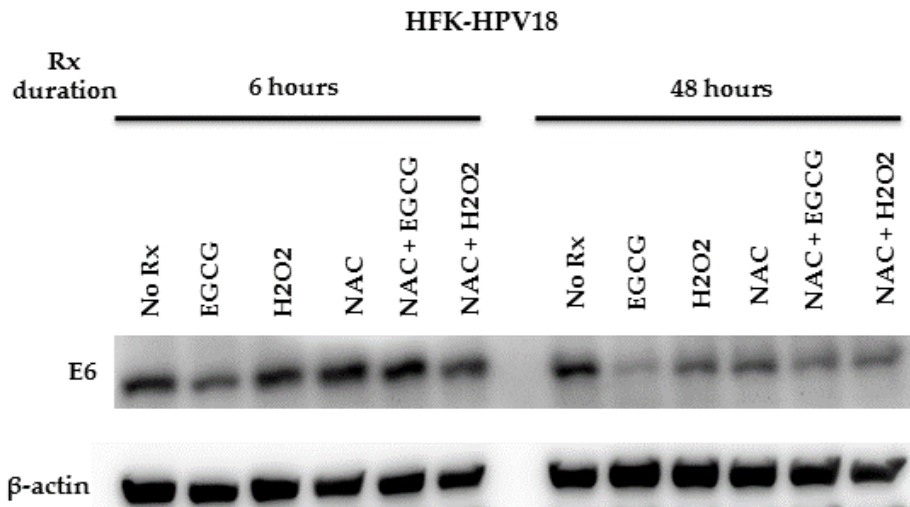


Figure 4.36: Expression of the HPV18 E6 protein is only marginally affected by ROS. HFK-HPV18 cells were treated with 100 μM EGCG; 500 μM hydrogen peroxide (H_2O_2); 5mM N-acetylcysteine (NAC); primed with 5mM NAC for 1hr then 100 μM EGCG; 5mM NAC then 500 μM H_2O_2 for 6hrs or 48hrs. Cells were lysed with RIPA buffer and sonicated. 30 μg of total protein lysate were resolved by SDS-PAGE prior to Western blotting with an antibody to HPV18 E6 or β -actin. This is a representative result of two experiments.

4.9 Discussion

Although an increasing body of evidence shows that green tea polyphenols, particularly EGCG, inhibit the growth and induce apoptosis in HR-HPV-positive cervical cancer cell lines, the underlying mechanism of action(s) remains to be elucidated. Of the studies that have evaluated the effects of EGCG treatment on the growth and behaviour of human cervical cancer cell lines [100, 101, 128, 145, 146], only two examined the impact of EGCG on expression of the HPV-encoded E6 and E7 oncogenes. Despite the lack of insight into its mechanism of action, EGCG has been made into an ointment (Veregen), and used successfully to treat genital warts [52]. However, while appearing effective, it is still unclear whether EGCG targets the virus, or whether it inhibits epithelial cell proliferation. As such, it remains to be discovered whether EGCG functions as an anti-viral in this disease.

Here, I have used a well-characterised human foreskin keratinocyte cell line, HFK-HPV18, to study potential anti-viral effects of EGCG in both monolayer and three-dimensional organotypic raft culture. Like other studies, we found that EGCG inhibits the growth of HPV18 infected keratinocytes and, at doses greater than 50 μ M, induces cell death by apoptosis. However, unlike the DNA-damaging agent Cisplatin [147], the effects of EGCG on growth and apoptosis took longer to develop at the doses used. Although studies using cervical cancer cell lines have shown that EGCG induces a G2/M cell-cycle arrest and increases the proportion of cells undergoing apoptosis (sub-G1 population) [101, 145], such effects were not observed in HFK-HPV18. However, a progressive increase in the proportion of cells in the sub-G1 population was observed when the duration of EGCG treatment was extended to 72 hours. Our findings are in

broad agreement with those of others who have shown that EGCG treatment of normal epidermal keratinocytes and the SCC cell line, SCC13, increases the size of the sub-G1 population without altering cell cycle *per se* [96, 97]. This indicates that EGCG-induced growth inhibition and apoptosis in keratinocytes and HFK-HPV18 is probably achieved through a mechanism(s) that is independent of any effects on the cell-cycle.

The effects of EGCG on cell proliferation was not limited to cells grown in monolayer culture, as growth inhibition was also observed in HFK-HPV18 cultured in a three-dimensional organotypic raft culture. Compared to untreated cells, EGCG treated cells produced thinner epithelial structures in raft culture, with a loss of the more mature suprabasal epithelial cell layers. These findings are in broad agreement with those of Yokoyama and colleagues who showed that EGCG treatment of HPV18 transformed ecto- and endo-cervical cell lines grown in raft culture, were significantly thinner than those of controls [100]. Furthermore, using BrdU labelling and Ki67 staining, I went on to show that cell proliferation was significantly reduced in EGCG treated rafts, indicating that EGCG imposes a major effect on cell proliferation. In normal epithelium, cell proliferation is confined to basal epithelial cells, while cells in the suprabasal layers are committed to terminal differentiation and no longer undergo mitosis. In HR-HPV infected epithelium, keratinocytes retain their ability to undergo mitosis even though they have migrated out of the basal layer (parakeratosis). This, in part, explains how HR-HPV infected keratinocytes give rise to a thicker, dysplastic epithelium when compared to their uninfected isogenic counterparts when grown in organotypic raft culture [148]. Treatment with EGCG inhibits the proliferative potential of HPV18 infected keratinocytes in the basal and suprabasal layers resulting

in rafts with a very thin epithelium as fewer basal cells are capable of undergoing differentiation. At this stage, it is unclear whether EGCG merely reverses the proliferative potential of HPV18 infected keratinocytes, by inhibiting the growth promoting functions of E6 and E7, forcing them to behave like normal uninfected cells. Despite numerous attempts, we were unable to culture NVK or the isogenic counterpart of HFK-HPV18 successfully in raft culture. Future studies are planned to examine the effects of EGCG on the normal uninfected keratinocytes.

Although treatment of HFK-HPV18 with EGCG resulted in overall thinner raft structures displaying less distinct suprabasal cell layers, it did not appear to affect their ability to undergo terminal differentiation. Expression of the high molecular weight keratins: K1/10 and the cross-linked envelope protein, involucrin, were maintained in the parabasal cells and a distinctive cornified layer was also observed on the rafts. K1/10 and involucrin are differentiation proteins synthesized in the stratum spinosum as keratinocytes undergo growth arrest in preparation for terminal differentiation. On closer inspection, the architecture of the suprabasal layers in EGCG treated rafts appeared distorted with less distinctive stratum spinosum and stratum granulosum when compared to control rafts. Whether EGCG influences more subtle aspects of the differentiation process in HFK-HPV18 requires further investigation.

The productive or lytic phase of the virus life cycle of human papillomavirus is intimately linked to keratinocyte differentiation. The HPV-encoded early and late genes are selectively expressed as the keratinocytes mature and migrate upwards out of the basal layer towards the stratum corneum. The HPV E4 gene is normally expressed late in the viral life cycle, where it is required for viral assembly and release.

The E4 protein, an insoluble amyloid protein, is abundantly expressed in the upper epithelial layers of productively infected HPV lesions/tissues. Indeed, its presence is often used as a biomarker to indicate viral replication or active, productive forms of viral infection [149]. HFK-HPV18 has been used extensively as a model to study the HPV life cycle *in vitro* [150]. These studies have shown that HFK-HPV18, which carries episomal forms of the virus, can be induced to express the E4 protein in organotypic raft culture [151]. Despite numerous attempts, I was unable able to detect expression of the E4 protein in HFK-HPV18 raft cultures. As a similar lack of staining was observed on EGCG-treated rafts, this precluded an assessment of the effects of EGCG on HR-HPV lytic replication. At this stage, it is unclear why we were unable to detect E4 expression, given that the raft structures displayed evidence of histomorphological differentiation. Although unlikely, I reasoned that the HPV18 genome might have become integrated in HFK-HPV18. Under these conditions, the virus is no longer capable of lytic replication. However, the PCR-based E2 disruption assay confirmed that the E2 region of the HPV18 genome was intact prior to culturing on rafts, indicating that the virus was still maintained in episomal form [108]. It is currently not clear why expression of the E4 protein was not observed in HFK-HPV18 rafts but is not due to incomplete terminal differentiation of cells in the raft culture system.

When measuring the relative change in viral copy number in HFK-HPV18 cultured in monolayer, little or no change in relative viral copy number was observed when EGCG treated keratinocytes were compared to untreated cells using a sensitive qPCR-based assay. This led us to speculate that viral genome maintenance is probably not affected by EGCG, at least in response to short-term treatment. In the context of organotypic

raft culture treated, it is possible that the virus is still able to maintain episomal replication in the basal epithelium but fails to undergo genome amplification and lytic replication as the epithelium is no longer in a highly proliferative or "hyperplastic state" that may be required for lytic viral replication. Using my newly derived primary keratinocyte cell line which harbours episomal forms of HPV18 (VIN cl.11), I have shown that EGCG treatment impairs viral replication in organotypic raft culture, as shown by the lack of suprabasal E4 protein expression in EGCG treated rafts (see Chapter 5). This observation further strengthens our hypothesis that EGCG probably affects the lytic vegetative phase of the viral life cycle by modulating the behaviour of the keratinocytes. We speculate that chronic EGCG treatment probably inhibits the growth potential of the HPV18-immortalised keratinocytes so that they are unable to expand the pool of undifferentiated keratinocytes that are destined for terminal differentiation. This may explain why treatment with the Veregen ointment requires a protracted treatment regime, where the ointment is applied three times daily for 16 weeks to achieve complete resolution of genital warts [52]. Further experiments are planned to evaluate the effect of chronic EGCG exposure (at least 30 days treatment) on HFK-HPV18 raft cultures.

Having evaluated the phenotypic consequences of EGCG treatment on HPV18 infected keratinocytes in both monolayer and organotypic raft culture, I next examined potential molecular targets of EGCG. Two studies have shown that EGCG down-regulates expression of the key viral oncogenes E6 and E7 in cervical cancer cell lines, probably through mechanisms that involve transcriptional repression; however, the true molecular target(s) remain to be elucidated.

E6 and E7 are the key HPV-encoded oncogenes that disrupt cellular signalling pathways to create a cellular environment that favours viral lytic replication. The E7 oncoprotein binds to and destabilises members of the Retinoblastoma (Rb) family of proteins leading to the liberation of E2F transcription factors and activation of S-phase-specific genes. This forces basal and suprabasal cells to re-enter the cell cycle so that cell proliferation continues and consequently gives rise to a hyperproliferative epithelium. This is a feature observed in HFK-HPV18 raft cultures [152-154]. The increase in E2F activity, which promotes aberrant cell proliferation, normally triggers an increase in expression of the tumour suppressor gene p53, which functions to put a brake on cell proliferation and induce apoptosis in E7 expressing keratinocytes. To counteract this, the high-risk E6 proteins counter p53 upregulation by promoting its degradation through the ubiquitin-proteasome mediated pathway, thus reducing the total pool of p53 protein. E6 can also bind directly to p53 and inhibits its downstream transcriptional activity [66].

Findings presented in this chapter show that EGCG down-regulates expression of E6 and E7 oncoproteins in HFK-HPV18 and this, as predicted, was followed by increased expression of their putative targets: TP53 and pRB, respectively. Whether the upregulation of TSGs, in particular p53, is a direct consequence of E6 and E7 degradation or occurs independently as an "off-target" effect of EGCG, remains to be confirmed, as EGCG has been shown to directly stimulate expression of TSGs (e.g. p53, p21^{WAF1}, pRb) in a range of cancer cell lines. It has been suggested that EGCG increases the half-life of p53 by selectively phosphorylating serine residues on the protein, the net effect of which is to inhibit MDM2-mediated ubiquitin-proteasome degradation.

This results in protein stabilisation and activation of its downstream targets, p21^{WAF1} and BAX, which induce cell growth inhibition and apoptosis [155-158]. Consistent with other studies, I also found that the accumulation of p53 protein stimulates the upregulation of its downstream target gene, p21^{WAF1}. However, in monolayer culture the relative induction in p21^{WAF1} expression was modest and not statistically significant. However, this contrasted to its expression in raft cultures, where a clear induction in p21^{WAF1} protein was observed in response to EGCG treatment. The reason for the lack of difference in expression of p21^{WAF1} in control and EGCG treated cells, especially on day 3, is probably masked due to an upregulation in p21^{WAF1} expression as untreated cells attain confluence and cell growth becomes inhibited [159].

With respect to pRb, EGCG treatment was found to reduce the overall levels of Rb but it was unclear whether it selectively increased the pool of "hypophosphorylated" form of RB; the form responsible for binding and inactivating the E2F transcription factors [160-162]. Although the overall levels of Rb were increased in EGCG treated raft cultures, I failed to distinguish which of the two species (hypo- or hyper-phosphorylated forms), were selectively induced in response to EGCG treatment. Despite numerous attempts, I failed to demonstrate changes in the levels of hypo and hyper-phosphorylated forms of Rb as the antibody failed to work in immunoblotting experiments.

To further assess changes in additional molecular targets following down-regulation of the E6 and E7 proteins, the expression of MCM7 and p16^{INK4a}, and epigenetic regulators whose expression becomes dysregulated following HR-HPV infection, were also examined. p16^{INK4a} is overexpressed in keratinocytes expressing the HR-HPV E7

proteins as a result of the abrogation of the negative feedback of pRb [163]. As expected, the expression of p16^{INK4a} was down regulated as pRb expression was restored. Restoration of pRb expression is likely to inhibit the E2F1 activity binding leading to the down-regulation of its target gene, MCM7. MCM7 is used as a surrogate marker to indicate the presence of transcriptionally active HR-HPV oncogenes in HR-HPV-associated disorders, as expressed in these hyperproliferative cells in suprabasal layer [164-166]. Interesting, the expression of MCM7 in EGCG treated rafts was restored to the basal cells thus further confirming the abrogation of E6/E7 influence following EGCG treatment.

A series of epigenetic alterations have been reported following transfection of high-risk E6 and E7 oncogenes into primary human epidermal keratinocytes. These included upregulation of the methyltransferase, Enhancer of Zeste Homolog 2 (EZH2); the DNA methyltransferases, DNMT1 and DNMT3B; the histone demethylases, KDM6A and KDM6B, and down-regulation of the Polycomb group protein, BMI1 [136, 167-169]. Although it remains unclear how E6 and E7 modulate expression of these epigenetic modulators, some studies have found that this is linked indirectly to down-regulation of TP53 and pRb. For instance, the increase in the expression of EZH2 and DNMTs have been found to be mediated through the loss of p53 (induced by E6) [168, 170], and the expression of DNMT1 is thought to be regulated through the pRb/E2F pathway (induced by E7) [171]. EGCG has also been previously shown to be able to modulate the expression and the enzyme activities of polycomb group proteins and DNMTs through a mechanism that is yet to be defined. I found, for the first time, that EGCG treatment of keratinocytes with episomally maintained HPV18 reverses the expression

of the epigenetic modulators induced by HPV18 E6 and E7 described previously. The expression of EZH2, DNMT1 and DNMT3B were downregulated while the expression of BMI1 was upregulated in EGCG treated keratinocytes when compared to controls. We believe that the changes in the expression of these epigenetic modulators are due to either the down-regulation of E6/E7, the re-expressions of the TSGs or both. Interestingly, BMI1 expression, previously reported to be down-regulated following EGCG treatment in various cancer cell lines, was found to be upregulated in HFK-HPV18, and this probably suggests that the changes in the expressions in these epigenetic modulators are likely to be a consequence of the down-regulation of E6/E7 proteins. To determine if the changes in the expression of the epigenetic modulators are a consequence of the down-regulation of E6/E7 expression or a direct modulation by EGCG, I have planned future experiments using isogenic untransfected HFK to investigate whether similar epigenetic alterations also follow after EGCG treatment.

The down-regulation of E6 and E7 proteins following EGCG treatment appears to play a pivotal role in modulating the expression of key molecular targets (as discussed above) that subsequently modifies the behaviour of the keratinocytes. Therefore, I sought to understand the underlying mechanism of action EGCG in modulating the expression of E6 and E7 in HFK-HPV18. Contrary to previous studies [101], I found, using the HFK-HPV18 model system, that EGCG does not affect the transcription of E6 and E7 genes but does stimulate the turnover of the E6 and E7 viral oncoproteins through the ubiquitin-proteasome or other proteolytic pathways. To examine potential differences in the levels of E6/E7 mRNA pre- and post-EGCG treatment, I used primer and probe sets designed and validated by Lindh *et al.*, which measure

levels of the bicistronic HPV18 E6/E7 transcript [107]. Unlike the low-risk HPV subtypes, the high-risk HPV strains transcribe E6 and E7 as either bicistronic or polycistronic mRNAs [69]. I found that EGCG treatment did not affect expression of the bicistronic E6/E7 transcript in HFK-HPV18. Using qPCR primer/probe sets specific for E6 and E7, *Qiao et al.* found that EGCG treatment down regulated expression of both E6 and E7 containing mRNAs in the HeLa cell line [101]. The authors then went on to demonstrate that the reduction in E6 mRNA correlated with a reduction in the E6 protein. Unlike Qiao, we did not use separate qPCR primers to measure the levels of E6 and E7 mRNAs, but rather, opted to measure levels of the bicistronic E6/E7 transcript instead, given that E6 and E7 are transcribed from a full-length bicistronic mRNA or a spliced variant which generates the truncated E6* and E7 proteins. In HPV18, only one mRNA species is capable of expressing E6* while up to four mRNA species are known to express E6* in HPV16 [68, 69]. The E6 and E6* proteins are translated from the full length and spliced variant of E6* mRNAs, respectively, and both the spliced and non-spliced variant of E6 can encode E7 proteins (see Introduction). Analysis of the early transcripts encoded by HPV16 and HPV18 positive cervical cell lines, including HeLa, revealed that expression of E6*mRNA significantly outnumbered that of E6 mRNA. Therefore, we believe that by simply comparing differences in expression of E6 in control and EGCG treated HFK-HPV18 keratinocytes would not give an accurate account of changes in mRNA levels of the full-length E6 transcripts. Moreover, I was unable to validate the HPV18 E6 primer sets used by Qiao *et al.* in their study and, given that the bicistronic primer set chosen in our study is downstream of the splice region, these primers would not differentiate between full-length and spliced forms of the bicistronic transcript.

Ideally, it would have been interesting to measure differences in expression of E6, E6* and E7 in HFK-HPV18 pre- and post-EGCG treatment, but this proved to be technically quite challenging within the timeframe of the Ph.D. study. To date, most, if not all studies designed to examine the effects of E6* expression has been achieved by overexpressing plasmids in established cell lines. Attempts to measure endogenous E6* expression in primary human keratinocytes transfected with HR-HPV have proved difficult. The low levels of endogenous E6 and E6* proteins made them technically difficult to detect using standard immunoblotting assays. This, coupled with the fact that commercially available E6 antibodies do not differentiate between full-length E6 and E6* because of subtle differences in the two peptides that make them difficult to resolve. When ectopically expressed, E6 and E6* are often tagged with molecular tags such as HA or FLAG, which allows the two proteins to be distinguished by detecting their respective epitope tag. Although speculative, an interesting avenue to pursue would be to examine the effects of EGCG on the levels of endogenous E6 and E6*. E6* expression could be important, as E6* proteins have been found to antagonise the function of full-length E6 by preventing p53 from undergoing E6-mediated proteasomal degradation (see Introduction). Furthermore, overexpression of HPV18 E6* in the Caski cell line resulted in overexpression of p53 and cell growth inhibition [172]. It remains unclear whether EGCG can selectively modulate the expression of full-length E6 and E6*, by influencing transcription and splicing. Future work is planned to measure the differences in the levels of HPV18 E6, and E6* proteins expressed ectopically in keratinocytes pre- and post-EGCG treatment.

Having found no difference in the expression of the bicistronic E6/E7 mRNA transcripts in control and EGCG-treated HFK-HPV18 keratinocytes, we next investigated the effects of EGCG on the expression of the E6 and E7 proteins, given that EGCG has previously been shown to modulate the turnover of cellular proteins [173]. It has been suggested that turnover of the E6 and E7 proteins is mediated through the ubiquitin-proteasome pathway, given that inhibition of the 26S proteasome with MG132, increases the steady-state level of these oncoproteins [71]. Furthermore, I have shown that EGCG mediated E6 and E7 protein degradation is reduced by the addition of MG132, suggesting that EGCG promotes degradation of the E6 and E7 proteins through the ubiquitin-proteasome pathways. Jing *et al.* demonstrated that the omega-3 fatty acid, Docosahexaenoic acid (DHA), also promotes degradation of the HR-HPV-encoded E6 and E7 proteins through the ubiquitin-proteasome system by modulating the over production of mitochondrion reactive oxygen species (ROS) [141]. Findings from our pilot study suggested that contrary to expectation, EGCG possessed anti-oxidant properties, as it reduced the levels of ROS induced by hydrogen peroxide (H_2O_2) treatment in HFK-HPV18 keratinocytes, thus protecting them from oxidative stress damage. Furthermore, doses of H_2O_2 that induce substantial ROS failed to downregulate expression of the E6 protein, while the ROS scavenger, n-acetyl-cysteine (NAC), failed to inhibit EGCG-mediated E6 proteolysis. At face value, these findings suggest that EGCG does not stimulate E6 proteolysis through the ROS pathway.

Proteins earmarked for proteasomal degradation undergo post-translational modification prior to ubiquitination and proteasome-mediated proteolysis. For this

reason, I set out to determine whether EGCG enhances E6 and E7 degradation by increasing the pool of poly-ubiquitinated E6 and E7 protein. While it is well established that E6 targets p53 for proteasome-mediated degradation through its association with E6AP, few attempts have been made to demonstrate that the E6 protein is itself subject to ubiquitination and proteasome-mediated proteolysis. In one study, Kehmeier and colleagues showed that E6 proteins encoded by the HR-HPV subtypes achieved lower steady-state levels of expression in cells due to increased protein turnover [174]. Interestingly, this phenomenon did not appear to be dependent on their ability to bind p53 or the E3-ligase, E6AP. Building on this observation, Stewart and colleagues demonstrated that both low and high-risk HPV E6 proteins were ubiquitinated and targeted for degradation by the 26S proteasome [71]. Using an immunoprecipitation-based assay, they went on to identify multiple poly-ubiquitinated species of E6 in cells where the LR-HPV and HR-HPV E6 proteins were co-expressed with an epitope-tagged form of ubiquitin. While this study identified multiple species of poly-ubiquitinated forms of E6 migrating between 31kDa to 200kDa from a low-risk isolate (HPV11), a single high molecular weight species (migrating at approximately 200kDa), was observed for HPV18. Again, using a panel of mutant E6 proteins, they found that the domains of E6 required for p53 or hDlg degradation, or E6AP binding, were not involved in proteasome-mediated degradation of HPV-18 E6.

Consistent with these findings, we also found that the molecular weight of poly-ubiquitinated proteins found in HPV18 E6 immunoprecipitates was approximately 200kDa. Given that the E6 protein is approximately 17kDa, these high molecular

weight species would have a mass ten times greater than that of the non-ubiquitinated HPV18 E6 protein. Ubiquitin is a small molecule with an estimated molecular weight of 8.5kDa. Given that the E6 protein has a molecular weight of 17kDa, at least 20 ubiquitin molecules are required to generate a larger modified protein of approximately 200kDa. Although we cannot rule out the possibility that such modified forms of E6 exist, it is unclear why smaller molecular weight species were not identified in the E6 immunoprecipitates, as were found for the HPV11 E6 protein described in Stewart et al. Moreover, it is unclear whether the high molecular weight protein identified in the HPV18 E6 immunoprecipitation experiments described by Stewart *et al.* were indeed poly-ubiquitinated forms of the HPV18 E6 protein [71]. In their experiments, the E6 proteins were tagged with the FLAG epitope to facilitate purification and detection. While probing of the E6 immunoprecipitates identified high molecular weight proteins bound to ubiquitin, they were unable to identify convincingly, exogenous expressed FLAG-tagged E6 protein in the E6 immunoprecipitates.

The lack of multiple poly-ubiquitinated species of HPV18 E6 described in the study by Stewart and colleagues, coupled with findings from my study, led us to speculate whether the HPV18 E6 protein was indeed poly-ubiquitinated and whether this was influenced by EGCG. We reasoned that the high molecular weight poly-ubiquitinated proteins found in the E6 immunoprecipitates were probably E6-associated proteins whose association with E6 was maintained under non-denaturing conditions. E6 is known to associate with a wide range of proteins, forming complexes with E6AP and PDZ-containing proteins such as hDlg. Although we found little or no difference in the

level of expression of these poly-ubiquitinated protein complexes in the absence or presence of EGCG, attempts were made to determine whether the E6 protein was itself ubiquitinated. This was achieved by dissociating E6 from its binding partners after solubilisation in urea lysis buffer. The results from these experiments revealed that the E6 protein does not undergo extensive poly-ubiquitination, but rather, undergoes mono-ubiquitination. Interestingly, the level of mono-ubiquitination increased following MG132, EGCG or a combination of the two treatments. Given that these findings reveal the existence of a mono-ubiquitinated form of the HPV18 E6 protein species for the first time, it is not yet known what the function or relevance of this protein modification is, in relation to E6 protein biology. Mono-ubiquitination of proteins has previously been documented [175]. This modification has been shown to affect protein trafficking and the activity of transcription factors. Future studies will elucidate the functional relevance of this modification as it pertains to E6 function.

However, based on current evidence and those published by Stewart *et al.*, I do not have enough evidence to support the notion that E6 protein undergoes extensive poly-ubiquitination and proteasome-mediated degradation, as it does not appear that EGCG-induced turnover of HPV18 E6 is achieved through enhanced ubiquitination of the E6 protein. Findings presented here, along with others, show that EGCG selectively inhibits the Chymotrypsin-like activity of the proteasome, an observation that is at odds with the notion that EGCG stimulates HPV18 E6 protein degradation through the ubiquitin-proteasome pathway.

Despite our inability to confirm, unequivocally, that the HPV18 E6 protein was ubiquitinated, and that EGCG treatment augmented this effect, the central hypothesis

that EGCG promotes the degradation of the viral oncoproteins still holds, given that the half-life of E6 was reduced in response to EGCG treatment. Interestingly, the rate of protein degradation was only increased during the first 1.5 hours following EGCG treatment and, after that, proceeded at a rate similar to those of untreated controls. Although the mechanism(s) involved are unclear, it is possible that EGCG influences the degradation of a distinct "pool" of E6 protein. As previously discussed, HPV18 E6 proteins exist in two forms, full-length E6 and a spliced variant E6*, and they can be found distributed in the cell nucleus and cytosol [176]. It remained to be determined whether EGCG targets either the nucleus, cytosolic or both pools of E6 proteins, and I am planning further experiment to measure the level of this different pool of E6 and E6* proteins using nuclear fractionation methods to separately extract the two pools of E6 protein. Also, I am also planning to investigate other proteolysis systems that may be involved, and influenced by EGCG, in the degradation of E6 and E7 proteins.

In summary, our study reveals that EGCG inhibits the growth and induces apoptosis in HR-HPV18 infected keratinocytes both in monolayer and three-dimensional raft culture. Superficially, this appears to be achieved through down-regulation of the E6 and E7 oncoproteins and a concomitant increase in expression of the TSGs - p53, p21^{WAF1} and pRb. However, it remains unclear how expression of the E6 and E7 proteins is modulated by EGCG and whether the re-expression of the TSGs occurs as a consequence of E6 and E7 down-regulation or is due to a direct effect of EGCG on TSG expression. Although it has long been assumed that the E6 and E7 oncoproteins are degraded through the ubiquitin-proteasome pathway, the results of my studies fail to support this notion, as evidence for E6 protein poly-ubiquitination, a prerequisite for

proteasome targeting, proved inconclusive. Thus, I believe that the E6 and E7 proteins are probably degraded through an as yet unidentified pathway that may involve the activity of caspases, or other proteases. However, I have identified a potentially new species of E6 protein that undergoes mono-ubiquitination in response to EGCG treatment, and whose expression is preserved in the presence of the proteasome inhibitor, MG132, implicating a role for the proteasome in their degradation. The existence and function of this novel pool of mono-ubiquitinated E6 protein requires further investigation, as recent studies have shown that mono rather than poly-ubiquitination regulates different aspects of protein function [175].

Also, I have also demonstrated, using the three-dimensional organotypic raft culture system that EGCG modulates keratinocyte differentiation, an effect that appears to impact on lytic HPV replication. Whether complete vegetative viral replication is affected requires further investigation, although it is unlikely that this will proceed in the absence of E4. Future experiments are aimed at understanding the underlying mechanisms by which EGCG modulates expression of HR-HPV oncogenes as it will not only allow us to re-purpose the use of this relatively cheap and safe compound as primary or adjuvant therapy for other HR-HPV induced neoplasia, it will also allow us to identify new molecular targets that new compounds can be derived.

Chapter 5:

The isolation and characterisation of a
 premalignant uVIN-derived keratinocyte clone
 and its responsiveness to EGCG

5.1 Introduction

Whilst the HPV18 infected keratinocyte cell line, HFK-HPV18, served as a useful model to examine the effects of EGCG treatment on cell growth, differentiation and the virus life cycle, we reasoned that it would be relevant to examine these effects in a more appropriate keratinocyte cell line. To this end, attempts were made to isolate an HR-HPV positive pre-malignant keratinocyte cell line from an authentic uVIN biopsy. Findings outlined in this chapter document my attempts to characterise a single HPV18 positive premalignant clone from a resected uVIN biopsy and to study the effects of EGCG treatment on these cells.

Thus far, only two uVIN-derived keratinocyte cell lines have been established. One of these, KG, was found to harbour both episomal and integrated forms of HPV16, with the majority carrying episomal, non-integrated forms of the virus [177]. This cell line, although not extensively characterised, displayed an extended lifespan *in vitro* and generated a hyperplastic, well stratified epithelium in organotypic raft culture. Another uVIN-derived cell line, CU-VI-8, was found to contain integrated forms of HPV 16. Single cell cloning gave rise to 3 further clones upon serial propagation, all of which contained integrated forms of HPV16 [178]. The growth characteristics of these clones have not been characterised in detail. Unfortunately, none of these cell lines were available for study.

As part of this study, a panel of 11 clones were isolated from pooled primary keratinocyte cultures of a surgically resected uVIN specimen, and these further characterised after serial propagation *in vitro*. HPV typing of these clones by the

Scottish HPV Reference Laboratory, revealed the presence of multiple HPV strains. Of the 11 clones examined, one, VIN cl.11, tested positive for HPV18, and for this reason, was selected for further analysis. The first part of this chapter focuses on the derivation and characterization of VIN cl.11, while the second explores the effects of EGCG treatment on the behaviour of this clone *in vitro*.

5.2 Clinicopathological characteristic of the donor

5.2.1 Clinical history of donor

Tissue biopsies were obtained from a healthy 46-year old woman, patient S.M, who had undergone an anterior skinning vulvectomy for recurring uVIN at the Pan Birmingham Gynaecological Cancer Centre, City Hospital, Birmingham. The patient was first diagnosed with a synchronous multicentric intraepithelial neoplasia of the cervix, vagina and vulva 8 years ago. The patient had received a hysterectomy and partial vaginectomy for recurrent cervical and vaginal intraepithelial neoplasia, and multiple episodes of surgical excision to manage her recurrent uVIN. The tissue was obtained with written consent and the use of the biopsy material for research purposes had been approved by the Birmingham, East, North and Solihull Research Ethics Committee (Reference number 11/WM/0070).

5.2.2 Pathological description of the surgical specimen

The tissue specimen was fixed in formalin, cut into smaller sections and embedded in 12 separate paraffin blocks. Haematoxylin and Eosin (H&E)-stained sections were prepared by the Histopathology department at City hospital, Birmingham, for diagnostic purposes. This was a large surgical specimen of the anterior vulva,

measuring 64mm(W) x 44mm(L) x 12mm(D) in size, which contained normal vulval epithelium, vulvar condylomata, and epithelium with various degrees of dysplasia ranging from low to high grade. The dysplastic changes observed in the epithelium were most likely associated with infection by low- and/or high-risk human papillomavirus, as defined by the general changes in epithelial morphology. Figure 5.1 shows epithelium with changes associated with benign vulvar condyloma commonly associated with infection by low-risk HPV subtypes. The epithelium displayed exophytic papillomatous hyperplasia but lacked dermal hyperkeratosis, suggesting that this lesion was a resolving genital wart infection.

In Figure 5.1C and 5.1D, both epithelium displayed pre-malignant changes consistent with uVIN; an intraepithelial neoplasia caused by high-risk HPV subtypes. The keratinocytes in these sections showed hyperchromatic nuclei with high nuclear to cytoplasmic ratios and increased mitotic activity. These atypical keratinocytes were confined to the lower third of the epithelium in Figure 5.1C, a feature of low-grade intraepithelial neoplasia, while in Figure 5.1D these abnormal cells were found involving the full thickness of the epithelium, a feature of high grade intraepithelial neoplasia.

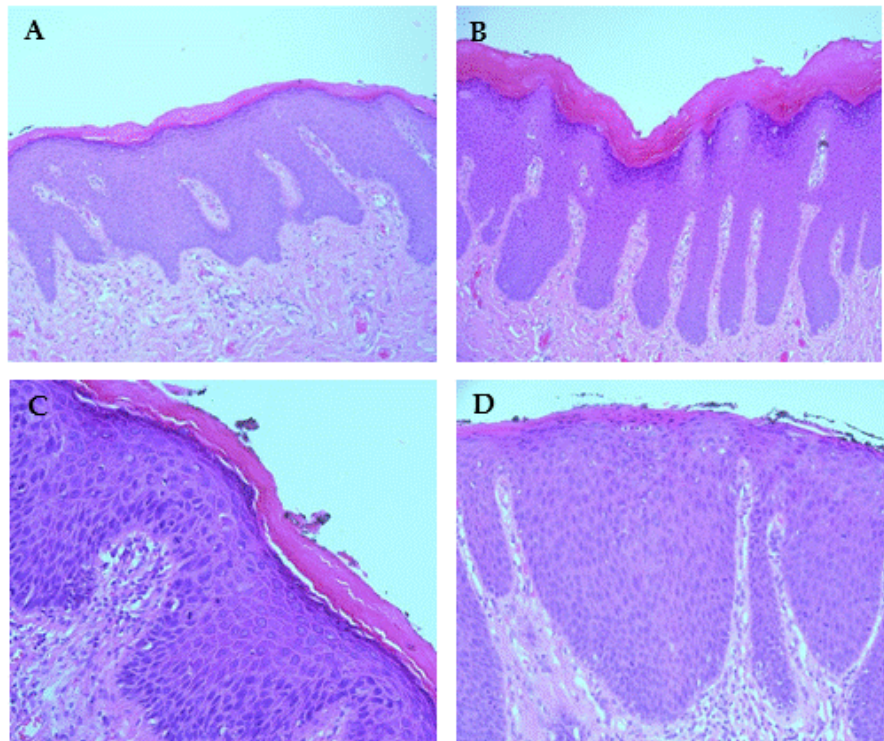


Figure 5.1: Representative sections of vulval squamous epithelium within the uVIN biopsies taken from patient Ms S.M. Haematoxylin and Eosin (H&E) stained sections of specimens obtained from an anterior vulvectomy for high grade HG-uVIN. The specimens consisted of a heterogeneous epithelium with normal to varying degree of dysplasia. (A) Well stratified normal vulval squamous epithelium; (B) Regressing vulvar wart showing features of exophytic papillomatous epidermal hyperplasia; (C) Low grade dysplasia (VIN 2) with immature keratinocytes confined to the lower third of the epithelium; (D) High grade dysplasia (VIN 3) with uniform and immature keratinocytes with large nuclei spanning the full thickness of the epithelium (parakeratosis). Images were taken using a Nikon Eclipse E600 microscope at x20 magnification.

5.2.3 HPV status of donor tissue

A distinctive feature of the resected uVIN lesions was the presence of koilocytes in a background of immature and incompletely keratinized surface epithelium; so-called parakeratosis, a feature characteristic of productive HPV infected epithelium (Figure 5.2A). A koilocyte is an abnormal squamous epithelial cell that displays morphological changes associated with HPV infection and is characterized by the presence of an enlarged, irregular and dense nucleus and a perinuclear halo (Figure 5.2A). Secondly, immunohistochemical (IHC) staining for p16^{INK4a}, a surrogate marker of high risk HPV infection, confirmed strong nuclear and cytoplasmic "block" staining in large areas of the uVIN lesions (Figure 5.2B). p16^{INK4a} IHC was performed by the Pathology laboratory at City hospital, Sandwell and West Birmingham NHS Trust.

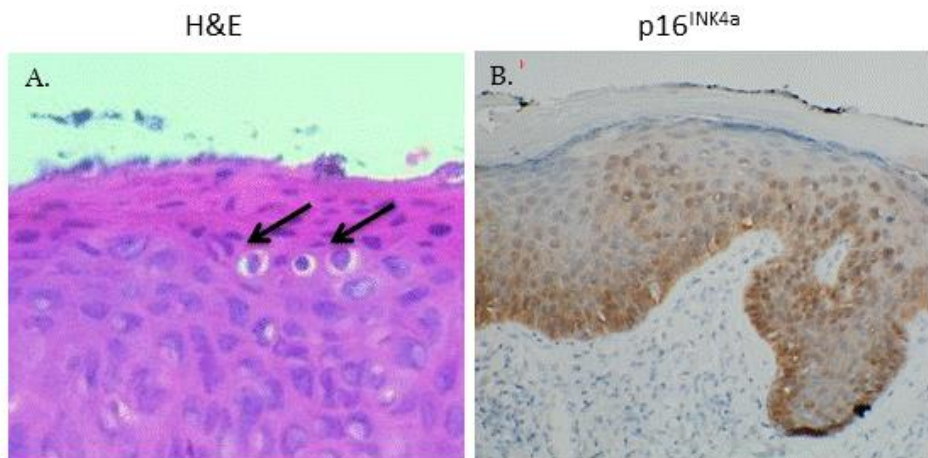


Figure 5.2: Sections of vulval squamous epithelium from biopsies taken from patient Ms S.M display evidence of HR-HPV infection: the presence of koilocytes, and contiguous block staining for p16^{INK4a} (A) H&E section showing the presence of koilocytes (arrows), a hallmark of active HR HPV infection, in the background of high grade VIN; 500x magnification. (B) p16^{INK4a} immunostaining of FFPE section showing diffuse nuclear and cytosolic "block" staining (brown); 200x magnification. The image was taken using a Nikon Eclipse E600 microscope.

To identify the HPV subtypes present within the uVIN lesions, DNA from 7 of the 12 formalin fixed paraffin embedded (FFPE) blocks was extracted and sent to the Scottish HPV Reference Laboratory for HPV genotyping using a sensitive Luminex-based multiplex PCR assay [179]. This assay detects the presence 27 mucosal HPV strains that include: 14 high-risk types (16, 18, 31, 33, 35, 39, 45, 51, 52, 56, 58, 59, 66 and 68), 6 possible high-risk types (26, 53, 67, 70, 73 and 82), and 7 low risk types (6, 11, 30, 42, 43, 44 and 69).

Six different HPV strains were detected in the biopsy specimens, of which one was a LR subtype (HPV42), one was a possible HR type (HPV 70), and four were HR subtypes (HPV 35, 51, 56 and 59). HPV42 and 70 are commonly found in genital condylomata accuminata while HPV 35 and 51 are found in high grade VIN. HPV 51, 56 and 59 are found in low grade VIN [180-183]. The heterogeneity of vulval dysplasia seen here in this patient is probably explained by infection with these different strains of HPV.

5.3 The establishment of primary keratinocytes from explanted uVIN biopsies

Tissue biopsies were taken from the surgical specimens and transported to the laboratory in iced-cold growth medium. After repeated washes in a PBS/antibiotic solution, tissue biopsies were minced into small 3-4mm fragments, seeded onto 9cm petri dishes and covered with 2mls of complete growth medium. Once the fragments had adhered to the petri dish (usually 24 hours), a further 8mls of growth medium was added to the dish. Dishes were cultured at 37°C in a CO₂ incubator.

5.3.1 The morphology of primary keratinocyte outgrowths from explanted VIN biopsies

Primary keratinocyte outgrowths were observed from tissue explants between 6-14 days after culture. Cells originating from the explanted biopsies displayed a cobblestone appearance typical of squamous epithelial cells (Figure 5.3A). Keratinocyte outgrowths were recovered by trypsinisation and 2×10^5 cells seeded into petri dishes containing irradiated 3T3-J2 fibroblasts. These primary cells formed small colonies with a characteristic polygonal and cobble stone appearance (Figure 5.3B). 10 days after seeding, keratinocyte colonies displaying different morphologies were observed with some cells maintaining their small polygonal appearance while others appeared elongated with pronounced protrusions (Figure 5.3C). The heterogeneity in cell morphology observed here suggests that these cell populations are derived from different epithelial origin given that the tissue specimens were heterogeneous in nature, containing normal tissue and tissue with varying degrees of epithelial dysplasia. Some of these keratinocytes underwent terminal differentiation after day 20 in culture and these differentiated cells appeared flattened and enlarged as seen in Figure 5.3D.

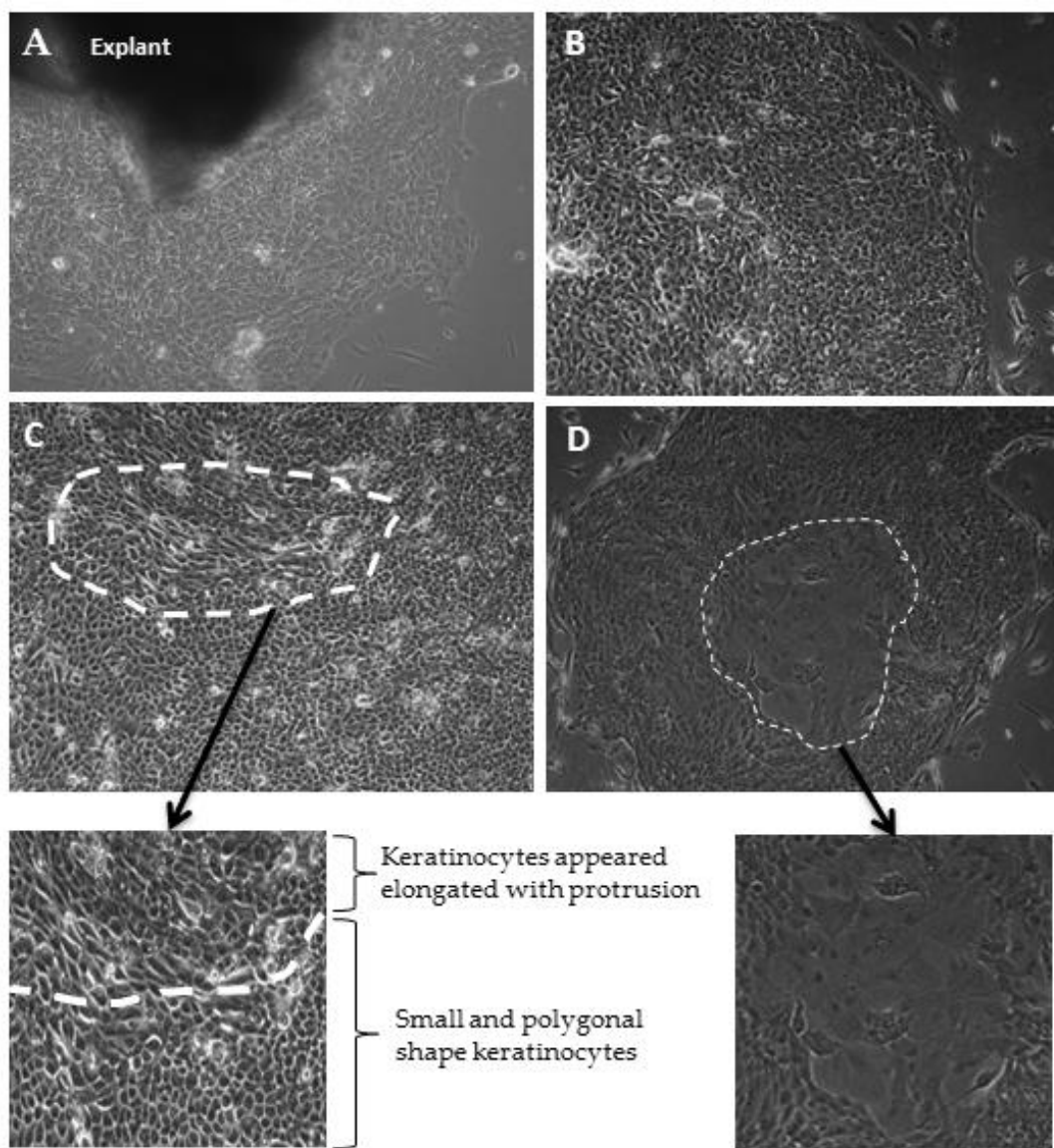


Figure 5.3: Primary keratinocyte outgrowths and early passage cultures from vulval tissue biopsies obtained from patient Ms S.M. (A) A primary keratinocyte outgrowth from a uVIN tissue explant cultured for 7 days. (B) Keratinocyte colonies displaying a characteristic polygonal and cobble stone appearance. (C) Colonies with heterogeneous morphology were observed after 6 days in primary culture. (D) Some of the keratinocytes became enlarged and flattened after 10 days in primary culture, a hallmark of keratinocyte differentiation. Phase contrast images were taken using a Nikon Eclipse E600 microscope at x200 magnification.

5.3.2 HPV analysis on primary VIN keratinocyte cultures

HPV genotyping was performed on primary keratinocytes derived from the uVIN outgrowths to detect the presence of the two most prevalent HR-HPV subtypes: HPV16 and HPV18. Primary keratinocytes were serially passaged and DNA extracted at each passage. HPV 16 and HPV18 genotyping was then performed by qPCR, using probes specific for the E6 gene [108]. While HPV16 and HPV18 genomes were detected in primary keratinocyte outgrowths harvested directly from the tissue explants, the presence of HPV16 and HPV18 DNA appeared to be lost upon serial propagation; firstly HPV18, and then HPV16 (Figure 5.4). While the presence of HPV18 genomes was not detected after only one passage, the presence of HPV16 DNA was undetectable after 3 passages.

Passage No.	HPV16 DNA		HPV18 DNA	
	Primary cells	SiHa cell	Primary cells	HeLa cell
p0	+	+	+	+
p1	+	+	-	+
p2	+	+	-	+
p4	-	+	-	+

Figure 5.4: HPV genotyping of primary and subcultured keratinocytes obtained from explanted uVIN biopsies. DNA isolated from primary and subcultured VIN-derived keratinocytes was tested for the presence of HPV16 and HPV18 DNA by qPCR using oligonucleotides for the E6 coding sequence. Both HPV16 and HPV18 E6 DNA were detected in cells from the primary outgrowths (at p0) but at p1 HPV18 DNA was not detectable; at p4, neither HPV16 nor HPV18 DNA were detected. SiHa and HeLa served as positive controls for HPV16 and HPV18 respectively.

5.4 The establishment of single cell clones from the primary VIN keratinocyte cultures

The presence of primary keratinocytes displaying a heterogeneous morphology, coupled with the loss of HPV16 and HPV18 DNA upon serial passage suggested that primary keratinocyte cultures from the uVIN biopsies comprised a mixture of normal uninfected and HPV infected keratinocytes, and that for some unknown reason, HPV16 and HPV18 infected keratinocytes were lost upon serial passage.

To explore the possibility that keratinocytes infected with HR-HPV strains were lost or outcompeted by other non-infected keratinocyte populations, single cell cloning was performed to purify clones derived from single cells. Single cell cloning was undertaken, using a metal ring cylinder strategically placed over the primary keratinocytes that were homogeneous in appearance. These cells were then isolated and cultured independently on lethally irradiated 3T3 J2 feeder cells.

5.4.1 Characterisation of single cell clones isolated from primary keratinocyte outgrowths of the VIN biopsies

A total of 23 single cell clones were isolated from primary keratinocyte cultures, but of these, only 11 clones grew and could be propagated beyond a single passage. All 11 clones displayed a homogeneous morphology and were successfully propagated for at least 5 passages before freezing and storage in liquid nitrogen. The remaining 12 clones that failed to propagate in culture either underwent terminal differentiation or senescence/apoptosis soon after colony formation

5.4.2 Characterization of HPV status of VIN cell lines using Luminex PCR

DNA from the 11 primary VIN clones was extracted and sent to the Scottish HPV reference laboratory for HPV genotyping. The HPV status of these 11 clones is illustrated in Figure 5.5. HPV 35, a high risk subtype, was detected in 8 of the clones (Clone 3, 4, 7, 10, 12, 20, 22 and 23), while HPV18 was detected in two of the clones (Clone 3 and 11). None of the 27 HPV subtypes were detected in Clone 8. Interestingly, Clone 3 appeared to be co-infected with two HR-HPV subtypes, HPV18 and 35. The assay failed to detect any HPV DNA in Clone 2 and the experiment was not repeated due to time and cost implications.

VIN clone 11 (cl.11) was subsequently selected for further experimentation for two reasons; firstly it harbours the more common HPV 18 strain, and secondly, it offers the opportunity to assess whether the consequence of EGCG treatment observed in HFK-HPV18 is recapitulated in this newly derived VIN keratinocyte cell line. The behaviour of VIN cl.11 and the physical status of the virus were profiled before the cells were subjected to EGCG treatment.

VIN clone	HPV subtype
Clone 2	Assay failed
Clone 3	18, 35
Clone 4	35
Clone 7	35
Clone 8	No HPV detected
Clone 10	35
Clone 11	18
Clone 12	35
Clone 20	35
Clone 22	35
Clone 23	35

Figure 5.5: Results of the HPV typing analysis performed on uVIN-derived clones using the Luminex multiplex PCR platform. DNA obtained from each of the primary VIN-derived single cell clones were extracted and sent for HPV subtype testing by Dr K. Cushieri at the Scottish HPV Reference Laboratory, Edinburgh, Scotland. The assay failed in Clone 2 and no HPV DNA was detected in Clone 8. For the remaining clones, HPV18 alone, HPV35 alone, or both, were detected.

5.5 Characterization of VIN cl. 11

5.5.1 Karyotypic characterisation of VIN cl.11

Chromosome analysis was performed on early passage cultures of VIN cl.11 by Dr Sally Jeffries at the West Midlands Regional Genetics laboratory, Birmingham Womens NHS Trust. 10 metaphase spreads from actively growing cell cultures were examined by G-band chromosome analysis. Of the 10 cells examined, 2 had abnormal near tetraploid karyotypes of 94 chromosomes, shown below as a composite karyotype. Clonal abnormalities included apparent loss of one copy each of chromosomes 2, 10, and 21; gain of two copies of chromosome 13; gain of three copies of chromosome 20; and unidentified material replacing the majority of one chromosome 10p. 6 cells had related abnormal near tetraploid karyotypes of 90~93 chromosomes shown below as a composite karyotype. Clonal abnormalities included those observed in the first clone and apparent loss of one copy of chromosome 19. 2 cells had related abnormal near tetraploid karyotypes of 90~93 chromosomes shown below as a composite. Clonal abnormalities include apparent loss of one copy each of chromosomes 2, 10, 19 and 21; gain of one copy of chromosome 13; gain of three copies of chromosome 20; and unidentified material replacing the majority of one chromosome 10p. The (10p) add observed in these cells is different to the add (10p) observed in the clones above.

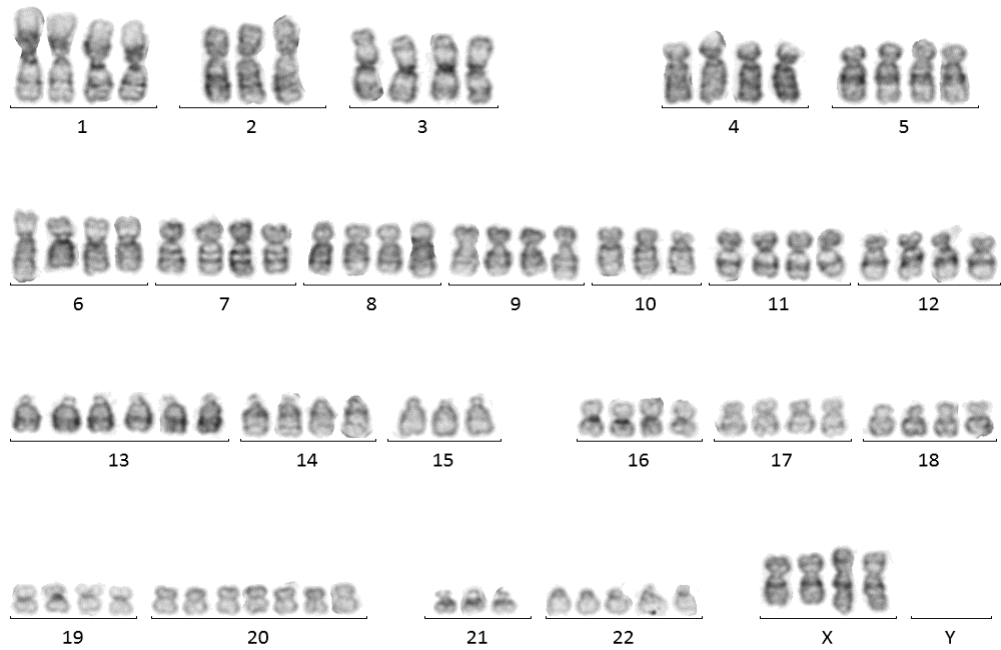
94<4n>,XXXX,-2,-10,add(10)(p11),+13,+13,+20,+20,+20,-21[cp2]/

90~93<4n>,XXXX,-2,-10,add(10)(p11),+13,+13,-19,+20,+20,+20,-21[cp6]/

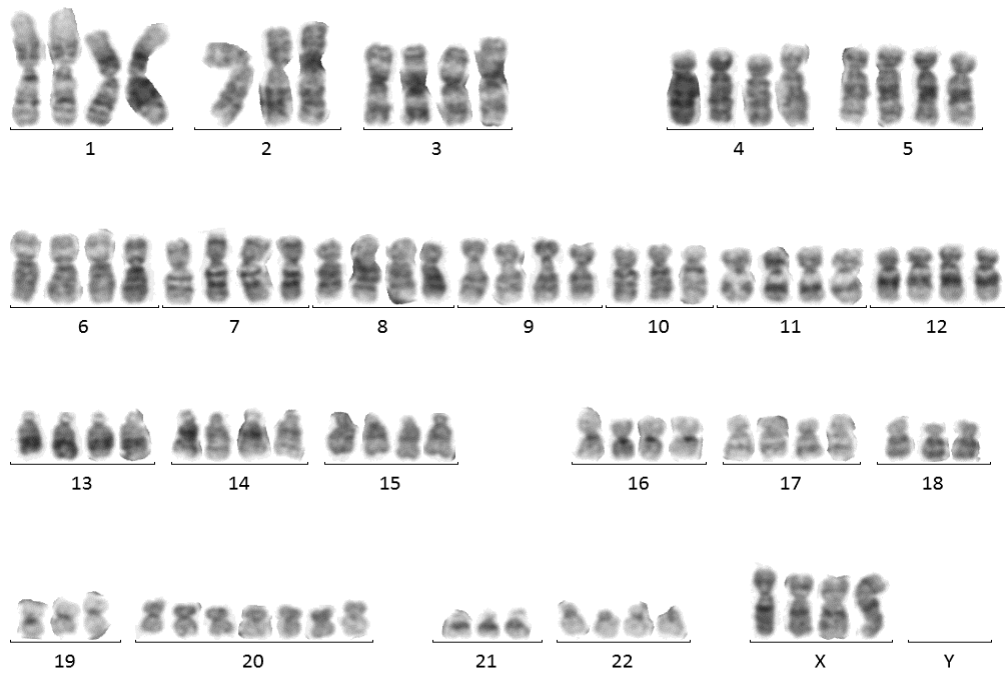
90~93<4n>,XXXX,-2,-10,add(10)(p11),+13,-19,+20,+20,+20,-21[cp2]

In summary, the results showed a female chromosome complement and an abnormal karyotype that were near tetraploid, consistent with neoplasia. Representative karyotypes are shown in Figure 5.6.

A



B



C.

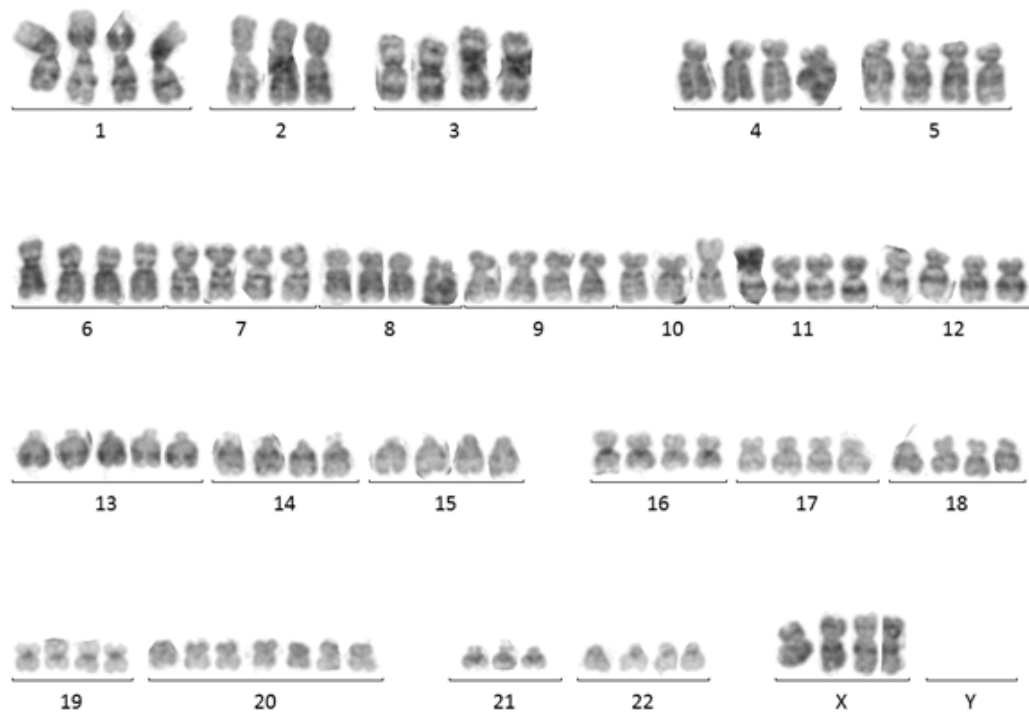


Figure 5.6: Representative karyotypes from three major clones identified in cultured VIN cl.11 cells. Chromosome alignment of G-banded chromosomes taken from the three major clones (A) clone 1, (B), clone 2 and (C), clone 3 found in early passage cultures of VIN cl.11. This analysis confirmed the near-tetraploid nature of chromosomes and the absence of a Y chromosome.

5.5.2 *The morphology of VIN cl.11 in monolayer culture*

A representative phase contrast photomicrograph of VIN cl.11 grown in monolayer culture is shown in Figure 5.7. Cells seeded at clonal density gave rise to small well-circumscribed colonies that displayed a polygonal morphology typical of epidermal keratinocytes cultured using the 3T3 feeder system. Small colonies, acquired a cobble stone-like appearance when they merged at confluence. However, unlike HFK-HPV18, VIN cl.11 failed to stratify and produce cells with a characteristic differentiated morphology. To confirm the keratinocyte origin of VIN cl. 11, total cell lysates were subjected to Western blotting analysis for the established keratinocytes markers, involucrin and keratin 14. As shown in Figure 5.8, VIN cl.11, like HFK-HPV18, expressed high levels of involucrin and keratin 14, whereas the HPV18 positive HeLa cell line, derived from an adenocarcinoma, was negative for both proteins. The murine fibroblast cell line 3T3-J2 was negative for these proteins. Collectively, these analyses confirmed the keratinocyte origin of VIN cl.11.

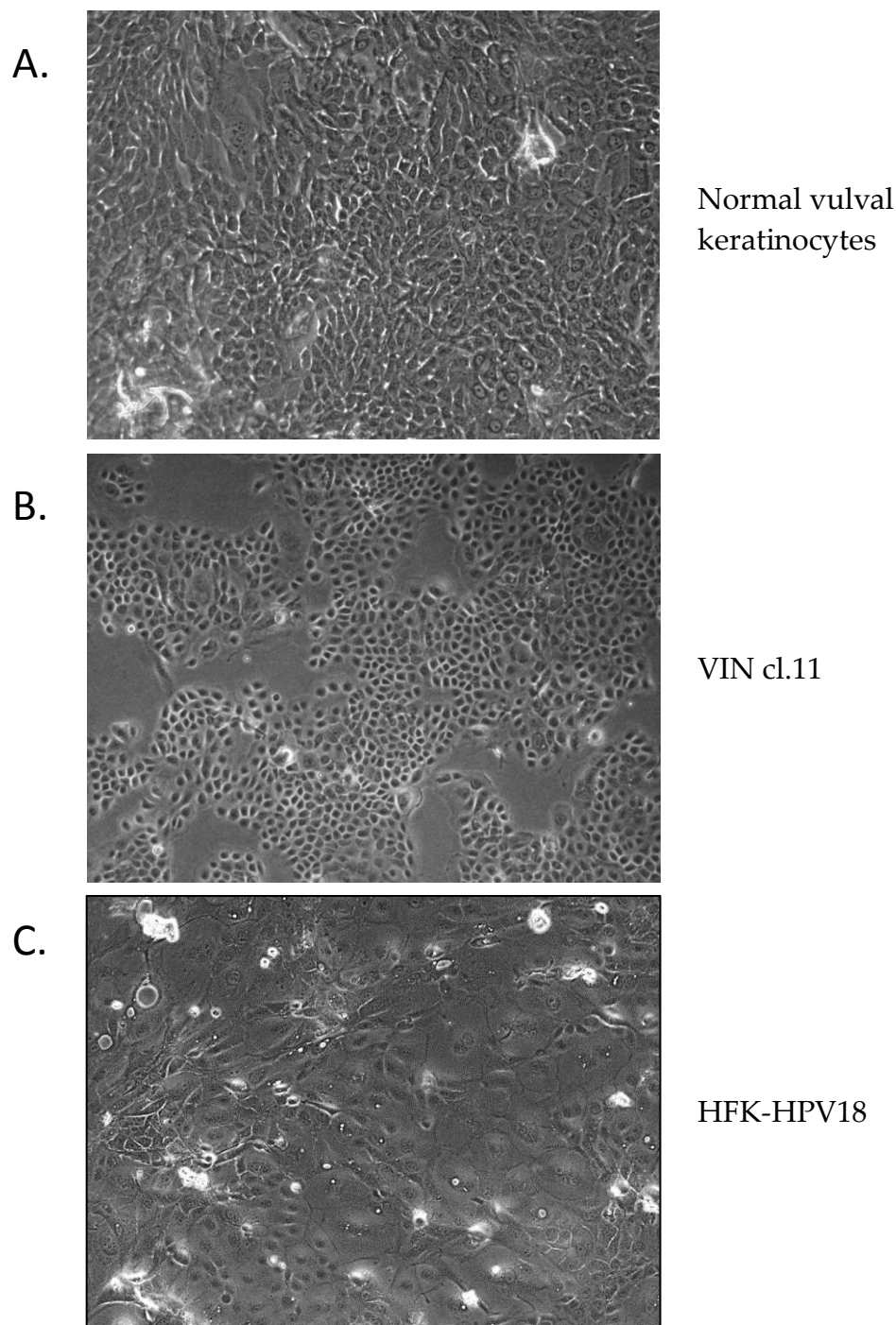


Figure 5.7: The morphology of VIN cl.11 in monolayer culture. The morphology of (A) normal vulvar keratinocytes, (B) VIN cl.11 and (C) HFK-HPV18 in monolayer cultures. Keratinocytes were seeded at clonal density on irradiated 3T3-J2 fibroblasts. After seven days, the feeder cells were removed and a phase contrast image taken using a Nikon Eclipse E600 microscope at x200 magnification.

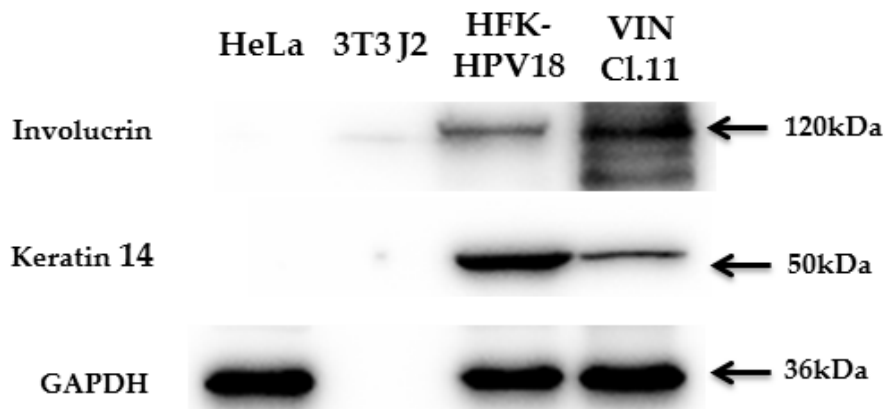


Figure 5.8: Western blotting analysis confirming the expression of keratinocyte-specific markers in HFK-HPV18 and VIN Cl.11. Total cell lysates were generated from subconfluent cultures of HeLa, Mouse 3T3 J2 fibroblasts, HFK-HPV18 and VIN Cl.11 cells. Lysates were resolved by SDS-PAGE and subjected to western blotting for the keratinocyte-specific proteins: involucrin and keratin 14. Both involucrin and keratin 14 were present in VIN Cl.11 confirming that cells were of keratinocyte origin.

5.5.3 *The morphology of VIN cl.11 in organotypic raft culture*

A characteristic feature of keratinocytes derived from squamous epithelium, is their ability to stratify and differentiate into a full thickness squamous epithelium when grown in organotypic raft culture. In this system, keratinocytes are seeded onto a collagen plug containing 3T3-J2 feeder cells and then raised in an air-liquid interface to allow the keratinocytes to stratify and differentiate. This three-dimensional culture system also made it possible to study the HPV life cycle as viral replication is intimately linked to keratinocyte differentiation [184]. For these reasons, attempts were made to examine the ability of VIN cl.11 to differentiate in organotypic raft cultures.

VIN cl.11 cells were seeded on collagen plug containing 3T3 feeder cells and raised to the air-liquid interface. Rafts were cultured for 13 days prior to fixation and sectioning. Figure 5.9 shows representative H&E stained sections of organotypic raft cultures generated from VIN cl.11 and HFK-HPV18; the latter were included for comparative purposes. VIN cl.11 and HFK-HPV18 were able to stratify into full thickness squamous epithelium with distinctive basal, spinous, granular, and cornified layers. This finding established that VIN cl.11 retained the ability to stratify and differentiate when cultured at the air-liquid interface. However, when compared to HFK-HPV18 the keratinocytes in VIN cl.11 appeared less organised with areas of immature and large nucleated cells extending to the granular layer, a feature suggestive of dysplastic changes that resembles uVIN.

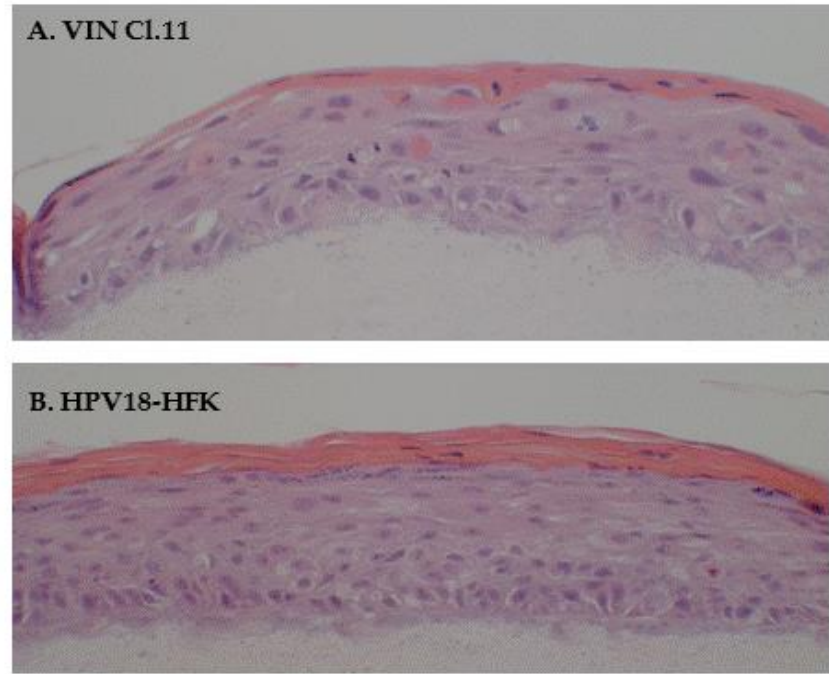


Figure 5.9: Typical morphology of VIN cl. 11 and HFK-HPV18 organotypic raft cultures. H&E stained sections from organotypic raft cultures grown at the air-liquid interface for 14 days. Both (A) VIN cl. 11 and (B) HFK-HPV18 rafts displayed evidence of parakeratosis but VIN cl.11 appeared less organised with area of immature and large nucleated cells extending to the granular layer, a feature suggestive of dysplastic changes that resembles uVIN. The image was taken using a Nikon Eclipse E600 microscope at x200 magnification.

5.5.4 The physical status of the HPV18 genome in VIN Clone 11

Genotyping with Luminex multiplex PCR at the Scottish HPV Reference Laboratory revealed the presence of HPV18 in VIN cl. 11. This result was further validated by qPCR using HPV18 E6 primers performed in house. These analyses confirmed that VIN cl.11 was infected with HPV18. Immunostaining of organotypic raft cultures generated from VIN cl.11 revealed strong nuclear and cytosolic staining for p16^{INK4a} in the basal and immediate suprabasal cell layers the epithelium (Figure 5.10). This so-called p16^{INK4a} “block” staining indicates the presence of functionally active HPV18 E6 and E7 proteins.

Given that HPV18 can exist as either episomal or integrated forms, the physical status of the HPV18 genome in VIN cl.11 was further examined using an E2 disruption PCR assay [108]. Briefly, previously published primer pairs spanning 4 regions of the HPV18 E2 coding region were used to amplify DNA isolated from VIN clone 11. As a reference, DNA isolated from HPV18-HFK, which contains episomal forms of HPV18, and HeLa, a cell line which carries 10-50 integrated copies of the HPV18 genome were included as positive controls. As shown in Figure 5.11, all four-primer sets amplified products from HPV18-HFK, indicating the presence of an intact E2 gene. In contrast, the same set of primer failed to amplify E2 sequences in HeLa, findings consistent with the fact that E2 gene is disrupted following viral genome integration. Examination of the E2 gene in VIN Clone 11 revealed the presence of episomal forms of HPV18, given that all four-primer successfully amplified E2 sequences (Figure 5.11).

In summary, evidence presented thus far shows that VIN cl.11 harbors episomal forms of HPV18, and the expression of the E4 protein in organotypic raft culture suggests

that the virus is capable of lytic replication under conditions that favour keratinocyte differentiation.

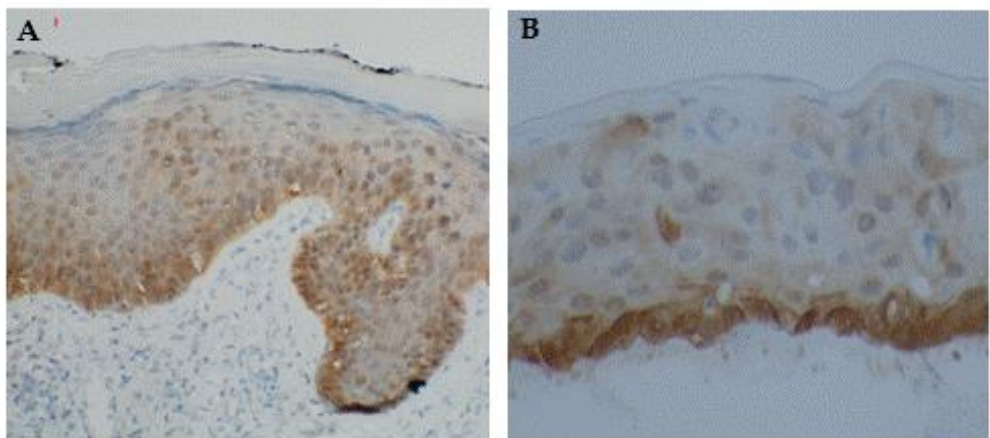


Figure 5.10: Representative immunostaining for p16^{INK4a} in organotypic raft cultures generated from VIN cl.11. (A) Immunostaining for p16^{INK4a} on a single uVIN biopsy taken from patient Ms S.M. (B) FFPE sections of organotypic raft cultures generated from VIN cl. 11 were stained for p16^{INK4a} by standard IHC. Epithelial cells within the raft culture showed diffused nuclear and cytosolic immunostaining for p16^{INK4a}. The image was taken using a Nikon Eclipse E600 microscope at x200 magnification.

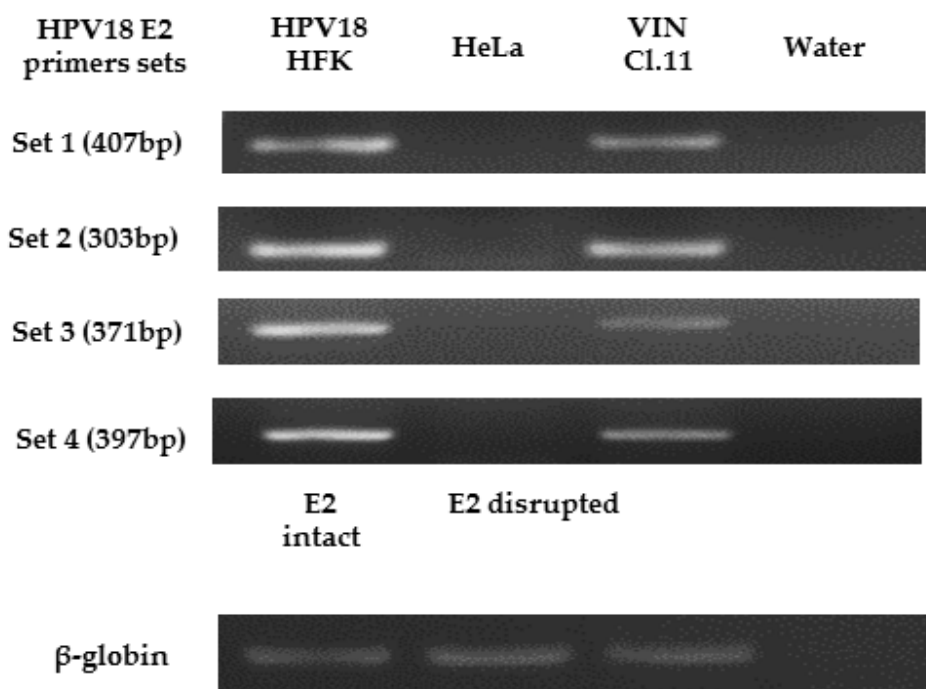


Figure 5.11: PCR-based HPV18 E2 disruption assay performed to detect the presence of integrated HPV18 genomes. DNA was extracted from HFK-HPV18, HeLa and VIN cl. 11, and amplified using defined HPV18 E2 primer sets 1 to 4 to detect the presence of an intact E2 gene. Left column: amplification of an intact E2 gene in HPV18 genome-containing human foreskin keratinocytes (HPV18-HFK), and from HeLa cells, which contain integrated, disrupted E2 genes. These were used as positive and negative controls respectively. Right column: results from VIN cl. 11: the E2 gene was not disrupted. β -globin globe was used as internal control. This is representative result of 3 experiments.

5.5.5 Expression of the HPV18-encoded E6 and E7 proteins in VIN cl. 11

Having confirmed that VIN cl. 11 contained episomal forms of HPV18, the expression of the two key viral oncoproteins, E6 and E7, was next examined by Western blotting.

Figure 5.12 shows the expression of E6 and E7 proteins in VIN cl. 11. Although E6 expression was readily detected at levels comparable to those observed in HFK-HPV18, the expression of E7 was only observed after over-exposure of the membrane. A short exposure time failed to show E7 expression (Figure 5.12), findings which suggest that VIN cl.11 expresses low levels of the E7 protein [149].

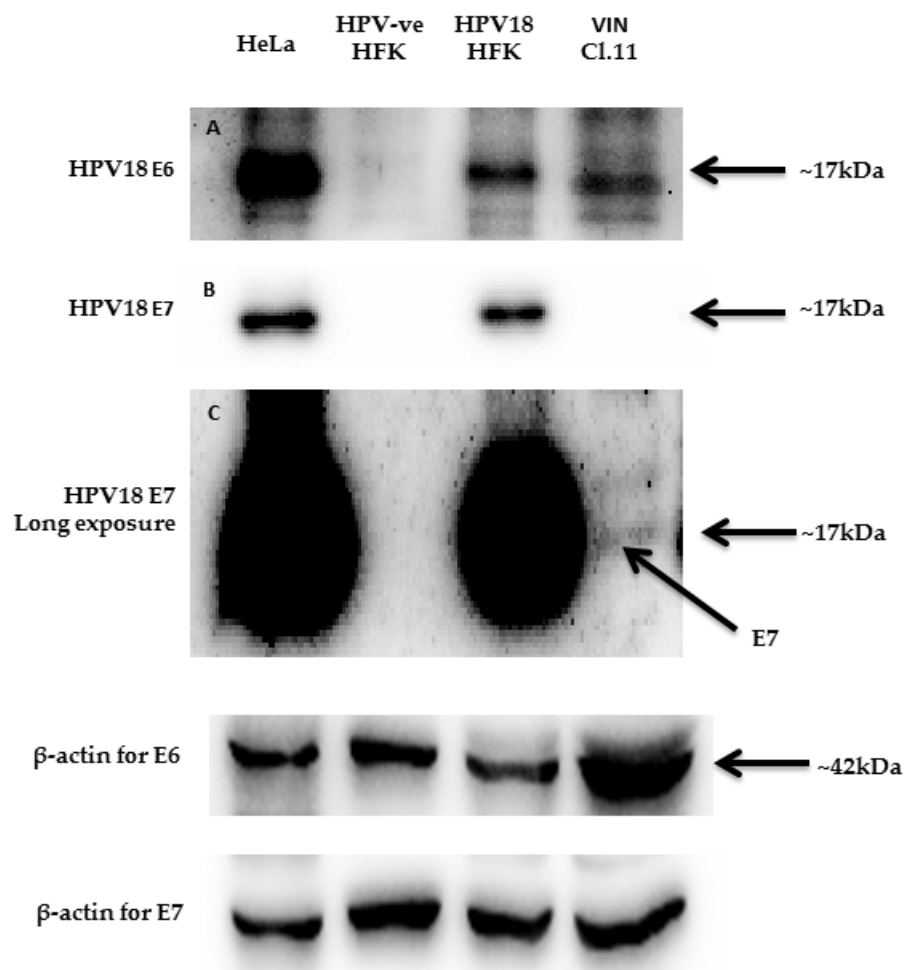


Figure 5.12: Western blot, confirming the expression of HPV18-encoded E6 and E7 proteins in VIN cl.11. Subconfluent cultures of HeLa, HFK-HPV18, its isogenic non-HPV18 infected counterpart, and VIN cl.11 were lysed in urea lysis buffer prior to resolving by SDS-PAGE and immunoblotting for anti-HPV18 E6 and E7. β -actin was used as internal control. The E7 protein was only detected in VIN cl.11 after prolonged exposure (twice the exposure time was taken to detect E7 protein in HeLa and HFK-HPV18). This is a representative result of 3 experiments.

5.6 The effects of EGCG treatment on VIN cl.11 in monolayer culture

Having confirmed that VIN cl.11 contained episomal forms of HPV18 and expressed the E6 and E7 proteins, I next sought to examine the effects of EGCG on the growth and differentiation of VIN cl.11 in both monolayer and organotypic raft culture, focussing on cell proliferation, apoptosis and terminal differentiation. To substantiate the effects observed on E6 protein expression in HFK-HPV18, the effects of EGCG on the turnover and stability of E6 in VIN cl.11 was also examined.

5.6.1 EGCG inhibits the proliferation of VIN cl.11 in monolayer culture

Actively growing VIN cl.11 cells were recovered by trypsinisation and single cell suspensions seeded into 96 well plates pre-coated with fibronectin (in triplicate). 24 hours later, cells were treated with increasing concentrations of EGCG. 72hours after treatment, cells were pulsed for 3 hrs with 10 μ M BrdU and cell proliferation measured using the BrdU ELISA assay kit (Roche) according to manufacturer's instructions. The experiment was repeated on three separate occasions.

As shown in Figure 5.13, a progressive reduction in cell proliferation was observed in VIN cl.11 cells treated with increasing concentrations of EGCG. Surprisingly however, a 0.2 fold increase in cell proliferation was observed at 20 μ M but this was not statistically significant (two tailed student t-test; P=0.27). The decrease in proliferation was only observed when VIN c.11 was treated with concentrations of 60 μ M and above. The concentration at which 50% of the cell proliferation was inhibited in VIN cl.11 (IC50 value) was at ~150 μ M (two-tailed student t-test; P= 0.02). The IC50 was higher than that of HFK-HPV18 which was at ~100 μ M.

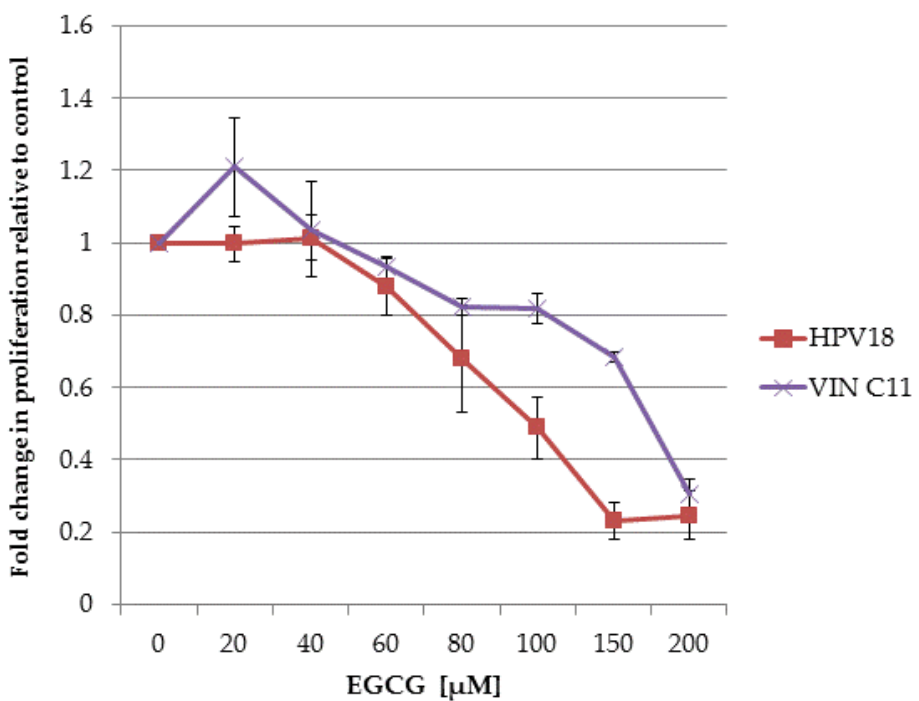


Figure 5.13: EGCG inhibits the proliferation of VIN cl.11 and HFK-HPV18 keratinocytes. Cells were treated with increasing concentrations of EGCG for three days prior to BrdU labelling. Cell proliferation was measured using the BrdU ELISA assay kit (Roche). Fold change in proliferation in EGCG treated cells were measured against untreated cells (control). Cell proliferation decreased as the concentration of EGCG increased. The IC₅₀ for VIN cl.11 and HFK-HPV18 were $\sim 100 \mu\text{M}$ and $\sim 150 \mu\text{M}$, respectively. Data shown is an average of 3 independent experiments.

5.6.2 EGCG treatment changes the morphology of VIN cl.11

To examine the effects of EGCG on cell morphology, VIN cl.11 cells were cultured in petri dishes pre-coated with fibronectin. The following day, cells were treated with 50, 100 or 150 μ M EGCG for an additional 72 hours, and the morphology of control and EGCG treated cells examined by phase microscopy. Figure 5.14 shows the changes in cell morphology of VIN cl.11 cells following EGCG treatment. Compared to untreated cells, cells treated with EGCG developed cytoplasmic vacuoles and assumed a spindle-like appearance. These changes were most apparent at a concentration of 150 μ M EGCG. In addition, EGCG treated cultures failed to proliferate, containing smaller colonies and fewer cells compared to untreated cells. The morphological changes induced by EGCG treatment on VIN cl.11 observed here are consistent with those observed in HFK-HPV18 following EGCG treatment and are suggestive of the cells undergoing apoptosis.

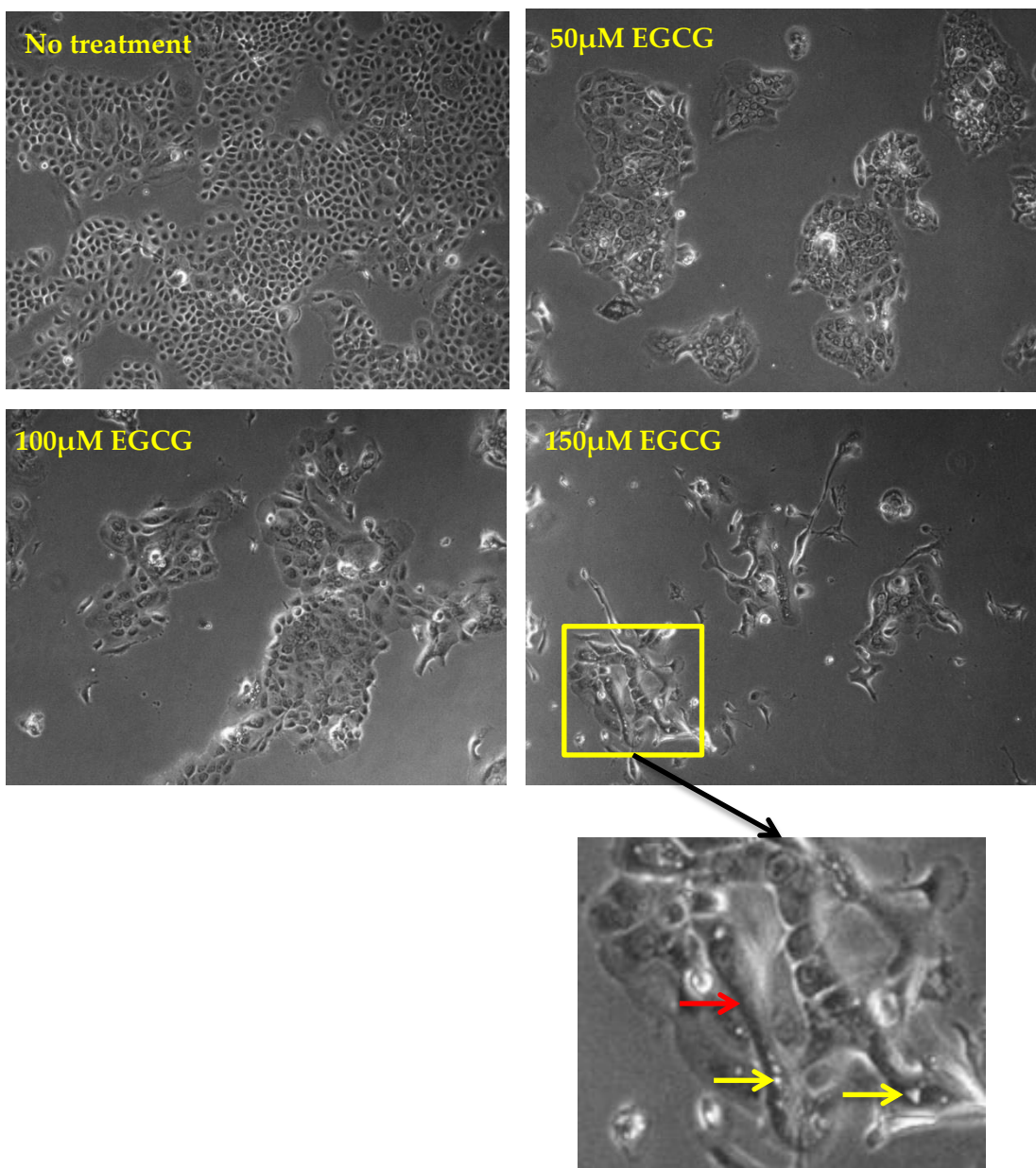


Figure 5.14: Changes in the morphology of VIN Cl.11 following three days of treatment with 25 μ M, 50 μ M and 100 μ M EGCG.

VIN cl.11 cells were plated onto fibronectin-coated petri dishes and allowed to establish colonies for three days prior to treatment with different concentrations of EGCG. Changes in cell morphology were evident after 72 hours with increasing concentration of EGCG. The cells assumed spindle-like appearance (red arrow) with intracellular vacuole (yellow arrows) at 100 μ M. Images were taken using a Nikon Eclipse E600 microscope at x200 magnification.

5.6.3 EGCG treatment does not influence a specific cell-cycle checkpoint, but does increase the proportion of cells undergoing apoptosis

Having observed that EGCG reduces cell proliferation and induces a profound change in the morphology of VIN cl.11 cells in monolayer culture, we set out to determine whether EGCG influenced cell proliferation by inducing cycle arrest at a specific check point. VIN cl.11 cells were treated with 150µM EGCG for 24, 48 and 72 hours. Cells were also treated with 100ng/ml Nocodazole for 12 hours, an agent used to disrupt cellular microtubules, which results in cell cycle arrest at the G2/M checkpoint. Control and EGCG treated cells were recovered as single cell suspensions, permeabilised in 70% ethanol, stained with 25µg/ml propidium iodide (PI) to stain DNA. Cells were then subjected to flow cytometric analysis and the data collected analysed with FlowJo v.10 software to build cell-cycle profiles. Figure 5.15 shows the results from a representative analysis of VIN cl.11 following EGCG treatment. Treatment of VIN cl.11 cells with Nocodazole for 12 hours increased the number of cells displaying a G2/M phase DNA content, and a corresponding decrease in the number of cells in the G1 and S phases of the cell cycle. There was a significant rise in sub-G1 cell population in cells treated with EGCG compared to untreated cells. Extending the treatment duration from 24 to 72 hours also increased the proportion of cells in Sub-G1 phase. Cells found in the sub-G1 phase have depleted DNA content as a result of loss of DNA fragments from permeabilized cells. DNA fragmentation is a characteristic hallmark of apoptosis and the accumulation of VIN cl.11 in sub-G1 showed that these cells have underwent apoptosis following EGCG treatment. However, there was no change in the overall cell cycle profile in VIN cl.11 after EGCG treatment.

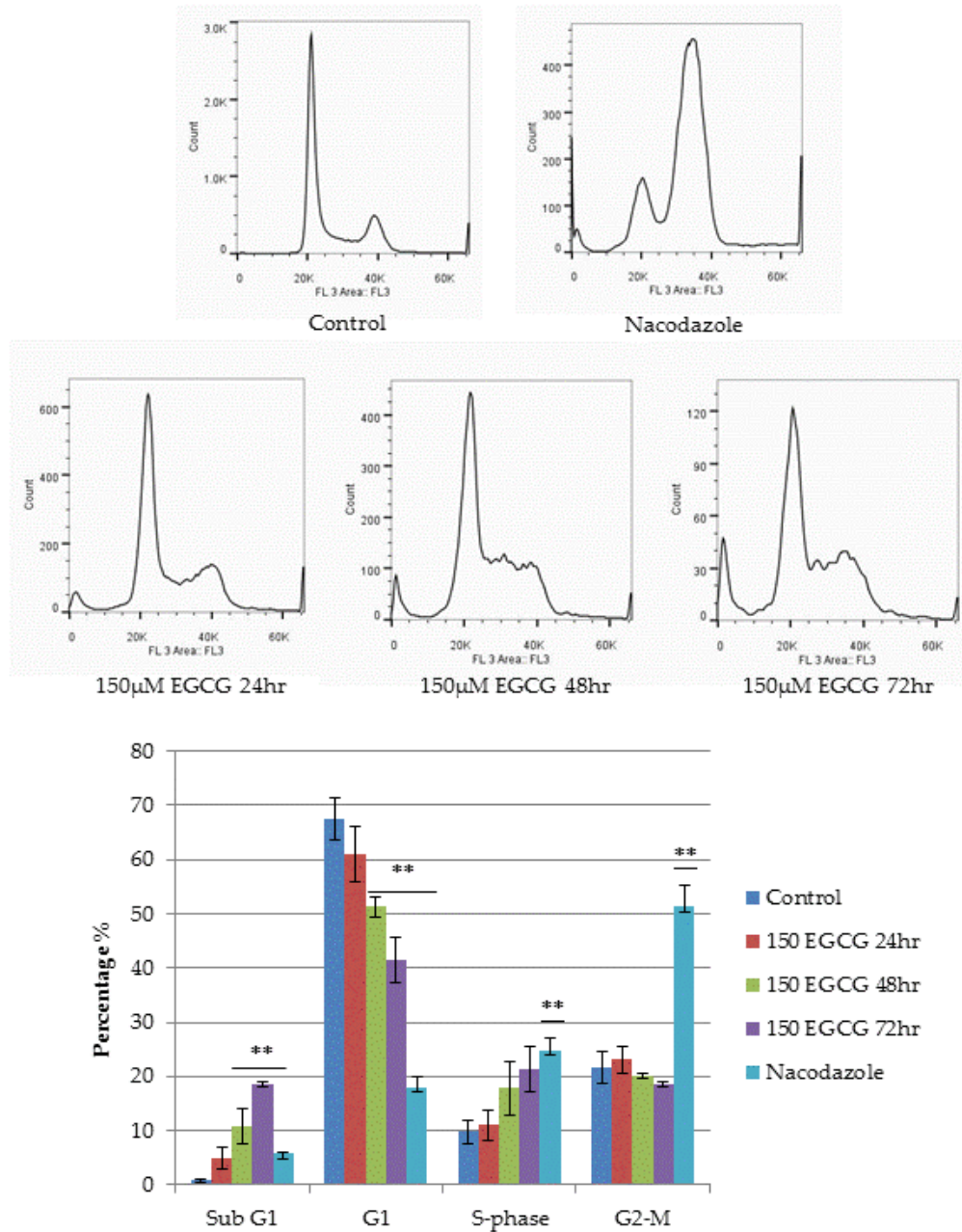


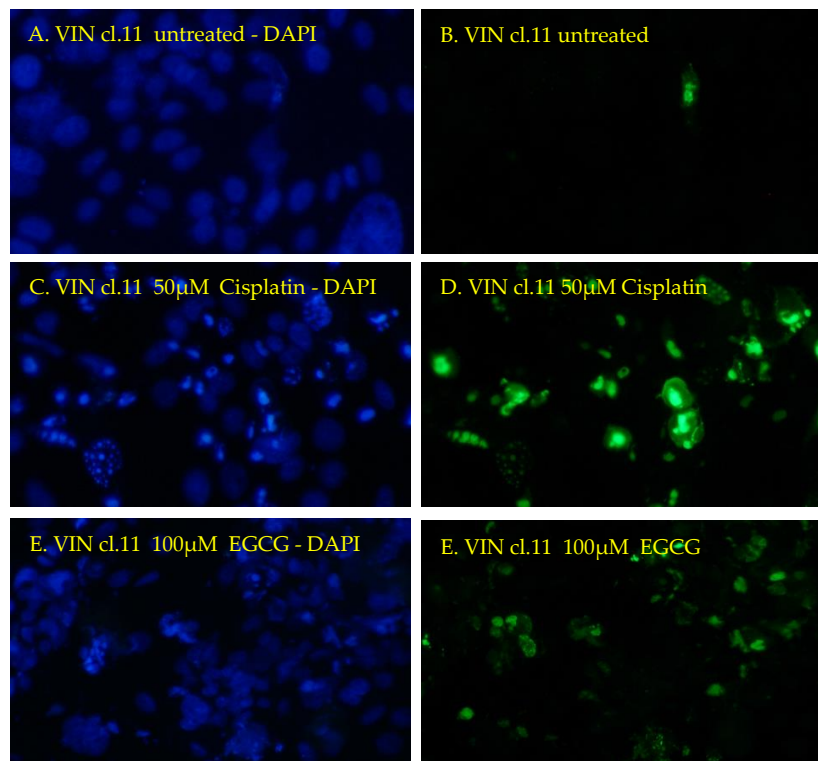
Figure 5.15: Cell cycle analysis of VIN Cl.11 in the presence or absence of EGCG treatment. Cells were treated with 150µM EGCG for 24, 48 and 72 hrs, and harvested, fixed and stained with propidium iodide for flow cytometry analysis. Nocodazole treatment was used as positive control for the assay. Data were analysed with FlowJo v.10. Data shown is an average of 3 independent experiments. Statistical significance was determined by two-tailed unpaired Student t-test.

5.6.4 EGCG treatment induces apoptosis in VIN cl.11

To complement findings from the cell cycle analysis, a TUNEL (TdT-mediated dUTP Nick-End Labeling) assay was performed to examine the extent of apoptosis induced by EGCG treatment. VIN cl.11 cells were seeded onto fibronectin-coated cover slips and, 24 hours later, treated with 100 μ M EGCG for 72 hours. As a positive control, cells were treated for 24 hours with 50 μ M Cisplatin to induce apoptosis. Cell nuclei were then labelled with TUNEL (visualised in green) and counterstained with DAPI (blue) to identify cell nuclei. Cell nuclei and TUNEL positive nuclei were counted and results were expressed as proportion of TUNEL positive nuclei as a percentage of total cell nuclei. Two tailed unpaired student t-test was used to determine the level of significance between the proportion of TUNEL positive cell in drug treated and untreated cells.

Figure 5.16 shows the proportion of TUNEL positive or apoptotic cells in Cisplatin, EGCG and untreated VIN cl.11 cells. The proportion of baseline apoptotic cells was just under 1% in untreated cells. Treatment of cells with Cisplatin for 24 hours induced apoptosis in almost half of the cell population. Approximately 51% of TUNEL positive cells were observed following EGCG treatment indicating that half of these cells were undergoing apoptosis after 72 hours of treatment. In comparison, the DNA damaging agent, Cisplatin, which is a more potent cytotoxic agent as a significantly less amount of drug and shorter treatment duration is sufficient to achieve the same level of apoptosis in EGCG treatment.

A.



B.

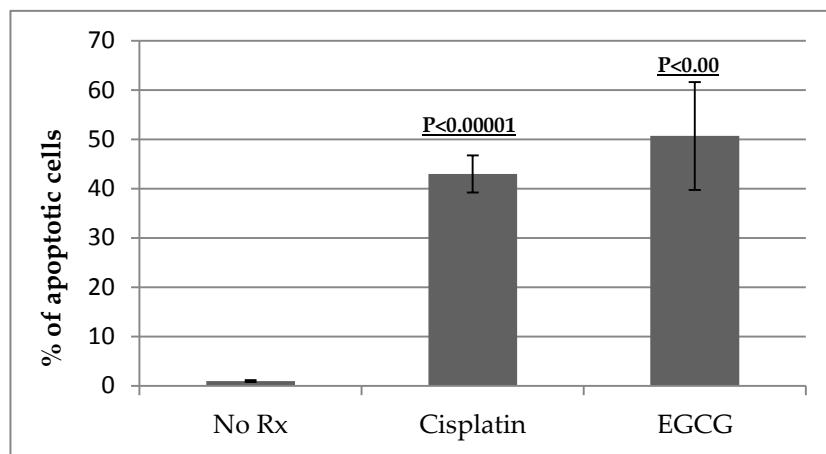


Figure 5.16: TUNEL assay demonstrating that EGCG treatment induces apoptosis in VIN cl.11. (A). VIN cl.11 cells were treated with 100 μ M EGCG for 72 hours or 50 μ M Cisplatin for 24 hours; the latter used as a positive control to induce apoptosis. The TUNEL assay was used to label apoptotic cell (green) and cell nuclei counter stained with DAPI (blue). Magnification $\times 200$. (B). TUNEL positive cells were counted and expressed as a percentage of total DAPI-stained cell nuclei. Unpaired Student t-test was used to determine the level of significance for the difference in the proportion of apoptotic cells in drug-treated and untreated cells. The experiments were repeated at twice in triplicate.

5.7 The effect of EGCG treatment on VIN cl.11 in organotypic raft culture

Having established that concentrations of EGCG greater than 60 μ M reduced cell growth and induced apoptosis in VIN cl.11 cells in monolayer culture, the effect of EGCG on cell growth and differentiation in a three dimensional organotypic raft culture system was subsequently investigated. VIN cl.11 cells were cultured on a collagen plug impregnated with 3T3-J2 feeder cells and transferred to a metal grid and allowed to differentiate for 10 days at the air-liquid interface before 150 μ M EGCG was added to the growth media for a further 10 days. Prior to fixation in formaldehyde, 25 μ g/ml of BrdU was added to growth media for 12 hours to label cells undergoing DNA replication.

5.7.1 EGCG reduces the proliferation of VIN cl.11 in organotypic raft culture

To assess the effect of EGCG on the morphology of VIN cl.11 in a three-dimensional culture system, FFPE sections of treated and untreated EGCG treated raft cultures were stained with H&E, and a FITC-conjugated anti-BrdU mAb. Sections were counter stained with DAPI to visualise cell nuclei.

H&E sections of untreated and EGCG-treated-EGCG rafts showed that the thickness of rafts treated with EGCG were significantly thinner than those of untreated rafts (Figure 5.17). Immunofluorescence staining for BrdU revealed that the number of proliferating cells was significantly reduced in EGCG-treated rafts compared to control rafts (Figure 5.18), indicating that fewer cells were undergoing DNA synthesis. To further confirm that cell proliferation was suppressed by EGCG, immunofluorescence staining was performed for Ki-67, a protein expressed in proliferating cells [185]. This

analysis revealed a significant reduction in nuclear staining in EGCG-treated rafts compared to untreated control rafts (Figure 5.18). These findings are consistent with those obtained from HFK-HPV18 raft cultures (Chapter 4 section 4.6.1), where EGCG was also shown to reduce cell proliferation.

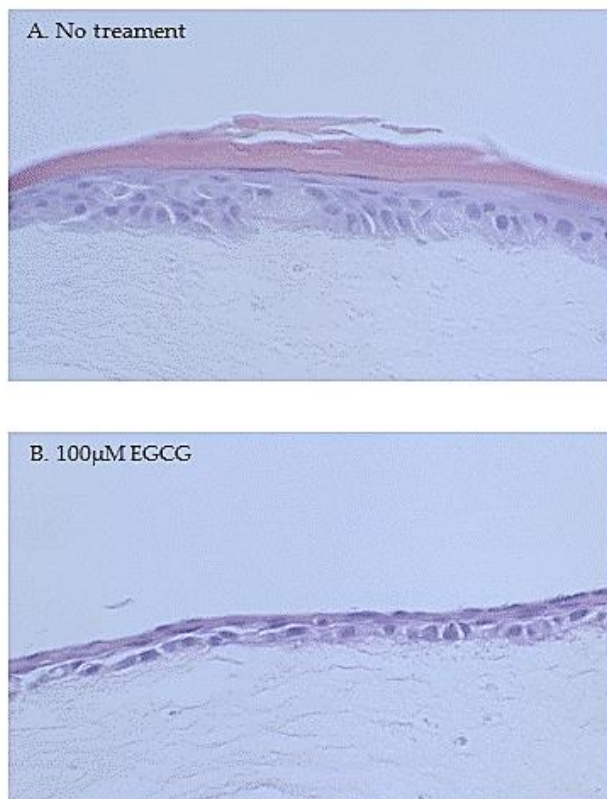


Figure 5.17: H&E staining showing the overall morphology of control and EGCG-treated VIN cl.11 keratinocytes grown in organotypic raft culture. Organotypic raft cultures were allowed to stratify for 10 days prior to the addition of 100 μ M EGCG, which was then added to the growth media for a further 10 days. Representative haematoxylin and eosin (H&E) stained sections of (A) control and (B) EGCG treated raft cultures. Note that the thickness of the epithelium was significantly reduced in response to EGCG treatment. Magnification x200.

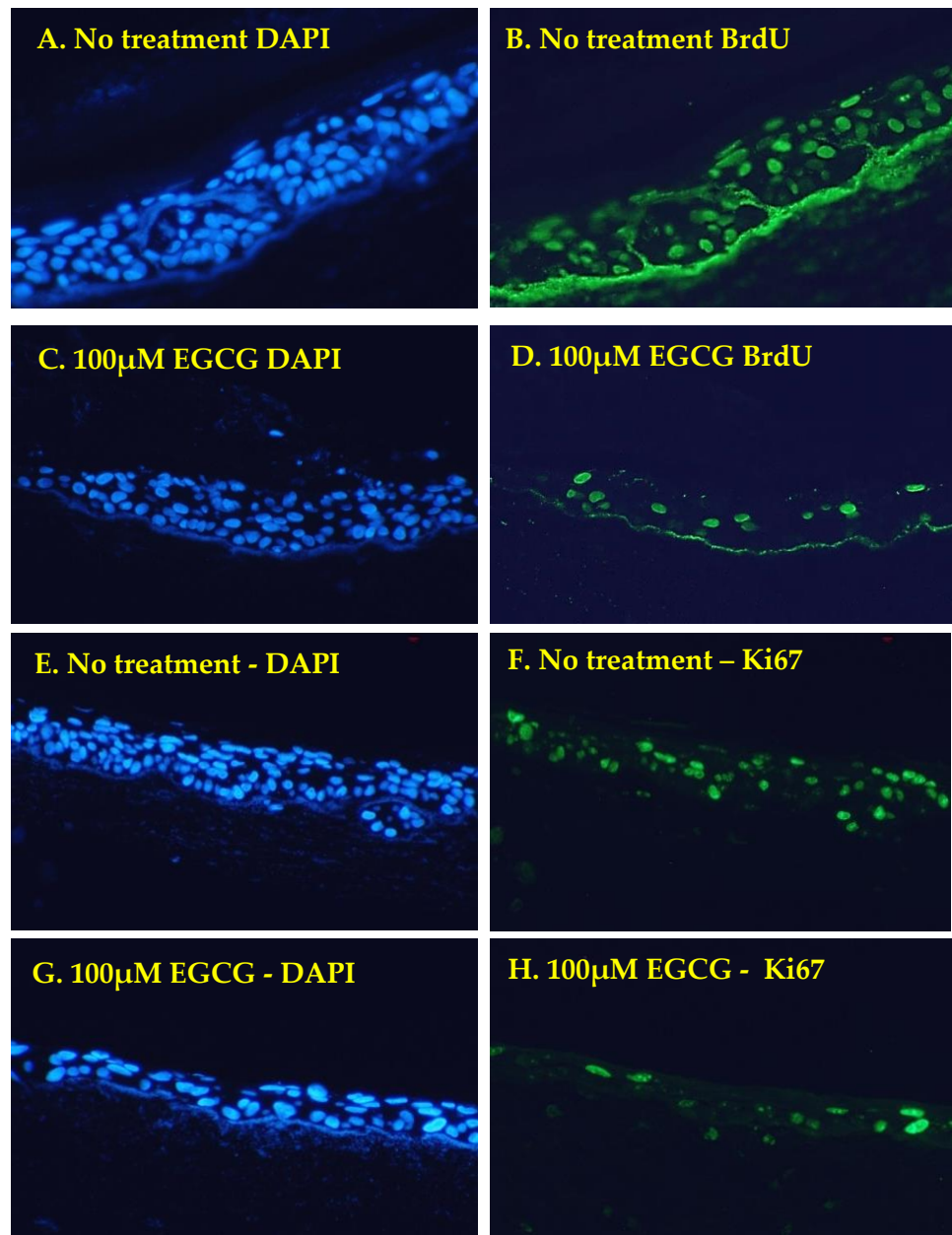


Figure 5.18: The incorporation of BrdU label and expression of the cell proliferation marker, Ki67, are reduced in VIN cl.11 raft cultures treated with EGCG. FFPE sections of control and EGCG-treated rafts were stained for (A-D) cells incorporating the BrdU label or (E-H) Ki67 (Green) and counterstained with DAPI (Blue) to label cell nuclei. The number of cell nuclei staining positive for BrdU label or Ki67 expression was significantly reduced in response to EGCG treatment. Magnification x200.

5.7.2 EGCG has little effect on expression of p16^{INK4A} and MCM7 in VIN cl.11 raft cultures

Having established that EGCG treatment inhibited cell proliferation in VIN cl.11 raft cultures, I set out to examine the effects of EGCG on expression of two established HR-HPV targets: p16^{INK4A} and MCM7. As mentioned previously, p16^{INK4A} and the MCM7 proteins are used as surrogate markers for HR-HPV infection as their expression is elevated in response to HR-HPV infection. Given that EGCG has been shown here to down regulate expression of the E7 protein in HFK-HPV18, I next examined whether this down-regulation impacted on the expression of p16^{INK4A}. IHC staining was performed on VIN cl.11 raft sections and p16^{INK4A} expression compared between untreated and EGCG treated rafts. Contrary to expectations, little or no change was observed in the levels of p16^{INK4A} expression in control and EGCG treated raft cultures, with strong basal and suprabasal expression observed in both control and untreated raft culture (Figure 5.19).

Expression of the DNA replication licensing factor, MCM7, is normally confined to cells within the basal layer of normal epidermis but expressed in basal and suprabasal cell layers in HR-HPV infected pre-neoplastic lesions such as cervical intraepithelial neoplasia (CIN); especially high-grade CIN3 [186]. Overexpression of MCM7 is induced by HPV-E7, as raft cultures generated from HPV E7 transfected keratinocytes, expressed MCM7 throughout the whole epithelium, spanning from the basal cell layer to the uppermost spinous cell layers [187]. Immunostaining of control and EGCG treated VIN cl.11 raft sections identified expression of MCM7 in the nuclei of VIN cl.11 spanning the entire thickness of the raft culture. However, following EGCG treatment

there was a modest change in the expression and distribution of MCM7 in VIN cl.11, although the pattern of staining became more polarised to the basal cell layer (Figure 5.19). The number of cell nuclei labelled with BrdU, or expressing Ki67 or MCM7 was counted manually in control and EGCG treated rafts ($n = 5$ fields) and these expressed as a proportion of the total number of DAPI stained cell nuclei. Results were presented as the proportion of cells stained positive for targeted proliferative markers. Two-tailed unpaired Student t-test was used to determine the difference in the proliferative marker expression of in EGCG treated rafts is significant when compared to control. Figure 5.20 shows the results of IF staining for BrdU, Ki67 and MCM7, shown as a percentage of total DAPI stained nuclei. BrdU and Ki67 expression were significantly reduced in response to EGCG treatment compared to control rafts, indicating that DNA replication and cell proliferation were inhibited by EGCG.

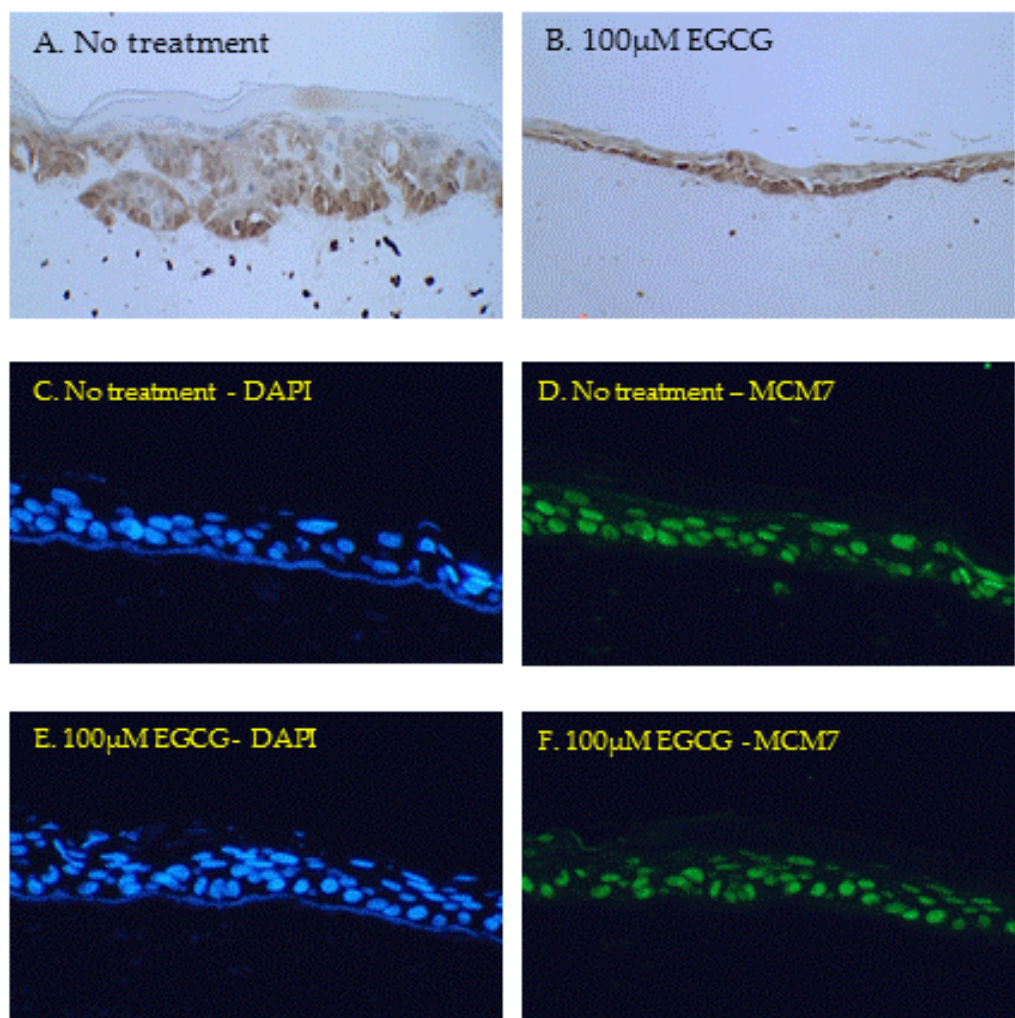


Figure 5.19: The expression and distribution of p16^{INK4a} and MCM7 are not affected by EGCG treatment in raft cultures of VIN cl11.

(A, B) Immunohistochemical (IHC) staining for p16^{INK4a} (Brown) on FFPE sections of VIN cl. 11 rafts cultured in the presence or absence of EGCG. (C-F) FFPE sections generated from VIN cl11 were stained for MCM7 (Green) and counterstained with DAPI (Blue) to label cell nuclei. MCM7 was expressed in the nuclei of basal and suprabasal keratinocytes, but the level of expression was unchanged following EGCG treatment. Magnification x200.

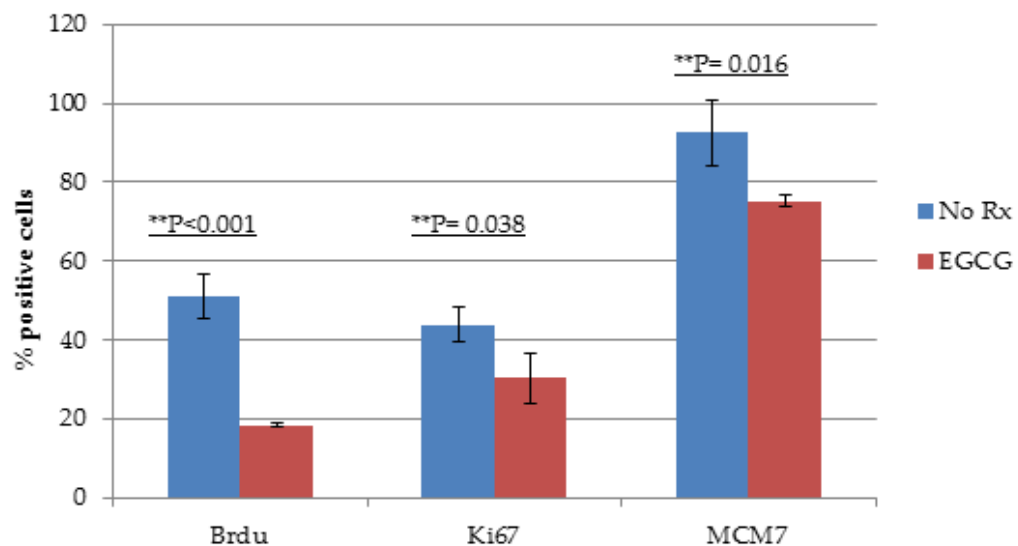


Figure 5.20: EGCG treatment inhibits the proliferation of VIN cl11 cells in organotypic raft culture. Summary of the results obtained from cells incorporating BrdU label or staining positive for the proliferation antigens Ki67 and MCM7 in control and EGCG treated organotypic raft cultures. The total number of cell nuclei (DAPI stained) and those nuclei expressing BrdU, Ki67 or MCM7 were counted manually. Results were presented as the proportion of cells stained positive for targeted proliferative markers. $**P < 0.05$, two-tailed Student unpaired t-test indicates that the difference in BrdU, Ki67 or MCM7 expression is significant when compared to control.

5.7.3 EGCG does not influence expression of keratinocyte differentiation markers

Previous studies have shown that EGCG promotes the differentiation of normal epidermal keratinocytes in monolayer culture, simulating expression of the keratinocyte differentiation markers, involucrin and transglutaminase [96]. To determine whether EGCG promotes the differentiation of VIN cl.11 cells, sections of EGCG treated and untreated raft cultures were stained with antibodies specific for two keratinocyte differentiation markers: involucrin and the high molecular keratins, K1/10. Representative IF staining of rafts sections with antibodies to involucrin and K1/10 (green), counterstained with the nuclear DAPI stain, (blue) are shown in Figure 5.21. While little difference in the level of involucrin was observed between control and EGCG treated rafts, higher levels of Keratin 1/10 were observed in EGCG treated rafts. Although preliminary, these findings suggest that EGCG may promote the differentiation of VIN cl.11 keratinocytes in organotypic raft culture.

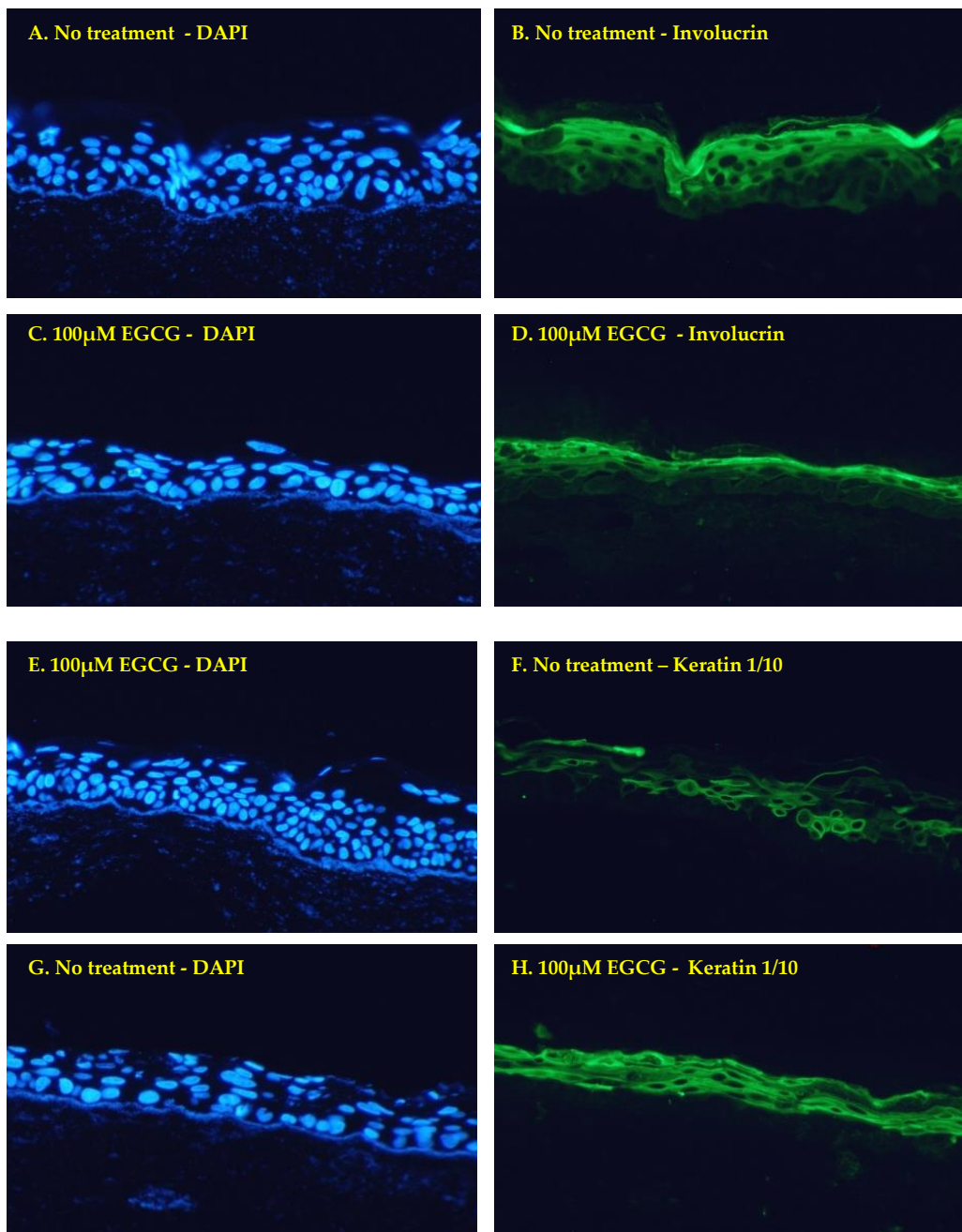


Figure 5.21: Expression of the differentiation markers, involucrin and Keratin 1/10 are not altered in VIN cl. 11 raft cultures treated with EGCG. FFPE sections of control and EGCG treated VIN cl.11 rafts were stained for (A-D) involucrin or (E-F) Keratin 1/10 (Green) and counterstained with DAPI (Blue) to label cell nuclei. Both involucrin and K1/10 were expressed in the cytoplasm of suprabasal differentiating keratinocytes, and their level of expression was unchanged following EGCG treatment. Magnification x200.

5.7.4 EGCG inhibits the expression of E4 in VIN cl.11 raft cultures

As previously discussed, the expression of E4 is indicative of productive viral infection. E4 is expressed prior to the late structural proteins L1 and L2, and distributed within the suprabasal layers of HPV-transfected raft cultures [188]. To examine the effects of EGCG on productive infection, IF staining was performed on FFPE sections of control and EGCG treated VIN cl.11 rafts for the E4 protein. As shown in Figure 5.22, E4 was expressed at high levels in the suprabasal layers of non-EGCG treated raft sections, whilst little, if any E4 was observed in EGCG treated rafts. This probably indicates that process of viral production is interrupted by EGCG at the later stage of the HPV life cycle.

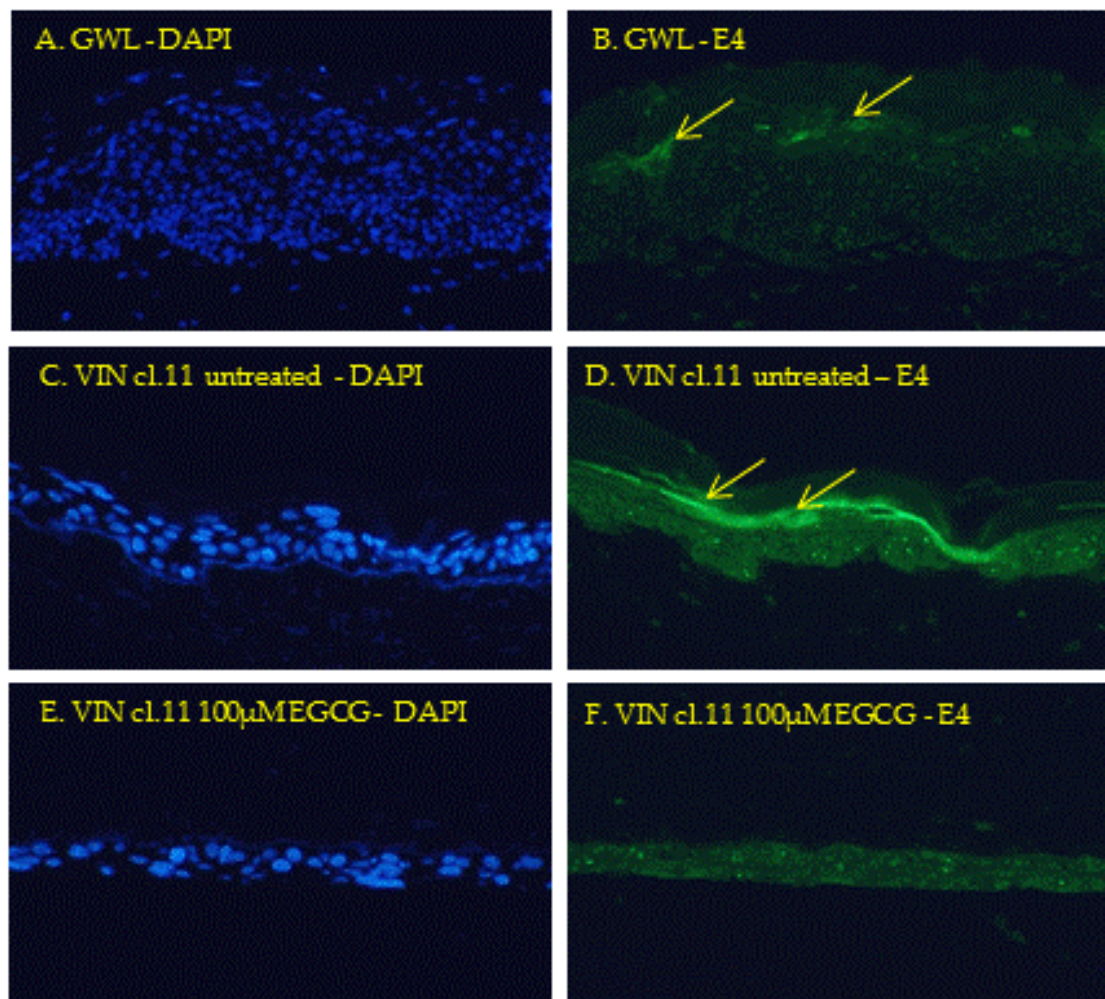


Figure 5.22: The HPV18 E4 protein is not expressed in VIN.cl11 raft cultures treated with EGCG. Panels A and B show staining for the E4 protein (green) in raft cultures generated from HFK-HPV18-E6GWL keratinocytes, which express the E4 protein and serve as a positive control. Cell nuclei were counter stained with DAPI (blue). Expression of the E4 protein was detected in differentiating suprabasal cells (yellow arrows). (C-F) show E4 protein staining (green) in VIN cl. 11 rafts grown in the presence or absence of EGCG; cell nuclei were counterstained with DAPI (blue). E4 expression was observed in the uppermost suprabasal layers (yellow arrows) of untreated, but not EGCG-treated rafts. Magnification x200.

5.8 The effect of EGCG treatment on expression of the HPV18-encoded E6 and E7 proteins and tumour suppressor gene (TSG) expression in VIN cl.11

In Chapter 2, I demonstrated that EGCG treatment was associated with down regulation of the HPV18-encoded E6 and E7 oncoproteins, in HFK-HPV18. This down regulation was accompanied by an up-regulation of their target TSGs, p53 and p21^{WAF1}. Thus far, I have demonstrated that VIN cl.11, harbours episomal forms of HPV18 and strongly expresses the HPV18-encoded E6 protein. When treated with EGCG, the proliferation of VIN cl.11 was inhibited in both monolayer and organotypic raft culture, with a proportion of cells undergoing apoptosis. Having shown that the morphological changes observed in monolayer and organotypic raft culture following EGCG treatment resembled that observed in HFK-HPV18, I went on to investigate whether EGCG also affected the expression of the viral oncoproteins and cellular TSGs.

To examine the expression of the HPV18-encoded E6 and E7 oncoproteins and their target TSGs, VIN cl.11 cells were treated with 100μM EGCG for 24, 48 and 72 hours. Control and EGCG treated cells were lysed *in situ* in RIPA buffer at the appropriate time and cell lysates resolved by SDS-PAGE. Western blotting was performed using antisera specific for E6, p53 and p21^{WAF1}; antibodies specific for GAPDH or β-actin were included as loading controls. In parallel, FFPE sections of organotypic rafts were stained with the same antisera to assess level of TSG expression in control and EGCG treated raft cultures.

5.8.1 EGCG treatment down regulates expression of the HPV18 E6 protein in VIN

cl.11

Expression of the HPV18-encoded E6 protein was down regulated following EGCG treatment (Figure 5.22). Densitometric analysis was performed on the E6 and β -actin bands using ImageJ software. The densitometry values for E6 were then normalised against the corresponding values for β -actin, and the fold change in E6 expression was compared against that of untreated cells (control). Two tailed unpaired student t-test was used to determine the level of significance in the difference between E6 expression before and after EGCG treatment. A representative experiment, shown in Figure 5.23, demonstrates that E6 is down regulated in response to EGCG treatment. A small reduction in E6 expression was observed 24 hours after treatment, but the difference was not significant, $P=0.51$. However, in keeping with earlier findings, the level of E6 protein was reduced by more than 50% after 48 and 72hours ($P= 0.01$ and 0.02 , respectively). It was not possible to examine the level of protein expression for E7 in VIN cl.11 because the endogenous protein level of E7 was below the limit of detection.

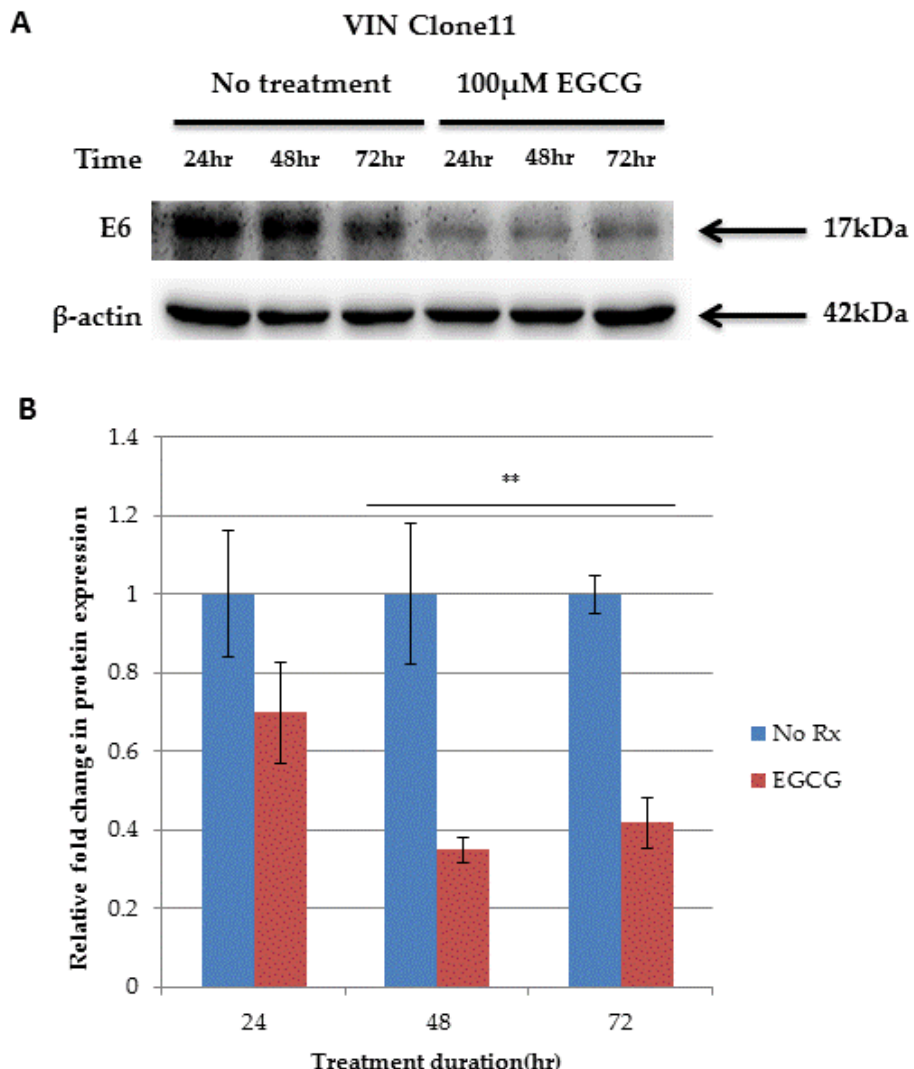


Figure 5.23: Western blot showing down-regulation of the HPV18 E6 oncoprotein in VIN cl. 11 following EGCG treatment. VIN cl.11 cells were treated with 150 μ M EGCG for 24, 48 and 72hrs prior to lysis in RIPA buffer. Total cell lysates were resolved by SDS-PAGE and immunoblotted for anti-HPV18 E6. (A) Western blot showing down regulation of HPV18 E6. (B) Densitometry analysis of the blots. E6 densitometry values were normalized against β -actin. The fold change in E6 expression was compared against untreated cells. Statistical significance was determined by two-tailed unpaired Student t-test. Data shown is an average of 3 independent experiments.

5.8.2 EGCG up regulates expression of p53 but not p21^{WAF1} in VIN cl.11

The down regulation of E6 expression was followed by the up regulation of its target TSG, p53 (Figure 5.24), and this was accompanied by an increase in expression of p21^{WAF1}, a downstream target of p53 (Figure 5.25). Densitometric analysis showed a gradual increase in p53 expression when EGCG treatment duration was extended from 24 to 72 hours. The rise in p53 protein level was only significant at 72 hours treatment when compared to no treatment (two tail unpaired student t-test, P=0.055). Although the levels of p21^{WAF1} were found to increase 24 and 72 hours after EGCG treatment, the difference was not statistically significant (P=0.49, P=0.19, respectively, by two tailed unpaired student t-test).

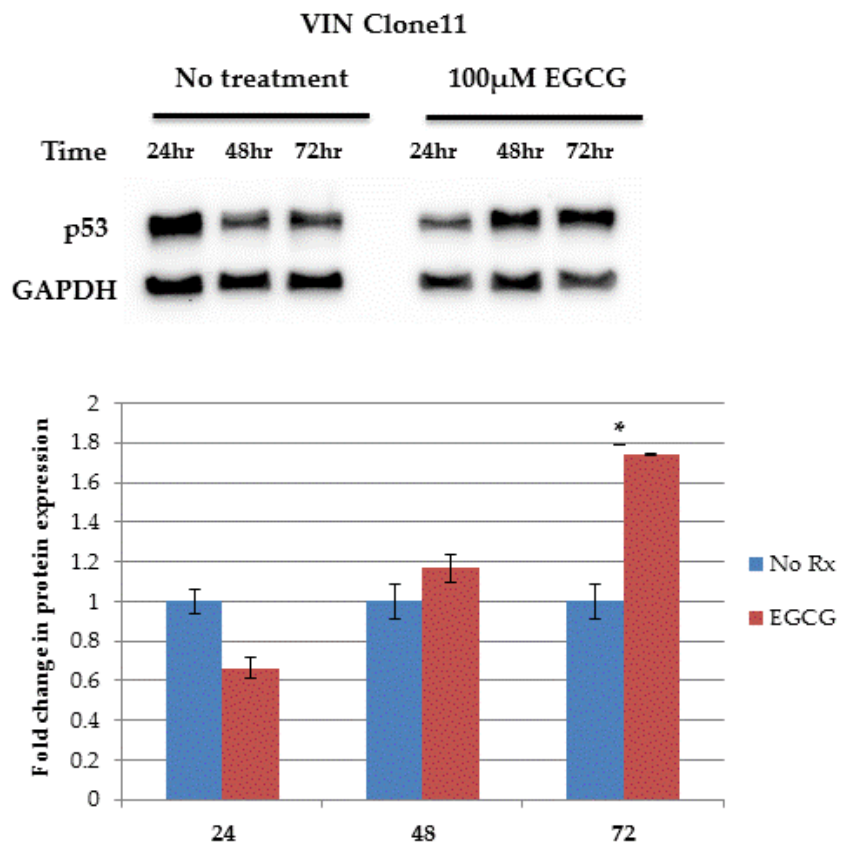


Figure 5.24: Western blot showing up-regulation of p53 expression in VIN cl. 11 following EGCG treatment. VIN cl.11 cells were treated with 150 μ M EGCG for 24, 48 and 72hrs prior to lysis in RIPA buffer. Total cell lysates were resolved by SDS-PAGE and immunoblotting performed for p53. (A) Western blot showing up-regulation of the p53 protein in EGCG treated VIN cl.11 cells. (B) Densitometric analysis of the blots. The densitometry values of p53 were normalized against GAPDH. The fold change in p53 expression was compared against untreated cells (control). *P=0. 055, unpaired student t-test indicates that the difference in p53 expression is significant when compared to controls. Data shown is an average of 3 independent experiments.

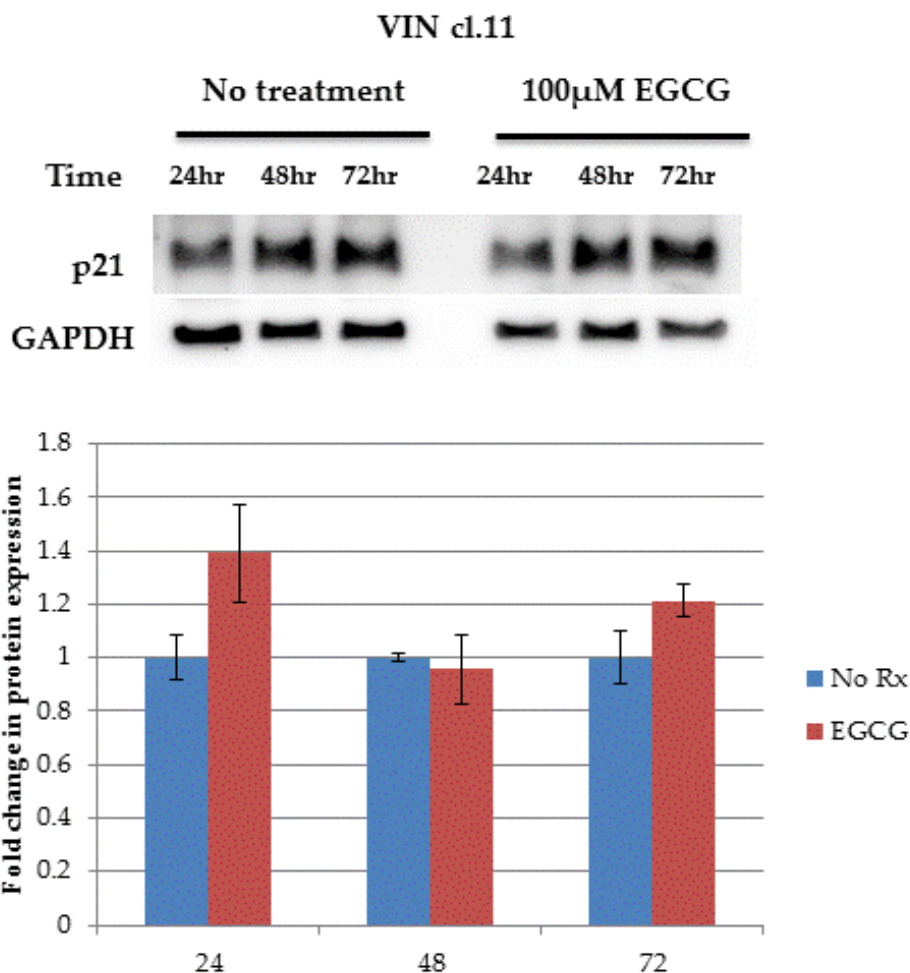
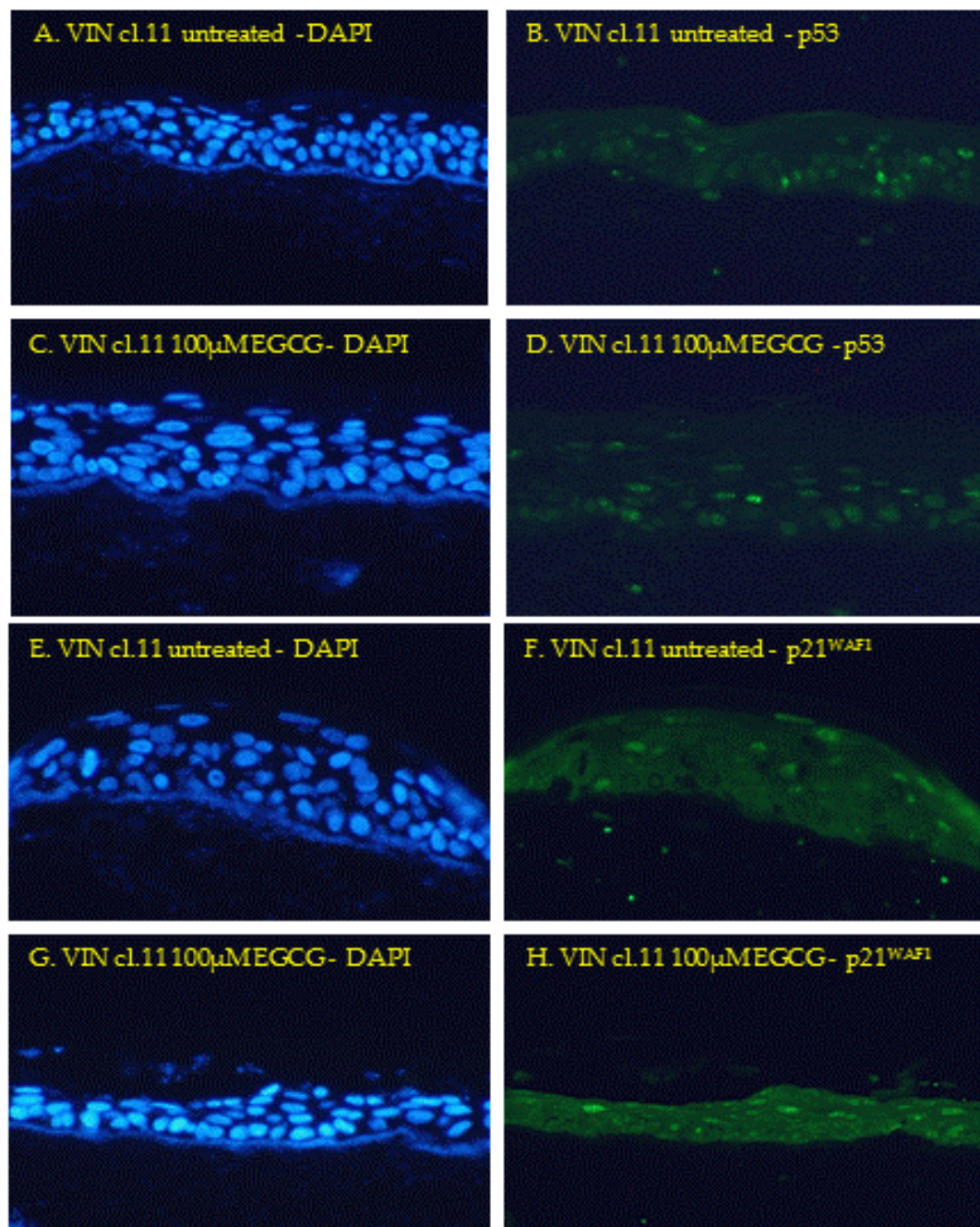


Figure 5.25: Western blot showing up-regulation of p21^{WAF1} expression in VIN cl. 11 following EGCG treatment. Cells were treated with 150 μ M EGCG for 24, 48 and 72hrs prior to lysis in RIPA buffer. Total cell lysates were resolved by SDS-PAGE prior to immunoblotting for p21^{WAF1}. (A) Western blot showing up-regulation of p21^{WAF1} protein at 24 and 72 hours post EGCG treatment. (B) Densitometry analysis of the blots. p21^{WAF1} densitometry value was normalized against GAPDH. The fold change in p21 expression was compared against untreated cells (control). The difference in p21 protein level before and after EGCG treatment was not statistically significant (two tailed unpaired student t-test). No Rx = no treatment. Data shown is an average of 3 independent experiments.

5.8.3 EGCG treatment stimulates expression of p53, p21^{WAF1} and pRb in VIN cl.11

raft cultures

The effects of EGCG treatment on the expression of p53, p21^{WAF1} and pRb in VIN cl.11 cells was examined by immunofluorescence staining of control and EGCG treated raft cultures using antibodies outlined in Chapter 2. Representative analyses (Figure 5.26) revealed that long-term exposure of VIN cl.11 rafts to EGCG led to an increase in the levels of nuclear p53, p21^{WAF1} and pRb. Although IF staining failed to differentiate between the under and hyperphosphorylated forms of pRb, EGCG treatment was associated with a general increase in the levels of nuclear pRb staining. Quantification of these results revealed that EGCG-treated rafts displayed a 40% increase in p53; a 48% increase in p21^{WAF1}; and a 72% increase in pRb expression (Figure 5.27).



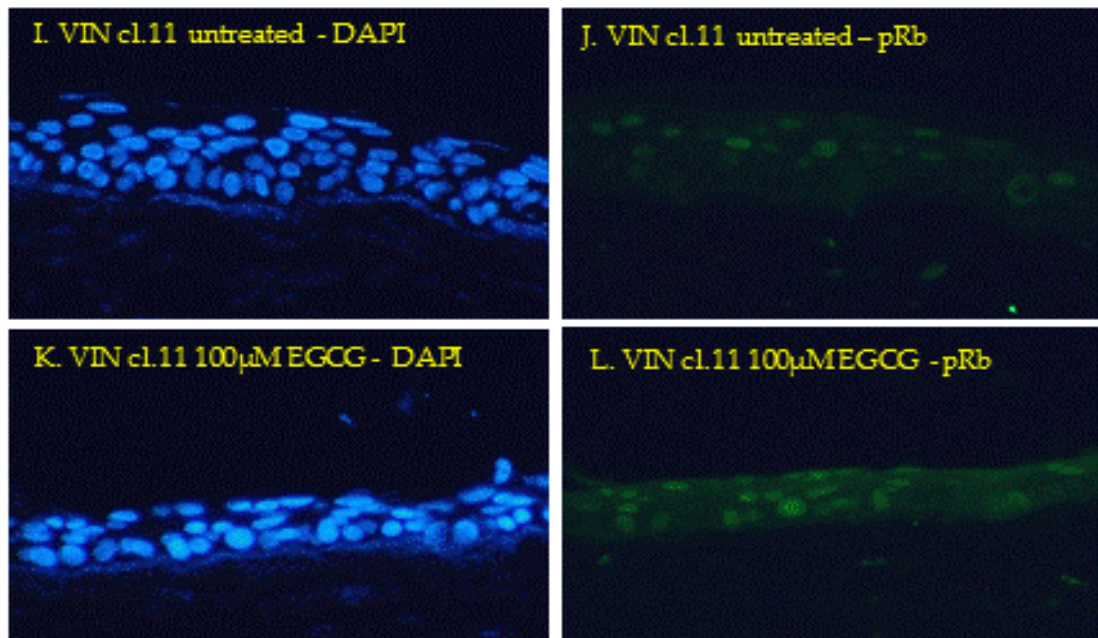


Figure 5.26: Expression of the p53, p21^{WAF1} and pRb are altered in response to EGCG treatment of VIN cl. 11 raft cultures. FFPE sections of VIN cl.11 raft cultures grown in the presence or absence of EGCG were stained for p53 (A-D), p21^{WAF1} (E-H) or pRb (I-L) (green) and cell nuclei counter stained with DAPI (blue). Panel A-D showing an increase in the nuclear staining of p53 following EGCG treatment. Panel E-H, showing a modest upregulation of nuclear p21^{WAF1} staining following EGCG treatment. Panel I-L, showing an increase in pRb expression following EGCG treatment. Magnification x200.

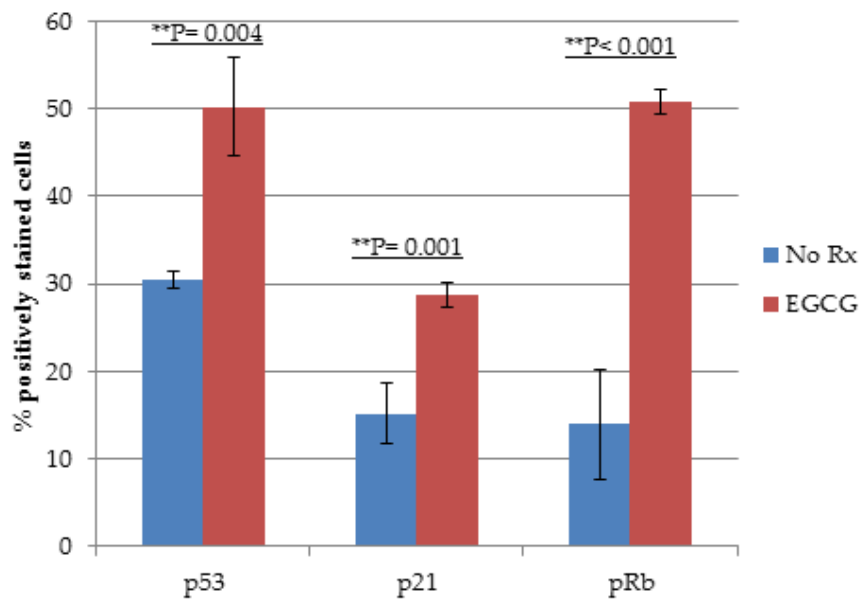


Figure 5.27: EGCG treatment upregulates expression of the key tumour suppressor genes, p53, p21^{WAF1} and pRb, targeted by the HPV oncoproteins, E6 and E7, indicating the functions of these TSGs were restored in VIN cl.11. Summary of the results of IF staining for p53, p21^{WAF1} and Rb expression in organotypic raft cultures of VIN cl.11 cultured in the presence or absence of EGCG. The total number of cell nuclei (DAPI stained) and those nuclei stained positive for p53, p21^{WAF1} or pRb were counted manually. Results were presented as proportion of cells stained positive for TSGs. **P<0.05, two-tailed student unpaired t-test indicates that the difference in the TSG expression is significant when compared to control. Summarized from three independent experimental repeats. No Rx = No treatment

5.8.4 EGCG treatment alters the distribution of Δ Np63 in VIN cl.11 raft cultures

Δ Np63, a homologue of p53, is a transcription factor required for maintaining and modulating stem cell populations in a number of epithelial tissues [189]. While expression of Δ Np63 is normally confined to the basal cell layer of normal squamous epithelium, its expression extends to suprabasal cell layers in dysplastic or pre-neoplastic epithelium, such as CIN 3. In vulvar epithelium, expression of Δ Np63 is also confined to the basal cell layer, but aberrantly expressed in suprabasal cell layers of differentiated VIN (dVIN), a HPV negative intraepithelial neoplasia of the vulva [43]. Interestingly, the role of Δ Np63 in uVIN, a HPV induced intraepithelial neoplasia of the vulva, has not been explored. Here I went on to examine the level and distribution of Δ Np63 in HFK-HPV18 and VIN cl.11 cells grown in organotypic raft culture. The effect of EGCG treatment on Δ Np63 expression was also studied.

FFPE sections of VIN cl.11 and HFK-HPV18 organotypic raft cultures were subjected to immunofluorescence staining for Δ Np63 using a rabbit antiserum; cell nuclei were counter stained with DAPI (Figure 5.28). Immunofluorescence staining revealed that Δ Np63 was confined to the nuclei of basal cells in raft cultures generated from HFK-HPV18 (see Figure 4.36), but expressed throughout most cell layers in VIN cl.11 rafts. EGCG treatment did not alter the level of expression and distribution of Δ Np63 in HFK-HPV18 (see Figure 4.36). However, while the levels of Δ Np63 expression were not altered, the distribution of Δ Np63 positive keratinocytes was confined to the basal layer following EGCG treatment.

These findings suggest that VIN cl.11 is likely to be more transformed than HFK-HPV18, given that Δ Np63 is not confined to the basal cell layer as it is in these HPV-

immortalised keratinocytes. Although speculative, it is unlikely that HPV18 directly influences Δ Np63 expression given that expression is confined to the basal layer in raft cultures generated from these cells. It is possible that HPV18 transformation of VIN cl.11 is followed by additional genetic changes that stimulate Δ Np63 expression in these pre-malignant keratinocytes. Whether Δ Np63 is required to maintain keratinocytes in a hyperproliferative state is unclear. However, the fact that EGCG inhibits the proliferation of VIN cl.11 cells and restores Δ Np63 expression to the basal cell layer suggests that Δ Np63 may play a role in maintaining cells in an undifferentiated state.

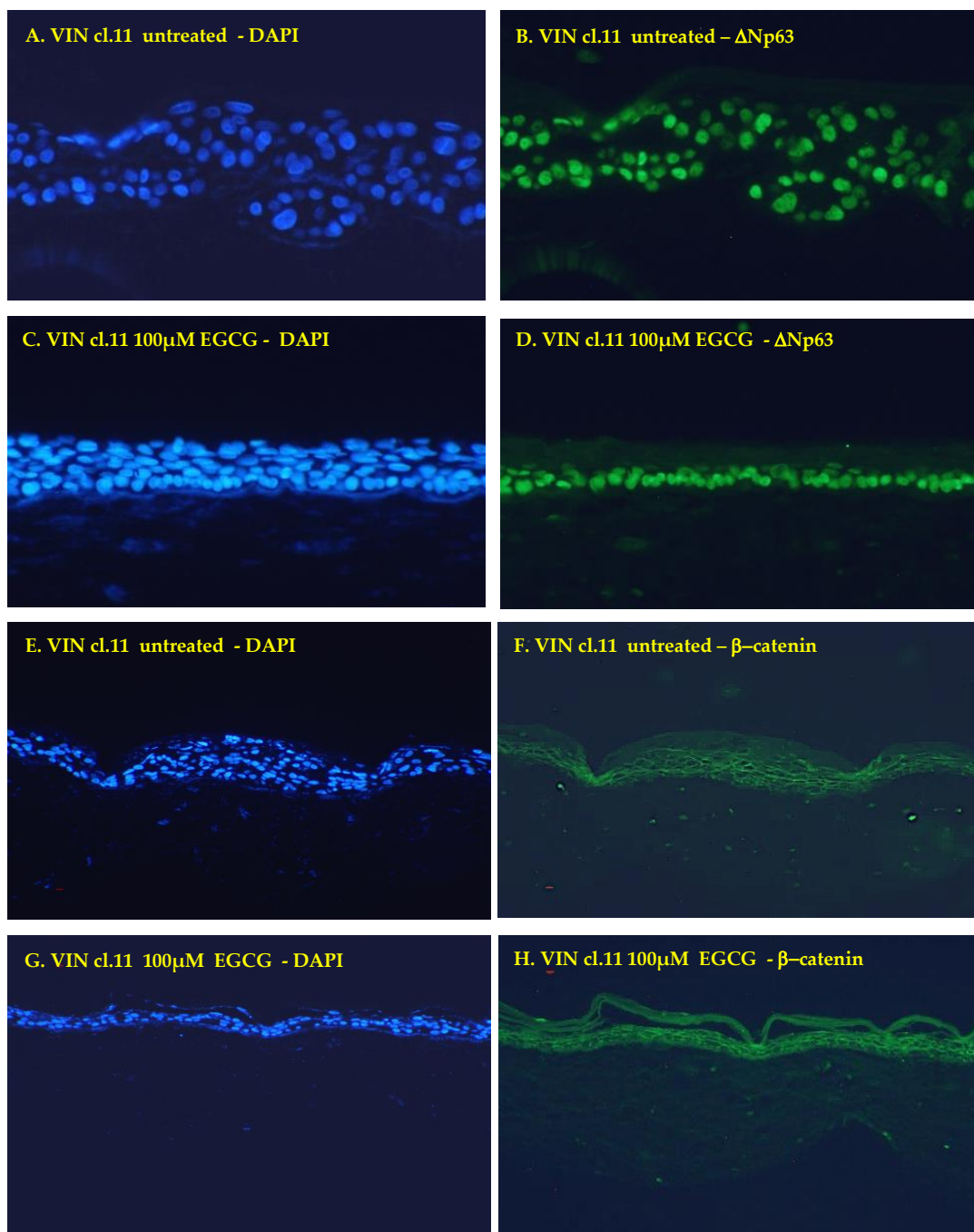


Figure 5.28: Unlike β -catenin, expression of the basal cell marker, Δ Np63, is altered in response to EGCG treatment in VIN cl. 11 raft cultures. FFPE sections of VIN cl. 11 raft cultures (panel A-H) cultured in the presence or absence of EGCG were stained for Δ Np63 or β -catenin (green) and cell nuclei counter stained with DAPI (blue). In VIN cl. 11, Δ Np63 is expressed throughout the full thickness of the raft culture. In response to EGCG treatment, Δ Np63 expression is confined to the basal cell layer. Panel E-H shows that EGCG treatment did not alter the distribution or level of expression of β -catenin in EGCG treated VIN cl.11 rafts. Magnification x200.

5.9 Discussion

As part of a pilot study designed to isolate an authentic uVIN-derived keratinocyte clone, primary epidermal keratinocytes were successfully grown from a resected biopsy obtained from a 46-year-old woman with histologically proven uVIN. These primary keratinocyte cultures were heterogeneous in appearance, suggesting that they were derived from a mixture of normal and HPV-infected keratinocytes. This heterogeneity most likely reflected the nature of the tissue specimens, which, after close inspection, were found to contain normal epithelium and tissue with varying degrees of epithelial dysplasia. Subsequent testing of the biopsies by Luminex PCR revealed the presence of six different HPV strains (HPV42, 70, 35, 51, 56 and 59), but the lack of HPV16 and HPV18. While the PCR methodology proved useful in identifying the strains of HPV, ISH may have to be performed to confirm the presence and relative abundance of each HPV strain within the resected uVIN lesions.

At face value, the results obtained were somewhat surprising given that analysis of primary keratinocyte cultures for HPV strains revealed the presence of HPV16 and HPV18 DNA using strain-specific E6 primers. However, subsequent testing of passaged primary keratinocytes indicated a loss of both HPV16 and 18 strains upon serial propagation. Given that primary cultures contained detectable amounts of HPV16 and HPV18 DNA, it is currently unknown why these were not found in the original uVIN biopsies using the more sensitive Luminex-based assay. The presence of HPV16 and HPV18-infected keratinocytes at p0 suggested that keratinocytes infected with these strains must have been present in the primary lesions; moreover, it is unclear at present why HPV16 and HPV18-infected keratinocytes were lost so quickly

upon serial propagation. It is possible that viral episomes were lost as a consequence of *in vitro* cultivation; either through genomic instability or differentiation/senescence [190, 191]. However, it is more likely that the number of HPV16 and HPV18 infected keratinocytes in the uVIN biopsy were so low, that they constituted a minority of keratinocytes infected with other HR-HPV strains and/or normal uninfected primary keratinocytes.

In an attempt to isolate clones that retained HPV16 or HPV18, single cell cloning was performed from primary p0 keratinocyte cultures. Of 23 independent clones, 11 were successfully grown and expanded for further investigation. Analysis of these 11 isogenic clones for HPV strains using the Luminex multiplex PCR platform revealed that seven were infected with HPV35, one with HPV18, one with both HPV18 and HPV35. One tested negative for all HR-HPV strains. None of the clones were found to contain HPV16 DNA.

While HPV16 and HPV18 infected keratinocytes were lost upon serial propagation, keratinocytes infected with the HPV35 strain were maintained, given that all but two of the clones examined tested positive for this virus. At first glance, this seemed surprising, as it was assumed that clones infected with HPV16 or HPV18 would possess a proliferative advantage over normal uninfected keratinocytes, or clones infected with low-risk HPV strains. However, HPV35 is classified as an HR-HPV strain and, as such, possesses the ability to stimulate keratinocyte growth. To our knowledge, this is the first demonstration of spontaneously isolated keratinocyte clones infected with HPV35, or co-infected with multiple HR-HPV strains. It is unclear whether clones infected with HPV35 are immortalised and how their behaviour compares to HPV16 or

HPV18 infected clones isolated from the same biopsies. Future studies are planned to compare the behaviour and growth characteristics of HPV18 and HPV35 infected clones. However, due to time constraints, we elected to focus on characterising VIN cl.11, as this was the only clone found to contain HPV18.

Like normal vulvar keratinocytes (NVK) and HFK-HPV18, VIN cl.11 formed colonies at clonal density on irradiated 3T3-J2 fibroblasts, eventually merging to form monolayers of homogenous, undifferentiated keratinocytes. However, unlike NVK or HFK-HPV18, VIN cl.11 failed to stratify and produce larger, more differentiated keratinocytes. In this respect, VIN cl.11 is similar to the KG cell line, the first HR-HPV infected uVIN keratinocyte line isolated by Grassmann and colleagues [177]. The keratinocyte origin of VIN cl.11 was confirmed, as cultured cells were found to express the keratinocyte-specific markers: keratin 14 (K14) and the cross-linked envelope protein, involucrin. Moreover, when grown in organotypic raft culture, VIN cl.11 underwent stratification and expressed Keratin 1 and 10 (K1/10), two high molecular weight keratins associated with terminal differentiation. Although it is not clear at this stage whether VIN cl.11 is immortalised, this clone has been successfully cultivated for over 20 passages, which is well beyond the normal lifespan of age-matched NVK *in vitro*; primary cultures of NVK have a proliferative capacity of <6 passages. Although VIN cl.11 has an extended lifespan *in vitro* and may possess pre-malignant properties, it failed to form colonies in anchorage-independent growth assays (Supplementary Figure 2), indicating that it is not fully transformed. Despite this, VIN cl.11 produced epithelial structures that exhibited abnormal, possibly pre-neoplastic features, with immature keratinocytes displaying a high nucleus-to-cytoplasmic ratio extending to

the upper layers of the raft structure and a poorly defined cornified layer. Expression of ΔNp63, a marker of basal keratinocytes was more extensive than that observed in HFK-HPV18, revealing the presence of an expanded immature basal cell layer, a feature commonly observed in intraepithelial neoplasia of the cervix (CIN), vulva (VIN), and VSCC, but not normal vulvar epithelium [43, 192]. This was confirmed, as BrdU labelling and Ki67 staining of VIN cl.11 rafts, revealed extensive staining of labelled nuclei throughout the lower two-thirds of the raft structure, indicating the presence of mitotically active immature basal cells.

Unlike previously isolated VIN cell lines, which carry episomal or integrated copies of HPV16 [177, 178], VIN cl.11 is unique in that it harbours the HPV18 strain. PCR analysis revealed that the E2 region, a site commonly disrupted during viral integration, was intact, suggesting that VIN cl.11 contains episomal forms of the virus. Furthermore, when cultured in organotypic raft culture, expression of the E4 protein was observed in the suprabasal layers of VIN cl.11 raft structures, confirming the presence of a productive HPV18 infection. The fact that E4 can only be expressed from intact viral episomes supports findings from the E2 disruption assay, confirming that VIN cl.11 carries episomal forms of HPV18. However, further studies are required to establish, unequivocally, the presence of viral episomes and possible integrants in this clone. The establishment and serial propagation of VIN cl.11 on irradiated 3T3 feeder cells appears to favour viral episome maintenance (Dr Sally Roberts – personal communication). Future studies will examine the impact of cell culture conditions on viral episome maintenance and viral integration. The growth and differentiation of clones carrying episomal and integrated forms of the virus may yield potentially

interesting insights into the behaviour of these pre-malignant clones, and how viral integration alters the growth and transformed properties of cells.

Having confirmed that VIN cl.11 harboured intact, episomal forms of HPV18 we next examined this clone for expression of the two viral oncoproteins, E6 and E7. While Western blotting confirmed that both E6 and E7 proteins were expressed in VIN cl.11, the level of E7 was significantly lower than that observed in HFK-HPV18; indeed, prolonged exposure of membranes was required to visualise the E7 protein. At this stage, it is unclear why levels of the E7 protein were significantly lower than that of E6 in VIN cl.11. Although speculative, one possible explanation for this is that the virus in VIN cl.11 selectively expresses a splice variant of the E6/E7 transcript that favours translation of the E6 protein rather than the E7 protein, resulting in a disproportionately higher amount of E6 protein. The E6 and E7 proteins are translated from a single bicistronic or polycistronic mRNA [69]. Although the E6 gene can undergo alternative splicing to generate truncated forms of the E6 protein; the so-called E6* protein, these alternatively spliced transcripts still contain the E7 ORF. It is possible that certain spliced variants of the E6/E7 transcripts may favour translation of one protein over the other, thus resulting in a different amount of E6 and E7 proteins being synthesised [70, 193, 194]. Further studies are required to examine the variant of E6/E7 transcripts expressed in VIN cl.11 to confirm the above hypothesis.

In the previous chapter, I showed that EGCG inhibited the growth of HFK-HPV18 keratinocytes, an effect that was accompanied by the induction of apoptosis. Furthermore, EGCG induced proteolysis and degradation of the E6 and E7 proteins, and increased expression of key TSGs (p53, p21^{WAF1}, pRb) in both monolayer and

organotypic raft culture. I next explored the phenotypic and molecular consequence of EGCG treatment on the newly derived uVIN cell line. Like HFK-HPV18, EGCG treatment inhibited the growth and induced apoptosis in VIN cl.11 in monolayer culture and, like HPV18-HFK downregulated expression of the E6 protein. However, the IC₅₀ of EGCG for VIN cl.11 (150μM) was higher than that of HFK-HPV18 (100μM), indicating that this VIN cl.11 was less sensitive to the anti-proliferative effects of EGCG. When grown in the organotypic raft culture system, cell proliferation was significantly impaired, as the incorporation of the BrdU label and expression of the proliferative marker Ki67 were significantly reduced in response to EGCG treatment. Interestingly, while cell proliferation was inhibited, very little effects were observed on the expression of p16^{INK4a} and MCM7. Although speculative, this suggests that while sufficient levels of E6 and E7 required to stimulate p16^{INK4a}, and MCM7 expression were maintained in EGCG-treated rafts, additional, possibly "off-target" effects of EGCG were activated to inhibit cell proliferation. In this context, it is interesting to note that the levels of pRb, p21^{WAF1} and p53 were all increased in response to EGCG treatment. Whether this occurred as a result of E6 and/or E7 degradation or an "off-target" effect of EGCG on TSG expression remains to be fully resolved. The lack of suitable reagents to examine the levels of E6 and E7 in raft cultures prohibited an examination of their levels in response to EGCG treatment.

Although there was only a subtle change in the levels of p16^{INK4a} and MCM7 in EGCG-treated raft cultures, expression of the HPV-encoded E4 protein was completely suppressed, indicating that the virus was unable to undergo complete vegetative propagation. As the HPV life cycle is closely linked to keratinocyte differentiation, we

believe that EGCG may disrupt certain aspects of the keratinocyte maturation process, thereby interfering with the lytic life-cycle. Although expression of the differentiation-specific markers involucrin and K1/10 were present in EGCG treated rafts, the distinct lack of a stratum granulosum and stratum corneum, suggests that EGCG interferes with keratinocyte maturation, impeding the formation of epithelial layers in which E4, L1 and L2 are expressed [115]. This effect appeared to be specific for the lytic phase, as episomal replication did not appear to be affected by EGCG treatment in HFK-HPV18 cultured in monolayer culture. These findings may suggest that the virus can maintain its replication at a low level in basal keratinocytes, but is unable to complete its life-cycle as keratinocyte maturation is impaired following EGCG treatment. Obviously, this has implications for the use of EGCG as a topical treatment for uVIN, as an incomplete eradication of the virus may occur, allowing for reactivation. Future experiments are planned to examine the effects of long-term EGCG treatment on HPV18 persistence in organotypic raft culture and whether EGCG influences expression of E1 and E2, two proteins required for efficient episomal replication.

Studies have shown that EGCG exerts differential effects on transformed and non-transformed keratinocytes; it induces apoptosis in squamous cancer cell lines but promotes differentiation in normal keratinocytes. EGCG stimulates expression of differentiation markers such as involucrin and keratin 1 [96, 103, 105] via engagement of the p38 Stress-activated protein kinase (SAPK) pathway and stimulation of AP1 and CREB transcription factors. However, while such effects have been studied in HPV-positive transformed cell lines (e.g. Hela, CaSki), the effects of EGCG on pre-malignant cancer cell lines (uVIN) or HPV-immortalised keratinocytes (HFK-HPV18) has not

been evaluated. In raft culture, little or no change in involucrin and K1/10 expression were observed in response to EGCG treatment, indicating that EGCG is unlikely to promote differentiation in VIN cl.11 or HFK-HPV18. It is also worth pointing out that all the studies described previously which showed that EGCG promotes differentiation in normal epidermal keratinocytes were performed on monolayer culture. While attempts to culture NVK in organotypic raft culture were unsuccessful, it would nonetheless be interesting to examine the effects of EGCG treatment on the growth and differentiation of normal vulvar keratinocytes in monolayer and organotypic raft culture.

Although the mechanism(s) by which EGCG influences keratinocyte maturation remain elusive, possible explanations come from the study of cell signalling pathways affected by EGCG. Although the signalling pathways influenced by EGCG are numerous, ones that are relevant in this context include the interleukin (IL)-1 α and IL1 β signalling pathways. IL1 α and IL1 β are pro-inflammatory cytokines that contribute to epidermal hyperplasia through the induction of growth factors and cytokines that stimulate keratinocyte growth and inflammation [195, 196]. EGCG attenuates IL1 α and IL1 β signalling through a variety of mechanisms, including the induction of the IL-1 receptor antagonist (IL1ra) and the attenuation of NF- κ B and AP-1 activity [197-199]. A number of studies have shown that EGCG, alone, or in combination with IL1ra, attenuate the transformed properties of a malignant osteosarcoma cell line [200], while others have shown that EGCG inhibits IL-1 β -mediated induction of IL8 through a mechanism involving I-kappa-B kinase (IKK) activation [196]. While data for uVIN is lacking, comprehensive gene expression

profiling has identified over-expression of IL1 α and IL1 β as a common feature in VSCC [201], suggesting that these cytokines are important in disease pathogenesis. A profiTabe line of enquiry might be the examination of IL1 α and IL1 β expression in uVIN biopsies and the newly derived VIN cl.11 cell line, given that EGCG attenuates IL1 α and IL1 β signalling. In this respect, IL1 α and IL1 β signalling may constitute an important target of EGCG action.

In addition to IL1 α and IL1 β , the effects of EGCG on Notch signalling might constitute an additional interesting line of enquiry. In normal epidermal keratinocytes, Notch signalling promotes cell-cycle withdrawal, stratification and terminal differentiation through a number of overlapping mechanisms [92]. Notch1 down-regulates Δ Np63, through a mechanism involving transcriptional silencing of interferon regulatory factor (IRF) 3 and IRF7 [202]. This is accompanied by an induction in expression of p21^{WAF1}, p27^{Kip}, NF- κ B, PPAR γ 1, which function to promote cell-cycle withdrawal and regulate various aspects of keratinocyte maturation [203]. This contrasts with fully transformed keratinocytes, where Notch signalling becomes "uncoupled" or down-regulated. In this context, the absence of Notch1 signalling favours cell proliferation [204]. Indeed, studies have shown that Notch1 gene dysregulation occurs in cervical neoplasia, where expression of Notch1 signalling is reduced as CIN progresses from low to high-grade disease [205-207].

A number of studies have shown that EGCG down-regulates Notch signalling in immortalised keratinocyte cell lines [208-210]. Given that Notch is required for correct spatiotemporal regulation of keratinocyte differentiation, EGCG inhibition may interfere with the normal maturation process, resulting in the loss of granular and

cornified cell layers in the pre-malignant and immortalised keratinocyte cell lines (VIN cl.11, HPV18-HFK). As vegetative replication of HPV18 is intricately linked to differentiation, EGCG-induced changes in the differentiation programme may influence late gene expression. Such a hypothesis may explain the lack of detectable E4 expression in EGCG-treated rafts. Future studies are planned to examine the effects of EGCG treatment on Notch1 expression/activity, and how this influences keratinocyte differentiation and HPV lytic replication.

As previously mentioned, Δ Np63 is expressed in immature keratinocyte populations confined to the basal layer of normal human epithelium and, as such, Δ Np63 is frequently used as a marker to identify this population in squamous epithelia and carcinomas. In raft culture, the number of cell layers expressing Δ Np63 was more extensive in VIN cl.11 compared to HFK-HPV18, where a single layer of Δ Np63 positive cells was observed. This, coupled with the observation that the number of cells incorporating the BrdU-label, or expressing Ki67 was more extensive in VIN cl.11 compared to HFK-HPV18, indicates that VIN cl.11 is more “transformed” than HFK-HPV18. Following EGCG treatment, we found that the expression of Δ Np63 in VIN cl.11 raft culture became more polarised, becoming restricted to a single cell layer at the basolateral surface of the raft structures. Interestingly, the change in distribution was not associated with a loss in the number of Δ Np63 positive cells. Rather, the upward migration of these cells was impeded as the number of Δ Np63-positive cells was increased within the basal cell layer. The fact that the level of Δ Np63 expression was not altered suggests that EGCG does not influence its expression (i.e. through the induction of Notch1 activity), but rather, influences some aspect of cell behaviour that influences their migration and possibly maturation.

Although the exact mechanism(s) by which EGCG reverses the pre-neoplastic features of VIN cl.11 remain to be elucidated, we hypothesize that it is achieved through a number of mechanisms. The loss of E4 expression following EGCG treatment indicates that the epithelium is unable to sustain viral lytic replication, possibility due to effects on keratinocyte maturation. Whether lytic replication *per se*, influences the malignant potential of the virus is unknown, although the ability to suppress lytic viral replication may actually promote viral integration and potentiate cell transformation.

EGCG was also found to promote rapid degradation of the key viral proteins E6 and E7 that are responsible for driving carcinogenesis, an effect that may prevent HPV-infected keratinocytes (VIN cl.11) from developing dysplastic features in organotypic raft culture. The increase in expression of tumour suppressor genes, p53, p21^{WAF1} and pRb is also likely to play a major role in preventing carcinogenesis. As discussed previously, these TSGs are normally suppressed following HR-HPV infection. Whether their re-expression is attributed to the down-regulation of the viral E6 and E7 proteins or induced directly in response to EGCG treatment remains to be elucidated. The re-expression of these TSGs may interfere or antagonize the increased proliferative potential of HR-HPV transformed keratinocytes leading to cell death by apoptosis. This may explain why EGCG treated rafts are considerably thinner and lack immature cells in the suprabasal layer when compared to untreated rafts, as cell proliferation is reduced due to TSG re-activation. Collectively, these findings suggest that EGCG influences the growth and pre-neoplastic properties of this uVIN-derived keratinocyte clone through mechanisms that influence the behaviour of the virus in addition to keratinocyte growth and maturation.

To summarise the findings presented in this chapter, a novel pre-malignant keratinocyte clone was isolated from an authentic uVIN biopsy and shown to harbour episomal forms of HPV18. When grown in organotypic raft culture, this clone stratified, generating an epithelium with pre-malignant features that superficially resembled uVIN. Moreover, under appropriate conditions, this clone was shown to sustain a productive lytic infection. For the first time, I have shown that treatment with EGCG reverses these pre-malignant features in organotypic raft culture, by impairing viral replication, down regulating expression of the E6 protein and re-activating expression of many TSGs. This cell line will not only offer us the opportunity to study and understand the process of carcinogenesis induced by HPV18 in vulvar keratinocytes, but it may also be used as a model to screen new therapeutic targets for uVIN or other HR-HPV induced proliferative disorders.

Chapter 6:

General Discussion & Future Work

General Discussion and Future Work

In Chapter 3, I set out to identify the iso prognostic factors which determine local cancer recurrence using a well characterized retrospective cohort of patients with primary VSCC, and have identified Lichen Sclerosus (LS) as the only independent risk factor after a multivariate analysis was performed using 12 prognostic variables (age, smoking status, disease stage, tumour size, disease focality, LS +/- VIN, LVSI, histology grade, HPV positivity, groin node status, excision margins, and chemo-radiotherapy) which have previously been shown to modulate the risks of local recurrence (see chapter 3 discussion). Paradoxically, women with uVIN, the putative precursor lesion for VSCC, were not at increased risk of developing local recurrences. Although speculative, there are a number of reasons why women with uVIN were less likely to develop local recurrences compared to those with LS. Firstly, women with chronic or persistent uVIN suffer debilitating symptoms and are more likely to be examined and treated in the clinic more frequently than those with LS. Secondly, women presenting with uVIN tended to be younger than those presenting with LS and, as such were more likely to seek medical help compared to patients with LS, who tended to be elderly. Thirdly, given the fact that these women had cancer previously, it is likely that clinicians would offer surgical intervention as a means to alleviate their symptoms and prevent disease progression. It is possible; therefore, that surgical intervention to excise persistent uVIN may have reduced the incidence of local recurrence observed in our cohort of patients who present with viral-associated VSCC. As for HPV-negative HNSCC, it remains unclear whether HR-HPV can induce a “field change” in vulvar epithelium, and whether excision of the dysplastic lesion is sufficient to remove all

molecularly altered clones [62]. Although uVIN is a pre-malignant lesion, its rate of malignant progression is comparatively low (approximately 5-10%), taking anything up to 5-10 years [24]. As a clearly visible lesion, surgical intervention is relatively straightforward. Naturally, this intervention interrupts the disease process and the possibility of progression to cancer. To establish if surgical intervention to remove uVIN confounded the outcome of local recurrence within our cohort, I have planned further analysis to assess the frequency and type of intervention women have received when uVIN was diagnosed after their primary cancer was removed.

Compared to women presenting with uVIN, women with LS were usually asymptomatic and from an older age group (see chapter 3 discussion). As such, these patients were probably examined less frequently in the clinic compared to those with uVIN. Unlike HPV-infected uVIN, there is no recognised premalignant lesion associated with LS that progress to cancer. It remains unclear if dVIN, which develops in a field of LS, is a precursor lesion of HPV-negative VSCC. dVIN is often found associated with VSCC and rarely exists on its own, which makes surveillance and treatment of dVIN difficult. My analysis also revealed that women with LS were not only twice more likely to have a local relapse (tumour recurring on a site previously occupied by the primary tumour), but were also 5 times more likely to develop recurrence away from the primary tumour (second field tumour). This observation raises two questions; firstly, did LS give rise to second field tumour (SFT) or indeed the primary tumour; and secondly, was SFT derived from the same clonal origin as its primary tumour. Studies on head and neck SCC (HNSCC) have found that patients with viral negative tumour were also more likely to recur in a molecularly altered

epithelium (field of cancerization) away from the site of primary tumour [62]. As mentioned previously, studies have showed that non-viral induced VSCC often bore similar genetic and epigenetic alterations to its adjacent LS, thus raising the possibility that chronic LS may generate a cancer field (see chapter 3 discussion). To confirm this, I have planned, using the DNAseq, RNAseq and pyrosequencing technology, to measure the frequency with which genetic and epigenetic alterations occur in tumour and its adjacent epithelium affected by LS on our well-characterized cohort of patients where paraffin embedded blocks have already been retrieved. If the primary tumour, recurrence tumour and adjacent LS all share similar molecular alterations, then these tumours were most likely to have derived from the same clonal origin and arose in a molecularly altered field generated by chronic LS. The molecular alterations identified can also be used as potential biomarkers to stratify patients into indolent LS and those at risk of malignant transformation. As LS cannot be treated with surgery, future work should focus on developing an effective chemopreventative treatment to minimise the risks of local recurrence in this group of patients.

The primary aim of chapter 4 was to investigate the effects of EGCG on the growth and differentiation of HPV18 transfected keratinocytes and establish whether this was due to effects on virus behaviour. Thus far, it is not clear whether EGCG functions solely as an anti-viral agent, as I was unable to demonstrate that EGCG clears cells of viral episomes. My findings revealed that episomal replication, as measured by viral copy number, was not affected by EGCG treatment in monolayer culture, albeit over a relatively short duration. However, the fact that HFK-HPV18 cells were undergoing growth inhibition and apoptosis at this stage suggests that episomal loss *per se* is not

important. This observation has interesting connotations in the clinical setting. If chronic exposure to EGCG ointment (Veregen®) does not eradicate viral episomes, there is a possibility that the virus may remain latent in subpopulations of long-lived basal keratinocytes such as stem/progenitor cells, and that these become reactivated once treatment is discontinued. Future studies are planned to examine the effects of EGCG on episomal maintenance in HFK-HPV18 and VIN cl.11 keratinocytes grown in raft culture for more protracted periods of time. Similarly, both treated and non-treated samples for the EPIVIN clinical trial, which evaluate the use of Veregen® in the treatment of uVIN, will be examined for the presence of HPV DNA using sensitive in-situ hybridisation. If EGCG treatment does induce complete or partial remission of uVIN lesions, the presence of HPV DNA in histologically normal epithelium from treated biopsies will prove informative.

Although EGCG did not appear to influence viral episome maintenance, I did find that it interfered with lytic replication of HPV18 in organotypic raft culture. While this could not be substantiated in HFK-HPV18, I found that treatment of VIN cl.11 with EGCG resulted in a loss of E4 protein expression in the differentiating cell layers. As lytic replication of HPV is intimately linked to keratinocyte differentiation [115], I speculate that EGCG may impair this process by modulating some subtle aspect of keratinocyte differentiation that is not evident by immunofluorescence staining for established epidermal differentiation markers. Another intriguing possibility is that efficient expression of E4, and other late structural proteins, requires E6 and E7, or that the hyperproliferative epithelium generated as a consequence of their action is necessary to create a suitable cellular environment in which they can be expressed [66].

Another striking effect of EGCG treatment in HFK-HPV18 cells was down regulation of the E6 and E7 proteins, the key HR-HPV-encoded oncogenes that drive keratinocyte proliferation. It is still unclear at present whether this ability is central to the effects of EGCG on HFK-HPV18 and VIN cl.11 growth and differentiation. To establish whether it is a cause or a consequence, the E6 and E7 proteins will be targeted using custom made siRNAs and the effects of silencing on growth, apoptosis and expression of TSGs examined. Using tetracycline-regulaTable retroviruses containing E6 and E7-specific shRNAs, clones of HFK-HPV18 and VIN cl.11 will be generated, and the effects of E6 and E7 silencing on growth, differentiation and TSG expression in organotypic raft cultured examined.

Although my study along with others has shown that the ability of EGCG to down regulate E6 and E7 expression is inhibited by the addition of the proteasome inhibitor [71, 141], MG132, it remains unclear if their turnover is actually mediated through the ubiquitin-proteasome pathway given that my studies, and those of others, have failed to confirm that the E6 and E7 proteins are polyubiquitinated. However, my study has identified a monoubiquitinated E6 species, whose expression is maintained in the presence of EGCG and MG132 treatment. Currently, the significance and function of this modified form of E6 is unknown, although this type of modification may regulate E6 function, potential interactions with other proteins (E6AP, hD1G Scribble - amongst others), and intracellular trafficking.

Given that E6, and possibly E7, do not appear to be poly-ubiquitinated in response to EGCG treatment, I plan to investigate whether other proteolytic pathways are involved in their degradation. As EGCG has been found to target a myriad of cell

signalling pathways, I will firstly focus on the role of Calpains and Caspases, given that EGCG has been shown to induce Calpain and Caspase activity (Caspase-3, 9) to induce apoptosis. Another interesting area of study would be to examine the expression and activity of protein tyrosine kinase and phosphatases that are involved in the post-translational modification of E6 and E7 [211]. One such pathway is Protein Kinase A (PKA), which phosphorylates and modulates E6 function. Whether EGCG stimulates PKA activity and whether PKA-mediated phosphorylation of E6 is a prerequisite to ubiquitination remains unknown.

Again, I am not able to distinguish if the upregulation of the TSGs, p53 and Rb, is a consequence of E6 and E7 protein downregulation or directly induced in response to EGCG treatment. To distinguish between the two mechanisms, I plan to treat the isogenic non-HPV18 transfected keratinocytes with EGCG and examine the expression of p53 and Rb; if their expression is increased in non-HPV transfected keratinocytes, then it is likely that EGCG directly stimulates their expression rather than their re-expression occurring as a consequence of E6 and E7 degradation.

In Chapter 5, I have achieved my primary objective of establishing a novel pre-malignant clone from an authentic uVIN biopsy, which harbours episomal forms of HPV 18 (VIN cl.11). When grown in organotypic raft culture, this clone stratified, generating an epithelium with pre-malignant features that resembled uVIN, which is also capable of sustaining a productive lytic infection. Molecular profiling of VIN cl.11 showed overexpression of p16^{INK4a} and aberrant expression of ΔNp63 in suprabasal cells in organotypic raft cultures, both features consistent with those found in high grade pre-neoplastic lesions of the cervix and vulva, indicating that cellular dysplasia

is driven by HPV18 [43, 192]. Furthermore, chromosomal analysis of VIN cl.11 showed tetraploid karyotype with abnormal chromosome rearrangements, another feature confirming the pre-neoplastic nature of this clone. Further work is currently underway, with the help from our regional genetics department, to complete the molecular profiling of VIN cl.11. DNA fingerprinting will be performed to establish unequivocally, the provenance of the cell line. Given the chromosome abnormalities I have observed from the karyotyping studies, I plan to perform DNA sequencing (DNASeq) to identify mutations within the host genome that may be of relevance to disease pathogenesis, and to establish whether any HPV18 genomes have become integrated into the host chromosome. At this stage, it is still unclear whether VIN cl.11 harbours both integrated and episomal forms of HPV 18.

Further work is also planned to study the HPV 18 virus in VIN cl.11 in greater detail. This will involve: measuring the absolute viral copy number in cells by Southern blotting; determining the levels of expression of the bicistronic E6/E7 transcripts and its splice variants, to establish if it contributes to the disparity seen in the level of expression of E6 and E7 proteins (see Figure 3.12); and to profile for the expression of the early (E1, E2 and E4) and late viral (L1 and L2) genes.

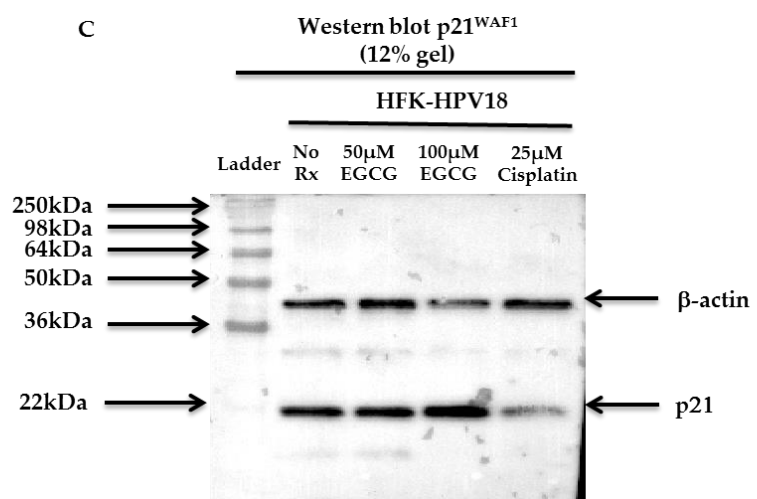
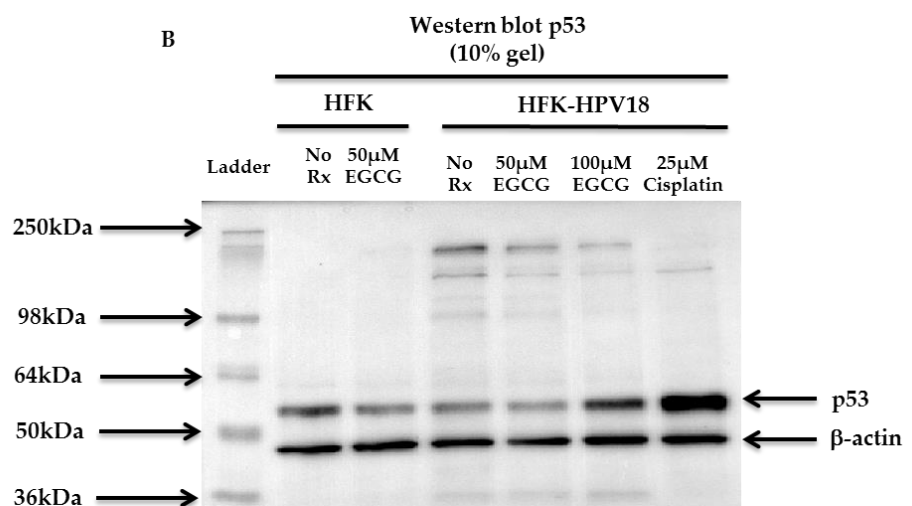
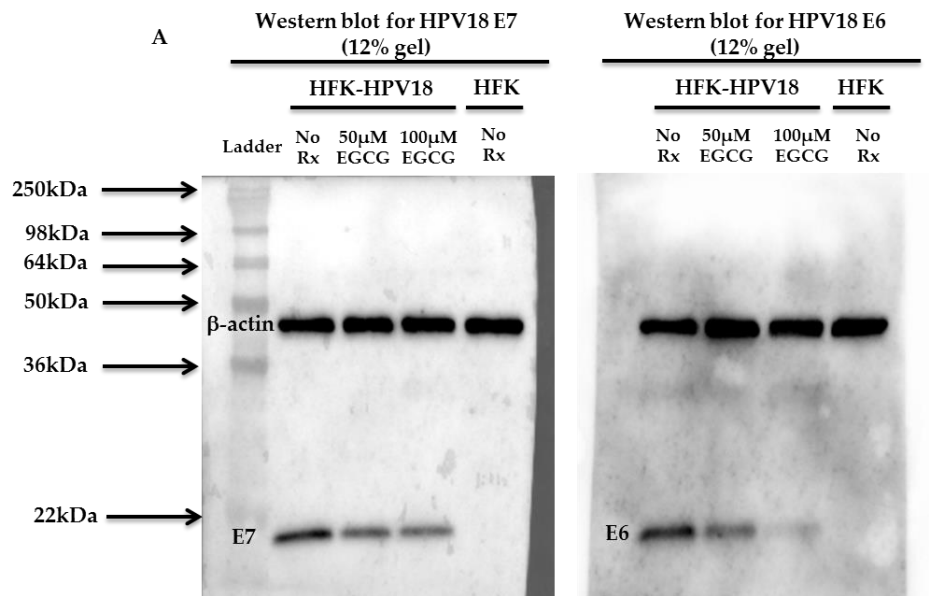
When VIN cl.11 was established, an additional ten isogenic clones were isolated by single cell cloning, and these have been frozen away at passage 2 or 3 (see Chapter 3, Figure 3.5). One of the clones, VIN cl.8, was tested negative for any HR-HPV strain and, as such, might serve as an isogenic normal control to examine differences in gene expression profiles between a HR-HPV negative and positive clone (VIN cl.11). Thus, my next priority is to characterize VIN cl.8 and compare its phenotype and molecular

profiles with VIN cl.11. If it is proven to be a normal isogenic keratinocytes to VIN cl.11 then it could be used in future as a negative control to study the pathogenesis of VIN and for drug screening.

In summary, I have shown, from my retrospective cohort study, that women with LS are at significantly increased risk of developing local recurrence; this result sets precedence for those women with VSCC arising in background of LS to be followed-up more closely in clinic after their primary tumour was resected; unless a more robust surveillance programme or chemoprevention treatment becomes available in the future. Although I have not been able to establish if EGCG affects the physical status of HPV, I have demonstrated that viral lytic replication is impaired following EGCG treatment as demonstrated by the inability of HPV18-infected keratinocytes to express E4 in organotypic raft culture. I have also shown that EGCG induced apoptosis of HR-HPV keratinocytes by inhibiting the expression of the E6 and E7 oncoproteins and inducing the expression of TSGs, p53 and Rb. EGCG treatment also restores the altered cell polarity observed in the HR-HPV transformed pre-malignant cell line, VIN cl.11, as demonstrated by the restoration of ΔNp63 to the basal cell layer following EGCG treatment. VIN cl.11 is a novel VIN cell line that harbours episomal forms of HPV 18 and can stratify in organotypic raft cultures generating a hyperplastic poorly differentiating epithelium. Phenotypically, the VIN cl.11 raft culture shows a hyperplastic and dysplastic feature that resembles uVIN. Furthermore, the culture of VIN cl.11 in the raft system supports lytic HPV 18 replication, making it a useful model to study the pathogenesis of uVIN and also for *in vitro* drug screening.

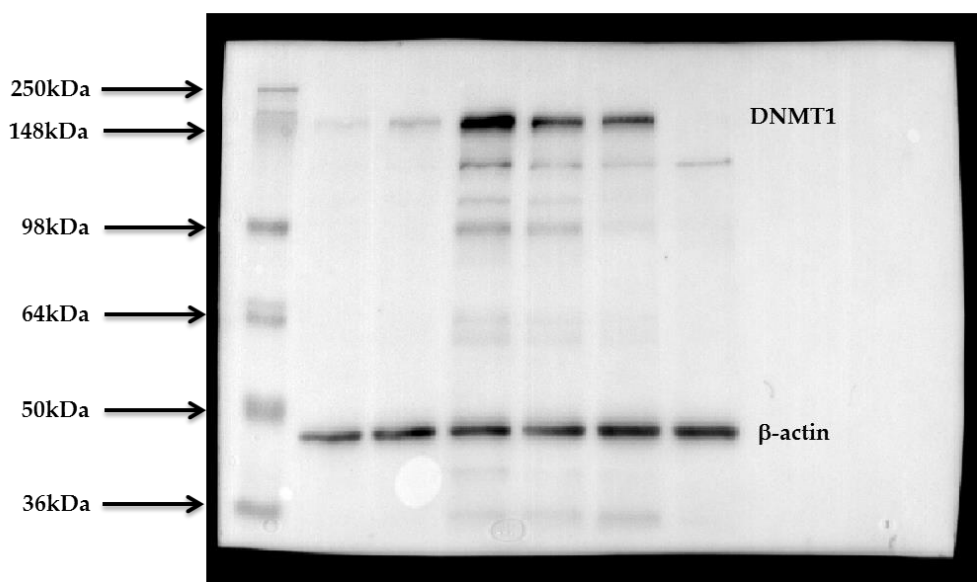
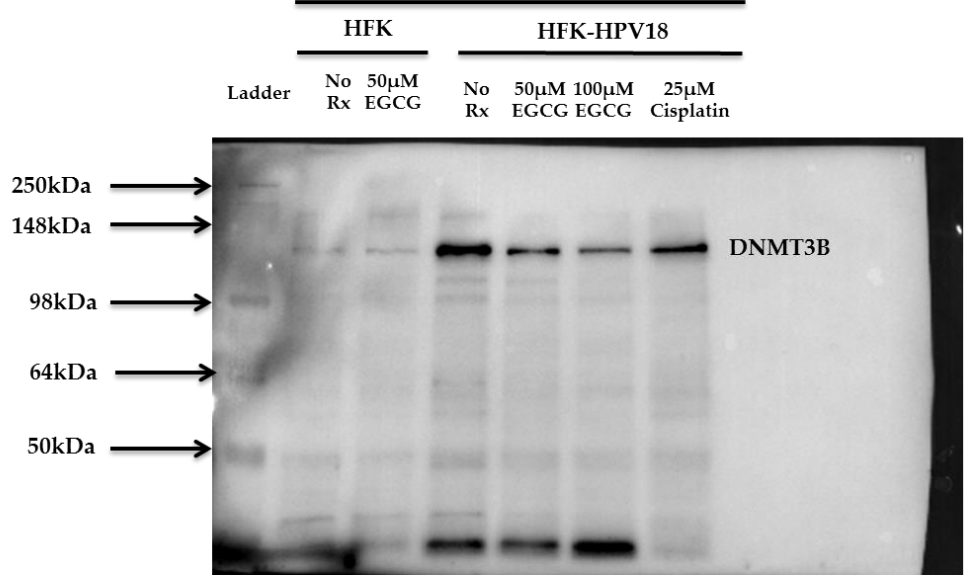
Chapter 7:

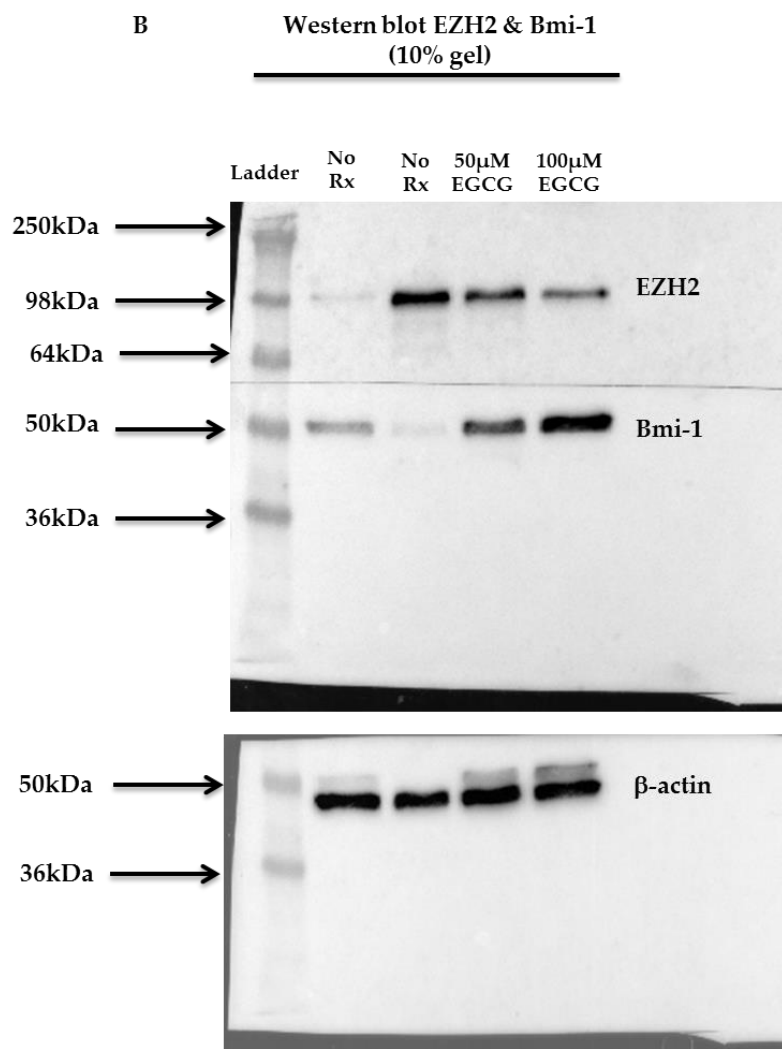
Supplementary Figures



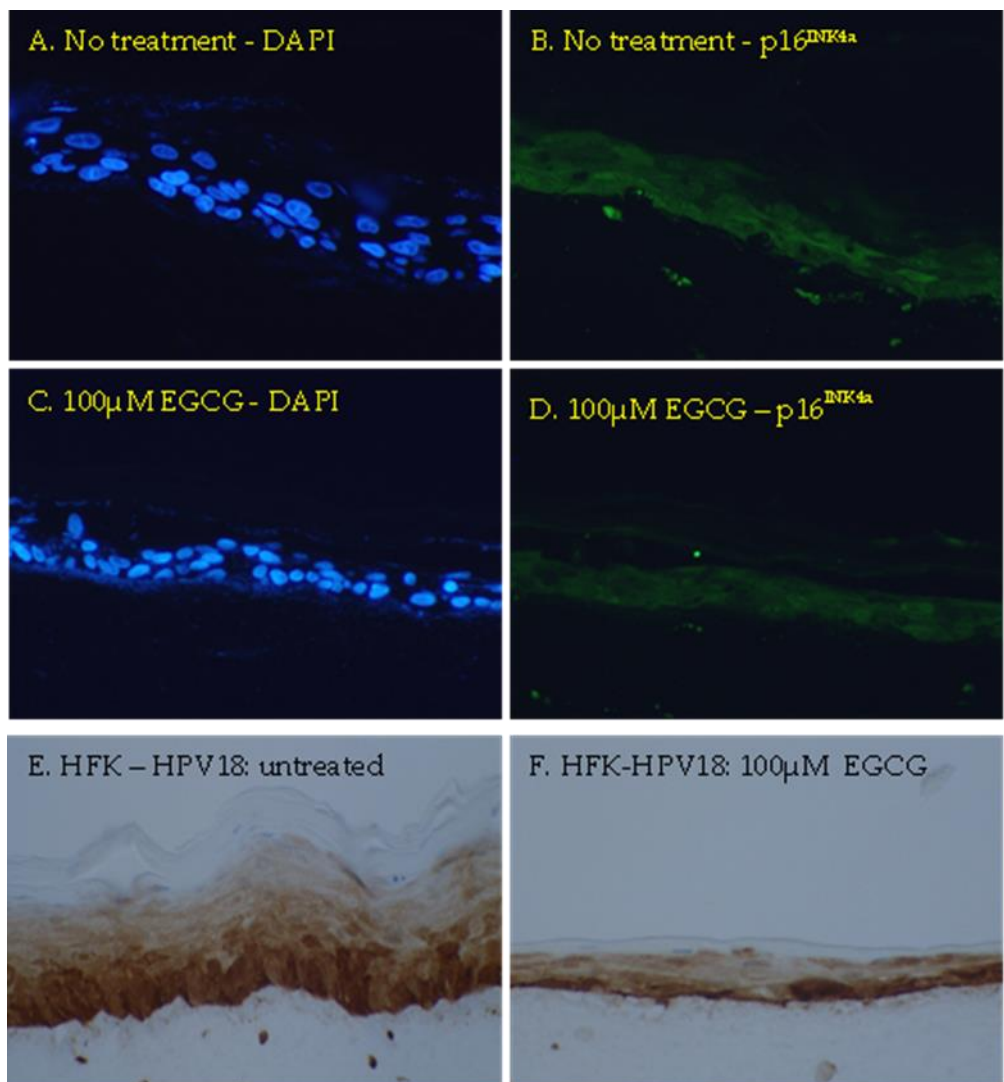
Supplementary Figure 1: Expanded image of Western blots taken from Figures 4.6 & 4.13. HFK-HPV18 cells were either left untreated or treated with 50 μ M or 100 μ M EGCG for three days. Where appropriate, HFK-HPV18 cells were treated for 24 hours with 25 μ M cisplatin to stimulate expression of p53. Cells were harvested by lysing in RIPA buffer. 30 μ g of total protein lysate were resolved by SDS-PAGE. The levels of HPV18 E6, HPV18 E7, p53, and p21WAF1 were determined by Western blotting using antibodies specific for the protein of interest. Membranes were stripped and reprobed with a mAb to β -actin to confirm equal protein loading. (A) Western blots for HPV18-encoded E7 protein (left) and HPV18-encoded E6 protein (right). The same membranes were reprobed with a mAb to β -actin to confirm equal loading. Lysates from isogenic normal keratinocytes (HFK) were included as a negative control. (B) Western blot for p53. The same membrane was reprobed with an mAb to β -actin to ensure equal protein loading. Lysates from isogenic normal keratinocytes (HFK) were included as a negative control. (C) Western blot for p21. The same membrane was reprobed with a mAb to β -actin to ensure equal protein loading.

A Western blot for DNMT1 and DNMT3B
(8% gel)

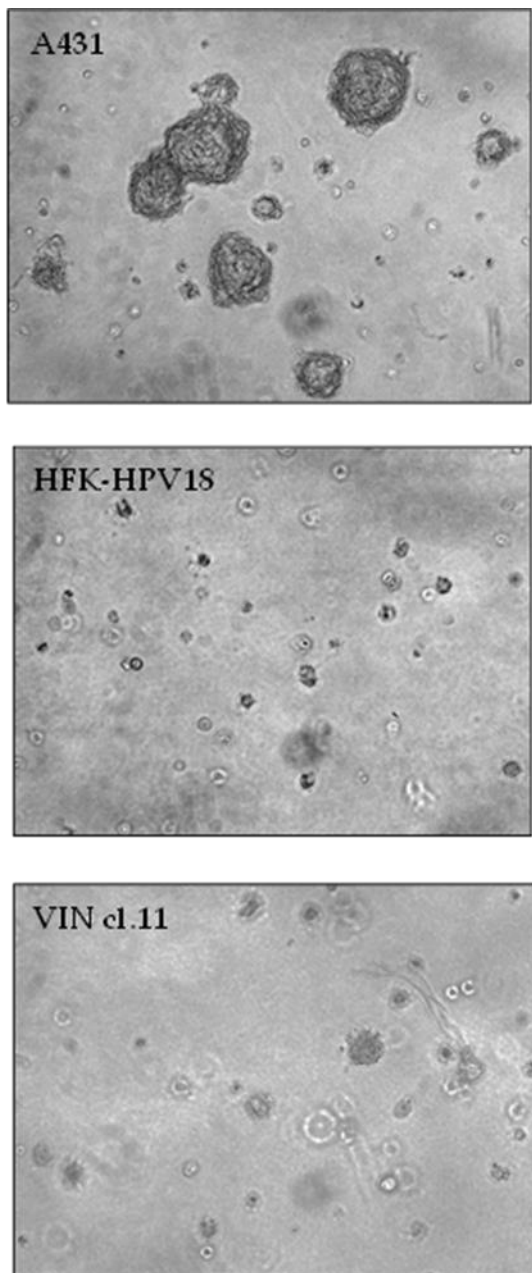




Supplementary Figure 2: Expanded image of Western blots taken from Figure 4.13. HFK-HPV18 cells were either left untreated or treated with 50 μ M or 100 μ M EGCG for three days. Where appropriate, HFK-HPV18 cells were treated for 24 hours with 25 μ M cisplatin. In some experiments, the isogenic normal uninfected counterpart of HFK-HPV18, (HFK), was included for comparison. Cells were harvested by lysing in RIPA buffer. 30 μ g of total protein lysate were resolved by SDS-PAGE. The levels of DNMT1, DNMT3B, EZH2 and BMI-1 were determined by Western blotting using antibodies specific for the protein of interest. Membranes were stripped and reprobed with a mAb to β -actin to confirm equal protein loading. (A) Western blots for DNMT3B (upper) and DNMT1 (lower). The DNMT1 membrane was stripped and reprobed with a mAb to β -actin to confirm equal loading. Lysates from isogenic normal keratinocytes (HFK) were included as a negative control. (B) Western blots for EZH2 and BMI-1. The same membrane was reprobed with an mAb to β -actin to ensure equal protein loading. Lysates from isogenic normal keratinocytes (HFK) were included as a negative control.



Supplementary Figure 3: Immunofluorescence and immunohistochemical staining for p16^{INK4a} on organotypic raft cultures generated from untreated and EGCG-treated HFK-HPV18 keratinocytes. Immunofluorescence (A-D) and immunostaining (E-F) of p16^{INK4a} were performed on HFK-HPV18 rafts sections. DAPI was used to counter stain cell nuclei in IF staining. Both the staining techniques consistently showed that the expression of p16 was not affected by EGCG treatment when compared to control.



Supplementary Figure 4: VIN cl. 11 fails to form colonies in soft-agarose colony formation assays. A431, HFK-HPV18 and VIN cl.11 cells were assayed for their ability to proliferate in an anchorage-independent manner by seeding cells into growth medium containing 0.5% soft agarose. Colony formation monitored after 3 weeks. Unlike the fully malignant A431 cell line, HFK-HPV18 and VIN cl.11 cells failed to form colonies.

Chapter 8:

References

References

1. CRUK. *Cancer Research UK Cancer Statistics*.
2. Akhtar-Danesh, N., L. Elit, and A. Lytwyn, *Trends in incidence and survival of women with invasive vulvar cancer in the United States and Canada: a population-based study*. Gynecologic oncology, 2014. **134**(2): p. 314-8.
3. Olsen, J., et al., *Incidence and cost of anal, penile, vaginal and vulvar cancer in Denmark*. BMC public health, 2012. **12**: p. 1082.
4. Somoye, G.O., A. Mocroft, and A. Olaitan, *Analysis of the incidence and mortality of vulval cancer in women in South East England 1960-1999*. Archives of gynecology and obstetrics, 2009. **279**(2): p. 113-7.
5. Kurman, R.J., T. Toki, and M.H. Schiffman, *Basaloid and warty carcinomas of the vulva. Distinctive types of squamous cell carcinoma frequently associated with human papillomaviruses*. The American journal of surgical pathology, 1993. **17**(2): p. 133-45.
6. Ueda, Y., et al., *Two distinct pathways to development of squamous cell carcinoma of the vulva*. Journal of skin cancer, 2011. **2011**: p. 951250.
7. Knopp, S., et al., *p14ARF, a prognostic predictor in HPV-negative vulvar carcinoma*. American journal of clinical pathology, 2006. **126**(2): p. 266-76.
8. Iwasawa, A., et al., *Human papillomavirus in squamous cell carcinoma of the vulva by polymerase chain reaction*. Obstetrics and gynecology, 1997. **89**(1): p. 81-4.
9. Pinto, A.P., et al., *Prognostic significance of lymph node variables and human papillomavirus DNA in invasive vulvar carcinoma*. Gynecologic oncology, 2004. **92**(3): p. 856-65.
10. Skapa, P., et al., *Human papillomavirus (HPV) profiles of vulvar lesions: possible implications for the classification of vulvar squamous cell carcinoma precursors and for the efficacy of prophylactic HPV vaccination*. The American journal of surgical pathology, 2007. **31**(12): p. 1834-43.
11. Lee, Y.Y., et al., *Carcinoma of the vulva: HPV and p53 mutations*. Oncogene, 1994. **9**(6): p. 1655-9.
12. Lindell, G., et al., *Presence of human papillomavirus (HPV) in vulvar squamous cell carcinoma (VSCC) and sentinel node*. Gynecologic oncology, 2010. **117**(2): p. 312-6.
13. De Vuyst, H., et al., *Prevalence and type distribution of human papillomavirus in carcinoma and intraepithelial neoplasia of the vulva, vagina and anus: a meta-analysis*. International journal of cancer. Journal international du cancer, 2009. **124**(7): p. 1626-36.
14. Carlson, J.A., et al., *Vulvar lichen sclerosus and squamous cell carcinoma: a cohort, case control, and investigational study with historical perspective; implications for chronic inflammation and sclerosis in the development of neoplasia*. Human pathology, 1998. **29**(9): p. 932-48.
15. Rhodes, C.A., C. Cummins, and M.I. Shafi, *The management of squamous cell vulval cancer: a population based retrospective study of 411 cases*. British journal of obstetrics and gynaecology, 1998. **105**(2): p. 200-5.
16. Yap, J.K., et al., *Impact of improving outcome guidance in gynaecological cancer on squamous cell carcinoma of the vulva in the West Midlands, UK*. Journal of obstetrics and gynaecology : the journal of the Institute of Obstetrics and Gynaecology, 2011. **31**(8): p. 754-8.
17. Pecorelli, S., *Revised FIGO staging for carcinoma of the vulva, cervix, and endometrium*. International journal of gynaecology and obstetrics: the official organ of the International Federation of Gynaecology and Obstetrics, 2009. **105**(2): p. 103-4.
18. RCOG (2014) *Guidelines for the diagnosis and management of vulval cancer*.

19. Woelber, L., et al., *Management of patients with vulvar cancer: a perspective review according to tumour stage*. Therapeutic advances in medical oncology, 2013. **5**(3): p. 183-92.
20. Heaps, J.M., et al., *Surgical-pathologic variables predictive of local recurrence in squamous cell carcinoma of the vulva*. Gynecologic oncology, 1990. **38**(3): p. 309-14.
21. Eva, L.J., et al., *Differentiated-type vulval intraepithelial neoplasia has a high-risk association with vulval squamous cell carcinoma*. International journal of gynecological cancer : official journal of the International Gynecological Cancer Society, 2009. **19**(4): p. 741-4.
22. Tantipalakorn, C., et al., *Outcome and patterns of recurrence for International Federation of Gynecology and Obstetrics (FIGO) stages I and II squamous cell vulvar cancer*. Obstetrics and gynecology, 2009. **113**(4): p. 895-901.
23. Regauer, S., *Residual anogenital lichen sclerosus after cancer surgery has a high risk for recurrence: a clinicopathological study of 75 women*. Gynecologic oncology, 2011. **123**(2): p. 289-94.
24. van Seters, M., M. van Beurden, and A.J. de Craen, *Is the assumed natural history of vulvar intraepithelial neoplasia III based on enough evidence? A systematic review of 3322 published patients*. Gynecologic oncology, 2005. **97**(2): p. 645-51.
25. Fehr, M.K., et al., *Disease progression and recurrence in women treated for vulvovaginal intraepithelial neoplasia*. Journal of gynecologic oncology, 2013. **24**(3): p. 236-41.
26. Hacker, N.F. and J. Van der Velden, *Conservative management of early vulvar cancer*. Cancer, 1993. **71**(4 Suppl): p. 1673-7.
27. Van der Zee, A.G., et al., *Sentinel node dissection is safe in the treatment of early-stage vulvar cancer*. Journal of clinical oncology : official journal of the American Society of Clinical Oncology, 2008. **26**(6): p. 884-9.
28. Underwood, M., et al., *The use of sentinel node sampling in vulval cancer*. Journal of obstetrics and gynaecology : the journal of the Institute of Obstetrics and Gynaecology, 2013. **33**(8): p. 892-7.
29. Maggino, T., et al., *Patterns of recurrence in patients with squamous cell carcinoma of the vulva. A multicenter CTF Study*. Cancer, 2000. **89**(1): p. 116-22.
30. Chan, J.K., et al., *Margin distance and other clinico-pathologic prognostic factors in vulvar carcinoma: a multivariate analysis*. Gynecologic oncology, 2007. **104**(3): p. 636-41.
31. Gonzalez Bosquet, J., et al., *Long-term survival and disease recurrence in patients with primary squamous cell carcinoma of the vulva*. Gynecologic oncology, 2005. **97**(3): p. 828-33.
32. Yoder, B.J., et al., *Stage IA vulvar squamous cell carcinoma: an analysis of tumor invasive characteristics and risk*. The American journal of surgical pathology, 2008. **32**(5): p. 765-72.
33. Groenen, S.M., P.J. Timmers, and C.W. Burger, *Recurrence rate in vulvar carcinoma in relation to pathological margin distance*. International journal of gynecological cancer : official journal of the International Gynecological Cancer Society, 2010. **20**(5): p. 869-73.
34. Woolderink, J.M., et al., *Patterns and frequency of recurrences of squamous cell carcinoma of the vulva*. Gynecologic oncology, 2006. **103**(1): p. 293-9.
35. Preti, M., et al., *Recurrent squamous cell carcinoma of the vulva: clinicopathologic determinants identifying low risk patients*. Cancer, 2000. **88**(8): p. 1869-76.
36. Rouzier, R., et al., *Prognostic significance of epithelial disorders adjacent to invasive vulvar carcinomas*. Gynecologic oncology, 2001. **81**(3): p. 414-9.

37. Woelber, L., et al., *Prognostic value of pathological resection margin distance in squamous cell cancer of the vulva*. Annals of surgical oncology, 2011. **18**(13): p. 3811-8.
38. Dakubo, G.D., et al., *Clinical implications and utility of field cancerization*. Cancer cell international, 2007. **7**: p. 2.
39. Slaughter, D.P., H.W. Southwick, and W. Smejkal, *Field cancerization in oral stratified squamous epithelium; clinical implications of multicentric origin*. Cancer, 1953. **6**(5): p. 963-8.
40. Rosenthal, A.N., et al., *Molecular evidence of a common clonal origin and subsequent divergent clonal evolution in vulval intraepithelial neoplasia, vulval squamous cell carcinoma and lymph node metastases*. International journal of cancer. Journal international du cancer, 2002. **99**(4): p. 549-54.
41. Burger, M.P., et al., *The importance of the groin node status for the survival of T1 and T2 vulval carcinoma patients*. Gynecologic oncology, 1995. **57**(3): p. 327-34.
42. van de Nieuwenhof, H.P., et al., *Differentiated vulvar intraepithelial neoplasia is often found in lesions, previously diagnosed as lichen sclerosus, which have progressed to vulvar squamous cell carcinoma*. Modern pathology : an official journal of the United States and Canadian Academy of Pathology, Inc, 2011. **24**(2): p. 297-305.
43. Pinto, A.P., et al., *Differentiated vulvar intraepithelial neoplasia contains Tp53 mutations and is genetically linked to vulvar squamous cell carcinoma*. Modern pathology : an official journal of the United States and Canadian Academy of Pathology, Inc, 2010. **23**(3): p. 404-12.
44. van Seters, M., et al., *In the absence of (early) invasive carcinoma, vulvar intraepithelial neoplasia associated with lichen sclerosus is mainly of undifferentiated type: new insights in histology and aetiology*. Journal of clinical pathology, 2007. **60**(5): p. 504-9.
45. Hillemanns, P. and X. Wang, *Integration of HPV-16 and HPV-18 DNA in vulvar intraepithelial neoplasia*. Gynecologic oncology, 2006. **100**(2): p. 276-82.
46. Judson, P.L., et al., *Trends in the incidence of invasive and in situ vulvar carcinoma*. Obstetrics and gynecology, 2006. **107**(5): p. 1018-22.
47. Baandrup, L., et al., *In situ and invasive squamous cell carcinoma of the vulva in Denmark 1978-2007-a nationwide population-based study*. Gynecologic oncology, 2011. **122**(1): p. 45-9.
48. van Beurden, M., et al., *Multifocal vulvar intraepithelial neoplasia grade III and multicentric lower genital tract neoplasia is associated with transcriptionally active human papillomavirus*. Cancer, 1995. **75**(12): p. 2879-84.
49. van Seters, M., et al., *Treatment of vulvar intraepithelial neoplasia with topical imiquimod*. The New England journal of medicine, 2008. **358**(14): p. 1465-73.
50. Todd, R.W., I.J. Etherington, and D.M. Luesley, *The effects of 5% imiquimod cream on high-grade vulval intraepithelial neoplasia*. Gynecologic oncology, 2002. **85**(1): p. 67-70.
51. Tristram, A., et al., *Activity, safety, and feasibility of cidofovir and imiquimod for treatment of vulval intraepithelial neoplasia (RT(3)VIN): a multicentre, open-label, randomised, phase 2 trial*. The Lancet. Oncology, 2014. **15**(12): p. 1361-8.
52. Tzellos, T.G., et al., *Efficacy, safety and tolerability of green tea catechins in the treatment of external anogenital warts: a systematic review and meta-analysis*. Journal of the European Academy of Dermatology and Venereology : JEADV, 2011. **25**(3): p. 345-53.
53. Powell, J.J. and F. Wojnarowska, *Lichen sclerosus*. Lancet, 1999. **353**(9166): p. 1777-83.
54. Cox, N.H., J.N. Mitchell, and W.N. Morley, *Lichen sclerosus et atrophicus in non-identical female twins*. The British journal of dermatology, 1986. **115**(6): p. 743.

55. Meyrick Thomas, R.H., C.M. Ridley, and M.M. Black, *The association of lichen sclerosus et atrophicus and autoimmune-related disease in males*. The British journal of dermatology, 1983. **109**(6): p. 661-4.
56. Meyrick Thomas, R.H., et al., *Lichen sclerosus et atrophicus and autoimmunity--a study of 350 women*. The British journal of dermatology, 1988. **118**(1): p. 41-6.
57. Wallace, H.J., *Lichen sclerosus et atrophicus*. Transactions of the St. John's Hospital Dermatological Society, 1971. **57**(1): p. 9-30.
58. Todd, P., et al., *Lichen sclerosus and the Kobner phenomenon*. Clinical and experimental dermatology, 1994. **19**(3): p. 262-3.
59. Chi, C.C., et al., *Systematic review and meta-analysis of randomized controlled trials on topical interventions for genital lichen sclerosus*. Journal of the American Academy of Dermatology, 2012. **67**(2): p. 305-12.
60. Reyes, M.C. and K. Cooper, *An update on vulvar intraepithelial neoplasia: terminology and a practical approach to diagnosis*. Journal of clinical pathology, 2014. **67**(4): p. 290-4.
61. Spiryda, L.B., A.F. Fuller, and A. Goodman, *Aggressive locally recurrent vulvar cancer: review of cases presented to Massachusetts General Hospital 1990 to present*. International journal of gynecological cancer : official journal of the International Gynecological Cancer Society, 2005. **15**(5): p. 884-9.
62. Leemans, C.R., B.J. Braakhuis, and R.H. Brakenhoff, *The molecular biology of head and neck cancer*. Nature reviews. Cancer, 2011. **11**(1): p. 9-22.
63. de Villiers, E.M., et al., *Classification of papillomaviruses*. Virology, 2004. **324**(1): p. 17-27.
64. Walboomers, J.M., et al., *Human papillomavirus is a necessary cause of invasive cervical cancer worldwide*. The Journal of pathology, 1999. **189**(1): p. 12-9.
65. de Sanjose, S., et al., *Worldwide human papillomavirus genotype attribution in over 2000 cases of intraepithelial and invasive lesions of the vulva*. European journal of cancer, 2013. **49**(16): p. 3450-61.
66. Moody, C.A. and L.A. Laimins, *Human papillomavirus oncoproteins: pathways to transformation*. Nature reviews. Cancer, 2010. **10**(8): p. 550-60.
67. Watt, F.M., *Epidermal stem cells: markers, patterning and the control of stem cell fate*. Philosophical transactions of the Royal Society of London. Series B, Biological sciences, 1998. **353**(1370): p. 831-7.
68. Pim, D. and L. Banks, *HPV-18 E6*I protein modulates the E6-directed degradation of p53 by binding to full-length HPV-18 E6*. Oncogene, 1999. **18**(52): p. 7403-8.
69. Pim, D., V. Tomaic, and L. Banks, *The human papillomavirus (HPV) E6* proteins from high-risk, mucosal HPVs can direct degradation of cellular proteins in the absence of full-length E6 protein*. Journal of virology, 2009. **83**(19): p. 9863-74.
70. Tang, S., et al., *The E7 oncoprotein is translated from spliced E6*I transcripts in high-risk human papillomavirus type 16- or type 18-positive cervical cancer cell lines via translation reinitiation*. Journal of virology, 2006. **80**(9): p. 4249-63.
71. Stewart, D., et al., *Ubiquitination and proteasome degradation of the E6 proteins of human papillomavirus types 11 and 18*. The Journal of general virology, 2004. **85**(Pt 6): p. 1419-26.
72. Munger, K., et al., *Complex formation of human papillomavirus E7 proteins with the retinoblastoma tumor suppressor gene product*. The EMBO journal, 1989. **8**(13): p. 4099-105.
73. Ishikawa, M., et al., *Overexpression of p16 INK4a as an indicator for human papillomavirus oncogenic activity in cervical squamous neoplasia*. International journal of gynecological cancer : official journal of the International Gynecological Cancer Society, 2006. **16**(1): p. 347-53.

74. Narisawa-Saito, M. and T. Kiyono, *Basic mechanisms of high-risk human papillomavirus-induced carcinogenesis: roles of E6 and E7 proteins*. Cancer science, 2007. **98**(10): p. 1505-11.
75. Durst, M., et al., *A papillomavirus DNA from a cervical carcinoma and its prevalence in cancer biopsy samples from different geographic regions*. Proceedings of the National Academy of Sciences of the United States of America, 1983. **80**(12): p. 3812-5.
76. von Knebel Doeberitz, M., *New markers for cervical dysplasia to visualise the genomic chaos created by aberrant oncogenic papillomavirus infections*. European journal of cancer, 2002. **38**(17): p. 2229-42.
77. Woodman, C.B., S.I. Collins, and L.S. Young, *The natural history of cervical HPV infection: unresolved issues*. Nature reviews. Cancer, 2007. **7**(1): p. 11-22.
78. van de Nieuwenhof, H.P., et al., *The etiologic role of HPV in vulvar squamous cell carcinoma fine tuned*. Cancer epidemiology, biomarkers & prevention : a publication of the American Association for Cancer Research, cosponsored by the American Society of Preventive Oncology, 2009. **18**(7): p. 2061-7.
79. Wilson, V.G., *The role of ubiquitin and ubiquitin-like modification systems in papillomavirus biology*. Viruses, 2014. **6**(9): p. 3584-611.
80. Vos, R.M., et al., *The ubiquitin-specific peptidase USP15 regulates human papillomavirus type 16 E6 protein stability*. Journal of virology, 2009. **83**(17): p. 8885-92.
81. Tomaic, V., et al., *Regulation of the human papillomavirus type 18 E6/E6AP ubiquitin ligase complex by the HECT domain-containing protein EDD*. Journal of virology, 2011. **85**(7): p. 3120-7.
82. Kelley, M.L., et al., *The global transcriptional effects of the human papillomavirus E6 protein in cervical carcinoma cell lines are mediated by the E6AP ubiquitin ligase*. Journal of virology, 2005. **79**(6): p. 3737-47.
83. Nagasaka, K., et al., *PDZ domains and viral infection: versatile potentials of HPV-PDZ interactions in relation to malignancy*. BioMed research international, 2013. **2013**: p. 369712.
84. Tomaic, V., et al., *Interaction of HPV E6 oncoproteins with specific proteasomal subunits*. Virology, 2013. **446**(1-2): p. 389-96.
85. Oh, K.J., A. Kalinina, and S. Bagchi, *Destabilization of Rb by human papillomavirus E7 is cell cycle dependent: E2-25K is involved in the proteolysis*. Virology, 2010. **396**(1): p. 118-24.
86. Classon, M. and N. Dyson, *p107 and p130: versatile proteins with interesting pockets*. Experimental cell research, 2001. **264**(1): p. 135-47.
87. Zhang, B., W. Chen, and A. Roman, *The E7 proteins of low- and high-risk human papillomaviruses share the ability to target the pRB family member p130 for degradation*. Proceedings of the National Academy of Sciences of the United States of America, 2006. **103**(2): p. 437-42.
88. Berezutskaya, E. and S. Bagchi, *The human papillomavirus E7 oncoprotein functionally interacts with the S4 subunit of the 26 S proteasome*. The Journal of biological chemistry, 1997. **272**(48): p. 30135-40.
89. Deyrieux, A.F., et al., *Sumoylation dynamics during keratinocyte differentiation*. Journal of cell science, 2007. **120**(Pt 1): p. 125-36.
90. Heaton, P.R., et al., *HPV E6 proteins target Ubc9, the SUMO conjugating enzyme*. Virus research, 2011. **158**(1-2): p. 199-208.
91. Simpson, C.L., D.M. Patel, and K.J. Green, *Deconstructing the skin: cytoarchitectural determinants of epidermal morphogenesis*. Nature reviews. Molecular cell biology, 2011. **12**(9): p. 565-80.

92. Dotto, G.P., *Crosstalk of Notch with p53 and p63 in cancer growth control*. Nature reviews. Cancer, 2009. **9**(8): p. 587-95.
93. Blanpain, C. and E. Fuchs, *Epidermal homeostasis: a balancing act of stem cells in the skin*. Nature reviews. Molecular cell biology, 2009. **10**(3): p. 207-17.
94. Steinmann, J., et al., *Anti-infective properties of epigallocatechin-3-gallate (EGCG), a component of green tea*. British journal of pharmacology, 2013. **168**(5): p. 1059-73.
95. Yang, C.S., et al., *Cancer prevention by tea: Evidence from laboratory studies*. Pharmacological research : the official journal of the Italian Pharmacological Society, 2011. **64**(2): p. 113-22.
96. Balasubramanian, S., et al., *Human epidermal keratinocytes undergo (-)-epigallocatechin-3-gallate-dependent differentiation but not apoptosis*. Carcinogenesis, 2005. **26**(6): p. 1100-8.
97. Balasubramanian, S., G. Adhikary, and R.L. Eckert, *The Bmi-1 polycomb protein antagonizes the (-)-epigallocatechin-3-gallate-dependent suppression of skin cancer cell survival*. Carcinogenesis, 2010. **31**(3): p. 496-503.
98. Choudhury, S.R., et al., *(-)-Epigallocatechin-3-gallate and DZNep reduce polycomb protein level via a proteasome-dependent mechanism in skin cancer cells*. Carcinogenesis, 2011. **32**(10): p. 1525-32.
99. Nandakumar, V., M. Vaid, and S.K. Katiyar, *(-)-Epigallocatechin-3-gallate reactivates silenced tumor suppressor genes, Cip1/p21 and p16INK4a, by reducing DNA methylation and increasing histones acetylation in human skin cancer cells*. Carcinogenesis, 2011. **32**(4): p. 537-44.
100. Yokoyama, M., et al., *The tea polyphenol, (-)-epigallocatechin gallate effects on growth, apoptosis, and telomerase activity in cervical cell lines*. Gynecologic oncology, 2004. **92**(1): p. 197-204.
101. Qiao, Y., et al., *Cell growth inhibition and gene expression regulation by (-)-epigallocatechin-3-gallate in human cervical cancer cells*. Archives of pharmacal research, 2009. **32**(9): p. 1309-15.
102. Thakur, V.S., K. Gupta, and S. Gupta, *Green tea polyphenols increase p53 transcriptional activity and acetylation by suppressing class I histone deacetylases*. International journal of oncology, 2012. **41**(1): p. 353-61.
103. Hsu, S., et al., *Green tea polyphenols induce differentiation and proliferation in epidermal keratinocytes*. The Journal of pharmacology and experimental therapeutics, 2003. **306**(1): p. 29-34.
104. Hsu, S., et al., *Green tea polyphenol-induced epidermal keratinocyte differentiation is associated with coordinated expression of p57/KIP2 and caspase 14*. The Journal of pharmacology and experimental therapeutics, 2005. **312**(3): p. 884-90.
105. Balasubramanian, S. and R.L. Eckert, *Keratinocyte proliferation, differentiation, and apoptosis--differential mechanisms of regulation by curcumin, EGCG and apigenin*. Toxicology and applied pharmacology, 2007. **224**(3): p. 214-9.
106. Lo, A.K., et al., *Alterations of biologic properties and gene expression in nasopharyngeal epithelial cells by the Epstein-Barr virus-encoded latent membrane protein 1*. Laboratory investigation; a journal of technical methods and pathology, 2003. **83**(5): p. 697-709.
107. Lindh, M., et al., *Real-time Taqman PCR targeting 14 human papilloma virus types*. Journal of clinical virology : the official publication of the Pan American Society for Clinical Virology, 2007. **40**(4): p. 321-4.
108. Collins, S.I., et al., *Disruption of the E2 gene is a common and early event in the natural history of cervical human papillomavirus infection: a longitudinal cohort study*. Cancer research, 2009. **69**(9): p. 3828-32.

109. Livak, K.J. and T.D. Schmittgen, *Analysis of relative gene expression data using real-time quantitative PCR and the 2(-Delta Delta C(T)) Method*. Methods, 2001. **25**(4): p. 402-8.
110. Dawson, C.W. and L.S. Young, *In vitro assays to study epithelial cell differentiation*. Methods in molecular biology, 2001. **174**: p. 173-80.
111. Rouzier, R., et al., *Local relapse in patients treated for squamous cell vulvar carcinoma: incidence and prognostic value*. Obstetrics and gynecology, 2002. **100**(6): p. 1159-67.
112. De Hullu, J.A., et al., *Vulvar carcinoma. The price of less radical surgery*. Cancer, 2002. **95**(11): p. 2331-8.
113. Rolfe, K.J., et al., *TP53 mutations in vulval lichen sclerosus adjacent to squamous cell carcinoma of the vulva*. British journal of cancer, 2003. **89**(12): p. 2249-53.
114. Vanin, K., et al., *Overexpression of wild-type p53 in lichen sclerosus adjacent to human papillomavirus-negative vulvar cancer*. The Journal of investigative dermatology, 2002. **119**(5): p. 1027-33.
115. Doorbar, J., et al., *The biology and life-cycle of human papillomaviruses*. Vaccine, 2012. **30 Suppl 5**: p. F55-70.
116. Yang, B. and W.R. Hart, *Vulvar intraepithelial neoplasia of the simplex (differentiated) type: a clinicopathologic study including analysis of HPV and p53 expression*. The American journal of surgical pathology, 2000. **24**(3): p. 429-41.
117. Choschzick, M., et al., *Role of TP53 mutations in vulvar carcinomas*. International journal of gynecological pathology : official journal of the International Society of Gynecological Pathologists, 2011. **30**(5): p. 497-504.
118. Del Pino, M., L. Rodriguez-Caruncho, and J. Ordi, *Pathways of vulvar intraepithelial neoplasia and squamous cell carcinoma*. Histopathology, 2013. **62**(1): p. 161-75.
119. Holway, A.H., et al., *Somatic mutation of PTEN in vulvar cancer*. Clinical cancer research : an official journal of the American Association for Cancer Research, 2000. **6**(8): p. 3228-35.
120. Woelber, L., et al., *EGFR gene copy number increase in vulvar carcinomas is linked with poor clinical outcome*. Journal of clinical pathology, 2012. **65**(2): p. 133-9.
121. Guerrero, D., et al., *Differential hypermethylation of genes in vulvar cancer and lichen sclerosus coexisting or not with vulvar cancer*. International journal of cancer. Journal international du cancer, 2011. **128**(12): p. 2853-64.
122. Pinto, A.P., et al., *Squamous cell carcinoma of the vulva in Brazil: prognostic importance of host and viral variables*. Gynecologic oncology, 1999. **74**(1): p. 61-7.
123. Monk, B.J., et al., *Prognostic significance of human papillomavirus DNA in vulvar carcinoma*. Obstetrics and gynecology, 1995. **85**(5 Pt 1): p. 709-15.
124. Bloss, J.D., et al., *Clinical and histologic features of vulvar carcinomas analyzed for human papillomavirus status: evidence that squamous cell carcinoma of the vulva has more than one etiology*. Human pathology, 1991. **22**(7): p. 711-8.
125. Molijn, A., et al., *Molecular diagnosis of human papillomavirus (HPV) infections*. Journal of clinical virology : the official publication of the Pan American Society for Clinical Virology, 2005. **32 Suppl 1**: p. S43-51.
126. Gupta, N., et al., *A case report of vulvar carcinoma in situ treated with simecatechins with complete response*. Gynecologic oncology case reports, 2013. **6**: p. 10-2.
127. Ahn, W.S., et al., *A major constituent of green tea, EGCG, inhibits the growth of a human cervical cancer cell line, CaSki cells, through apoptosis, G(1) arrest, and regulation of gene expression*. DNA and cell biology, 2003. **22**(3): p. 217-24.
128. Zou, C., et al., *Green tea compound in chemoprevention of cervical cancer*. International journal of gynecological cancer : official journal of the International Gynecological Cancer Society, 2010. **20**(4): p. 617-24.

129. Liang, Y.C., et al., *Suppression of extracellular signals and cell proliferation through EGF receptor binding by (-)-epigallocatechin gallate in human A431 epidermoid carcinoma cells*. Journal of cellular biochemistry, 1997. **67**(1): p. 55-65.
130. Sah, J.F., et al., *Epigallocatechin-3-gallate inhibits epidermal growth factor receptor signaling pathway. Evidence for direct inhibition of ERK1/2 and AKT kinases*. The Journal of biological chemistry, 2004. **279**(13): p. 12755-62.
131. Gupta, S., et al., *Essential role of caspases in epigallocatechin-3-gallate-mediated inhibition of nuclear factor kappa B and induction of apoptosis*. Oncogene, 2004. **23**(14): p. 2507-22.
132. Zheng, Z.M. and X. Wang, *Regulation of cellular miRNA expression by human papillomaviruses*. Biochimica et biophysica acta, 2011. **1809**(11-12): p. 668-77.
133. Shai, A., et al., *The human papillomavirus E6 oncogene dysregulates the cell cycle and contributes to cervical carcinogenesis through two independent activities*. Cancer research, 2007. **67**(4): p. 1626-35.
134. Brake, T., et al., *Comparative analysis of cervical cancer in women and in a human papillomavirus-transgenic mouse model: identification of minichromosome maintenance protein 7 as an informative biomarker for human cervical cancer*. Cancer research, 2003. **63**(23): p. 8173-80.
135. Ukpo, O.C., et al., *High-risk human papillomavirus E6/E7 mRNA detection by a novel in situ hybridization assay strongly correlates with p16 expression and patient outcomes in oropharyngeal squamous cell carcinoma*. The American journal of surgical pathology, 2011. **35**(9): p. 1343-50.
136. Hyland, P.L., et al., *Evidence for alteration of EZH2, BMI1, and KDM6A and epigenetic reprogramming in human papillomavirus type 16 E6/E7-expressing keratinocytes*. Journal of virology, 2011. **85**(21): p. 10999-1006.
137. Thrower, J.S., et al., *Recognition of the polyubiquitin proteolytic signal*. The EMBO journal, 2000. **19**(1): p. 94-102.
138. Adams, J., *The proteasome: structure, function, and role in the cell*. Cancer treatment reviews, 2003. **29 Suppl 1**: p. 3-9.
139. Luker, G.D., et al., *Imaging 26S proteasome activity and inhibition in living mice*. Nature medicine, 2003. **9**(7): p. 969-73.
140. Lee, D.H. and A.L. Goldberg, *Proteasome inhibitors: valuable new tools for cell biologists*. Trends in cell biology, 1998. **8**(10): p. 397-403.
141. Jing, K., et al., *Docosahexaenoic acid induces the degradation of HPV E6/E7 oncoproteins by activating the ubiquitin-proteasome system*. Cell death & disease, 2014. **5**: p. e1524.
142. Manohar, M., et al., *(-)-Epigallocatechin-3-gallate induces apoptosis in human endometrial adenocarcinoma cells via ROS generation and p38 MAP kinase activation*. The Journal of nutritional biochemistry, 2013. **24**(6): p. 940-7.
143. Li, G.X., et al., *Pro-oxidative activities and dose-response relationship of (-)-epigallocatechin-3-gallate in the inhibition of lung cancer cell growth: a comparative study in vivo and in vitro*. Carcinogenesis, 2010. **31**(5): p. 902-10.
144. Aruoma, O.I., et al., *The antioxidant action of N-acetylcysteine: its reaction with hydrogen peroxide, hydroxyl radical, superoxide, and hypochlorous acid*. Free radical biology & medicine, 1989. **6**(6): p. 593-7.
145. Singh, M., et al., *Regulation of cell growth through cell cycle arrest and apoptosis in HPV 16 positive human cervical cancer cells by tea polyphenols*. Investigational new drugs, 2010. **28**(3): p. 216-24.
146. Tyring, S.K., *Effect of Sinecatechins on HPV-Activated Cell Growth and Induction of Apoptosis*. The Journal of clinical and aesthetic dermatology, 2012. **5**(2): p. 34-41.

147. Dasari, S. and P.B. Tchounwou, *Cisplatin in cancer therapy: molecular mechanisms of action*. European journal of pharmacology, 2014. **740**: p. 364-78.
148. McCance, D.J., et al., *Human papillomavirus type 16 alters human epithelial cell differentiation in vitro*. Proceedings of the National Academy of Sciences of the United States of America, 1988. **85**(19): p. 7169-73.
149. Doorbar, J., *The E4 protein; structure, function and patterns of expression*. Virology, 2013. **445**(1-2): p. 80-98.
150. Delury, C.P., et al., *The role of protein kinase A regulation of the E6 PDZ-binding domain during the differentiation-dependent life cycle of human papillomavirus type 18*. Journal of virology, 2013. **87**(17): p. 9463-72.
151. Wilson, R., et al., *The full-length E1E4 protein of human papillomavirus type 18 modulates differentiation-dependent viral DNA amplification and late gene expression*. Virology, 2007. **362**(2): p. 453-60.
152. Zerfass, K., et al., *Sequential activation of cyclin E and cyclin A gene expression by human papillomavirus type 16 E7 through sequences necessary for transformation*. Journal of virology, 1995. **69**(10): p. 6389-99.
153. Stevaux, O. and N.J. Dyson, *A revised picture of the E2F transcriptional network and RB function*. Current opinion in cell biology, 2002. **14**(6): p. 684-91.
154. Cheng, S., et al., *Differentiation-dependent up-regulation of the human papillomavirus E7 gene reactivates cellular DNA replication in suprabasal differentiated keratinocytes*. Genes & development, 1995. **9**(19): p. 2335-49.
155. Hastak, K., et al., *Ablation of either p21 or Bax prevents p53-dependent apoptosis induced by green tea polyphenol epigallocatechin-3-gallate*. FASEB journal : official publication of the Federation of American Societies for Experimental Biology, 2005. **19**(7): p. 789-91.
156. Hastak, K., et al., *Role of p53 and NF-kappaB in epigallocatechin-3-gallate-induced apoptosis of LNCaP cells*. Oncogene, 2003. **22**(31): p. 4851-9.
157. Garland, S.M., et al., *Natural history of genital warts: analysis of the placebo arm of 2 randomized phase III trials of a quadrivalent human papillomavirus (types 6, 11, 16, and 18) vaccine*. The Journal of infectious diseases, 2009. **199**(6): p. 805-14.
158. Jin, L., et al., *Epigallocatechin gallate promotes p53 accumulation and activity via the inhibition of MDM2-mediated p53 ubiquitination in human lung cancer cells*. Oncology reports, 2013. **29**(5): p. 1983-90.
159. Cho, Y.S., et al., *HIF-1alpha controls keratinocyte proliferation by up-regulating p21(WAF1/Cip1)*. Biochimica et biophysica acta, 2008. **1783**(2): p. 323-33.
160. Ahmad, N., et al., *Role of the retinoblastoma (pRb)-E2F/DP pathway in cancer chemopreventive effects of green tea polyphenol epigallocatechin-3-gallate*. Archives of biochemistry and biophysics, 2002. **398**(1): p. 125-31.
161. Masuda, M., M. Suzui, and I.B. Weinstein, *Effects of epigallocatechin-3-gallate on growth, epidermal growth factor receptor signaling pathways, gene expression, and chemosensitivity in human head and neck squamous cell carcinoma cell lines*. Clinical cancer research : an official journal of the American Association for Cancer Research, 2001. **7**(12): p. 4220-9.
162. Liberto, M. and D. Cobrinik, *Growth factor-dependent induction of p21(CIP1) by the green tea polyphenol, epigallocatechin gallate*. Cancer letters, 2000. **154**(2): p. 151-61.
163. Gronhoj Larsen, C., et al., *Correlation between human papillomavirus and p16 overexpression in oropharyngeal tumours: a systematic review*. British journal of cancer, 2014. **110**(6): p. 1587-94.
164. Vasilev, I., et al., *[Expression of human papilloma virus (HPV) and P16ink4a in cervical intraepithelial neoplasia (CIN) and papilloma]*. Akusherstvo i ginekologiya, 2006. **45**(1): p. 27-31.

165. Strati, K., H.C. Pitot, and P.F. Lambert, *Identification of biomarkers that distinguish human papillomavirus (HPV)-positive versus HPV-negative head and neck cancers in a mouse model*. Proceedings of the National Academy of Sciences of the United States of America, 2006. **103**(38): p. 14152-7.
166. Zhang, J., et al., *The protein levels of MCM7 and p63 in evaluating lesion severity of cervical disease*. International journal of gynecological cancer : official journal of the International Gynecological Cancer Society, 2013. **23**(2): p. 318-24.
167. McLaughlin-Drubin, M.E., C.P. Crum, and K. Munger, *Human papillomavirus E7 oncoprotein induces KDM6A and KDM6B histone demethylase expression and causes epigenetic reprogramming*. Proceedings of the National Academy of Sciences of the United States of America, 2011. **108**(5): p. 2130-5.
168. Holland, D., et al., *Activation of the enhancer of zeste homologue 2 gene by the human papillomavirus E7 oncoprotein*. Cancer research, 2008. **68**(23): p. 9964-72.
169. Leonard, S.M., et al., *Oncogenic human papillomavirus imposes an instructive pattern of DNA methylation changes which parallel the natural history of cervical HPV infection in young women*. Carcinogenesis, 2012. **33**(7): p. 1286-93.
170. Au Yeung, C.L., et al., *HPV-16 E6 upregulation of DNMT1 through repression of tumor suppressor p53*. Oncology reports, 2010. **24**(6): p. 1599-604.
171. McCabe, M.T., J.N. Davis, and M.L. Day, *Regulation of DNA methyltransferase 1 by the pRb/E2F1 pathway*. Cancer research, 2005. **65**(9): p. 3624-32.
172. Pim, D., P. Massimi, and L. Banks, *Alternatively spliced HPV-18 E6* protein inhibits E6 mediated degradation of p53 and suppresses transformed cell growth*. Oncogene, 1997. **15**(3): p. 257-64.
173. Singh, B.N., S. Shankar, and R.K. Srivastava, *Green tea catechin, epigallocatechin-3-gallate (EGCG): mechanisms, perspectives and clinical applications*. Biochemical pharmacology, 2011. **82**(12): p. 1807-21.
174. Kehmeier, E., et al., *Cellular steady-state levels of "high risk" but not "low risk" human papillomavirus (HPV) E6 proteins are increased by inhibition of proteasome-dependent degradation independent of their p53- and E6AP-binding capabilities*. Virology, 2002. **299**(1): p. 72-87.
175. Hicke, L., *Protein regulation by monoubiquitin*. Nature reviews. Molecular cell biology, 2001. **2**(3): p. 195-201.
176. Nicolaides, L., et al., *Stabilization of HPV16 E6 protein by PDZ proteins, and potential implications for genome maintenance*. Virology, 2011. **414**(2): p. 137-45.
177. Grassmann, K., et al., *Identification of a differentiation-inducible promoter in the E7 open reading frame of human papillomavirus type 16 (HPV-16) in raft cultures of a new cell line containing high copy numbers of episomal HPV-16 DNA*. Journal of virology, 1996. **70**(4): p. 2339-49.
178. Bryant, D., et al., *mRNA sequencing of novel cell lines from human papillomavirus type-16 related vulval intraepithelial neoplasia: consequences of expression of HPV16 E4 and E5*. Journal of medical virology, 2014. **86**(9): p. 1534-41.
179. Cuschieri, K., et al., *Effect of HPV assay choice on perceived prevalence in a population-based sample*. Diagnostic molecular pathology : the American journal of surgical pathology, part B, 2013. **22**(2): p. 85-90.
180. de Villiers, E.M., et al., *Presence of papillomavirus sequences in condylomatous lesions of the mamillae and in invasive carcinoma of the breast*. Breast Cancer Res, 2005. **7**(1): p. R1-11.
181. Hiller, T., et al., *Comparative analysis of 19 genital human papillomavirus types with regard to p53 degradation, immortalization, phylogeny, and epidemiologic risk classification*. Cancer Epidemiol Biomarkers Prev, 2006. **15**(7): p. 1262-7.

182. Garland, S.M., et al., *Human papillomavirus infections and vulvar disease development*. Cancer Epidemiol Biomarkers Prev, 2009. **18**(6): p. 1777-84.
183. Srodon, M., et al., *The distribution of low and high-risk HPV types in vulvar and vaginal intraepithelial neoplasia (VIN and VaIN)*. Am J Surg Pathol, 2006. **30**(12): p. 1513-8.
184. McLaughlin-Drubin, M.E. and C. Meyers, *Propagation of infectious, high-risk HPV in organotypic "raft" culture*. Methods in molecular medicine, 2005. **119**: p. 171-86.
185. Scholzen, T. and J. Gerdes, *The Ki-67 protein: from the known and the unknown*. Journal of cellular physiology, 2000. **182**(3): p. 311-22.
186. Shin, M.K., et al., *Human papillomavirus E7 oncoprotein overrides the tumor suppressor activity of p21Cip1 in cervical carcinogenesis*. Cancer research, 2009. **69**(14): p. 5656-63.
187. Buitrago-Perez, A., et al., *A humanized mouse model of HPV-associated pathology driven by E7 expression*. PloS one, 2012. **7**(7): p. e41743.
188. Middleton, K., et al., *Organization of human papillomavirus productive cycle during neoplastic progression provides a basis for selection of diagnostic markers*. Journal of virology, 2003. **77**(19): p. 10186-201.
189. Koster, M.I. and D.R. Roop, *Transgenic mouse models provide new insights into the role of p63 in epidermal development*. Cell cycle, 2004. **3**(4): p. 411-3.
190. Edwards, T.G., et al., *Human papillomavirus episome stability is reduced by aphidicolin and controlled by DNA damage response pathways*. Journal of virology, 2013. **87**(7): p. 3979-89.
191. Edwards, T.G., et al., *HPV episome levels are potently decreased by pyrrole-imidazole polyamides*. Antiviral research, 2011. **91**(2): p. 177-86.
192. Quade, B.J., et al., *Expression of the p53 homologue p63 in early cervical neoplasia*. Gynecologic oncology, 2001. **80**(1): p. 24-9.
193. Roggenbuck, B., et al., *Human papillomavirus type 18 E6*, E6, and E7 protein synthesis in cell-free translation systems and comparison of E6 and E7 in vitro translation products to proteins immunoprecipitated from human epithelial cells*. Journal of virology, 1991. **65**(9): p. 5068-72.
194. Smotkin, D. and F.O. Wettstein, *The major human papillomavirus protein in cervical cancers is a cytoplasmic phosphoprotein*. Journal of virology, 1987. **61**(5): p. 1686-9.
195. Hoffmann, J., et al., *EGCG downregulates IL-1RI expression and suppresses IL-1-induced tumorigenic factors in human pancreatic adenocarcinoma cells*. Biochemical pharmacology, 2011. **82**(9): p. 1153-62.
196. Wheeler, D.S., et al., *Epigallocatechin-3-gallate, a green tea-derived polyphenol, inhibits IL-1 beta-dependent proinflammatory signal transduction in cultured respiratory epithelial cells*. The Journal of nutrition, 2004. **134**(5): p. 1039-44.
197. Barthelman, M., et al., *(-)-Epigallocatechin-3-gallate inhibition of ultraviolet B-induced AP-1 activity*. Carcinogenesis, 1998. **19**(12): p. 2201-4.
198. Nomura, M., et al., *Inhibition of ultraviolet B-induced AP-1 activation by theaflavins from black tea*. Molecular carcinogenesis, 2000. **28**(3): p. 148-55.
199. Ahmad, N., S. Gupta, and H. Mukhtar, *Green tea polyphenol epigallocatechin-3-gallate differentially modulates nuclear factor kappaB in cancer cells versus normal cells*. Archives of biochemistry and biophysics, 2000. **376**(2): p. 338-46.
200. Honicke, A.S., S.A. Ender, and J. Radons, *Combined administration of EGCG and IL-1 receptor antagonist efficiently downregulates IL-1-induced tumorigenic factors in U-2 OS human osteosarcoma cells*. International journal of oncology, 2012. **41**(2): p. 753-8.
201. Pappa, K.I., et al., *Expression profiling of vulvar carcinoma: clues for deranged extracellular matrix remodeling and effects on multiple signaling pathways combined with discrete patient subsets*. Translational oncology, 2011. **4**(5): p. 301-13.

202. Nguyen, B.C., et al., *Cross-regulation between Notch and p63 in keratinocyte commitment to differentiation*. Genes & development, 2006. **20**(8): p. 1028-42.
203. Nickoloff, B.J., et al., *Jagged-1 mediated activation of notch signaling induces complete maturation of human keratinocytes through NF-kappaB and PPARgamma*. Cell death and differentiation, 2002. **9**(8): p. 842-55.
204. Henken, F.E., et al., *The functional role of Notch signaling in HPV-mediated transformation is dose-dependent and linked to AP-1 alterations*. Cellular oncology, 2012. **35**(2): p. 77-84.
205. Maliekal, T.T., et al., *The role of Notch signaling in human cervical cancer: implications for solid tumors*. Oncogene, 2008. **27**(38): p. 5110-4.
206. Talora, C., et al., *Specific down-modulation of Notch1 signaling in cervical cancer cells is required for sustained HPV-E6/E7 expression and late steps of malignant transformation*. Genes & development, 2002. **16**(17): p. 2252-63.
207. Talora, C., et al., *Constitutively active Notch1 induces growth arrest of HPV-positive cervical cancer cells via separate signaling pathways*. Experimental cell research, 2005. **305**(2): p. 343-54.
208. Liu, X., et al., *The effect of green tea extract and EGCG on the signaling network in squamous cell carcinoma*. Nutrition and cancer, 2011. **63**(3): p. 466-75.
209. Lee, S.H., et al., *Epigallocatechin-3-gallate attenuates head and neck cancer stem cell traits through suppression of Notch pathway*. European journal of cancer, 2013. **49**(15): p. 3210-8.
210. Jin, H., et al., *Epigallocatechin gallate inhibits the proliferation of colorectal cancer cells by regulating Notch signaling*. OncoTargets and therapy, 2013. **6**: p. 145-53.
211. Thomas, M., et al., *Human papillomaviruses, cervical cancer and cell polarity*. Oncogene, 2008. **27**(55): p. 7018-30.